

International Journal for

Computational Civil and Structural Engineering

**Международный журнал по расчету
гражданских и строительных конструкций**

EXECUTIVE EDITOR

Vladimir I. Travush,
Full Member of RAACS, Professor, Dr.Sc.,
Vice-President of the Russian Academy
of Architecture and Construction Sciences;
Urban Planning Institute
of Residential and Public Buildings;
24, Ulitsa Bolshaya Dmitrovka, 107031, Moscow, Russia

EDITORIAL DIRECTOR

Valery I. Telichenko,
Full Member of RAACS, Professor, Dr.Sc.,
The First Vice-President of the Russian Academy
of Architecture and Construction Sciences;
Honorary President of National Research
Moscow State University of Civil Engineering;
24, Ulitsa Bolshaya Dmitrovka, 107031, Moscow, Russia

EDITOR-IN-CHIEF

Vladimir N. Sidorov,
Corresponding Member of RAACS, Professor, Dr.Sc.,
Russian University of Transport (RUT – MIIT);
Russian University of Friendship of Peoples;
Moscow Institute of Architecture (State Academy);
Perm National Research Polytechnic University;
Kielce University of Technology (Poland);
9b9, Obrazcova Street, Moscow, 127994, Russia

MANAGING EDITOR

Nadezhda S. Nikitina,
Professor, Ph.D.,
Director of ASV Publishing House;
National Research Moscow State University
of Civil Engineering;
26, Yaroslavskoe Shosse, 129337, Moscow, Russia

ASSOCIATE EDITORS

Pavel A. Akimov,
Full Member of RAACS, Professor, Dr.Sc.,
Acting Rector of National Research
Moscow State University of Civil Engineering;
Tomsk State University of Architecture and Building;
Russian University of Friendship of Peoples;
26, Yaroslavskoe Shosse, 129337, Moscow, Russia

Alexander M. Belostotsky,
Corresponding Member of RAACS, Professor, Dr.Sc.,
Research & Development Center “STADYO”;
Russian University of Transport (RUT – MIIT);
Russian University of Friendship of Peoples;
Perm National Research Polytechnic University;
Tomsk State University of Architecture and Building;
Irkutsk National Research Technical University;
8th Floor, 18, ul. Tretya Yamskogo Polya,
125040, Moscow, Russia

Vladimir Belsky, Ph.D.,
Dassault Systèmes Simulia;
1301 Atwood Ave Suite 101W
02919 Johnston, RI, United States

Mikhail Belyi, Professor, Dr.Sc.,
Dassault Systèmes Simulia;
1301 Atwood Ave Suite 101W
02919 Johnston, RI, United States

Vitaly Bulgakov, Professor, Dr.Sc.,
Micro Focus;
Newbury, United Kingdom

Nikolai P. Osmolovskii, Professor, Dr.Sc.,
Systems Research Institute, Polish Academy of
Sciences; Kazimierz Pulaski University
of Technology and Humanities in Radom;
29, ul. Malczewskiego, 26-600, Radom, Poland

Gregory P. Panasenکو, Professor, Dr.Sc.,
Equipe d'Analyse Numerique; NMR CNRS 5585
University Gean Mehnet;
23 rue. P.Michelon 42023, St.Etienne, France

Leonid A. Rozin, Professor, Dr.Sc.,
Peter the Great Saint-Petersburg
Polytechnic University;
29, Ul. Politechnicheskaya,
195251 Saint-Petersburg, Russia

Scientific coordination is carried out by the Russian Academy of Architecture and Construction Sciences (RAACS)

PUBLISHER

ASV Publishing House
(ООО «Издательство ACB»)
19/1,12, Yaroslavskoe Shosse, 120338, Moscow, Russia
Tel. +7(925)084-74-24; E-mail: iasv@iasv.ru; Интернет-сайт: <http://iasv.ru/>

ADVISORY EDITORIAL BOARD

Robert M. Aloyan,
Corresponding Member
of RAACS, Professor, Dr.Sc.,
Russian Academy of Architecture
and Construction Sciences;
24, Ul. Bolshaya Dmitrovka,
107031, Moscow, Russia

Vladimir I. Andreev,
Full Member of RAACS,
Professor, Dr.Sc.,
National Research Moscow State
University of Civil Engineering;
Yaroslavskoe Shosse 26,
Moscow, 129337, Russia

Mojtaba Aslami, Ph.D,
Fasa University; Daneshjou blvd,
Fasa, Fars Province, Iran

Klaus-Jurgen Bathe, Professor
Massachusetts Institute
of Technology;
Cambridge, MA 02139, USA

Yuri M. Bazhenov,
Full Member of RAACS,
Professor, Dr.Sc.,
National Research Moscow State
University of Civil Engineering;
Yaroslavskoe Shosse 26,
Moscow, 129337, Russia

Alexander T. Bekker,
Corresponding Member
of RAACS, Professor, Dr.Sc.,
Far Eastern Federal University;
Russian Academy of Architecture
and Construction Sciences;
8, Sukhanova Street, Vladivostok,
690950, Russia

Tomas Bock, Professor, Dr.-Ing.,
Technical University of Munich,
Arcisstrasse 21, D-80333
Munich, Germany

Jan Buynak, Professor, Ph.D.,
University of Žilina;
1, Univerzitná, Žilina, 010 26,
Slovakia

Evgeniy M. Chernishov,
Full Member of RAACS,
Professor, Dr.Sc.,
Voronezh State Technical
University; 14, Moscow Avenue,
Voronezh, 394026, Russia

Vladimir T. Erofeev,
Full Member of RAACS,
Professor, Dr.Sc.,
Ogarev Mordovia State
University; 68, Bolshhevistskaya
Str., Saransk 430005, Republic of
Mordovia, Russia

Victor S. Fedorov,
Full Member of RAACS,
Professor, Dr.Sc.,
Russian University of Transport
(RUT – MIIT);
9b9 Obrazcova Street, Moscow,
127994, Russia

Sergey V. Fedosov,
Full Member of RAACS,
Professor, Dr.Sc.,
Russian Academy of Architecture
and Construction Sciences;
24, Ul. Bolshaya Dmitrovka,
107031, Moscow, Russia

Sergiy Yu. Fialko,
Professor, Dr.Sc.,
Cracow University of
Technology;
24, Warszawska Street, Kraków,
31-155, Poland

Vladimir G. Gagarin,
Corresponding Member
of RAACS, Professor, Dr.Sc.,
Research Institute of Building
Physics of Russian Academy
of Architecture and Construction
Sciences;
21, Lokomotivny Proezd,
Moscow, 127238, Russia

Alexander S. Gorodetsky,
Foreign Member of RAACS,
Professor, Dr.Sc.,
LIRA SAPR Ltd.;
7a Kiyanovsky Side Street
(Pereulok), Kiev, 04053, Ukraine

Vyatcheslav A. Ilyichev,
Full Member of RAACS,
Professor, Dr.Sc.,
Russian Academy of Architecture
and Construction Sciences;
Podzemproekt Ltd.;
24, Ulitsa Bolshaya Dmitrovka,
Moscow, 107031, Russia

Marek Iwański,
Professor, Dr.Sc.,
Kielce University of Technology;
7, al. Tysiąclecia Państwa
Polskiego Kielce, 25 – 314,
Poland

Sergey Yu. Kalashnikov,
Advisor of RAACS,
Professor, Dr.Sc.,
Volograd State Technical
University; 28, Lenin avenue,
Volograd, 400005, Russia

Semen S. Kaprielov,
Corresponding Member
of RAACS, Professor, Dr.Sc.,
Research Center of Construction;
6, 2nd Institutsкая St., Moscow,
109428, Russia

Nikolay I. Karpenko,
Full Member of RAACS,
Professor, Dr.Sc.,
Research Institute of Building
Physics of Russian Academy
of Architecture and Construction
Sciences; Russian Academy of
Architecture and Construction
Sciences; 21, Lokomotivny
Proezd, Moscow, 127238, Russia

Vladimir V. Karpov,
Professor, Dr.Sc.,
Saint Petersburg State University
of Architecture and Civil
Engineering;
4, 2-nd Krasnoarmeiskaya Steet,
Saint Petersburg, 190005, Russia

Galina G. Kashevarova,
Corresponding Member
of RAACS, Professor, Dr.Sc.,
Perm National Research
Polytechnic University;
29 Komsomolsky pros., Perm,
Perm Krai, 614990, Russia

John T. Katsikadelis,
Professor, Dr.Eng, PhD, Dr.h.c.,
National Technical University of
Athens; Zografou Campus
9, Iroon Polytechniou str
15780 Zografou, Greece

Vitaly I. Kolchunov,
Full Member of RAACS,
Professor, Dr.Sc.,
Southwest State University;
Russian Academy of Architecture
and Construction Sciences;
94, 50 let Oktyabrya, Kursk,
305040, Russia

Markus König, Professor
Ruhr-Universität Bochum;
150, Universitätsstraße, Bochum,
44801, Germany

Sergey B. Kositsin,
Advisor of RAACS,
Professor, Dr.Sc.,
Russian University of Transport
(RUT – MIIT); 9b9 Obrazcova
Street, Moscow, 127994, Russia

Sergey B. Krylov,
Corresponding Member
of RAACS, Professor, Dr.Sc.,
Research Center of Construction;
6, 2nd Institutskaya St., Moscow,
109428, Russia

Sergey V. Kuznetsov,
Professor, Dr.Sc.,
Ishlinsky Institute for Problems
in Mechanics of the Russian
Academy of Sciences;
101-1, Prosp. Vernadskogo,
Moscow, 119526, Russia

Vladimir V. Lalin,
Professor, Dr.Sc.,
Peter the Great Saint-Petersburg
Polytechnic University;
29, Ul. Politechnicheskaya,
Saint-Petersburg, 195251, Russia

Leonid S. Lyakhovich,
Full Member of RAACS,
Professor, Dr.Sc.,
Tomsk State University
of Architecture and Building;
2, Solyanaya Sq., Tomsk,
634003, Russia

Rashid A. Mangushev,
Corresponding Member
of RAACS, Professor, Dr.Sc.,
Saint Petersburg State University
of Architecture and Civil
Engineering;
4, 2-nd Krasnoarmeiskaya Steet,
Saint Petersburg, 190005, Russia

Ilizar T. Mirsayapov,
Advisor of RAACS,
Professor, Dr.Sc., Kazan State
University of Architecture and
Engineering; 1, Zelenaya Street,
Kazan, 420043, Republic
of Tatarstan, Russia

Vladimir L. Mondrus,
Corresponding Member
of RAACS, Professor, Dr.Sc.,
National Research Moscow State
University of Civil Engineering;
Yaroslavskoe Shosse 26,
Moscow, 129337, Russia

Valery I. Morozov,
Corresponding Member
of RAACS, Professor, Dr.Sc.,
Saint Petersburg State University
of Architecture and Civil
Engineering;
4, 2-nd Krasnoarmeiskaya Steet,
Saint Petersburg, 190005, Russia

Anatoly V. Perelmuter,
Foreign Member of RAACS,
Professor, Dr.Sc., SCAD Soft;
Office 1,2, 3a Osvity street,
Kiev, 03037, Ukraine

Alexey N. Petrov,
Advisor of RAACS, Professor,
Dr.Sc., Petrozavodsk State
University; 33, Lenina Prospekt,
Petrozavodsk, 185910,
Republic of Karelia, Russia

Vladilen V. Petrov,
Full Member of RAACS,
Professor, Dr.Sc.,
Yuri Gagarin State Technical
University of Saratov;
77 Politechnicheskaya Street,
Saratov, 410054, Russia

Jerzy Z. Piotrowski,
Professor, Dr.Sc.,
Kielce University of Technology;
al. Tysiąclecia Państwa Polskiego
7, Kielce, 25 – 314, Poland

Chengzhi Qi, Professor, Dr.Sc.,
Beijing University of Civil
Engineering and Architecture;
1, Zhanlanlu, Xicheng District,
Beijing, China

Vladimir P. Selyaev,
Full Member of RAACS,
Professor, Dr.Sc., Ogarev
Mordovia State University;
68, Bolshevistskaya Str., Saransk
430005, Republic of Mordovia,
Russia

Eun Chul Shin,
Professor, Ph.D.,
Incheon National University;
(Songdo-dong)119 Academy-ro,
Yeonsu-gu, Incheon, Korea

D.V. Singh,
Professor, Ph.D.,
University of Roorkee;
Roorkee, India, 247667

Wacław Szczęśniak,
Foreign Member of RAACS,
Professor, Dr.Sc.,
Lublin University of Technology;
Ul. Nadbystrzycka 40,
20-618 Lublin, Poland

Tadatsugu Tanaka,
Professor, Dr.Sc.,
Tokyo University; 7-3-1 Hongo,
Bunkyo, Tokyo, 113-8654, Japan

Josef Vican,
Professor, Ph.D.,
University of Žilina;
1, Univerzitná, Žilina, 010 26,
Slovakia

Zbigniew Wojcicki,
Professor, Dr.Sc.,
Wrocław University
of Technology;
11 Grunwaldzki Sq., 50-377,
Wrocław, Poland

Artur Zbiciak, Ph.D.,
Warsaw University of
Technology;
Pl. Politechniki 1, 00-661
Warsaw, Poland

Segrey I. Zhavoronok, Ph.D.,
Institute of Applied Mechanics of
Russian Academy of Sciences;
Moscow Aviation Institute
(National Research University);
7, Leningradsky Prt.,
Moscow, 125040, Russia

Askar Zhussupbekov,
Professor, Dr.Sc.,
Eurasian National University;
5, Munaitpassov street, Astana,
010000, Kazakhstan

TECHNICAL EDITOR

Taymuraz B. Kaytukov,
Advisor of RAACS,
Associate Professor, Ph.D.,
Vice-Rector of National Research
Moscow State University
of Civil Engineering;
Yaroslavskoe Shosse 26,
Moscow, 129337, Russia

EDITORIAL TEAM

Vadim K. Akhmetov, Professor, Dr.Sc., National Research Moscow State University of Civil Engineering; 26, Yaroslavskoe Shosse, 129337 Moscow, Russia

Pavel A. Akimov, Full Member of RAACS, Professor, Dr.Sc., Acting Rector of National Research Moscow State University of Civil Engineering; Tomsk State University of Architecture and Building; Russian University of Friendship of Peoples; 26, Yaroslavskoe Shosse, 129337, Moscow, Russia

Alexander M. Belostotsky, Corresponding Member of RAACS, Professor, Dr.Sc., Research & Development Center "STADYO"; Russian University of Transport (RUT – MIIT); Russian University of Friendship of Peoples; Perm National Research Polytechnic University; Tomsk State University of Architecture and Building; Irkutsk National Research Technical University; 8th Floor, 18, ul. Tretya Yamskogo Polya, 125040, Moscow, Russia

Vladimir Belsky, Ph.D., Dassault Systèmes Simulia; 1301 Atwood Ave Suite 101W 02919 Johnston, RI, United States

Mikhail Belyi, Professor, Dr.Sc., Dassault Systèmes Simulia; 1301 Atwood Ave Suite 101W 02919 Johnston, RI, United States

Vitaly Bulgakov, Professor, Dr.Sc., Micro Focus; Newbury, United Kingdom

Charles El Nouty, Professor, Dr.Sc., LAGA Paris-13 Sorbonne Paris Cite; 99 avenue J.B. Clément, 93430 Villetaneuse, France

Natalya N. Fedorova, Professor, Dr.Sc., Novosibirsk State University of Architecture and Civil Engineering (SIBSTRIN); 113 Leningradskaya Street, Novosibirsk, 630008, Russia

Darya Filatova, Professor, Dr.Sc., Probability, Assessment,

Reasoning and Inference Studies Research Group, EPHE Laboratoire CHART (PARIS) 4-14, rue Ferrus, 75014 Paris

Vladimir Ya. Gecha, Professor, Dr.Sc., Research and Production Enterprise All-Russia Scientific-Research Institute of Electromechanics with Plant Named after A.G. Iosiphyan; 30, Volnaya Street, Moscow, 105187, Russia

Taymuraz B. Kaytukov, Advisor of RAACS, Associate Professor, Ph.D, Vice-Rector of National Research Moscow State University of Civil Engineering; 26, Yaroslavskoe Shosse, 129337, Moscow, Russia

Amirlan A. Kusainov, Foreign Member of RAACS, Professor, Dr.Sc., Kazakh Leading Architectural and Civil Engineering Academy; Kazakh-American University, 9, Toraighyrov Str., Almaty, 050043, Republic of Kazakhstan

Marina L. Mozgaleva, Professor, Dr.Sc., National Research Moscow State University of Civil Engineering; 26, Yaroslavskoe Shosse, 129337 Moscow, Russia

Nadezhda S. Nikitina, Professor, Ph.D., Director of ASV Publishing House; National Research Moscow State University of Civil Engineering; 26, Yaroslavskoe Shosse, 129337 Moscow, Russia

Nikolai P. Osmolovskii, Professor, Dr.Sc., Systems Research Institute Polish Academy of Sciences; Kazimierz Pulaski University of Technology and Humanities in Radom; 29, ul. Malczewskiego, 26-600, Radom, Poland

Gregory P. Panasenkov, Professor, Dr.Sc., Equipe d'Analyse Numerique NMR CNRS 5585 University Gean Mehnet; 23 rue. P.Michelon 42023, St.Etienne, France

Andreas Rauh, PD Dr.-Ing. habil. Chair of Mechatronics

University of Rostock Justus-von-Liebig-Weg 6 D-18059 Rostock, Germany

Leonid A. Rozin, Professor, Dr.Sc., Peter the Great Saint-Petersburg Polytechnic University; 29, Ul. Politechnicheskaya, 195251 Saint-Petersburg, Russia

Zhan Shi, Professor LPSM, Université Paris VI 4 place Jussieu, F-75252 Paris Cedex 05, France

Marina V. Shitikova, Advisor of RAACS, Professor, Dr.Sc., Voronezh State Technical University; 14, Moscow Avenue, Voronezh, 394026, Russia

Igor L. Shubin, Corresponding Member of RAACS, Professor, Dr.Sc., Research Institute of Building Physics of Russian Academy of Architecture and Construction Sciences; 21, Lokomotivny Proezd, Moscow, 127238, Russia

Vladimir N. Sidorov, Corresponding Member of RAACS, Professor, Dr.Sc., Russian University of Transport (RUT – MIIT); Russian University of Friendship of Peoples; Moscow Institute of Architecture (State Academy); Perm National Research Polytechnic University; Kielce University of Technology (Poland); 9b9 Obrzeczowa Street, Moscow, 127994, Russia

Valery I. Telichenko, Full Member of RAACS, Professor, Dr.Sc., The First Vice-President of the Russian Academy of Architecture and Construction Sciences; National Research Moscow State University of Civil Engineering; 24, Ulitsa Bolshaya Dmitrovka, 107031, Moscow, Russia

Vladimir I. Travush, Full Member of RAACS, Professor, Dr.Sc., Vice-President of the Russian Academy of Architecture and Construction Sciences; Urban Planning Institute of Residential and Public Buildings; 24, Ulitsa Bolshaya Dmitrovka, 107031, Moscow, Russia

INVITED REVIEWERS

Akimbek A. Abdikalikov, Professor, Dr.Sc.,
Kyrgyz State University of Construction, Transport and Architecture n.a. N. Isanov;
34 Malydybayeva Str., Bishkek, 720020, Biskek, Kyrgyzstan

Vladimir N. Alekhin, Advisor of RAACS, Professor, Dr.Sc.,
Ural Federal University named after the first President of Russia B.N. Yeltsin;
19 Mira Street, Ekaterinburg, 620002, Russia

Irina N. Afanasyeva, Ph.D.,
University of Florida; Gainesville, FL 32611, USA

Ján Čelko, Professor, PhD, Ing.,
University of Žilina; Univerzitná 1, 010 26, Žilina, Slovakia

Tatyana L. Dmitrieva, Professor, Dr.Sc.,
Irkutsk National Research Technical University; 83, Lermontov street, Irkutsk, 664074, Russia

Petr P. Gaidzhurov, Advisor of RAACS, Professor, Dr.Sc.,
Don State Technical University; 1, Gagarina Square, Rostov-on-Don, 344000, Russia

Jacek Grosel, Associate Professor, Dr inz.
Wroclaw University of Technology; 11 Grunwaldzki Sq., 50-377, Wrocław, Poland

Stanislaw Jemioło, Professor, Dr.Sc.,
Warsaw University of Technology; 1, Pl. Politechniki, 00-661, Warsaw, Poland

Konstantin I. Khenokh, M.Ing., M.Sc.,
General Dynamics C4 Systems; 8201 E McDowell Rd, Scottsdale, AZ 85257, USA

Christian Koch, Dr.-Ing.,
Ruhr-Universität Bochum;
Lehrstuhl für Informatik im Bauwesen, Gebäude IA, 44780, Bochum, Germany

Gaik A. Manuylov, Professor, Ph.D.,
Moscow State University of Railway Engineering; 9, Obratsova Street, Moscow, 127994, Russia

Alexander S. Noskov, Professor, Dr.Sc.,
Ural Federal University named after the first President of Russia B.N. Yeltsin;
19 Mira Street, Ekaterinburg, 620002, Russia

Grzegorz Świt, Professor, Dr.hab. Inż.,
Kielce University of Technology; 7, al. Tysiąclecia Państwa Polskiego, Kielce, 25 – 314, Poland

AIMS AND SCOPE

The aim of the Journal is to advance the research and practice in structural engineering through the application of computational methods. The Journal will publish original papers and educational articles of general value to the field that will bridge the gap between high-performance construction materials, large-scale engineering systems and advanced methods of analysis.

The scope of the Journal includes papers on computer methods in the areas of structural engineering, civil engineering materials and problems concerned with multiple physical processes interacting at multiple spatial and temporal scales. The Journal is intended to be of interest and use to researches and practitioners in academic, governmental and industrial communities.

ОБЩАЯ ИНФОРМАЦИЯ О ЖУРНАЛЕ

International Journal for Computational Civil and Structural Engineering
(Международный журнал по расчету гражданских и строительных конструкций)

Международный научный журнал “*International Journal for Computational Civil and Structural Engineering* (Международный журнал по расчету гражданских и строительных конструкций)” (IJCCSE) является ведущим научным периодическим изданием по направлению «Инженерные и технические науки», издаваемым, начиная с 1999 года (ISSN 2588-0195 (Online); ISSN 2587-9618 (Print) Continues ISSN 1524-5845). В журнале на высоком научно-техническом уровне рассматриваются проблемы численного и компьютерного моделирования в строительстве, актуальные вопросы разработки, исследования, развития, верификации, апробации и приложений численных, численно-аналитических методов, программно-алгоритмического обеспечения и выполнения автоматизированного проектирования, мониторинга и комплексного наукоемкого расчетно-теоретического и экспериментального обоснования напряженно-деформированного (и иного) состояния, прочности, устойчивости, надежности и безопасности ответственных объектов гражданского и промышленного строительства, энергетики, машиностроения, транспорта, биотехнологий и других высокотехнологичных отраслей.

В редакционный совет журнала входят известные российские и зарубежные деятели науки и техники (в том числе академики, члены-корреспонденты, иностранные члены, почетные члены и советники Российской академии архитектуры и строительных наук). Основным критерием отбора статей для публикации в журнале – их высокий научный уровень, соответствие которому определяется в ходе высококвалифицированного рецензирования и объективной экспертизы, поступающих в редакцию материалов.

Журнал входит в Перечень ВАК РФ ведущих рецензируемых научных изданий, в которых должны быть опубликованы основные научные результаты диссертаций на соискание ученой степени кандидата наук, на соискание ученой степени доктора наук по научным специальностям и соответствующим им отраслям науки:

- 01.02.04 – Механика деформируемого твердого тела (технические науки),
- 05.13.18 – Математическое моделирование численные методы и комплексы программ (технические науки),
- 05.23.01 – Строительные конструкции, здания и сооружения (технические науки),
- 05.23.02 – Основания и фундаменты, подземные сооружения (технические науки),
- 05.23.05 – Строительные материалы и изделия (технические науки),
- 05.23.07 – Гидротехническое строительство (технические науки),
- 05.23.17 – Строительная механика (технические науки).

В Российской Федерации журнал индексируется Российским индексом научного цитирования (РИНЦ).

Журнал входит в базу данных Russian Science Citation Index (RSCI), полностью интегрированную с платформой Web of Science. Журнал имеет международный статус и высылается в ведущие библиотеки и научные организации мира.

Издатели журнала – Издательство Ассоциации строительных высших учебных заведений /АСВ/ (Россия, г. Москва) и до 2017 года Издательский дом Begell House Inc. (США, г. Нью-Йорк). Официальными партнерами издания является Российская академия архитектуры и строительных наук (РААСН), осуществляющая научное курирование издания, и Научно-исследовательский центр СтаДиО (ЗАО НИЦ СтаДиО).

Цели журнала – демонстрировать в публикациях российскому и международному профессиональному сообществу новейшие достижения науки в области вычислительных ме-

тодов решения фундаментальных и прикладных технических задач, прежде всего в области строительства.

Задачи журнала:

- предоставление российским и зарубежным ученым и специалистам возможности публиковать результаты своих исследований;
- привлечение внимания к наиболее актуальным, перспективным, прорывным и интересным направлениям развития и приложений численных и численно-аналитических методов решения фундаментальных и прикладных технических задач, совершенствования технологий математического, компьютерного моделирования, разработки и верификации реализующего программно-алгоритмического обеспечения;
- обеспечение обмена мнениями между исследователями из разных регионов и государств.

Тематика журнала. К рассмотрению и публикации в журнале принимаются аналитические материалы, научные статьи, обзоры, рецензии и отзывы на научные публикации по фундаментальным и прикладным вопросам технических наук, прежде всего в области строительства. В журнале также публикуются информационные материалы, освещающие научные мероприятия и передовые достижения Российской академии архитектуры и строительных наук, научно-образовательных и проектно-конструкторских организаций.

Тематика статей, принимаемых к публикации в журнале, соответствует его названию и охватывает направления научных исследований в области разработки, исследования и приложений численных и численно-аналитических методов, программного обеспечения, технологий компьютерного моделирования в решении прикладных задач в области строительства, а также соответствующие профильные специальности, представленные в диссертационных советах профильных образовательных организациях высшего образования.

Редакционная политика. Политика редакционной коллегии журнала базируется на современных юридических требованиях в отношении авторского права, законности, плагиата и клеветы, изложенных в законодательстве Российской Федерации, и этических принципах, поддерживаемых сообществом ведущих издателей научной периодики.

За публикацию статей плата с авторов не взимается. Публикация статей в журнале бесплатная. На платной основе в журнале могут быть опубликованы материалы рекламного характера, имеющие прямое отношение к тематике журнала.

Журнал предоставляет непосредственный открытый доступ к своему контенту, исходя из следующего принципа: свободный открытый доступ к результатам исследований способствует увеличению глобального обмена знаниями.

Индексирование. Публикации в журнале входят в системы расчетов индексов цитирования авторов и журналов. «Индекс цитирования» — числовой показатель, характеризующий значимость данной статьи и вычисляющийся на основе последующих публикаций, ссылающихся на данную работу.

Авторам. Прежде чем направить статью в редакцию журнала, авторам следует ознакомиться со всеми материалами, размещенными в разделах сайта журнала (интернет-сайт Российской академии архитектуры и строительных наук (<http://raasn.ru>); подраздел «Издания РААСН» или интернет-сайт Издательства АСВ (<http://iasv.ru>); подраздел «Журнал IJCCSE»): с основной информацией о журнале, его целях и задачами, составом редакционной коллегии и редакционного совета, редакционной политикой, порядком рецензирования направляемых в журнал статей, сведениями о соблюдении редакционной этики, о политике авторского права и лицензирования, о представлении журнала в информационных системах (индексировании), информацией о подписке на журнал, контактными данными и пр. Журнал рабо-

тает по лицензии Creative Commons типа cc by-nc-sa (Attribution Non-Commercial Share Alike) – Лицензия «С указанием авторства – Некоммерческая – Копилефт».

Рецензирование. Все научные статьи, поступившие в редакцию журнала, проходят обязательное двойное слепое рецензирование (рецензент не знает авторов рукописи, авторы рукописи не знают рецензентов).

Заемствования и плагиат. Редакционная коллегия журнала при рассмотрении статьи проводит проверку материала с помощью системы «Антиплагиат». В случае обнаружения многочисленных заимствований редакция действует в соответствии с правилами COPE.

Подписка. Журнал зарегистрирован в Федеральном агентстве по средствам массовой информации и охраны культурного наследия Российской Федерации. Индекс в общероссийском каталоге РОСПЕЧАТЬ – 18076.

По вопросам подписки на международный научный журнал “International Journal for Computational Civil and Structural Engineering (Международный журнал по расчету гражданских и строительных конструкций)” обращайтесь в Агентство «Роспечать» (Официальный сайт в сети Интернет: <http://www.rospechat.ru/>) или в издательство Ассоциации строительных вузов (АСВ) в соответствии со следующими контактными данными:

ООО «Издательство АСВ»

Юридический адрес: 129337, Россия, г. Москва, Ярославское ш., д. 26, офис 705;

Фактический адрес: 129337, Россия, г. Москва, Ярославское ш., д. 19, корп. 1, 5 этаж, офис 12 (ТЦ Соле Молл);

Телефоны: +7 (925) 084-74-24, +7 (926) 010-91-33;

Интернет-сайт: www.iasv.ru. Адрес электронной почты: iasv@iasv.ru.

Контактная информация. По всем вопросам работы редакции, рецензирования, согласования правки текстов и публикации статей следует обращаться к главному редактору журнала члену-корреспонденту РААСН Сидорову Владимиру Николаевичу (адреса электронной почты: sidorov.vladimir@gmail.com, sidorov@iasv.ru, iasv@iasv.ru, sidorov@raasn.ru) или к техническому редактору журнала советнику РААСН Кайтукову Таймуразу Батразовичу (адреса электронной почты: tkaytukov@gmail.com; kaytukov@raasn.ru). Кроме того, по указанным вопросам, а также по вопросам размещения в журнале рекламных материалов можно обращаться к генеральному директору ООО «Издательство АСВ» Никитиной Надежде Сергеевне (адреса электронной почты: iasv@iasv.ru, nsnikitina@mail.ru, ijccse@iasv.ru).

Журнал становится технологичнее. Издательство АСВ с сентября 2016 года является членом Международной ассоциации издателей научной литературы (Publishers International Linking Association (PILA)), осуществляющей свою деятельность на платформе CrossRef. Оригинальным статьям, публикуемым в журнале, будут присваиваться уникальные номера (индексы DOI – Digital Object Identifier), что значительно облегчит поиск метаданных и местонахождение полнотекстового произведения. DOI – это система определения научного контента в сети Интернет.

С октября 2016 года стал возможен прием статей на рассмотрение и рецензирование через онлайн систему приема статей Open Journal Systems на сайте журнала (электронная редакция): <http://ijccse.iasv.ru/index.php/IJCCSE>.

Автор имеет возможность следить за продвижением статьи в редакции журнала в личном кабинете Open Journal Systems и получать соответствующие уведомления по электронной почте.

В феврале 2018 года журнал был зарегистрирован в Directory of open access journals (DOAJ) (это один из самых известных поисковых сервисов в мире, который предоставляет открытый доступ к материалам и индексирует не только заголовки журналов, но и научные статьи), в сентябре 2018 года включен в продукты EBSCO Publishing.

International Journal for
Computational Civil and Structural Engineering

(Международный журнал по расчету гражданских и строительных конструкций)

Volume 16, Issue 1

2020

Scientific coordination is carried out by the Russian Academy of Architecture and Construction Sciences (RAACS)

CONTENTS

Efficiency Evaluation of Apartment Houses Reconstruction with Optimizational Criteria Application	<u>14</u>
<i>Alexander N. Biryukov, Igor N. Kravchenko, Evgeny O. Dobryshkin, Yuri A. Biryukov, Valery I. Kondrashchenko</i>	
Intergal Parameters of Concrete Diagrams for Calculations of Strength of Reinforced Concrete Elements Using the Deformation Model	<u>25</u>
<i>Vladimir A. Eryshev, Nickolay I. Karpenko, Artur O. Zhemchuyev</i>	
Study of Stress-Strain States of a Regular Hinge-Rod Constructions with Kinematically Oriented Shape Change	<u>38</u>
<i>Peter P. Gaydzhurov, Elvira R. Iskhakova, Nadezhda G Tsaritova</i>	
Finite Elements of the Plane Problem of the Theory of Elasticity with Drilling Degrees of Freedom	<u>48</u>
<i>Viktor S. Karpilovskiy</i>	
To Assess the Horizontal Displacement of Piles Caused by Excavation of the Soil of the Pit	<u>73</u>
<i>D.S. Kolesnik, Rashid A. Mangushev</i>	
Using the Criterion of the Minimum Material Capacity of Rods Under Stability Restrictions for the Case of Multiple Critical Load	<u>86</u>
<i>Leonid S. Lyakhovich, Pavel A. Akimov, Anatoly P. Malinowski</i>	
A Probabilistic Approach to Evaluation of the Ultimate Load on Flexural RC Element on Crack Length	<u>98</u>
<i>Sergey A. Solov'yev</i>	
A.A. Ilyushin's Final Relation, Alternative Equivalent Relations and Versions of Its Approximation in Problems of Plastic Deformation of Plates and Shells Part 1: A.A. Ilyushin's Final Relation	<u>106</u>
<i>Aleksandr V. Starov, Sergei Yu. Kalashnikov</i>	

Bending of Ring Plates, Performed from an Orthotropic Nonlinear Differently Resistant Material	<u>130</u>
<i>Alexandr A. Treschev, Evgeniy A. Zhurin</i>	
Investigations of Historical Cities of Uzbekistan and Kazakhstan as Objects of the Silk Way	<u>147</u>
<i>A.Zh. Zhussupbekov, F.S. Temirova, A.A. Riskulov, A.R. Omarov</i>	
Optimization Problems of Mathematical Modelling of a Building as a Unified Heat and Power System	<u>156</u>
<i>Yuri A. Tabunshchikov, Marianna M. Brodach</i>	
To the Anniversary of Prof. Alexander Gorodetsky	<u>162</u>

International Journal for
Computational Civil and Structural Engineering

(Международный журнал по расчету гражданских и строительных конструкций)

Volume 16, Issue 1

2020

Scientific coordination is carried out by the Russian Academy of Architecture and Construction Sciences (RAACS)

СОДЕРЖАНИЕ

Оценка эффективности реконструкции жилых домов с применением оптимизационного критерия	<u>14</u>
<i>А.Н. Бирюков, И.Н. Кравченко, Е.О. Добрышкин, Ю.А. Бирюков, В.И. Кондращенко</i>	
Интегральные параметры диаграмм бетона в расчетах прочности железобетонных элементов по деформационной модели	<u>25</u>
<i>В.А. Ерышев, Н.И. Карпенко, А.О. Жемчужев</i>	
Исследование напряженно-деформированного состояния регулярной шарнирно-стержневой конструкции при кинематически ориентированном изменении формы	<u>38</u>
<i>П.П. Гайджуков, Э.Р. Исхакова, Н.Г. Царитова</i>	
Конечные элементы плоской задачи теории упругости с вращательными степенями свободы	<u>48</u>
<i>В.С. Карпиловский</i>	
К оценки горизонтального смещения свай вызванного экскавацией грунта котлована	<u>73</u>
<i>Д.С. Колесник, Р.А. Мангушев</i>	
Использование критерия минимальной материалоемкости стержней при ограничениях по устойчивости для случая кратной критической нагрузки	<u>86</u>
<i>Л.С. Ляхович, П.А. Акимов, А.П. Малиновский</i>	
Вероятностный подход к определению допустимой нагрузки на изгибаемый железобетонный элемент по критерию длины трещины	<u>98</u>
<i>С.А. Соловьев</i>	
Конечное соотношение А.А. Ильюшина, альтернативные эквивалентные зависимости и варианты его аппроксимации в задачах пластического деформирования пластин и оболочек.	
Часть 1: Конечное соотношение А.А. Ильюшина	<u>106</u>
<i>А.В. Старов, С.Ю. Калашиников</i>	

Изгиб кольцевых пластин, выполненных из ортотропного нелинейно разносопротивляющегося материала	<u>130</u>
<i>А.А. Трещев, Е.А. Журин</i>	
Исследования исторических городов Узбекистана и Казахстана как объектов Шелкового Пути	<u>147</u>
<i>А.Ж. Жусупбеков, Ф.С. Темирова, А.А. Рискулов, А.Р. Омаров</i>	
Оптимизационные задачи математического моделирования здания как единой теплоэнергетической системы	<u>156</u>
<i>Ю.А. Табунчиков, М.М. Бродач</i>	
Александр Сергеевич Городецкому – 85 лет	<u>162</u>

EFFICIENCY EVALUATION OF APARTMENT HOUSES RECONSTRUCTION WITH OPTIMIZATIONAL CRITERIA APPLICATION

*Alexander N. Biryukov¹, Igor N. Kravchenko², Evgeny O. Dobryshkin¹,
Yuri A. Biryukov¹, Valery I. Kondrashchenko³*

¹ Military Academy of Logistics named after Army General A.V. Khrulev, Saint-Petersburg, RUSSIA

² Russian State Agrarian University – Moscow Agricultural Academy named after K.A. Timiryazev,
Moscow, RUSSIA

³ Russian University of Transport, Moscow, RUSSIA

Abstract. The subject of the study, considered in the article, is the technical condition of the housing stock of the Russian Federation, which is a totality of objects with a characteristic variety of structural and space-planning decisions and increased values of physical wear. The objective of the study conducted by the authors was to develop an optimization criterion for assessing the effectiveness of restoration of housing facilities based on determining the ratio of one-time costs for restoration work and current projected costs for operation and maintenance of an apartment house. Since an important stage in reproduction of the housing stock is preparation of design estimates for reasonable implementation of capital investments by property owners and government support measures for restoration of buildings, the topic discussed in this article is relevant. The scientific novelty of the study conducted by the authors is to develop a method for assessing the effectiveness of overhaul (reconstruction, modernization) of buildings, where the criterion is the choice of innovative design solutions and building materials when planning the restoration of housing facilities.

Keywords: housing stock, housing facilities, restoration, overhaul, reconstruction, modernization, variant design

ОЦЕНКА ЭФФЕКТИВНОСТИ РЕКОНСТРУКЦИИ ЖИЛЫХ ДОМОВ С ПРИМЕНЕНИЕМ ОПТИМИЗАЦИОННОГО КРИТЕРИЯ

*А.Н. Бирюков¹, И.Н. Кравченко², Е.О. Добрышкин¹, Ю.А. Бирюков¹,
В.И. Кондращенко³*

¹ Военная академия логистики имени генерала армии А.В. Хрулева, г. Санкт-Петербург, РОССИЯ

² Российский государственный аграрный университет - Московская сельскохозяйственная академия
им. К.А. Тимирязева, г. Москва, РОССИЯ

³ Российский университет транспорта, г. Москва, РОССИЯ

Аннотация. Предметом исследования, рассматриваемого в статье, является техническое состояние жилого фонда Российской Федерации, представляющего собой совокупность объектов с характерным разнообразием конструктивных и планировочных решений и повышенными значениями физического износа. Целью исследования, проведенного авторами, была разработка оптимизационного критерия оценки эффективности восстановления объектов жилья на основе определения соотношения разовых затрат на восстановительные работы и текущих проектных затрат на эксплуатацию и содержание жилого дома. Поскольку важным этапом восстановления жилого фонда является подготовка проектно-сметной документации для обоснованного осуществления капитальных вложений собственниками и меры государственной поддержки для осуществления зданий, тема, обсуждаемая в этой статье, является актуальной. Научная новизна исследования, проведенного авторами, заключается в разработке метода оценки эффективности капитального ремонта (реконструкции, модернизации) зданий, где критерием является выбор инновационных проектных решений и строительных материалов при планировании восстановления объектов жилья.

Ключевые слова: жилищный фонд, объекты жилья, реставрация, капитальный ремонт, реконструкция, модернизация, вариантное проектирование

INTRODUCTION

Currently, the legislation of the Russian Federation defines housing stock as a totality of all residential premises located on the territory of the Russian Federation [1].

In the context of the reform of infrastructure sectors of the economy in the Russian Federation, one of the most important tasks is implementation of socio-economic transformations in the Russian Federation, and mainly in the housing and communal sector, since market and administrative approaches are particularly acute in this sector. Therefore, it is difficult to find a compromise between economic feasibility of restoring residential buildings, the ability of owners to provide proper control over implementation of work, as well as the ability of the state to provide financial support to owners in order to create a comfortable urban environment [2].

However, the growing degradation of the housing stock in the Russian Federation, the disordered legal relationships in it put society and the state in need of making drastic decisions and taking measures aimed at improving the current situation with the technical condition of residential buildings in the country. This problem becomes particularly urgent in the context of regular amendments to the Housing Code of the Russian Federation, within the framework of which the powers of participants are expanded when managing an apartment house, responsibility is transferred for their (apartment houses) maintenance to the owners of premises, and the role of state and municipal authorities is changing in the housing and communal services market.

Important is the fact that the housing stock of the Russian Federation is characterized by a historically developed variety of constructive and space-planning decisions (Table 1). The building of a significant number of cities on the territory of the Russian Federation has a long history and

is characterized by increased values of development of physical wear of building structures.

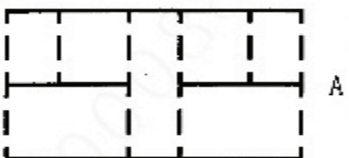
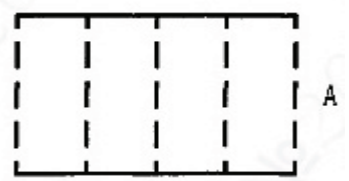


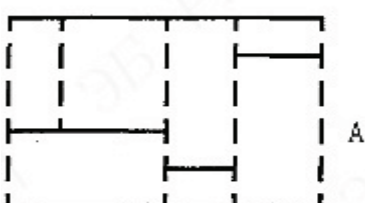
Thus, the housing stock of the Russian Federation totals about 3 billion square meters of total area, which makes up more than 30% of all reproducible property. At the present stage, deterioration of the housing stock of most Russian cities is about 70%. Residential buildings that have been in operation in disrepair for more than 25 years without restoration work represent about 300 million square meters [3]. Housing facilities subject to demolition due to an emergency technical condition make up about 90 million square meters (3,2% of the total housing area), where according to rough estimates about 5 million citizens of the Russian Federation live [3].

It will be advisable to consider in more detail the technical condition of residential buildings on the example of Leningrad region, since building of this constituent entity of the Russian Federation has been formed for more than 300 years of formation of the state in the European part of Russia and for 2017 consisted of 18,127 apartment houses. It is necessary to bring some clarity to the concept of “apartment house” (since these buildings are a structural component of the country’s housing stock) in accordance with the explanations of the Ministry of Economic Development of the Russian Federation, according to which any residential building with more than one apartment is an apartment house [4].

At the present stage, 42% of houses or 64% of the total area of apartment houses in Leningrad region were built in the period 1971-1995, and 2% of the total area of apartment houses are characterized by the presence of wooden walling (Figures 1, 2) [5].

The current legislation of Leningrad region provides for annual collection of data on the technical condition of apartment houses [6].

Table 1. Design schemes of residential buildings of old construction in Saint-Petersburg.

Design scheme type	Design scheme	Design scheme description	Main parameters, m		Repeatability, %
			A	B	
1	2	3	4	5	6
1		Double span with medium longitudinal bearing wall	10 – 18	12– 30	52
2		Multi-span with transverse bearing walls	4 – 16	12 –20	8
3		Single span with external load-bearing walls	4 –14	12 –22	13
4		Three-span with two longitudinal inner walls	12 –24	12 – 38	10
5		Mixed scheme	9 – 18	up to 25	17

The authors of the article analyzed the technical condition of 12 981 housing facilities. The results obtained by the authors allow us to conclude that

a significant number of buildings in emergency condition with increased values of physical wear are in operation:

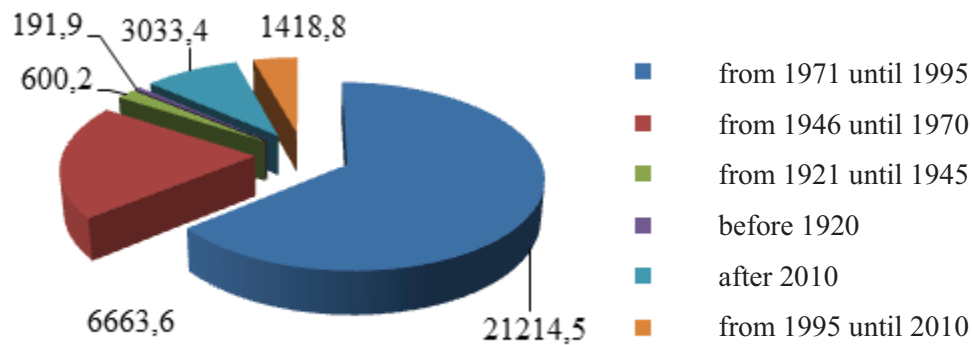


Figure 1. Analysis of the housing stock of Leningrad region by year of construction, m².

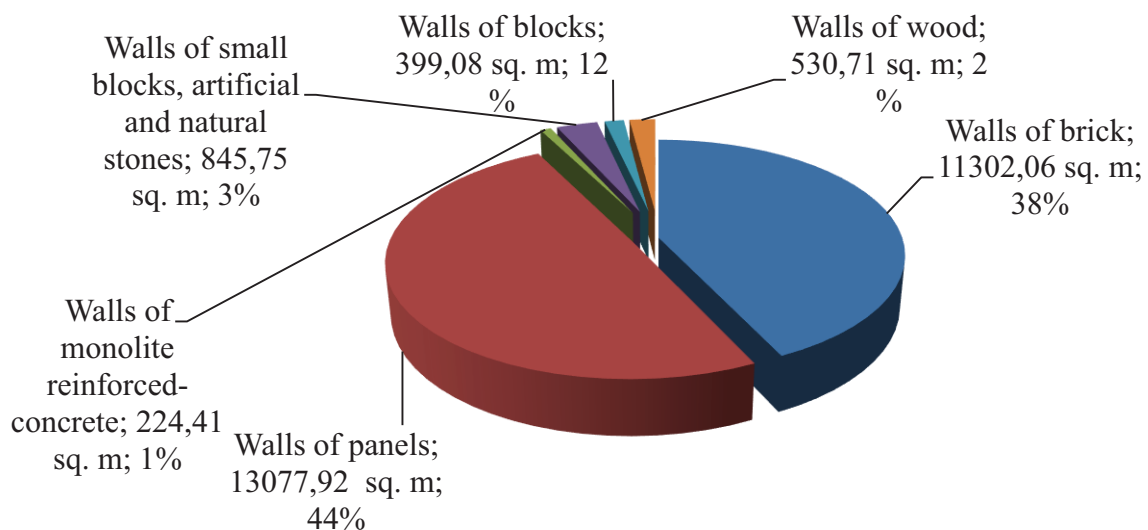


Figure 2. Classification of the housing stock of Leningrad region by the material of walls, m².

0-20 % – 1660 apartment houses with total area of 7626,2 thous. m²; 21-40 % – 3341 apartment houses 9603,5 thous. m²; 41-70 % – 3387 apartment houses 5417,6 thous. m²; over 70% – 988 apartment houses 1091,2 thous. m².

The largest number of apartment houses with a physical depreciation value of more than 70% are in Slantsevsky and Volkhovsky districts (38% and 20% of the total, respectively). The analysis of the technical condition of structural elements of 12981 apartment houses performed by the authors shows that 30% of foundations, 31% of roofing, 35% of facades require major repairs [6].

MATERIALS AND METHODS

In the course of the study, the authors determined that overhaul should be considered as one of the ways to preserve and update the housing stock along with current repair, reconstruction, modernization and new construction [7, 8, 9]. Moreover, in the absence of economic feasibility of repairs and reconstruction of buildings, preference should be given in favor of new construction. However, new construction often requires demolition of emergency apartment houses, which entails the need for resettlement of residents, while during overhaul or reconstruction, resettlement of owners is carried out only with comprehensive performance of

restoration work. It is advisable to organize reproduction of the housing stock by demolishing old facilities and new construction when the high level of physical wear of residential buildings does not allow the efficient use of capital investments of owners and state support funds for reconstruction work. In addition, demolition of old buildings, design, preparation of the territory and construction itself significantly increases commissioning time and cost of the future building [10, 11]. Thus, overhaul costs are 30-35%, modernization - 50-55%, reconstruction - 60-70% of the cost of 1 m² of the total area for new construction according to the Russian Academy of Architecture and Building Sciences [12]. Therefore, given the current state of the housing stock in the Russian Federation, the most appropriate is reproduction of housing through overhaul, reconstruction and modernization, implementation of these processes in the framework of this article, the authors accept as restoration work to eliminate physical wear of an apartment house.

One of the main stages of reconstruction of the housing stock by means of overhaul, reconstruction and modernization is preparation of design estimates for all design decisions on redevelopment, functional reassignment of premises, replacement of structures, engineering systems or their installation again, landscaping and other similar work. As part of the study, the authors used the analytical method and deduction, it was determined that a significant number of scientists whose scientific results were analyzed and summarized when writing the article were involved in the study of the issue of efficiency in implementation of investment construction projects (including reconstruction and overhaul projects [13, 14, 15]).

RESEARCH RESULTS AND DISCUSSION

In the framework of the study, the authors developed an approach to implementation of planning for restoration work based on variant design (Figure 3).

In accordance with the algorithm developed by the authors, preparation of projects for restoration of an apartment house should be preceded by a survey of the apartment house in order to determine the category of technical condition based on [16, 17].

The effectiveness of planning the reconstruction of the housing stock can be achieved by evaluating the restoration projects (overhaul, reconstruction or modernization) of the housing stock. It is advisable to accomplish this task by comparing variation of one-time and current costs when implementing a project for restoration of an apartment house on the basis of the following: increasing one-time costs of restoring a building to a certain level leads to a decrease in subsequent current costs for operation and maintenance (Figure 4) [11, 12]. So, overhaul of the facade of an apartment house can be carried out according to the standard option, i.e. sealing the external joints of a closely located urban area, repairing plaster and painting the facade, and an external insulation system using hinged ventilated facades can be used [18, 19].

The advantages of the latter option are reduction of heat losses, increase in the service life of load-bearing enclosing structures by eliminating condensation of water vapor in the load-bearing wall, possibility of reconstructing a house without resettling residents, and reducing the cost of repairing building envelopes, since the system in question plays the role of corrosion protection [20]. The key factor that determines the use of the system of ventilated facades is to increase durability and service life in relation to the standard overhaul period of operation of the facade in traditional stucco finishing.

In order to compare projects for restoration of an apartment house proposed for implementation, it is necessary to introduce a number of designations.

We will take K_i as one-time costs of restoration of a building in accordance with the i -th project for restoration of an apartment house.

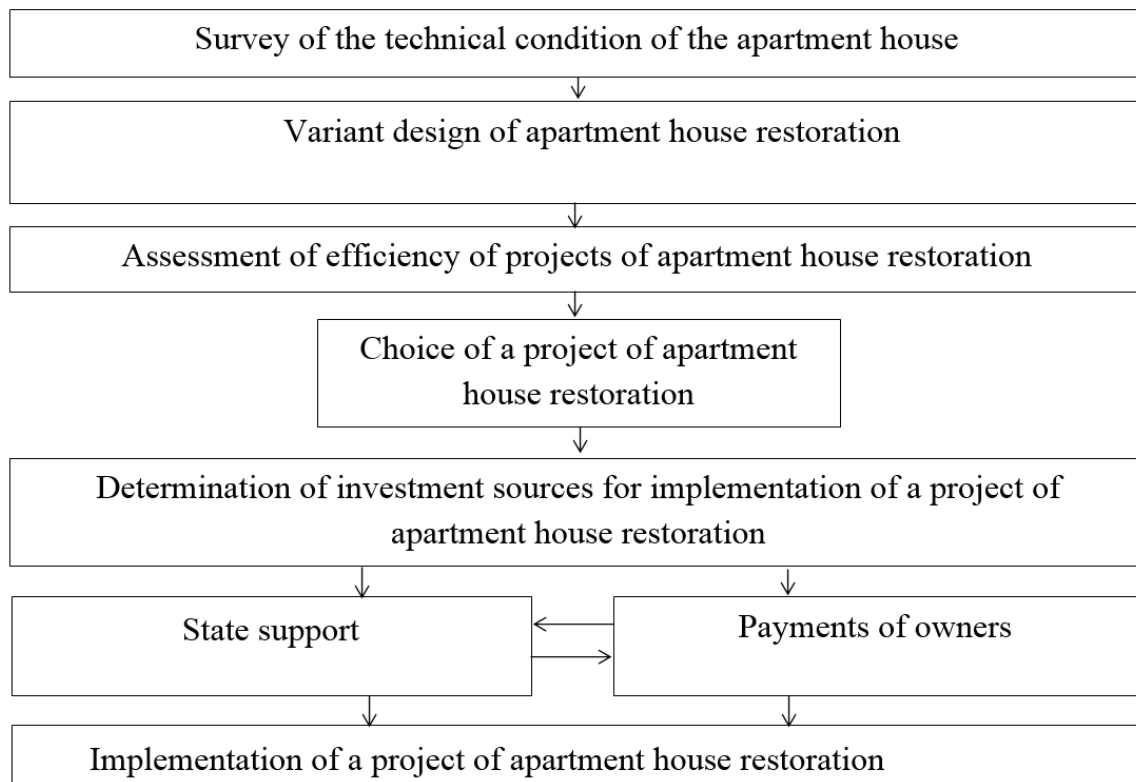


Figure 3. Algorithm of planning of restoration works based on variant design.

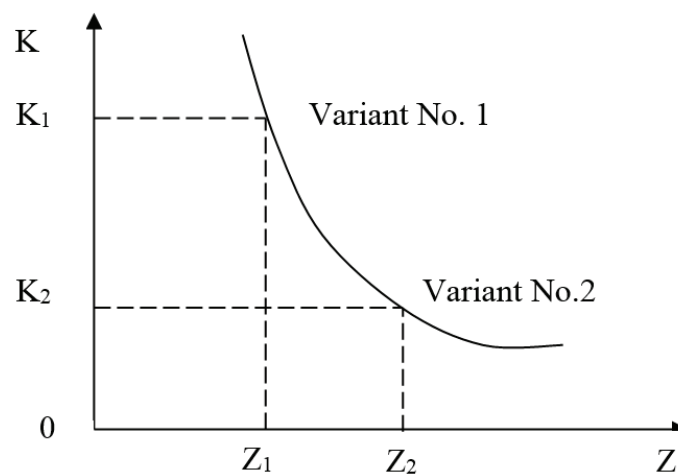


Figure 4. Graph of dependence between current and one-time costs (K – one-time costs, Z – current costs).

We will consider S_{vi} as operating costs for maintenance of an apartment house for the v -th year of operation ($v = 1, 2, 3, \dots, g$) during implementation of the i -th project of restoration of a house, and C_{vi} – costs of ongoing repairs, if necessary, for the v -year year of operation of the house during implementation of the i -th project. Then the effectiveness of the building restoration

project can be determined by the ratio of the sum of the costs of operation and maintenance to the number of one-time costs of the project:

$$P_i = \frac{K_i}{S_i + C_i} \quad (1)$$

At the same time, planning of current repairs and distribution of costs for operation of an apartment house are carried out for a certain period of time after restoration of the housing stock, which sets the task of taking into account annual inflation in assessing the effectiveness of restoration projects for an apartment house. Then the costs of the current repair and maintenance of the apartment house will be set in the form:

$$S_{vi} (1+p)^{v-l} \quad (2)$$

and

$$C_{vi} (1+p)^{v-l} \quad (3)$$

where p - inflation in fractions of a unit, taken for the v -th year of operation of the housing stock after its restoration.

Then the criterion for effectiveness of the projects under consideration for the accepted horizon of calculation (in years) should be determined by the following mathematical expression:

$$PI = \frac{K_i}{e_{v=1}^g (S_{vi}(1+p)^{v-1} + C_{vi}(1+p)^{v-1})} \quad (4)$$

Thus, the decision to restore apartment houses on the basis of variant design allows the selection of projects for restoration of housing facilities with the highest PI values. The next stage of work planning in accordance with the algorithm developed by the authors (Figure 3) is to determine the share of owners in implementation of the corresponding project and the amount of state support in restoration of an apartment house. The key point of the considered stage is selection of the contractor in accordance with the lowest price criterion [21, 22] during the auction, and at the same time, the quality of contractor work to comply with the interests of the owners (in the form of ensuring a quality standard of living for citizens) and the interests of the state (with formation of the comfortable urban environment). The ultimate goal of the process in question is to implement the project and reduce the level of physical wear of the housing facility.

CONCLUSIONS

As a result of the study, it was determined that an increase to a certain level of one-time costs for restoration of an apartment house allows to increase the overhaul periods of operation, which allows to reduce the amount of costs for the current repair of the building. In addition, the choice of innovative design solutions and building materials when planning restoration of housing facilities can reduce the costs of current operation of an apartment house, since in the long run, taking into account inflation, the cost of operating an apartment house requires a significant amount of investment. Since the owner will continue to bear the costs of current maintenance of an apartment house, he is interested in optimizing the consumption of fuel and energy resources as a result of restoration (major repairs, reconstruction or modernization) and minimizing the loss of heat and other energy, as well as reducing operational housing facility expenses. The results of the scientific research of the authors are especially relevant in view of the fact that the current stage of the need to improve the energy efficiency of buildings is one of the key tasks facing the world scientific community in a number of countries.

REFERENCES

1. Zhilishchnyi kodeks Rossiiskoy Federacii ot 29.12.2004 g. № 188-FZ [Housing code of the Russian Federation of 29.12.2004 № 188-FZ] (v red. ot 22.01.2019) [in the wording 22.01.2019] (in Russian).
2. **Yakuntsev D.S.** Organizacionno-ekonomicheskii mekhanizm predostavleniya uslug kapital'nogo remonta mnogokvartirnykh domov [The organizational and economic mechanism of providing services of apartment houses capital repairs]. Diss. kand. ekonom. nauk [Dissertation of economical science]. Moscow, Izd. dom Moskovskogo institute

- kommunalnogo khozyaistva i stroitel'stva, 2008, 155 pages (in Russian).
3. Federal State Statistics Service [Electronic resource, Section "Housing conditions"]. URL: <http://www.gks.ru> (Accessed 15.10.2018).
4. Vopros: Ob osobennostyah gosudarstvennoi registracii prav na nekotorye ob'ekty nedvizhimosti, a takzhe priznakah otneseniya ob'ekta nedvizhimosti k mnogokvartitnym zhilym domam [Question: about the features of the state registration of rights to some real estate objects, as well as signs of attributing the property to apartment houses]. Pis'mo Minekonomrazvitiya RF ot 23.06.2010 No. D23-2280 [Letter of the Russian Federation Ministry of economic development of 23.06.2010 № D23-2280]. {Consultant Plus} (in Russian).
5. Doklad o tehnichestkom sostoyanii mnogokvartirnykh domov, raspologennykh na territorii Leningradskoy oblasti [Report on the technical condition of apartment buildings located in the Leningrad region]. Komitet gosudarstvennogo zhilichnogo nadzora i kontrolya Leningradskoy oblasti, Pravitel'stvo Leningradskoy oblasti [Committee of state housing supervision and control of the Leningrad region, the government of the Leningrad region], 2017, 22 pages (in Russian).
6. Oblastnoy zakon Leningradskoy oblasti ot 29.11.2013 No. FZ-O3 "Ob otdelnykh voprosakh organizacii i provedeniya kapital'nogo remonta obschego imuchestva v mnogokvartirnykh domah, raspologennykh na territorii Leningradskoy oblasti" [Regional law of the Leningrad region of 29.11.2013 No. 82-OZ "On certain issues of organization and overhaul of common property in multi-apartment buildings located in the Leningrad region"]. Red. ot 29.12.2018 [Edited on 29.12.2018] (in Russian).
7. **Chernyshov L.N., Astaf'ev S.A., Vakulina V.P.** Kapitalnyi remont mnogokvartirnykh domov: problemy formirovaniya i napravleniya razvitiya [Capital repair of apartment buildings: problems of formation and direction of development]. // *Izvestiya Irkutskoy gosudarstvennoy ekonomicheskoy akademii*, 2015, No. 25, Vol. 1, pp. 85-94 (in Russian).
8. **Nurullina O.V.** Zhilishchniy fond: metodika otbora domov dlya okazaniya remontnykh eslug [Housing stock: methods of selecting houses to provide repair services]. // *Rossiskoe predprinimatel'stvo*, 2011, No. 12(1), pp. 135-140 (in Russian).
9. **Kashina E.V., Stepanova A.V.** Analiz i ozhenka mekhanizmov razvitiya modelei vosproizvodstva zhilichnogo fonda [Analysis and evaluation of development mechanisms of housing reproduction models]. *Izvestiya vuzov. Stroitel'stvo. Neddvizhimost'*, 2016, No. 3(18), pp. 22-27 (in Russian).
10. **Biryukov A.N.** Osnovnye organizacionno-tehnologichskie resheniya i ekonomicheskaya celesoobraznost' snosa zdaniy [The main organizational and technological solutions and economic feasibility of building demolition]. *Vestnik grazhdanskikh inzhenerov*, 2012, No. 5, p. 103-109 (In Russian).
11. **Biryukov A.N., Denisov V.N., Biryukov Yu.A.** Snos zdaniy i sooruzheiy v sovremennykh usloviyakh (monografiya) [Demolition of buildings and structures in modern conditions]. Saint-Petersburg, 2014, 256 pages (in Russian).
12. **Andreev A.S., Arkhipov V. L., Biryukov A. N., Bulanov A.I., Biryukov Yu. A., Kulikov D. N., Ivanov D. V.** Ekonomika stroitelstva [Economics of construction]. Saint-Petersburg, 2016, 370 pages (in Russian).
13. **Ustinovichius L.** Determination of efficiency of investments in construction. // *International Journal of Strategic Property Management*, 2004, No. 8, Vol. 1, pp. 25-43.
14. **Farahani A., Wallbaum H., Dalenbäck J.-O.** Optimized maintenance and renovation

scheduling in multifamily buildings – a systematic approach based on condition state and life cycle cost of building components. // *Construction Management and Economics*, 2018, No. 11, pp. 1-17.

15. **Zavadskas E.K., Turskis Z., Tamošaitienė J.** Risk assessment of construction projects. // *Journal of Civil Engineering and Management*, 2010, No. 16, Vol. 1, pp. 33-46.
16. **Biryukov A.N., Marugin V.M., Lazarev A.N., Moroz A.M., Chmyrev V.A.** Ekspertnye formy kontrolya (na primerah ocenki stroitelnykh ob'ektov i samoocenki stroitelnykh predpriyatii) (monographiya) [Expert forms of control (on the evaluation of construction projects and self-assessment of construction enterprises]. Saint-Petersburg, Izdatel'stvo 'Politehnika', 2012, 213 pages (in Russian).
17. GOST 31937-2011 ot 27 dekabrya 2012 goda [GOST 31937-2011 of December 27, 2012] "Zdaniya i sooruzheniya. Pravila obsledovaniya i monitoring tekhnicheskogo sostoyaniya" [Buildings and structures. Rules of inspection and monitoring of technical condition] (in Russian).
18. **Biryukov A.N., Kazakov Yu.N.** Effektivnost' novoi tekhnologii ustroystva navesnykh ventiliruemykh fasadov [Efficiency of new technology of ventilated facades]. // *Materialy 11-i Mezhdunarodnoi nauchno-practichskoi konferencii «Novosti peredovoi nauki» [Materials of the 11th International scientific and practical conference «News of advanced science»]*, 2015, Vol. 17. Tekhnologii. Stroitel'stvo i arkhitektura. Sofia, "Beliy gorod BG", pp. 79-84 (in Russian).
19. **Biryukov A., Kazakov Y.** Fast assembly of quality suspended ventilated facades. // *Architecture and Engineering*, 2017, No. 2, Vol. 1, pp. 11-19.
20. **Biryukov A.N., Denisov V.N., Shvarts M.S.** Rol' teplovoy inercii v zachite ograzhdauychikh konstrukcii ot promerzaniya v sibirskikh regionah [The role of thermal inertia in the protection of

enclosing structures from freezing in the Siberian regions]. // *Stroitel'nyye i dorozhnyye mashiny*, 2016, No. 3, pp. 45-50 (in Russian).

21. **González-Cruz C.** Scoring rules and abnormally low bids criteria in construction tenders: a taxonomic review. // *Construction Management and Economics*, 2015, No. 33, Vol. 4, pp. 259-278.
22. **Zeiler W., Gvozdenović K., De Bont K., Maassen W.** Toward cost-effective nearly zero energy buildings: The Dutch Situation. // *Science and Technology for the Built Environment*, 2016, No. 22, Vol. 7, pp. 911-927.
23. **Melnikas B., Jakubavičius A., Strazdas R.** The Development of innovation activities in building construction by saving heating resources. // *Statyba*, 1998, No. 4, Vol. 3, pp. 235-242.
24. **Berg F., Fuglseth M.** Life cycle assessment and historic buildings: energy-efficiency refurbishment versus new construction in Norway. // *Journal of Architectural Conservation*, 2018, No. 24, Vol. 2, pp. 152-167.

REFERENCES

1. Жилищный кодекс Российской Федерации (Федеральный закон (ФЗ) от 29 декабря 2004 г. №188-ФЗ (в редакции от 22 января 2019 г.).
2. **Якунцев Д.С.** Организационно-экономический механизм предоставления услуг капитального ремонта многоквартирных домов. Диссертация на соискание ученой степени кандидата экономических наук по специальности 08.00.05 – Экономика и управление народным хозяйством (экономика, организация и управление предприятиями, отраслями, комплексами – сфера услуг; экономика, организация и управление предприятиями, отраслями, комплексами – строительство. – М.:

- Российский государственный университет туризма и сервиса, 2008. – 155 с.
3. Интернет-сайт Федеральной службы государственной статистики. URL: <http://www.gks.ru> (Дата доступа: 15 октября 2018 г.).
 4. Вопрос: Об особенностях государственной регистрации прав на некоторые объекты недвижимости, а также признаках отнесения объекта недвижимости к многоквартирным жилым домам. Письмо Минэкономразвития России от 23 июня 2010 г. № Д23-2280.
 5. Доклад о техническом состоянии многоквартирных домов, расположенных на территории Ленинградской области. Комитет государственного жилищного надзора и контроля Ленинградской области, 2017. – 22 с.
 6. Областной закон Ленинградской области от 29 ноября 2013 г. №ФЗ-ОЗ «Об отдельных вопросах организации и проведения капитального ремонта общего имущества в многоквартирных домах, расположенных на территории Ленинградской области» (редакция от 29 декабря 2018 г.).
 7. Чернышов Л.Н., Астафьев С.А., Вакулина В.П. Капитальный ремонт многоквартирных домов: проблемы формирования и направления развития. // *Известия Иркутской государственной экономической академии*, 2015, том 25, №1, с. 85-94.
 8. Нуруллина О.В. Жилищный фонд: методика отбора домов для оказания ремонтных услуг. // *Российское предпринимательство*, 2011, №12(1), с. 135-140.
 9. Кашина Е.В., Степанова А.В. Анализ и оценка механизмов развития моделей воспроизводства жилищного фонда. // *Известия высших учебных заведений. Строительство. Недвижимость*, 2016, №3(18), с. 22-27.
 10. Бирюков А.Н. Основные организационно-технологические решения и экономическая целесообразность сноса зданий. // *Вестник гражданских инженеров*, 2012, №5, с. 103-109.
 11. Бирюков А.Н., Денисов В.Н., Бирюков Ю.А. Снос зданий и сооружений в современных условиях. – СПб., 2014. – 256 с.
 12. Андреев А.С., Архипов В.Л., Бирюков А.Н., Буланов А.И., Бирюков Ю.А., Куликов Д.Н., Иванов Д.В. Экономика строительства. – СПб., 2016. – 370 с.
 13. Ustinovichius L. Determination of efficiency of investments in construction. // *International Journal of Strategic Property Management*, 2004, No. 8, Vol. 1, pp. 25-43.
 14. Farahani A., Wallbaum H., Dalenbäck J.-O. Optimized maintenance and renovation scheduling in multifamily buildings – a systematic approach based on condition state and life cycle cost of building components. // *Construction Management and Economics*, 2018, No. 11, pp. 1-17.
 15. Zavadskas E.K., Turskis Z., Tamošaitiene J. Risk assessment of construction projects. // *Journal of Civil Engineering and Management*, 2010, No. 16, Vol. 1, pp. 33-46.
 16. Бирюков А.Н., Маругин В.М., Лазарев А.Н., Мороз А.М., Шмырев В.А. Экспертные формы контроля (на примерах оценки строительных объектов и самооценки строительных предприятий). – СПб.: Издательство «Политехника», 2012. – 213 с.
 17. ГОСТ 31937-2011 «Здания и сооружения. Правила обследования и мониторинга технического состояния» (редакция от 27 декабря 2012 г.).
 18. Бирюков А.Н., Казаков Ю.Н. Эффективность новой технологии устройства навесных вентилируемых фасадов. // *Материалы одиннадцатой научно-практической конференции «Новости передовой науки»*, 2015, №17, Технологии. Строительство и архитектура. – София: Белый город БГ, с. 79-84.

19. **Biryukov A., Kazakov Y.** Fast assembly of quality suspended ventilated facades. // *Architecture and Engineering*, 2017, No. 2, Vol. 1, pp. 11-19.
20. **Бирюков А.Н., Денисов В.Н., Шварц М.С.** Роль тепловой инерции в защите ограждающих конструкций от промерзания в сибирских регионах. // *Строительные и дорожные машины*, 2016, №3, с. 45-50.
21. **González-Cruz C.** Scoring rules and abnormally low bids criteria in construction tenders: a taxonomic review. // *Construction Management and Economics*, 2015, No. 33, Vol. 4, pp. 259-278.
22. **Zeiler W., Gvozdenović K., De Bont K., Maassen W.** Toward cost-effective nearly zero energy buildings: The Dutch Situation. // *Science and Technology for the Built Environment*, 2016, No. 22, Vol. 7, pp. 911-927.
23. **Melnikas B., Jakubavičius A., Strazdas R.** The Development of innovation activities in building construction by saving heating resources. // *Statyba*, 1998, No. 4, Vol. 3, pp. 235-242.
24. **Berg F., Fuglseth M.** Life cycle assessment and historic buildings: energy-efficiency refurbishment versus new construction in Norway. // *Journal of Architectural Conservation*, 2018, No. 24, Vol. 2, pp. 152-167.

Alexander N. Biryukov, Doctor of technical sciences, professor, chief of department, Military Institute (engineering), Military Academy of Logistics named after Army General A.V. Khrulev, Zakharyevskaya st., 22, St. Petersburg, 191123, Russian Federation; Phone: +7 (921) 751-67-52; e-mail: aleks_bir@mail.ru.

Igor N. Kravchenko, Doctor of technical sciences, professor, professor of the Department of Technical Service of Machinery and Equipment, Russian State Agrarian University-Moscow Agricultural Academy named after K.A. Timiryazev, 49, Timiryazev street, Moscow, Moscow, 127550, Russian Federation; phone: +7 (985) 994-02-20; E-mail: kravchenko-in71@yandex.ru.

Evgeny O. Dobryshkin, Post-graduate student, Military Institute (engineering), Military Academy of Logistics

named after Army General A.V. Khrulev, Zakharyevskaya st., 22, St. Petersburg, 191123, Russian Federation; phone: +7 (921) 555-97-02; e-mail: edobryshkin@mail.ru.

Yuri A. Biryukov, Doctoral student, Military Institute (engineering), Military Academy of Logistics named after Army General A.V. Khrulev, Zakharyevskaya st., 22, St. Petersburg, 191123, Russian Federation; phone: +7 (905) 255-36-97; e-mail: uabiryukov@mail.ru.

Valery I. Kondrashchenko, Doctor of technical sciences, professor of the Department of "Construction materials and technologies", Russian University of Transport (MIIT), Obraptsova Street, 9, 9b, Moscow, 127994, Russian Federation, phone +7 (926) 211-84-17; E-mail: kondrashchenko@mail.ru

Бирюков Александр Николаевич, профессор, доктор технических наук, заведующий кафедрой; Военный институт (инженерно-технический), Военная академия материально-технического обеспечения имени генерала армии А.В. Хрулева (ВА МТО им. генерала армии А.В. Хрулева), ул. Захарьевская, 22, Санкт-Петербург, 191123, Российская Федерация; Тел.: 8 (921) 751-67-52; e-mail: aleks_bir@mail.ru.

Кравченко Игорь Николаевич, профессор, доктор технических наук, профессор кафедры технического сервиса машин и оборудования, Российский государственный аграрный университет – МСХА имени К.А. Тимирязева, ул. Тимирязевская, 49, Москва, 127550, Российской Федерации; тел. +7 (985) 994-02-20; E-mail: kravchenko-in71@yandex.ru.

Добрышкин Евгений Олегович, адъюнкт, Военный институт (инженерно-технический), Военная академия материально-технического обеспечения имени генерала армии А.В. Хрулева (ВА МТО им. генерала армии А.В. Хрулева), ул. Захарьевская, 22, Санкт-Петербург, 191123, Российская Федерация; тел. +7 (921) 555-97-02; e-mail: edobryshkin@mail.ru.

Бирюков Юрий Александрович, докторант, Военный институт (инженерно-технический), Военная академия материально-технического обеспечения имени генерала армии А.В. Хрулева (ВА МТО им. генерала армии А.В. Хрулева), ул. Захарьевская, 22, Санкт-Петербург, 191123, Российская Федерация; тел.: +7 (905) 255-36-97; e-mail: uabiryukov@mail.ru.

Кондращенко Валерий Иванович, доктор технических наук, профессор кафедры «Строительные материалы и технологии» Российского университета транспорта, ул. Образцова, д. 9, стр. 9, Москва, 127994, Российская Федерация; тел. +7(926) 211-84-17; E-mail: kondrashchenko@mail.ru.

INTEGRAL PARAMETERS OF CONCRETE DIAGRAMS FOR CALCULATIONS OF STRENGTH OF REINFORCED CONCRETE ELEMENTS USING THE DEFORMATION MODEL

Vladimir A. Eryshev¹, Nickolay I. Karpenko², Artur O. Zhemchuyev¹

¹ Togliatti State University, Togliatti, RUSSIA

² Research Institute of Construction Physics of the Russian Academy of Architecture and Construction Sciences,
Moscow, RUSSIA

Abstracts: In accordance with the requirements of regulatory documents, restrictions are introduced on stress levels at the end of the falling branch of the diagrams at the maximum normalized strain values. We have developed mathematical models that establish a uniform sequence for calculating the unambiguous values of deformations at the base points of concrete diagrams, taking into account the accepted functional relationships and the rules for their use according to the tables of normative documents. It was shown that for equal values of deformations and stresses at base points, analytical expressions of diagram recommended by regulatory documents, even if it differs in structure, give identical outlines, diagram branches coincide. The correlation between the calculation models by Russian and foreign regulatory documents was established by comparing the values of the integral parameters of the diagrams and the ultimate forces obtained by calculating the reinforced concrete element according to the deformation model. As integral parameters of concrete deformation diagrams, it was recommended to use areas bounded by diagram branches and diagram completeness coefficients. Analytical modeling of integral parameters allowed us to exclude the procedure for numerically summing stresses along elementary strips in a section and solving nonlinear equations by the method of successive approximations when calculating the strength of an element.

Keywords: strength, deformations, concrete diagram, integral parameters,
deformation model

ИНТЕГРАЛЬНЫЕ ПАРАМЕТРЫ ДИАГРАММ БЕТОНА В РАСЧЕТАХ ПРОЧНОСТИ ЖЕЛЕЗОБЕТОННЫХ ЭЛЕМЕНТОВ ПО ДЕФОРМАЦИОННОЙ МОДЕЛИ

В.А. Ерышев¹, Н.И. Карпенко², А.О. Жемчуев¹

¹ Тольяттинский государственный университет, г. Тольятти, РОССИЯ

Научно-исследовательский институт строительной физики

² Российской академии архитектуры и строительных наук, г. Москва, РОССИЯ

Аннотация: В соответствии с требованиями нормативных документов, введены ограничения на уровни напряжений в конце ниспадающей ветви диаграмм при максимальных нормированных значениях деформаций. Разработаны математические модели, устанавливающие единообразную форму вычисления однозначных значений деформаций в базовых точках диаграмм бетона, с учетом принятых функциональных связей и правил их назначения по таблицам нормативных документов. Показано, что при равных значениях деформаций и напряжений в базовых точках, рекомендованные нормативными документами аналитические выражения описания диаграмм, разные по своей структуре, дают одинаковые их очертания, ветви диаграмм совпадают. Соотношение между расчетными моделями в редакции российских и зарубежных нормативных документов устанавливается сравнением значений интегральных параметров диаграмм и предельных усилий, полученных расчетом железобетонного элемента по деформационной модели. В качестве интегральных параметров диаграмм деформирования бетона рекомендуется использовать площади областей, ограниченных ветвями диаграмм и коэффициенты полноты диаграмм. Аналитическое моделирование интегральных параметров позволяет исключить из расчета прочности элемента процедуры численного суммирования напряжений по

элементарным полоскам в сечении и решения нелинейных уравнений путем последовательного приближения.

Ключевые слова: прочность, деформации, диаграмма бетона, интегральные параметры, деформационная модель.

INTRODUCTION

The regulatory documents [1, 2, 3, 4] recommend different types of concrete deformation diagrams and analytical dependencies that establish the relationship between deformations and stresses " $\varepsilon_b - \sigma_b$ " under axial compression and tension. The curvilinear diagram with ascending and descending deformation branches corresponds to the physical properties of concrete and the experimental test data for standard concrete specimens most fully. When describing curved diagrams of concrete deformation under compression, the authors of Russian and foreign publications [5, 6, 7, 8, 9] use the base points: at the top of the diagram on the ascending branch; at the end of the falling branch, in which the deformations reach their maximum values. The differences between analytical dependencies of the diagrams, the differences between calculation methods for determining of deformations and design values of concrete strength in the base points that is contained in regulatory documents leads to a mutual discrepancy between the values of ultimate forces in the strength calculations of reinforced concrete elements. In addition, difficulties arise in the comparative evaluation of the efficiency of computational models. In calculations by the deformation model, the numerical integration of stresses in the selected elementary strips of concrete over the thickness of the element and the solution of nonlinear equations satisfying the condition of equilibrium of forces by the method of successive approximation (iterations) is a laborious procedure in the calculations of complex engineering systems. The transition from the real stress diagram to the conventional stress diagram of a rectangular shape for the compressed zone of an element is important to simplify the computer modeling technique in

the calculations of generalized internal forces. The performed studies are important for the discrete-continuum approach in numerical modeling of the behavior of the load-bearing systems of high-rise buildings [10], the improvement of computational models of power resistance of reinforced concrete [11] and the development of the survivability theory of structural systems of buildings and structures [12, 13, 14].

THE PURPOSE AND OBJECTIVES OF THE RESEARCH

The first purpose of this research is developing of a mathematical model for calculating deformations at the base points of concrete diagrams, taking into account the accepted functional relationships and the rules for their accepting in accordance with the tables of normative documents. The second purpose is to include the integral parameters of concrete diagrams in the calculation method based on the deformation model and establish the relationships between the ultimate forces for the respective classes of concrete using the compressive strength. The third purpose is to propose a simplified method for calculating the strength of an element, excluding the procedure of the numerical integration of stresses over the thickness and solving nonlinear equations by the iteration method. Finally, it is to establish a relationship between the parameters of the deformation model and the method of ultimate forces for the ultimate state of an element.

METHOD

The normative documents [2, 3] sign the concrete class for the axial compression strength

by the letter C and numbers, for example, C12 / 15. The first number means the value of normative resistance f_{ck} i.e. the compressive strength of cylinders of 150 mm in diameter and 300 mm in height, tested in age 28 days. The second number is the value of the guaranteed strength of the concrete cube of 150 x 150 x 150 mm with a statistical security of 0.95 ($f_{c,cube}^G$).

Russian standards are based on the strength of the cube. In accordance with these principles, we established the correspondence between classes C and B (table 1). For example, concrete class B15 corresponds to class C12/15, etc. Further, we found respectively the normative concrete resistance under axial compression R_{bn} (prismatic strength) and f_{ck} (cilindric strength) for compressive strength classes of concrete B and C using tables of regulatory documents. The design values of concrete resistance R_b and f_{cd} (Table 1) are calculated dividing a value of the normative concrete resistance under compression, respectively, R_{bn} by the reliability coefficient for concrete under compression $\gamma_b = 1.3$ and f_{ck} by the safety coefficient for concrete $\gamma_c = 1.5$. When calculating RC elements for the limit states of the first group for high-strength concrete of class C, the work [2] takes into account the partial coefficient γ_{HSC} . The values of the initial modulus of elasticity of concrete E_b and E_{cm} for the compressive strength class of concrete B and C are taken according to the tables of normative documents. When evaluating the deformation properties of concrete, the works [2, 3] introduce the average values of compressive strength f_{cm} . Concrete compression diagrams are plotted in the coordinates " $\varepsilon_b(\varepsilon_c) - \sigma_b(f_c)$ ". Here, parentheses contain the denotations of deformations and stresses accepted in [2,3]. The base points of curvilinear diagrams for strength calculations are the following ones: the top of

the ascending branch of the diagram which takes coordinates $\hat{\varepsilon}_b(\varepsilon_{c1}), R_b(f_{cd})$; the end of the descending branch which takes the maximum strain value and coordinates $\varepsilon_{bu}(\varepsilon_{cu1}), \sigma_{bu}(f_{cu})$. The work [3] (table 6.1) normalizes the strain values at the base points ε_{c1} and ε_{cu1} which uses when calculating the stresses for concrete compression class C. The dependence stress – strain is constructed using the current values of strains

$$\eta_c = \varepsilon_c / \varepsilon_{c1} (|\varepsilon_c| \leq |\varepsilon_{cu1}|).$$

The stress value f_c takes its maximum value at $\eta_c = 1$ in the top of the diagram:

$$f_c = f_{cd}$$

– applied at the calculations for the first limiting state and

$$f_c = f_{ck}$$

– applied at the calculations for the second limiting state. Normative document [1] normalizes the magnitude of maximum strains ε_{bu} . Deformations $\hat{\varepsilon}_b$ at the top of the diagram, in contrast to [2, 3], are not assigned according to the tables of norms, but it is calculated by the formula, which takes into account the class and type of concrete. The relative stress level

$$\eta_b = \eta_{bu} = 0.85$$

($\eta_{bu} = 1$ for high-strength concrete) limits the descending branch of the diagram. Transforming the formula that describes the diagram, calculations can be performed both through stress and through deformation.

Table 1. Calculation parameters of concrete deformation diagrams.

Building Code of Belarus SNB [3]	Compressive class of concrete	C12	C25	C35	C50	C60	C70	C80	C90
	f_{cd} , MPa	8.0	16,7	23.3	33.3	39.2	42.6	47.6	50.2
	ε_{c1} [‰]	1.9	2,16	2.3	2.48	2.58	2.67	2.76	2.83
	ε_{cu1} [‰]	3.5	3.5	3.47	3.35	3.24	3.11	2.98	2.83
	S_{dc}	24.9	50,37	67.75	89.4	99.2	101.6	105.1	102.9
	ω_{dc}	0.89	0,86	0.845	0.8	0.78	0.768	0.744	0.725
	ε_{cc} [‰]	1.89	1.95	1.96	1.94	1.9	1.84	1.79	1.71
	$M_{c,ult}$, kN m	309	630	861	1191	1367	1450	1560	1590
Building Code of Russia SP [1]	Compressive class of concrete	B15	B30	B45	B60	B75	B85	B95	B105
	R_b , MPa	8.5	17.0	25.0	33.0	39.0	42.5	45.75	49.0
	$\hat{\varepsilon}_b$ [‰]	1.9	2.18	2.36	2.5	2.62	2.68	2.75	2.8
	ε_{bu} [‰]	3.5	3.5	3.44	3.31	3.2	3.04	2.92	2.8
	S_{db}	26.04	50.9	71.0	87.2	95.1	97.6	98.2	97.6
	ω_{db}	0.875	0.855	0.826	0.8	0.762	0.755	0.735	0.711
	ε_{bc} [‰]	1.88	1.948	1.95	1.92	1.87	1.82	1.77	1.71
	σ_{bc} MPa	8.41	15.3	21.3	25.4	27.8	28.8	29.5	29.9
	$M_{b,ult}$, kN m	321	636	916	1173	1341	1422	1482	1528

Currently, a curvilinear diagram is effectively used in structural calculations for the second limiting state, in which the accuracy of the calculation in comparison with the experimental data is determined by the analytical description of the ascending branch of the diagram. It should be noted that some discrepancy between the strain values $\hat{\varepsilon}_b$ and ε_{c1} at the top of the diagram for concrete classes B and C as amended by normative documents [1] and [2] does not lead to significant differences in the outline of the ascending branch of the diagrams and, respectively, the stress values for given strains. Strength calculations use the full concrete deformation diagram for compression. There are increasing requirements for the description of the descending branch of the diagram, for compliance with the

recommendations of the norms on limiting the values of both stresses and strains.

Analytical expressions for the description of concrete deformation diagrams characterize short-term loading models. The standard is the test mode of specimens at constant strain growth rates, which allows you to identify two branches of concrete deformation diagrams. In experiments, the rate of change in the load on the test equipment can be accepted arbitrary, the descending branch may appear partially or completely absent. The parameters of the diagram in the edition of normative documents [2, 3] were investigated in experiments with monotonically increasing compression strains, at a speed $\dot{\varepsilon}_c^* \approx 0,015$ ‰ / sec. It is assumed that the nonlinear properties of concrete for the corresponding concrete classes B and C for a given compression test mode of concrete

specimens of prisms and cylinders are manifested equally, and deformations at the base points have the same values:

$$\hat{\varepsilon}_b = \varepsilon_{c1}; \varepsilon_{bu} = \varepsilon_{cu1}.$$

Deformation values at base points are determined according to the rules of the rules depending on the average stresses f_{cm} in the formulas (1), (2) and concrete class B – in the formula (3). This means that the strain values at the base points can be used in the calculations for the limiting states of both the first and second groups.

According to the analytical dependencies presented in the regulatory documents [1,2,3,4], taking into account (5), concrete diagrams “ $\varepsilon_b(\varepsilon_c) - \sigma_b(f_c)$ ” are constructed. The branches of these diagrams pass through the base points, whose values are calculated from expressions (1), (2), (3) and (4). The shape of the concrete diagrams corresponds to the shape of the stress diagrams in the compressed zone of the element (Figures 1, 2).

The dependences for the calculating of deformations at base points. When conducting calculations in software systems, it is more convenient to use analytical dependencies in which the functional relationship is preserved when assigning normalized parameters from the tables. Deformations ε_{c1} increase with increasing concrete strength at maximum compression stress. Meyer (1998) proposed a mathematical model for their calculation:

$$\varepsilon_{c1} = 1,6(f_{cm}/10MIIa)^{0,25} / 1000, \quad (1)$$

where $f_{cm} = f_{ck} + \Delta f$ ($\Delta f = 8$ MPa).

It is proposed calculating the ultimate compressive strain of concrete ε_{cu1} , normalized in tabular form [2, 3], by the formula:

$$\varepsilon_{cu1} = \varepsilon_{c1} \left(1 - \frac{f_{cm} - f_{cm}^*}{81MIIa} \left(\frac{10MIIa}{f_{cm}} \right)^{0,2} \right), \quad (2)$$

where f_{cm}^* is the fixed value of the average concrete strength for the concrete class, in which the descending branch is excluded from the calculation and the equalities $|\varepsilon_{c1}| = |\varepsilon_{cu1}|$ and $f_{cd} = f_{cu}$ are satisfied (assumed that $f_{cm}^* = 98$ MPa).

The analytical dependencies uniform by the structure with (1) and (2), are introduced for heavy concrete in order to determine deformations at base points $\hat{\varepsilon}_b$ and ε_{bu} (Table 1):

$$\hat{\varepsilon}_b = 1,75 \left(\frac{B}{10MIIa} \right)^{0,2} / 1000; \quad (3)$$

$$\varepsilon_{bu} = \hat{\varepsilon}_b \left(1 - \frac{B - B^*}{98MIIa} \left(\frac{10MIIa}{B} \right)^{0,2} \right)$$

where B^* is a fixed class of concrete, in which the descending branch is excluded from the calculation and the equalities

$$|\hat{\varepsilon}_b| = |\varepsilon_{bu}| \quad \text{and} \quad \sigma_{bu} = R_b$$

are satisfied (assumed that $B^* = 105$ MPa).

When working with diagrams, there is a general rule. If deformations are assigned and stresses are calculated during the construction of diagrams, then the maximum values of deformations are limited by values ε_{cu1} (2) and ε_{bu} (4). If stresses are assigned and deformations are calculated [1, 4], then the minimum stress values on the descending branch are limited by the relative stress value η_{bu} calculated by the formula:

$$\eta_{bu} = 1 + \lambda_b \frac{B - B^*}{B + B^*}, \quad (4)$$

where, $\eta_{bu} = \sigma_{bu} / R_b$, here, B^* is a fixed class of concrete, in which the descending branch of a diagram is excluded from the calculation (assumed that $B^* = 105$ MPa).

If we take into account foreign experience, then from formula (1) it follows that the minimum value of the relative stresses on the descending branch

$$\eta_{cu} = f_{cu} / f_{cd}$$

for $\sigma_c = f_{cu}$.

When increasing the class of concrete accepted by compressive strength, it varies linearly from 0.9 to 1. In norms [1, 4], it is recommended to take the value of 0.85 for low-strength concrete, then

$$\lambda_b = 0.2$$

in the formula (4) and the linear relationship for η_{bu} is maintained for concrete classes ranging from 0.85 to 1.

A drop-down branch is carried out from the expression:

$$\eta_b = 1 + (\eta_{bu} - 1) \left(\frac{\eta_d - 1}{\eta_{du} - 1} \right)^2, \quad (5)$$

where,

$$\eta_{du} = \varepsilon_{bu} / \hat{\varepsilon}_b, \quad \eta_d = \varepsilon_b / \hat{\varepsilon}_b$$

are the current values of strains.

The values of deformations at the base points are determined according to the rules of norms depending on the average stresses f_{cm} in the formula (1, 2) and concrete class B in the formula (3). This means that the strain values at the base points can be used in the calculations for the limiting states of both the first and second groups.

According to the analytical dependencies presented in the regulatory documents [1, 2, 3, 4] taking into account (5), concrete diagrams " $\varepsilon_b(\varepsilon_c) - \sigma_b(f_c)$ " are constructed. The branches of these diagrams pass through the base points, whose values are calculated from expressions (1), (2), (3) and (4). The outline of the stress diagrams in the compressed zone of the element corresponds to outline of the concrete deformation diagrams (Figures 1, 2).

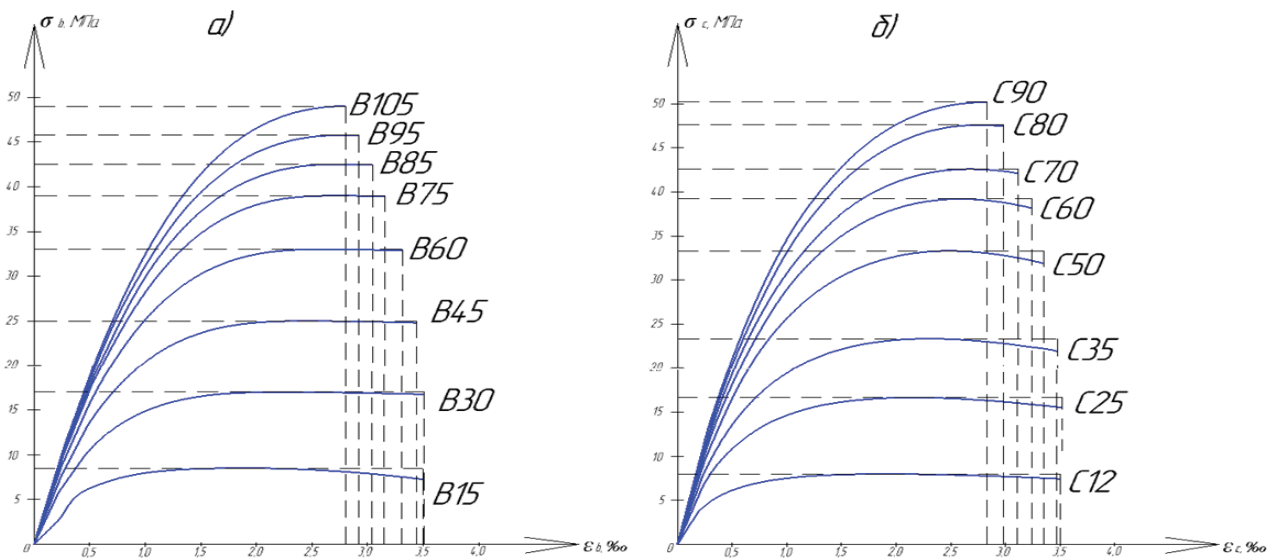


Figure 1. Diagrams of deforming of concrete by regulatory documents:
(a) Building Code of Russia SP 63.13330.2012 and (b) Building Code of Belarus SNB 5.03.01-02 taking in account formulas (1) – (5).

ENERGY MODEL FOR CALCULATING THE STRENGTH OF A REINFORCED CONCRETE ELEMENT USING MATERIAL DEFORMATION DIAGRAMS

Figure 2 (d) presents the stress diagram and diagram of internal forces for a rectangular cross-section with reinforcement in the lower zone A_s and in the upper zone A'_s (Fig. 2b), taking into account the distribution of the deformations of concrete and reinforcement according to the linear law (Fig. 2c). The relations for curvature based on the linear law of the deformations' distribution along the height of the element takes the following form,

$$\frac{1}{\rho} = \chi = \frac{\varepsilon_{sn}}{h_0 - x} = \frac{\varepsilon_{bn}}{x} = \frac{\varepsilon_{bn} + \varepsilon_{sn}}{h_0}, \quad (6)$$

where h_0 is the working height of the section; x is the height of the compressed zone; ε_{bn} – is deformations of the outer fiber of the compressed zone of concrete; χ - curvature of the element; ρ - radius of curvature; ε_{sn} - deformations in tensile reinforcement.

The values of the internal forces in the reinforcement, respectively in the stretched and compressed zone, are

$$N_s = R_s A_s, \quad N'_s = \sigma'_s A'_s = \varepsilon'_s E_s A'_s.$$

Here the deformation of the reinforcement is determined by the formula:

$$\varepsilon'_s = \varepsilon_{bn} - \chi a'. \quad (7)$$

The value of the force N_b perceived by a concrete strip of unit width ($b = 1$) in the compressed zone at the limiting state is calculated by the formula

$$N_b = S_{db} / \chi. \quad (8)$$

Taking into account the obtained dependences, the equilibrium equation for the limiting state for a symmetric section of width b is written in the form

$$\begin{aligned} \frac{S_{db} b}{\chi} + \sigma'_s A'_s - R_s A_s &= 0 \\ \text{or} \\ \frac{S_{db} x b}{\varepsilon_{bu}} + \sigma'_s A'_s - R_s A_s &= 0. \end{aligned} \quad (9)$$

In the general case, when the ascending and descending branches of the diagram are described by nonlinear equations, small sections are plotted along the deformation axis using computer simulation (Figure 2a) $\Delta\varepsilon_{b,i}$ (i section numbers).

The height of the elementary area of the section

$$\Delta h_{b,i} = \Delta\varepsilon_{b,i} / \chi$$

with the value of the stress $\sigma_{b,i}$ corresponds to deformations on the diagrams $\Delta\varepsilon_{b,i}$ in the compressed zone of the element.

For each i -th section, it can be determined the following parameters using the diagrams: $\sigma_{b,i}$ - stress value; $\varepsilon_{b,i}$ - deformations in the coordinate system ε_b 0 σ_b ;

$$A_{b,i} = \Delta\varepsilon_{b,i} \sigma_{b,i}$$

- area of the i -th section;

$$S_{db} = \sum_{i=1}^n A_{b,i} = \sum_{i=1}^n \sigma_{b,i} \Delta\varepsilon_{b,i}$$

- the area of the field bounded by the branches of the diagram.

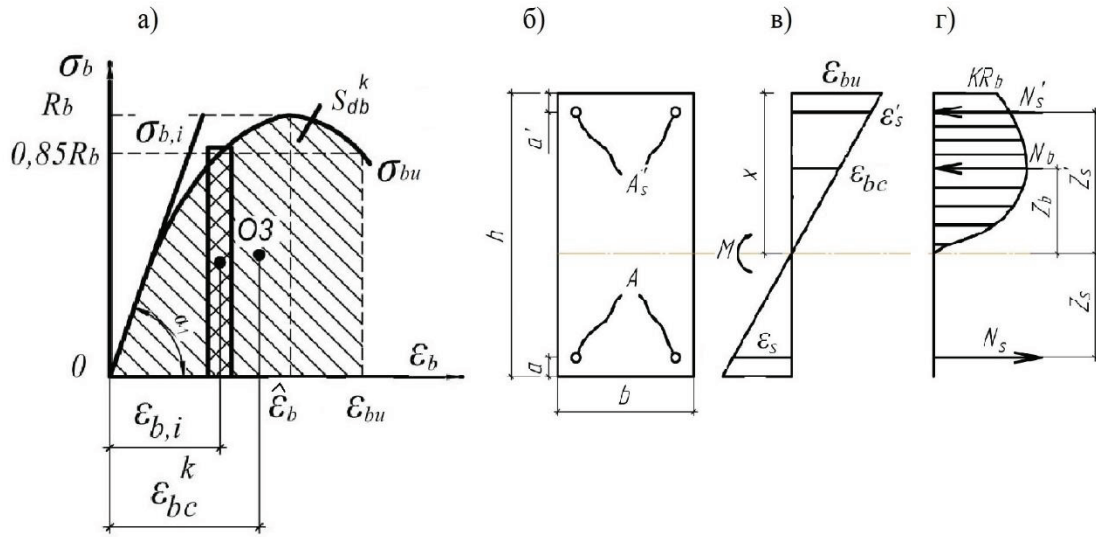


Figure 2. Schemes for explaining the methodic for calculating strength of an element using deformation model (in accordance with regulatory documents [2,3] index 'b' changed by index 'c'): (a) deformation diagram of concrete under compression and scheme for determining the integral parameters; (b) cross-section of an element; (c) linear distribution of deformations along the height of a cross-section; (d) stress diagram for compressed zone and scheme of internal forces into concrete and reinforcement.

The verification of the equilibrium equation (9) is performed by the method of successive approximations (iteration method), in which the variable is the element curvature χ determined from relations (6).

Strength calculation uses the complete concrete diagram (Fig. 2, a). The area of the field bounded by the branches of the diagram S_{db} (S_{dc}) remains constant. An integral characteristic of a concrete deformation diagram is the coefficient of completeness of the diagram ω_{db} (ω_{dc}). This coefficient characterizes the deviation of the actual area of the curved diagram S_{db} (S_{dc}) from the area of the rectangle S_{db}^* (S_{dc}^*) that describes the diagram by base points. The area of the complete diagram S_{db} (S_{dc}) for each class of concrete is calculated by numerical methods or using graphical computer programs (Table). The area of the rectangular diagram is calculated by the formula

$$S_{db}^* = R_b \epsilon_{bu} \quad \text{or} \quad S_{dc}^* = f_{cd} \epsilon_{cu1},$$

where R_b, f_{cd} are the design concrete resistances for the limiting states of the first group for concrete of compressive strength classes B and C, respectively; ϵ_{bu} (ϵ_{cu1}) - normalized values of ultimate strains are calculated by formulas (2) and (3). Coefficients of completeness of the diagram

$$\omega_{db} = S_{db} / S_{db}^*$$

and

$$\omega_{dc} = S_{dc} / S_{dc}^*$$

are calculated by the formulas

$$\begin{aligned} \omega_{db} &= 0,71 - 0,2 \frac{B - B^*}{B^*}; \\ \omega_{dc} &= 0,724 - 0,2 \frac{f_{cm} - f_{cm}^*}{f_{cm}^*}, \end{aligned} \quad (10)$$

where B^* is a fixed class of concrete, for which the descending branch is excluded from the calculation and the equalities

$$|\hat{\varepsilon}_b| = |\varepsilon_{bu}| \text{ and } \sigma_{bu} = R_b$$

are satisfied (assumed that $B^* = 105 \text{ MPa}$); f_{cm}^* - a fixed value of the average concrete strength for the concrete class, for which the descending branch is excluded from the calculation and the equalities

$$|\varepsilon_{c1}| = |\varepsilon_{cu1}| \text{ and } f_{cd} = f_{cu}$$

are satisfied (assumed that $f_{cm}^* = 98 \text{ MPa}$).

For an increase of the class of concrete, the curvature of the diagram decreases, approaching to the elastic one (Table), however $\omega_{db} > 0.5$. If condition (9) is satisfied the value of the ultimate bending moment M_{ult} perceived by the cross-section of an element is determined relatively to a fixed zero line:

$$M_{ult} = \frac{S_{db}}{\chi} b z_b + R_s A_s z_s + \sigma_s' A_s' z_s'. \quad (11)$$

The distances from the generalized forces N_s', N_s and N_b in the reinforcement and concrete to the neutral axis, respectively, are:

$$\begin{aligned} z_s' &= \frac{\varepsilon_b^{(k)} - a' \chi^{(k)}}{\chi^{(k)}}; \\ z_s &= \frac{\chi^{(k)} h_0 - \varepsilon_b^{(k)}}{\chi^{(k)}}; \\ z_b &= \frac{W_{db}}{\chi^{(k)} S_{db}} = \frac{\varepsilon_{bc}}{\chi^{(k)}}, \end{aligned} \quad (12)$$

where

$$W_{db} = \sum_{i=1}^n A_{b,i} \varepsilon_{b,i} = \sum_{i=1}^n \sigma_{b,i} \Delta \varepsilon_{b,i} \varepsilon_{b,i}$$

is the moment that numerically equal to the sum of the products of the areas of the elementary section on the concrete diagrams and the distances of their centers of gravity to the stress axis σ_b ;

$$\varepsilon_{bc} = W_{db} / S_{db}$$

- deformations at the level of the center of gravity of the diagram O_3 (Fig. 2a); $\chi^{(k)}$ - the curvature of an element after satisfying the equilibrium condition (9) at the k -th iteration.

From the formula (12) for z_b , it follows that the deformations at the level of the center of gravity of the stress diagram in the concrete of the compressed zone of an element are equal to the deformations ε_{bc} at the center of gravity of the full diagram. Studies indicate that the ratios between the values of strains at the center of gravity of the diagrams and strains at the top of the diagrams

$$\eta_{bc} = \varepsilon_{bc} / \hat{\varepsilon}_b \quad (\eta_{cc} = \varepsilon_{cc} / \hat{\varepsilon}_{c1})$$

are a monotonically decreasing functions (for increasing concrete class B and average concrete strength f_{cm}) that can be described by analytical expressions:

$$\begin{aligned} \eta_{bc} &= \left(\frac{0,75 M \Pi a}{B} \right)^{0,1} - 0,29 \frac{B - B^*}{B^*}; \\ \eta_{cc} &= \left(\frac{0,65 M \Pi a}{B} \right)^{0,1} - 0,35 \frac{f_{cm} - f_{cm}^*}{f_{cm}^*}, \end{aligned} \quad (13)$$

where the parameters B^* and f_{cm}^* are taken from (10).

Modeling of the parameters of the diagrams by analytical dependencies allows us to exclude from the calculations of the strength of elements the procedure of the numerical integration of the areas of elementary sections and the solution of nonlinear equations by the iteration method. The calculation of the strength of the element, taking into account the proposed dependencies, is performed in the following sequence:

- it is assigned a class of concrete, section, reinforcement: A_s, A'_s ;
- for a given class of concrete, the coefficient of completeness of the concrete deformation diagram ω_{db} is calculated by formula (10), for the area of a rectangular diagram S_{db}^* , the area S_{db} of the region bounded by the branches of the diagram is calculated;
- taking into account (6) and (7), equation (9) is converted into a quadratic equation with respect to the actual height of the compressed zone x :

$$x^2 \frac{S_{db} b}{\varepsilon_{bn}} + x(\varepsilon_{bn} E_s A'_s - R_s A_s) - a' \varepsilon_{bn} E_s A'_s = 0; \quad (14)$$

- according to formula (11) and taking into account (12), the moment value in the limiting state is calculated, where the force distances to the neutral axis are not determined with the parameter $\chi^{(k)}$ obtained by the sequential approximation procedure, but by solving the quadratic equation for the height of the compressed zone (14) and calculating the element curvature from formula (6).

TRANSITION TO THE METHOD OF ULTIMATE FORCES

For calculation by the method of ultimate forces, a simple rectangular diagram of normal stresses in the compressed zone of concrete was adopted. The relationship between the curvilinear stress diagram and the rectangular

stress diagram is established from the condition of equality of the forces in these diagrams

$$\frac{S_{db} x b}{\varepsilon_{bu}} = R_b x^* b, \quad (15)$$

from which a relationship between the heights of the compressed zone, respectively x and x^* is established for a given cross-section, reinforcement and class of concrete compressive strength. The value of the bending moment M_{ult}^* perceived by the cross-section of the element, according to ultimate forces, is calculated by the formula:

$$M_{ult}^* = R_b b x^* (h_0 - 0,5x) + R_{sc} A'_s (h_0 - a'). \quad (16)$$

A comparative analysis of the methods for calculating strength is performed for a reinforced concrete section with dimensions $h = 60$ cm, $b = 30$ cm. Reinforcement in the stretched zone is periodical steel rebars of A400 class. The condition of the equilibrium of forces in the normal section is satisfied by the reinforcement saturation of the stretched zone at given strain values: in the reinforcement

$$\varepsilon_s = R_s / E_s, \text{ where } R_s = 355 \text{ MPa};$$

in the outer concrete fiber of the compressed zone ε_{bu} , calculated by the formula (3). For the simple case of bending, the calculations are carried out in the same sequence, just for given deformations using the formulas (6), the element curvature and the actual height of the compressed zone x are calculated. Using the equilibrium equation (9) and without taking into account the reinforcement in the compressed zone, the reinforcement area A_s is determined. The forces in concrete for given concrete class of compressive strength are equal to the forces in the reinforcement.

*Table 2. Design values of parameters for limiting state by deformation model (A)
and the method of ultimate forces (B)*

Compressive class of concrete		B15	B30	B45	B60	B75	B85	B95	B105
A	x , cm	37.3	37.2	37.0	36.4	35.8	35.4	34.9	34.3
	M_{ult} , kN m	317.7	644.8	824.3	1178.7	1342.7	1419.5	1478.0	1523.1
B	x^* , cm	32.2	32.0	30.7	29.2	27.7	26.6	25.5	24.3
	M_{ult}^* , kN m	327	653	834.8	1196.4	1366.0	1449.8	1514.2	1566.5

The curvature of the element and the height of the compressed zone x decrease due to a reduction in the limit values of nonlinear deformations in high-strength concrete when increasing the class of concrete, and the value of the ultimate moment M_{ult} increases (Table 2, A). The height of the compressed zone x^* of rectangular shape is smaller than the actual height of the compressed zone x , however, the increase in the shoulder of the inner pair of forces compensates the difference between the values of the limiting moments calculated by formula (16) without taking into account the reinforcement in the compressed zone (Table 2, B).

CONCLUSION

The ratio of ultimate efforts when calculating the strength of elements according to the deformation model is determined by the integral parameters of the diagrams of concrete deformation under compression, the analytical modeling of which allows us to exclude from the calculation of strength the procedure for numerically summing of stresses along elementary strips in a section and solving nonlinear equations by successive approximations. Replacing a curvilinear stress diagram with a rectangular one does not introduce a significant error in the calculation of ultimate forces, since a decrease in the height of the compressed zone with a rectangular diagram is compensated by an increase in the shoulder of the internal pair of forces.

REFERENCES

1. Building Code of Russia SP 63.13330.2012. Betonnyye i zhelezobetonnyye konstruksii. Osnovnyye polozheniya. Aktualizirovannaya redaktsiya SNiP 52-01-2003 [Concrete and reinforced concrete structures. The main provisions. Updated edition of SNiP 52-01-2003]. Moscow, Minregion Rossii, 2013, 175 pages (in Russian).
2. ENV 1992-1-1: Eurocod 2: Design of Concrete Structures. Part 1: General rules and Rules for Building. European Prestandart. June, 1992.
3. Building Code of Belarus SNB 5.03.01-02 Betonnyye i zhelezobetonnyye konstruksii [Concrete and reinforced concrete structures]. Minsk, Minstroyarkhitektury, 2003, 149 pages (in Russian).
4. Posobiye po proyektirovaniyu betonnykh i zhelezobetonnykh konstruksiy iz tyazhelogo betona bez predvaritel'nogo napryazheniya armatury (k SP 52-101-2003) [A guide for the design of concrete and reinforced concrete structures made of heavy concrete without prestressing reinforcement (to Building Code of Russia SP 52-101-2003)]. TSNIIPromzdaniy, NIIZHB. Moscow, OAO "TSNIIPromzdaniy", 2005, 214 pages (in Russian).
5. **Karpenko N.I.** Obshchiye modeli mekhaniki zhelezobetona [General models of mechanics of reinforced concrete]. Moscow, Stroyizdat, 1996, 412 pages (in Russian).

6. **Karpenko N.I., Eryshev V.A., Latysheva E.V.** Stress-strain Diagrams of Concrete Under Repeated Loads with Compressive Stresses. // *Procedia Engineering*, 2015, Volume 111.
7. **Eryshev V.A.** Energy Model in Calculating the Strength Characteristics of the Reinforced Concrete Components. // *Materials Science Forum*, 2018, Vol. 931, pp. 36-41.
8. **Kodysh E.N., Nikitin I.K., Trekin N.N.** Raschet zhelezobetonnykh konstruktsiy iz tyazhelogo betona po prochnosti, treshchinostoykosti i deformatsiyam [Calculation of reinforced concrete structures of heavy concrete for strength, crack resistance and deformation]. Moscow, Izdatel'stvo Assotsiatsii stroitel'nykh vuzov, 2010, 352 pages (in Russian).
9. **Murashkin G.V., Mordovskiy S.S.** Primeneniye diagramm deformirovaniya dlya rascheta nesushchey sposobnosti vnetsentrenno szhatykh zhelezobetonnykh elementov [The use of strain diagrams for calculating the bearing capacity of eccentrically compressed reinforced concrete elements]. // *Zhilishchnoye stroitel'stvo*, 2013, No. 3, pp. 38-40 (in Russian).
10. **Akimov P.A.** O razvitii diskretno-kontinual'nogo podkhoda k chislenному моделиrovaniyu sostoyaniya nesushchikh sistem vysotnykh zdaniy [On the development of a discrete-continuum approach to numerical modeling of the state of load-bearing systems of high-rise buildings]. // *Promyshlennoye i grazhdanskoye stroitel'stvo*, 2015, No 3, pp. 16-20 (in Russian).
11. **Bondarenko V.M., Kolchunov V.I.** Raschetnyye modeli silovogo soprotivleniya zhelezobetona [Calculation models of strength resistance of reinforced concrete]. Moscow, Izdatel'stvo ASV, 2004, 472 pages (in Russian).
12. **Travush V.I., Kolchunov V.I., Klyuyeva N.V.** Nekotoryye napravleniya razvitiya teorii zhivuchesti konstruktivnykh sistem zdaniy i sooruzheniy [Some directions of the development of the theory of survivability of structural systems of buildings and structures]. // *Promyshlennoye i grazhdanskoye stroitel'stvo*, 2015, No 3, pp. 4-11 (in Russian).
13. **Shah S.P., Jehu R.** Strain rate effects an mode crack propagation in Concrete. // "Fract. Toughness and Fract. Energy". Coner. Proc. Conf. Lensaune. Oct. 1-3, 1985, Amsterdam e. a. 1986, pp. 453-465.
14. **Bazant Z.P., Oh B.H.** Crack Baut theczy for fracture of Concrete. // *Marer. Et. Conctr.*, 1983, Vol. 16, Issue 93, pp. 155-177.

СПИСОК ЛИТЕРАТУРЫ

1. СП 63.13330.2012. Бетонные и железобетонные конструкции. Основные положения. Актуализированная редакция СНиП 52-01-2003. – М.: Минрегион России, 2013. – 175 с.
2. ENV 1992-I-1: Eurocod 2: Design of Concrete Structures. Part 1: General rules and Rules for Building. European Prestandart. Iune, 1992.
3. СНБ 5.03.01-02 Бетонные железобетонные конструкции. – Минск: Минстройархитектуры, 2003. – 149 с.
4. Пособие по проектированию бетонных и железобетонных конструкций из тяжелого бетона без предварительного напряжения арматуры (к СП 52-101-2003). ЦНИИПромзданий, НИИЖБ. – М.: ОАО «ЦНИИПромзданий», 2005. – 214 с.
5. **Карпенко Н.И.** Общие модели механики железобетона. – М.: Стройиздат, 1996. – 412 с.
6. **Karpenko N.I., Eryshev V.A., Latysheva E.V.** Stress-strain Diagrams of Concrete

- Under Repeated Loads with Compressive Stresses. // *Procedia Engineering*, 2015, Volume 111.
7. **Eryshev V.A.** Energy Model in Calculating the Strength Characteristics of the Reinforced Concrete Components. // *Materials Science Forum*, 2018, Vol. 931, pp. 36-41.
 8. **Кодыш Э.Н., Никитин И.К., Трекин Н.Н.** Расчет железобетонных конструкций из тяжелого бетона по прочности, трещиностойкости и деформациям. – М.: АСВ, 2010. – 352с.
 9. **Мурашкин Г.В., Мордовский С.С.** Применение диаграмм деформирования для расчета несущей способности внецентренно сжатых железобетонных элементов. // *Жилищное строительство*, 2013, №3, с. 38-40.
 10. **Акимов П.А.** О развитии дискретно-континуального подхода к численному моделированию состояния несущих систем высотных зданий. // *Промышленное и гражданское строительство*, 2015, №3, с. 16 – 20.
 11. **Бондаренко В.М., Колчунов В.И.** Расчетные модели силового сопротивления железобетона. – М.: АСВ, 2004. – 472 с.
 12. **Травуш В.И., Колчунов В.И., Ключева Н.В.** Некоторые направления развития теории живучести конструктивных систем зданий и сооружений. // *Промышленное и гражданское строительство*, 2015, №3, с. 4 -11.
 13. **Shah S.P., Jehu R.** Strain rate effects an mode crack propagation in Concrete. // “*Fract. Toughness and Fract. Energy*”. Coner. Proc. Conf. Lensaune. Oct. 1-3, 1985, Amsterdam e. a. 1986, pp. 453-465.
 14. **Bazant Z.P., Oh B.H.** Crack Baut theczy for fracture of Concrete. // *Marer. Et. Conctr.*, 1983, Vol. 16, Issue 93, pp. 155-177.
- Dr.Sc.; Togliatti State University, Belorusskaya, 14, Togliatti, 445020, Russia;
E-mail: gsx@tltsu.ru.
- Nickolay I. Karpenko, Full Member of the Russian Academy of Architecture and Construction Sciences, Professor, Dr.Sc.; Federal State Budgetary Institution “Research Institute of Construction Physics of the Russian Academy of Architecture and Construction Sciences” (RICP RAACS) ; тел. +7(495) 482-40-76; факс: +7(495) 482-40-60; e-mail: niisf@niisf.ru.
- Artur O. Zhemchuyev, Togliatti State University, Belorusskaya, 14, Togliatti, 445020, Russia;
E-mail: gsx@tltsu.ru.
- Ерышев Валерий Алексеевич, советник Российской академии архитектуры и строительных наук (РААСН), профессор, доктор технических наук; профессор кафедры «Городское строительство и хозяйство», Тольяттинский государственный университет; 445020, Россия, г. Тольятти, ул. Белорусская, д. 14; тел. 53-91-50;
E-mail: gsx@tltsu.ru.
- Карпенко Николай Иванович, академик РААСН), профессор, доктор технических наук; федеральное государственное бюджетное учреждение «Научно-исследовательский институт строительной физики Российской академии архитектуры и строительных наук» (НИИСФ РААСН); 127238, Россия, г. Москва, Локомотивный проезд, д. 21; тел. +7(495) 482-40-76; факс: +7(495) 482-40-60; E-mail: niisf@niisf.ru.
- Жемчуев Артур Олегович, Тольяттинский государственный университет; 445020, Россия, г. Тольятти, ул. Белорусская, д. 14;
E-mail: gsx@tltsu.ru.

STUDY OF STRESS-STRAIN STATES OF A REGULAR HINGE-ROD CONSTRUCTIONS WITH KINEMATICALLY ORIENTED SHAPE CHANGE

Peter P. Gaydzhurov¹, Elvira R. Iskhakova², Nadezhda G Tsaritova²

¹ Don State Technical University, Rostov-on-Don, Russia

² Platov South-Russian State Polytechnic University, Novocherkassk, Russia

Abstract: For regular hinge-rod structures, an engineering method for analyzing the stress-strain state is developed, taking into account the transformation of the form by folding repeated fragments of the structure. For the software implementation of the proposed calculation algorithm, a macro is compiled in the APDL language, which is built into the ANSYS software package. A step-by-step procedure that simulates the transformation of the farm geometry was tested.

Keywords: hinge-rod structures, finite element method, truss element stiffness matrix, the stiffness matrix of a mechanical drive, the stress-strain state

ИССЛЕДОВАНИЕ НАПРЯЖЕННО-ДЕФОРМИРОВАННОГО СОСТОЯНИЯ РЕГУЛЯРНОЙ ШАРНИРНО-СТЕРЖНЕВОЙ КОНСТРУКЦИИ ПРИ КИНЕМАТИЧЕСКИ ОРИЕНТИРОВАННОМ ИЗМЕНЕНИИ ФОРМЫ

П.П. Гайджуров¹, Э.Р. Исхакова², Н.Г. Царитова³

¹Донской государственный технический университет, г. Ростов-на-Дону, Россия

²Южно-Российский государственный политехнический университет (НПИ) имени М.И. Платова,
г. Новочеркасск, РОССИЯ

Аннотация: для регулярных шарнирно-стержневых конструкций разработана инженерная методика анализа напряженно-деформированного состояния с учетом трансформации формы путем сворачивания повторяющихся фрагментов конструкции. Для программной реализации предлагаемого алгоритма расчета составлен макрос на языке APDL, встроенного в программный комплекс ANSYS. Выполнено тестирование шаговой процедуры, моделирующей процесс трансформации геометрии пространственной фермы.

Ключевые слова: шарнирно-стержневые конструкции, метод конечных элементов, матрица жесткости ферменного элемента, матрица жесткости механического привода, напряженно-деформированное состояние

INTRODUCTION

One of the creative directions in modern architecture is the so-called kinematic design, based on a controlled change in the geometry of the structure in order to obtain the required space planning decisions [1,2]. According to the principle of transformation of geometry, building structures can be divided into the following groups [3]:

- moving in space along the guides;
 - performing a rotation about the axis of rotation;
 - folding or rolling on the principle of a fan.
- The technology of constructions made of origami, which are capable, compressing and stretching, to qualitatively change shape should be added to this. The idea of creating such building structures was taken from the field of aerospace systems such as solar panels and mir-

rors with a large surface [4].

As examples of existing original transformable building structures, Thomas Heterwick's folding bridge [5], built in London in 2004 and the folding bridge in Germany (1997), which is called «Horn», which became a landmark of Kiel [6], can be mentioned.

At the same time, there is practically no information in the literature of structural mechanics about the mathematical modeling of transformable building systems taking into account the form change. In this regard, the direction associated with the development of an engineering methodology, the calculation of geometrically variable structures using the finite element method (FEM) is relevant.

In FEM, the relationship between deformations at an arbitrary point of a finite element and the corresponding nodal displacements is generally represented in matrix form [7]

$$\{\varepsilon\} = [\Phi]\{u\} \quad (1)$$

where $\{\varepsilon\}$ and $\{u\}$ – are the column vectors of the components of the strain tensor and nodal displacements; $[\Phi]$ – is a matrix of form functions, depending on the type of the finite element and the approximating functions.

By the hypothesis of infinitesimal deformations, it is generally accepted that the matrix does not change during loading on element. This assumption is the basis of the so-called infinitesimal theory of deformations, i.e., a theory when deformations are considered infinitesimal quantities. The use of this theory is quite justified if a change in the nodal coordinates of the finite element mesh can be neglected, during the deformation of the structure. However, in some cases, due to large elasto-plastic strains or large translational and angular displacements of the model, in order to obtain an exact solution, it is necessary to take into account the change of the matrices of finite elements. Such a theory is called the theory of finite strains. In the framework of the theory of finite strains, various step-by-step procedures are applied for the numerical implementation of calculations, the essence of

which is to represent the loading process in the form of a stepwise or continuous increase in the load parameter. Moreover, at each step, as a rule, a scheme for iterative refinement of the solution is provided.

The method to describe the current deformed state of the finite element model and the initial coordinates are used is called the method of Lagrange. In case of large displacements, for example during structural modification at the beginning of each loading step, the initial coordinates are used. This method of representing deformations is called the modified method of Lagrange [8]. The present work is devoted to the extension of the modified Lagrange method to the problem of analyzing the stress-strain state of a spatial truss structure with kinematically directed shape transformation in the plane of minimal stiffness.

2. CALCULATION METHOD

To analyze the stress-strain state of a hinged structure with a regular structure, we use the ANSYS Mechanical software [9], which implements the FEM in the form of a displacement method. As an object of research we consider a space truss structured in the form of repeating semi-octahedron (Figure 1).

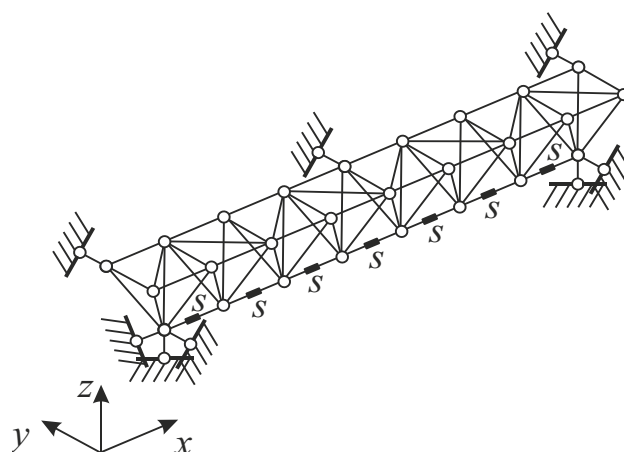


Figure 1. Initial state of the truss.

The geometrical dimension of the truss are set in the global Cartesian coordinate system

x, y, z . The truss shape transformation is provided using, located in the back bar of the structure, rods-drives with variable length. In this case, the process of forming takes place in such a way that the lengths of the rods of the top-chord and the lattice of the truss practically do not change. In Figure 1, the drive rods are indicated by s . Note that the operating mechanism of these rods provides a direct and reverse stroke, i.e., mounting and dismounting of the structure. To simulate the process of kinematically oriented structural change, we use the finite element (FE) LINK 11 (Figure 2), which allows you to change the distances s between nodes i and j .

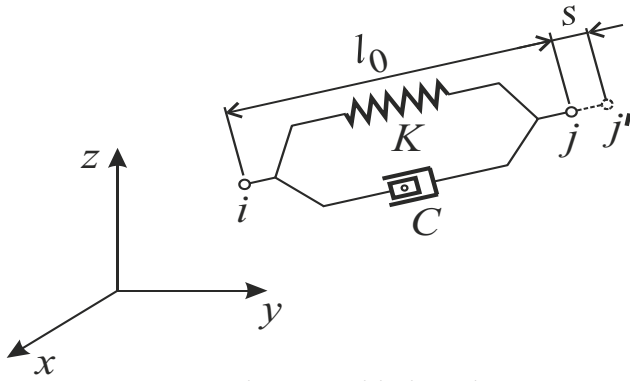


Figure 2. FE with a variable length LINK 11.

We model the rods of the top-chord and lattice with 3D truss elements of the LINK 180 type (Figure 3). In this figure the next symbols are marked: l – the length of the rod; EF – longitudinal stiffness.

The axis \bar{x} of the truss CE forms with the axes x, y, z the angles directing cosines, which are determined by the formulas:

$$\cos(x\bar{x}) = \frac{x_i - x_j}{l}; \quad \cos(y\bar{x}) = \frac{y_i - y_j}{l}; \quad \cos(z\bar{x}) = \frac{z_i - z_j}{l}. \quad (2)$$

Let's introduce the notation:

$$t_{11} = \cos(x\bar{x}), \quad t_{12} = \cos(y\bar{x}), \quad t_{13} = \cos(z\bar{x}).$$

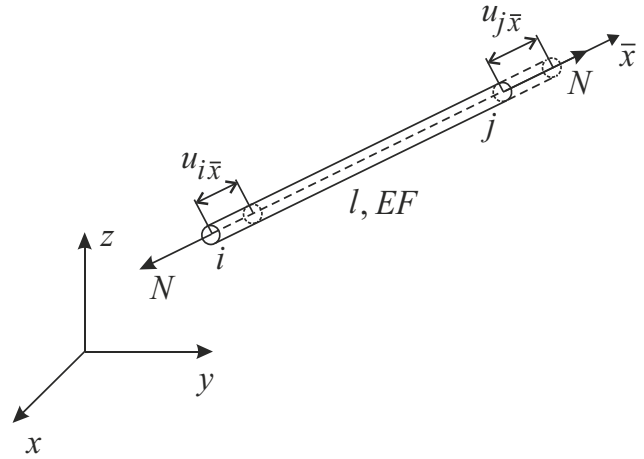


Figure 3. Truss FE LINK 180.

The relationship between the FE nodal displacements $u_{i\bar{x}}$ and $u_{j\bar{x}}$ and their projections u_{ix}, u_{iy}, u_{iz} and u_{jx}, u_{jy}, u_{jz} on the global coordinate axes is described by the relations:

$$u_{i\bar{x}} = u_{ix}t_{11} + u_{iy}t_{12} + u_{iz}t_{13};$$

$$u_{j\bar{x}} = u_{jx}t_{11} + u_{jy}t_{12} + u_{jz}t_{13}.$$

Hereinafter, the first index corresponds to the FE node number.

Axial force N in the axes x, y, z is decomposed into the following nodal components:

$$F_{ix} = -Nt_{11}; \quad F_{iy} = -Nt_{12}; \quad F_{iz} = -Nt_{13};$$

$$F_{jx} = Nt_{11}; \quad F_{jy} = Nt_{12}; \quad F_{jz} = Nt_{13}.$$

The equilibrium equation of truss FE in the axes x, y, z in matrix form has the form

$$[\mathbf{h}]\{\mathbf{u}\} = \{\mathbf{F}\}, \quad (3)$$

where column vectors of nodal displacements and forces

$$\{\mathbf{u}\} = \{u_{ix} u_{iy} u_{iz} u_{jx} u_{jy} u_{jz}\}^T;$$

$$\{\mathbf{F}\} = \{F_{ix} F_{iy} F_{iz} F_{jx} F_{jy} F_{jz}\}^T$$

(T – the symbol of matrix transposition operation); finite element stiffness matrix

$$[\mathbf{h}] = \frac{EF}{l}[\mathbf{t}], \quad (4)$$

direction cosines matrix

$$[\mathbf{t}] = \begin{bmatrix} t_{11}^2 & t_{11}t_{12} & t_{11}t_{13} & -t_{11}^2 & -t_{11}t_{12} & -t_{11}t_{13} \\ & t_{12}^2 & t_{12}t_{13} & -t_{12}t_{11} & -t_{12}^2 & -t_{12}t_{13} \\ & & t_{13}^2 & -t_{13}t_{11} & -t_{13}t_{12} & -t_{13}^2 \\ & & & t_{11}^2 & t_{11}t_{12} & t_{11}t_{13} \\ & & & & t_{12}^2 & t_{12}t_{13} \\ & & & & & t_{13}^2 \end{bmatrix}$$

As is obvious, the matrix elements $[\mathbf{h}]$ depend on the nodal coordinates x_i, y_i, z_i and x_j, y_j, z_j , which, with large displacements of the rod, change significantly compared to the initial values.

The LINK 11 element (Figure 2), having a length in the initial state l_0 , is endowed with longitudinal stiffness properties K and viscoelastic damping C . The latter is not used in this analysis. The stiffness matrix of the LINK 11 element in the global coordinate system can be represented in the form

$$[\mathbf{h}_{np}] = K[\mathbf{t}], \quad (5)$$

The components of the corresponding column vector of nodal forces are written as $\{\mathbf{F}_{ax}\} = N_{ax} \{-t_{11} -t_{12} -t_{13} \ t_{11} \ t_{12} \ t_{13}\}^T$ where $N_{ax} = Ks$ – axial force, due to the stroke of the drive s .

Thereafter, we accept the following assumptions:

- to describe the deformation of the structure in the process of shaping, we apply the modified method of Lagrange;
- the process of transformation of the structure represents a quasistatic sequence of steps $k=1, 2, \dots, n$ of discrete change in the lengths of elements LINK 11 by a small amount s ;

- rectilinear rods before deformation remain rectilinear after deformation;
- the cross sections of each rod remain normal to its longitudinal axis during deformation;
- we neglect the change in the longitudinal stiffness of the rods during the structural modification, i.e. we believe that the behavior of the material throughout the course of form-change obeys Hooke's law;
- in the process of transformation of the structure, the achieved level of the stress state of the rods is remain intact.

The geometry and stress state transformation of the rod modeled by the LINK 180 element is schematically shown in Figure 4. We emphasize that the transition from the current position of the rod to the subsequent position is accompanied by small increments in the values of the nodal coordinates.

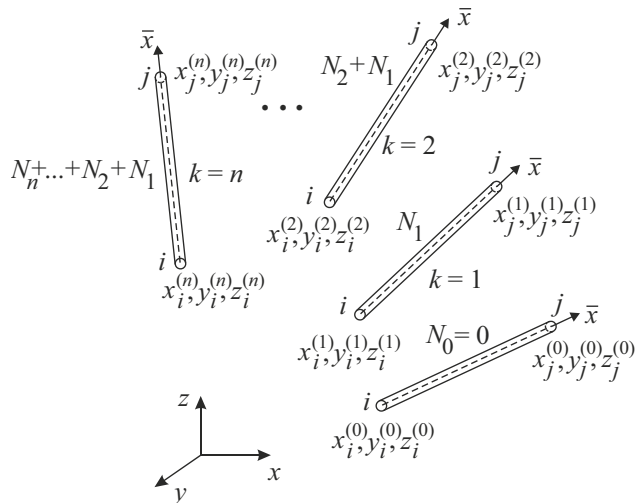


Figure 4. Visualization of the process of transformation of the rod.

The flow diagram of the algorithm developed on the basis of the accepted assumptions is shown in Figure 5. Abbreviations are introduced here: BC – boundary conditions; SLAE – simultaneous linear algebraic equations. APDL programming language is used For the software implementation of this algorithm [10], which is built into the ANSYS Mechanical. Created on the basis of this language the application macro is entered into the command window, after which

each line of the macro is processed by the APDL interpreter and, if the result is positive, is immediately launched. Thus, the macro allows you to automatically create the geometry of the structure, build a finite element mesh, set the boundary conditions and load, start the solver to perform the calculation, as well as carry out intermediate operations associated with extracting information from the ANSYS database at the current loading step and generating working arrays by performing the necessary algebraic procedures. In addition to the above actions, the macro contains commands to delete the finite element model at the current calculation step.

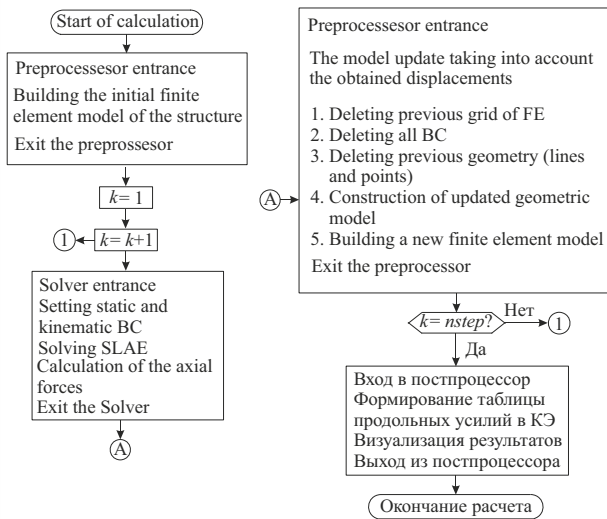


Figure 5. The block diagram of the transformable hinged structure calculating algorithm

Note that in the proposed macro the procedure of direct calculation of the axial forces in the truss rods using the formula

$$N_k = \frac{EF}{l_{k-1}} (l_k - l_{k-1}). \quad (6)$$

This approach is explained by the fact that when using LINK 180 FE values N_k are calculated in relation to the initial (undeformed) element length. With the proposed step-by-step method of representing the process of structural modification, this method leads to incorrect results.

2. NUMERICAL CONVERGENCE OF CONVERGENCE

Testing the developed algorithm and the corresponding macro is feasible on the example of the spatial truss shown in Fig. 1. Initial data: rods of the top-chord and lattice have a tubular cross-sectional area of $F = 0,113 \cdot 10^{-3} \text{ m}^2$; modulus of elasticity of the material of the rods (steel) $E = 2,1 \cdot 10^5 \text{ МПа}$; specific density $\gamma = 7800 \text{ kg/m}^3$. Overall dimensions in meters for a repeating fragment of the truss (semi-octahedron) are shown in Figure 6.

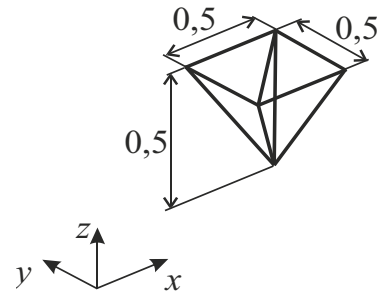


Figure 6. The repeating fragment of the truss

Stiffness coefficient and mass of the mechanical drive modeled by the LINK 11 element is $K = 1 \cdot 10^{10} \text{ N/m}$; $m_{ax} = 20 \text{ kg}$.

In Figure 7 shows graphs of changes in the height of the lift h and the bay l_{ax} of the truss depending on the stroke of the drive s and taking into account its own weight.

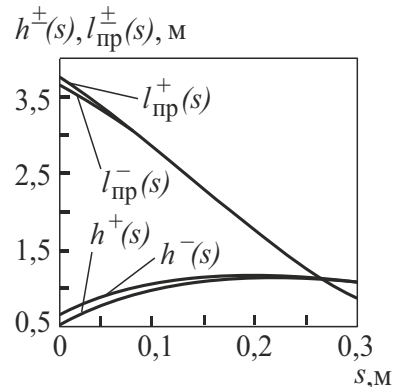


Figure 7. Graphs $h^{\pm}, l_{\pm}^{\pm} \sim s$ for $s = 0,01 \text{ m}$ and $nstep = 30$.

Here, the «+» sign corresponds to the forward stroke (camber of truss), the «-» sign to the reverse stroke (returning the truss to the initial state). The graphs in Figure 7 are obtained with the stroke value at the transformation step $s=0,01\text{m}$ and the number of transformation $nstep = 30$. Visualization of the patterns of the forward and reverse transformation of the truss for these parameters s and $nstep$ are presented in Figure 8.

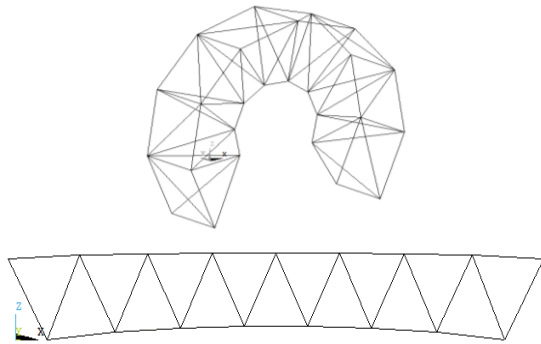


Figure 8. Visualization of the patterns of direct and reverse transformation of the farm $s=0,01\text{ m}$ and $nstep=30$.

Analyzing the graphs in Figure 7 and the type of structure after the reverse transformation, we establish that the geometry of the model as a result of the assembly-disassembly cycle is not restored to its original state and in this case there is a residual deflection of the truss top chord and truss back bar.

Figures 9 and 10 show the results of a similar calculation for the values of the parameters $s=0,001\text{m}$ and $nstep=300$. For comparison, the values of the parameters $h^+(0,3)$ and $l_{ax}^+(0,3)$ amounted to: for $s=0,01\text{ m}$ and $nstep=30$ – $h^+(0,3)=1,071\text{ m}$, $l_{np}^+(0,3)=0,8553\text{ m}$; for $s=0,001\text{m}$ and $nstep=300$ – $h^+(0,3)=1,036\text{ m}$, $l_{ax}^+(0,3)=0,9263\text{ m}$.

From the data presented it follows that with a tenfold decrease in the parameter s and the same increase in the parameter $nstep$ a satisfactory coincidence of the simulation results with a picture of the real behavior of the structure under consideration during direct and reverse transfor-

mation is observed.

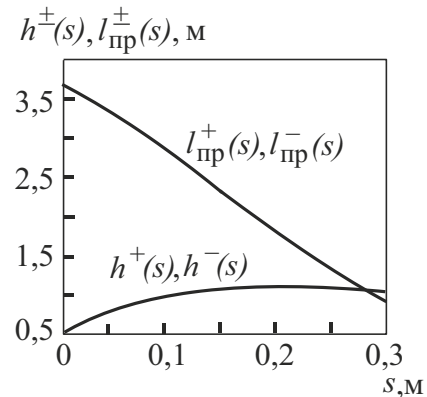


Figure 9. Graphs $h^{\pm}, l_{np}^{\pm} \sim s$ for $s=0,001\text{m}$ and $nstep=300$.



Figure 10. Visualization of the picture of the reverse transformation of the truss for $s=0,001\text{ m}$ and $nstep=300$.

Axial force diagram N in the rods of the top chord and the lattice of the test truss for various values of the parameters s and $nstep$ are shown in Figures 10 and 11. From the above data it can be seen that the values N in the truss rods substantially depend on the calculated parameters s and $nstep$.

For comparison, Figure 12 shows a picture of the transformation of a test truss with a direct forward stroke of actuators by a value. $s=0,3\text{m}$. This solution was obtained as part of a linear calculation.

As you can see the picture of the farm in a deformed state, shown in Figure 12, differs qualitatively from the picture obtained in the step-by-step transformation scheme of Figure 8.

When using the option of accounting for large displacements («Large Displacement Static») in the case of simultaneous calculation ($s=0,3\text{m}$) we obtain a picture of the structure in the transformed state similar to that shown in Figure 8.

The values of the transformation parameters are $h^+(0,3)=1,037\text{ m}$, $l_{np}^+(0,3)=0,9034\text{ m}$.

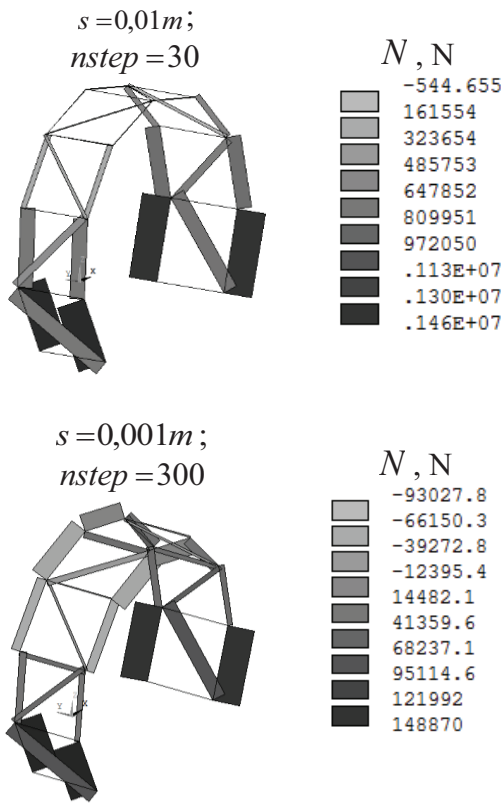


Figure 10. Axial force diagram N in the rods of the truss top chord

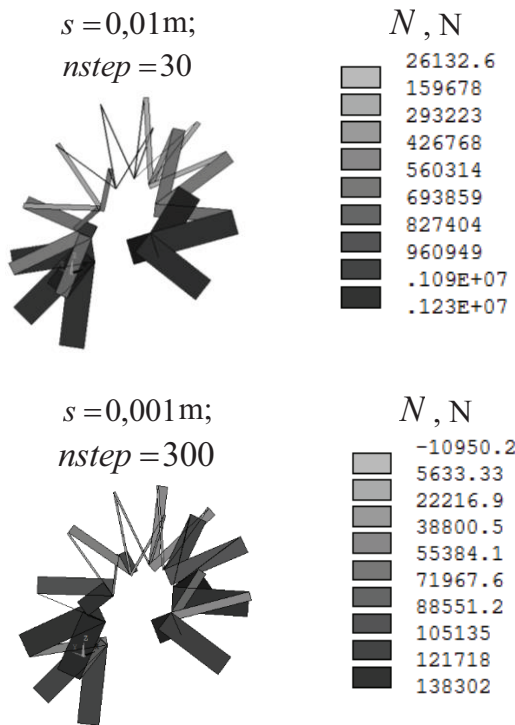


Figure 11. Axial force diagram N in the rods of the truss lattice

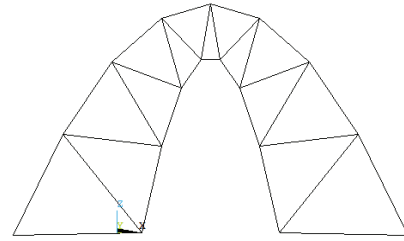


Figure 12. Simultaneous transformation of the truss for $s = 0,3m$.

However, it was found that the calculation in a geometrically nonlinear setting does not allow to take into account the installation history. The obtained values of the longitudinal forces in the truss rods are very underestimated.

3. EXAMPLE.

As a demonstration example, consider an industrially significant truss formed by 24 semi-octahedron (Figure 13).

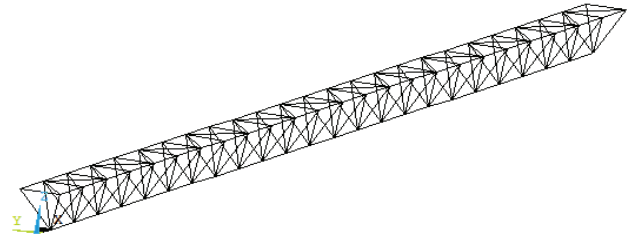


Figure 13. Initial truss position.

Initial data: rods of the top chord and lattice have a tubular cross section with an area of $F = 0,2901 \cdot 10^{-2} \text{ m}^2$; modulus of elasticity of the material of the rods (aluminum alloy D16T) $E = 7,2 \cdot 10^4 \text{ MPa}$; specific density $\gamma = 2885 \text{ kg/m}^3$. The value of the temporary resistance of the material $\sigma_{tol} = 420 \text{ MPa}$. The overall dimensions of the semi-octahedron are tripled in comparison with the test example (Figure 6). Mounting process is simulated by analogy with a test example, accepting $s = 0,001$, $nstep = 200$. The initial bay $l_{np} = 35 \text{ m}$.

The results of finite element modeling are presented in Figures 13-16.

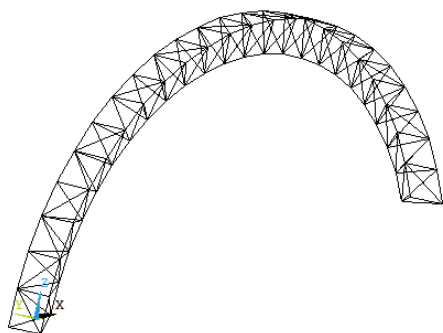


Figure 14. The truss position after the form transformation.

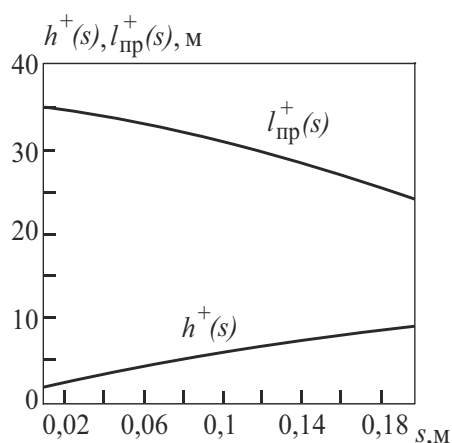


Figure 15. Graphs $h^{\pm}, l_{np}^{\pm} \sim s$.

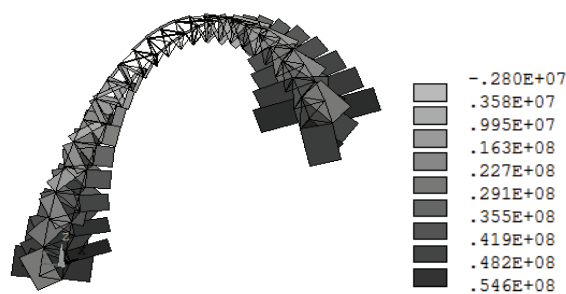


Figure 16. Axial force diagram N .

The resulting height of the form was $h^+(0,2) = 8,43$ m, and the total bay $l_{np}^+(0,2) = 25$ m (Figures 14, 15).

Figure 16 shows that the maximum value of compressive axial force $N_{\max} = -2800$ kN arises in the elements of the «boss» of the arch. This val-

ue N_{\max} corresponds to the maximum compressive stress $\sigma_{\max} = -0,965$ MPa, which is significantly less than the value σ_{σ} .

The critical value of the axial force for a axial compressed rod with a given size and mechanical characteristics is equal. $N_{cr} = 9044$ kN.

Safety factor for a compression rod

$$n_y = N_{cr} / |N_{\max}| = 3,23.$$

Thus, the initial stress state of the arched type structure under consideration fully satisfies the requirements of operation.

CONCLUSIONS

1. An engineering method for calculating the stress-strain state of regular hingerod structures with a kinematical oriented shape change has been developed.
2. A numerical study of the convergence of the step procedure modeling the process of controlled shaping of a regular hinged rod structure was carried out.

REFERENCES

1. Tumasov A.A., Tsaritova N.G., Kurbanov A.I., Kalinina A.A. Geometricheskie parametry sterzhnevyyh transformiruemyh arochnyyh system [Geometric parameters of rod-shaped transformable arch systems]. // *Construction and Architecture*, 2017, Vol. 2(15), pp. 135-140 (in Russian).
2. Tumasov A.A., Tsaritova N.G. Geometricheskie zakonomernosti obrazovaniya obemno-prostranstvennyh form v arhitekture iz ploskiy kinematicheskikh struktur [Geometric patterns of the formation of volumetric-spatial forms in architecture from flat kinematic structures]. // *Reporter of the Belgorod State Technologi-*

- cal University V.G. Shukhov*, 2019, Vol. 2, pp. 122-130 (in Russian).
3. **Usukin V.I.** Stroitel'naja mehanika konstrukcij kosmicheskoy tehniki [Structural mechanics of space systems]. Moscow, Mechanical Engineering, 1988. 392 pages (in Russian).
4. **Semenov V.S., Akbaraliev R.** Transformiruemye konstrukcii pokrytij v sovremennoj arhitekture [Transformable roof structures in modern architecture]. // *Vestnik of KRSU*, 2010, Vol. 10, Issue 2, pp. 25-31 (in Russian).
5. **Tornhill C.** London Bridge is rolling up: The spectacular Rolling Bridge that unfolds every Friday at noon. Daily Mail. 22.09.2018.
6. https://www.kiel.de/de/kultur_freizeit/museum/stadtmuseum_warleberger_hof.php.
7. **Sakharov A.S., Altrnbach I.** (Eds.) Metod konechnyh jelementov v mehanike tverdyh tel [The finite element method in the mechanics of solids]. Kiev, Vishcha school, 1982, 480 pages (in Russian).
8. **Hibbitt H.D., Marcal H.V., Rice J.R.** A finite element formulation for problems of the large strain and large displacement. // *International Journal of Solids Structures*, 1970, Vol. 6, pp. 1069-1086.
9. **Basov K.A.** ANSYS: spravochnik pol'zovatelja [ANSYS: user guide]. Moscow, DMK Press, 2012, 640 pages.
10. **Morozov E.M., Muizemnek A.Yu., Shadsky A.S.** ANSYS v rukah inzhenera: Mehanika razrushenija [ANSYS in the hands of an engineer: Mechanics of destruction]. Moscow, LENAND, 2008, 456 pages (in Russian).
2. **Тумасов А.А., Царитова Н.Г.** Геометрические закономерности образования объемно-пространственных форм в архитектуре из плоских кинематических структур. // *Вестник Белгородского государственного технологического университета им. В.Г. Шухова*, 2019, №2, с. 122-130.
3. **Усюкин В.И.** Строительная механика конструкций космической техники. – М.: Машиностроение, 1988. – 392 с.
4. **Семенов В.С. Акбаралиев Р.** Трансформируемые конструкции покрытий в современной архитектуре. // *Вестник КРСУ*, 2010, Том 10, №2, с. 25-31.
5. **Tornhill C.** London Bridge is rolling up: The spectacular Rolling Bridge that unfolds every Friday at noon. Daily Mail. 22.09.2018.
6. https://www.kiel.de/de/kultur_freizeit/museum/stadtmuseum_warleberger_hof.php.
7. **Сахаров А.С., Альтенбах И.** (ред.) Метод конечных элементов в механике твердых тел. – Киев: Вища школа, 1982. – 480 с.
8. **Hibbitt H.D., Marcal H.V., Rice J.R.** A finite element formulation for problems of the large strain and large displacement. // *International Journal of Solids Structures*, 1970, Vol. 6, pp. 1069-1086.
9. **Басов К.А.** ANSYS: справочник пользователя. – М.: ДМК Пресс, 2012. – 640 с.
10. **Морозов Е.М., Муйземнек А.Ю., Шадский А.С.** ANSYS в руках инженера: Механика разрушения. – М.: ЛЕНАНД, 2008. – 456 с.

СПИСОК ЛИТЕРАТУРЫ

1. **Тумасов А.А., Царитова Н.Г., Курбанов А.И., Калинина А.А.** Геометрические параметры стержневых трансформируемых арокных систем. // *Стро-*

Petr P. Gaydzhurov, Advisor of the Russian Academy of Architecture and Construction Sciences, Professor, Doctor of Technical Sciences, Department of Technical Mechanics; Don State Technical University; Gagarin square 1, Rostov-on-Don, 344000, Russia; phone 8 800 100-19-30; e-mail: reception@donstu.ru.

Elvira R. Iskhakova, Head of the Department of Building Structures, LLC Southern Project Institute (Rostov-on-

Don); Platov South-Russian State Polytechnic University (NPI); Prosveshcheniya St. 132, Rostov region, Novocherkassk, 346428, Russia; phone: 8 (8635) 25-51-51; E-mail: pressa_npi@mail.ru.

Nadezhda G Tsaritova, Ph.D., Associate Professor, Department of "Urban planning, design of buildings and structures"; Platov South-Russian State Polytechnic University (NPI); Prosveshcheniya St. 132, Rostov region, Novocherkassk, 346428, Russia; phone: 8 (8635) 25-51-51; e-mail: pressa_npi@mail.ru.

Гайджуров Петр Павлович, советник Российской академии архитектуры и строительных наук, профессор, доктор технических наук; федеральное государственное бюджетное образовательное учреждение высшего образования «Донской государственный технический университет»; 344000, Россия, ЮФО, Ростовская область, г.Ростов-на-Дону, пл. Гагарина, 1; тел. 8 800 100-19-30; e-mail: reception@donstu.ru.

Исхакова Э.Р., федеральное государственное бюджетное образовательное учреждение высшего образования «Южно-Российский государственный политехнический университет (НПИ) имени М.И. Платова»; 346428 Россия, г. Новочеркасск, Ростовская обл., ул. Просвещения 132; тел. 8 (8635) 25-51-51; E-mail: pressa_npi@mail.ru.

Царитова Н.Г., федеральное государственное бюджетное образовательное учреждение высшего образования «Южно-Российский государственный политехнический университет (НПИ) имени М.И. Платова»; 346428 Россия, г. Новочеркасск, Ростовская обл., ул. Просвещения 132; тел. 8 (8635) 25-51-51; E-mail: pressa_npi@mail.ru.

FINITE ELEMENTS OF THE PLANE PROBLEM OF THE THEORY OF ELASTICITY WITH DRILLING DEGREES OF FREEDOM

Viktor S. Karpilovskyi

ScadGroup Ltd., Kyiv, UKRAINE

Abstract: Twelve new finite elements with drilling degrees of freedom have been developed: triangular and quadrangular elements based on a modified hypothesis about the value of approximating functions on the sides of the element, which made it possible to avoid dimensional instability when all rotation angles are zero; incompatible and compatible triangular and quadrangular elements which can have additional nodes on the sides. Approximating functions satisfy the following condition: the value of the rotational degree of freedom of a node is nonzero and equal to one only for one of them. Numerical examples illustrate estimated minimum orders of convergence for displacements and stresses. All created elements retain the existing symmetry of the design models.

Keywords: finite elements, drilling degrees, plane problem, triangular element, rectangular element, quadrangular element

КОНЕЧНЫЕ ЭЛЕМЕНТЫ ПЛОСКОЙ ЗАДАЧИ ТЕОРИИ УПРУГОСТИ С ВРАЩАТЕЛЬНЫМИ СТЕПЕНЯМИ СВОБОДЫ

В.С. Карпиловский

ООО ScadGroup, г. Киев, УКРАИНА

Аннотация: Построено двенадцать новых конечных элементов с вращательными степенями свободы: треугольные и четырехугольные элементы на основе модифицированной гипотезы о значении аппроксимирующих функций на сторонах элемента, позволившей исключить геометрическую изменяемость при равенстве нулю всех углов поворота; несовместные и совместные треугольные и четырехугольные элементы, которые могут иметь дополнительные узлы на сторонах. При этом аппроксимирующие функции удовлетворяют условию: значение вращательной степени свободы узла только для одной из них отлично от нуля и равно единице. Приведены оценки минимальных порядков сходимости по перемещениям и напряжениям, иллюстрированные численными примерами. Все построенные элементы сохраняют существующую симметрию расчетных схем.

Ключевые слова: конечные элементы, вращательные степени свободы, плоская задача, треугольный элемент, прямоугольный элемент, четырехугольный элемент

1. INTRODUCTION

Let us consider the Lagrange functional of the plane problem of the theory of elasticity:

$$\Pi(\mathbf{u}) = \frac{1}{2} \int_{\Omega} (\mathbf{A}\mathbf{u})^T \mathbf{D}\mathbf{A}\mathbf{u} d\Omega - \int_{\Omega} \mathbf{f}^T \mathbf{u} d\Omega \quad (1)$$

where: Ω – plate of thickness h : solid body with a midplane XOY ;

$$\mathbf{u}(\mathbf{x}) = \begin{Bmatrix} u(\mathbf{x}) \\ v(\mathbf{x}) \end{Bmatrix}$$

– displacements of the point,

$$\mathbf{x} = \begin{Bmatrix} x \\ y \end{Bmatrix}, \quad \mathbf{f}(\mathbf{x}) = \begin{Bmatrix} f_x(\mathbf{x}) \\ f_y(\mathbf{x}) \end{Bmatrix}$$

– area load.

The geometry operator \mathbf{A} and the elasticity matrix \mathbf{D} (for an isotropic material) are:

$$\mathbf{A}^T = \begin{bmatrix} \frac{\partial}{\partial x} & 0 & \frac{\partial}{\partial y} \\ 0 & \frac{\partial}{\partial y} & \frac{\partial}{\partial x} \end{bmatrix}, \quad \mathbf{D} = \frac{E}{1-\nu^2} \begin{bmatrix} 1 & \nu & 0 \\ \nu & 1 & 0 \\ 0 & 0 & \frac{1-\nu}{2} \end{bmatrix}, \quad (2)$$

E – Young's modulus, ν – Poisson's ratio.

Classic finite elements have two degrees of freedom in each node: nodal displacements $u_i, v_i, i=1,2,\dots,N$, where N is the number of element nodes. There are also more complex elements with three degrees of freedom in a node, when the following values can be taken into account in addition to the displacement values:

- averaged rotation angle:

$$\omega_i = \omega_z(\mathbf{x}_i), \quad \omega_z = \frac{1}{2} \left(\frac{\partial v}{\partial x} - \frac{\partial u}{\partial y} \right) \quad (3)$$

According to [1] the value ω_z characterizes the rotation of an infinitesimal volume surrounding a point. This value is invariant with respect to orthogonal transformations of coordinate systems.

- the paper [2] proposes and the papers [3-5 et al.] develop the approach when the degrees of freedom θ_j with the following hypotheses are introduced at the nodes:

- a) tangential displacement u_τ varies linearly on the side ij ;
- b) normal displacement u_n varies according to the law:

$$u_n = (1-\xi)u_{ni} + \xi u_{nj} + \frac{a_{ij}}{2} (\theta_j - \theta_i) \xi (1-\xi), \quad (4)$$

$$\mathbf{x} = \mathbf{x}_i + \xi(\mathbf{x}_j - \mathbf{x}_i), \quad \boldsymbol{\tau}_{ij} = (\mathbf{x}_j - \mathbf{x}_i) / a_{ij}$$

$$a_{ij} = |\mathbf{x}_j - \mathbf{x}_i|$$

– side length;

- in order to avoid dimensional instability which can occur when all degrees of freedom are equal θ_j according to the hypothesis (4), we will assume that the normal displacement u_n varies according to the law proposed in [6]:

$$u_n = (1-\xi)u_{ni} + \xi u_{nj} + \frac{a_{ij}}{2} \xi (1-\xi) (\theta_j - \theta_i + \varepsilon (\theta_j + \theta_i) (1-2\xi)), \quad (5)$$

$\varepsilon = \text{const.}$

Degrees of freedom θ_j , created according to the hypothesis (5) will be called **quasi-rotational**. And for the function $\boldsymbol{\varphi}_i(\mathbf{x})$, corresponding to the degree of freedom θ_i :

$$\omega_z(\boldsymbol{\varphi}_i(\mathbf{x})) \Big|_{\mathbf{x}_j} = \begin{cases} 0.5(1-\varepsilon), & i=j, \\ -0.25(1+\varepsilon), & i \neq j, \text{ side} \\ 0, & i \neq j, \text{ diagonal} \end{cases} \quad (6)$$

If we substitute $\varepsilon = -1$ into (6), we obtain:

$$u_n = (1-\xi)u_{ni} + (1-\xi)u_{nj} + a_{ij} \xi (1-\xi) (\theta_j \xi - \theta_i (1-\xi)) \quad (7)$$

and $\omega_z(\boldsymbol{\varphi}_i(\mathbf{x})) \Big|_{\mathbf{x}_j} = \delta_{ij}^j, \quad i,j=1,2,\dots,N$.

The direction of the normal vector to the side \mathbf{n}_{ij} for (4) and (5) is selected in such a way so that the system $\mathbf{n}_{ij}, \boldsymbol{\tau}_{ij}$ and \mathbf{OZ} is right-hand. The *compatibility* of the respective system of approximating functions is provided in both cases.

However, (4) has the following disadvantages:

- a) since the degrees of freedom θ_j in (4) are included only as a difference between the values on the sides, it is necessary to create additional constraints in order to avoid degeneracy of the system or to introduce fictitious rigidities;
- b) the calculated values θ_j can be quite far from the actual rotation angles.

Additional constraints are not required for (5). As shown by numerical experiments we obtain

good accuracy of the results for small values of ε , which almost coincides with that of the results for displacements and stresses with the elements according to the hypothesis (4). The values of the “rotation angles” θ_j are more realistic.

For hypotheses (4) and (5):

a) moment loads are **incorrect**;

b) when creating elements with intermediate nodes on the sides, it is almost impossible to agree the physical meaning of θ_j at the vertices and on the sides. Therefore, θ_j are either not determined on the sides as in [7], or are determined artificially as in [8].

The degrees of freedom θ_j for (4) and (5) no longer have an exact physical meaning. They can hardly be interpreted as “**rotation angles**”. However, the corresponding approximating functions do not contradict the ideology of the FEM as a projection-grid method and show good results in shell analysis.

A large number of elements with rotational degrees of freedom based on formulations other than the Lagrange functional were created: hybrid elements based on a mixed functional [9], elements based on the Trefftz method [10], on the expansion by displacement modes [11] etc. [12,13,14 at al.]. The list of publications on this subject is obviously not complete. The elements considered in this paper are based on the Lagrange functional.

As confirmed by numerical experiments, the load can be given as moments: both nodal and distributed over an element (for example, along the side), for elements which have degrees of freedom ω_z and ensure convergence of the method. The reduced nodal moments are calculated according to a standard formula:

$$M_i = \int_{\Omega} M(x, y) \omega_z(\boldsymbol{\varphi}_i) d\Omega \quad (8)$$

When there are three degrees of freedom in a node, finite elements have $3N$ unknowns, which are arranged in the following order during the generation of a stiffness matrix of the element:

$$\{u_1, v_1, \omega_1, \dots, u_N, v_N, \omega_N\} \text{ and, accordingly,} \\ \{u_1, v_1, \theta_1, \dots, u_N, v_N, \theta_N\}, \quad (9)$$

which have a corresponding system of approximating functions:

$$\left\{ \boldsymbol{\varphi}_{ij}(x, y), \boldsymbol{\varphi}_{ij} = \begin{Bmatrix} \varphi_{ij,u} \\ \varphi_{ij,v} \end{Bmatrix}, i = 1 \div N, j = 1, 2, 3 \right\} \quad (10)$$

For example, the displacement field for the degrees of freedom θ_j is represented as:

$$\mathbf{u}(x, y) = \sum_{i=1}^N (u_i \boldsymbol{\varphi}_{i1} + v_i \boldsymbol{\varphi}_{i2} + \theta_i \boldsymbol{\varphi}_{i3}) = \\ \sum_{i=1}^N \begin{Bmatrix} u_i \varphi_{i1,u} + v_i \varphi_{i2,u} + \theta_i \varphi_{i3,u} \\ u_i \varphi_{i1,v} + v_i \varphi_{i2,v} + \theta_i \varphi_{i3,v} \end{Bmatrix}, \quad (11)$$

Functions satisfying (5) will be represented as follows:

$$\boldsymbol{\varphi}_{i3}(\mathbf{x}) = \boldsymbol{\chi}_i(\mathbf{x}) + \varepsilon \boldsymbol{\zeta}_i(\mathbf{x}), \quad i = 1, 2, \dots, N, \quad (12)$$

where $\boldsymbol{\chi}_i$ functions obtained from hypothesis (4), $\boldsymbol{\zeta}_i$ – correction functions.

Let us introduce the notation L_{ij} for operators of degrees of freedom:

$$L_{i1}(\boldsymbol{\varphi}(\mathbf{x})) = \varphi_u(\mathbf{x}_i), \quad L_{i2}(\boldsymbol{\varphi}(\mathbf{x})) = \varphi_v(\mathbf{x}_i), \\ L_{i3}(\boldsymbol{\varphi}(\mathbf{x})) = \omega_z(\boldsymbol{\varphi}(\mathbf{x}))|_{\mathbf{x}_i}, \quad i = 1, 2, \dots, N. \quad (13)$$

For $i=1, 2$ – these are nodal displacements in the respective directions.

The following condition has to be satisfied:

$$L_{ij}(\boldsymbol{\varphi}_{km}(\mathbf{x})) = \delta_{ij}^{km}, \quad i = 1, 2, \dots, N, \quad (14)$$

$j=1, 2$ for (4) and (5) and $j=1, 2, 3$ for ω_z .

Convergence criteria

Criteria for proving the convergence of both compatible and incompatible finite elements for problems with elliptic differential equilibrium equations of arbitrary order were proposed in

[15–17] and were used in [15] to create new elements.

Let us formulate them for the plane problem of the theory of elasticity. Equalities of the completeness criterion of the minimum order for the degrees of freedom u_i , v_i , ω_i :

$$\begin{aligned} \sum_{i=1}^N \boldsymbol{\varphi}_{i1}(\mathbf{x}) &\equiv \begin{Bmatrix} 1 \\ 0 \end{Bmatrix}, & \sum_{i=1}^N x_i \boldsymbol{\varphi}_{i1}(\mathbf{x}) &\equiv \begin{Bmatrix} x \\ 0 \end{Bmatrix}, \\ \sum_{i=1}^N (y_i \boldsymbol{\varphi}_{i1}(\mathbf{x}) + \boldsymbol{\varphi}_{i3}(\mathbf{x})) &\equiv \begin{Bmatrix} y \\ 0 \end{Bmatrix}, \\ \sum_{i=1}^N \boldsymbol{\varphi}_{i2}(\mathbf{x}) &\equiv \begin{Bmatrix} 0 \\ 1 \end{Bmatrix}, & \sum_{i=1}^N y_i \boldsymbol{\varphi}_{i2}(\mathbf{x}) &\equiv \begin{Bmatrix} 0 \\ y \end{Bmatrix}, \\ \sum_{i=1}^N (x_i \boldsymbol{\varphi}_{i2}(\mathbf{x}) - \boldsymbol{\varphi}_{i3}(\mathbf{x})) &\equiv \begin{Bmatrix} 0 \\ x \end{Bmatrix} \end{aligned} \quad (15)$$

Conditions (15) must be satisfied for the approximations according to (4) and (5), if we assume that $\boldsymbol{\varphi}_{i3} = 0$. Adding independent approximations can only increase the order of the completeness criterion.

When (15) is satisfied, it guarantees the displacement of a finite element as a rigid body, and for compatible approximations according to [15,16], the method will converge in displacements with the 2-nd order, and in stresses with the 1-st order.

An *incompatibility criterion* is introduced for incompatible approximating functions. For the considered problem it lies in finding such a compatible system of functions

$$\{ \boldsymbol{\psi}_{ij}(x, y), \quad i=1, 2, \dots, N, \quad j=1, 2, 3 \}, \quad (16)$$

that must guarantee the displacement of the finite element as a rigid body (or the fulfillment of all equalities (14), which are more strict conditions) and satisfy the equations

$$\int_{\Omega} \begin{bmatrix} \frac{\partial}{\partial x} & \frac{\partial}{\partial y} & 0 & 0 \\ 0 & 0 & \frac{\partial}{\partial x} & \frac{\partial}{\partial y} \end{bmatrix}^T (\boldsymbol{\varphi}_{ij} - \boldsymbol{\psi}_{ij}) d\Omega = \begin{Bmatrix} 0 \\ 0 \\ 0 \\ 0 \end{Bmatrix}, \quad (17)$$

$i=1, 2, \dots, N, \quad j=1, 2, 3.$

When performing (15) and (17) for incompatible approximations, according to [15,16], the method will converge in displacements with the 2-nd order, and in stresses with the 1-st order. When analyzing incompatible approximations for elements with rotational degrees of freedom, approximations of classic elements with two degrees of freedom of a node can be used as a compatible system of functions (16). The incompatibility criterion enables to analyze the approximations for one finite element unlike the piecewise testing [18,19,20], which requires the analysis of all possible stars of elements.

Functions for some nodes corresponding to the rotational degrees of freedom ω_z will be determined as follows for some elements:

$$\boldsymbol{\varphi}_{i3}(\mathbf{x}) = \boldsymbol{\mu}_i(\mathbf{x}) + \boldsymbol{\lambda}_i(\mathbf{x}), \quad (18)$$

where $\boldsymbol{\mu}_i(\mathbf{x})$ and $\boldsymbol{\lambda}_i(\mathbf{x})$ are *compatible* and *incompatible* approximations, respectively.

It follows from the incompatibility criterion (17) that $\boldsymbol{\lambda}_i(\mathbf{x})$ must satisfy the equations:

$$\int_{\Omega} \begin{bmatrix} \frac{\partial}{\partial x} & \frac{\partial}{\partial y} & 0 & 0 \\ 0 & 0 & \frac{\partial}{\partial x} & \frac{\partial}{\partial y} \end{bmatrix}^T \boldsymbol{\lambda}_{ij}(\mathbf{x}) d\Omega = \begin{Bmatrix} 0 \\ 0 \\ 0 \\ 0 \end{Bmatrix} \quad (19)$$

The aim of the work is to build 12 new finite elements with rotational degrees of freedom using the above convergence criteria, ensuring the convergence of the finite element method.

2. FINITE ELEMENTS

2.1. Finite Elements with Quasi-rotational Degrees of Freedom

a) Three-node Element

Let us consider a triangle in the local coordinate system shown in Figure 1a. After changing the coordinates (20), it is transformed into a right triangle with unit legs shown in Figure 1b.

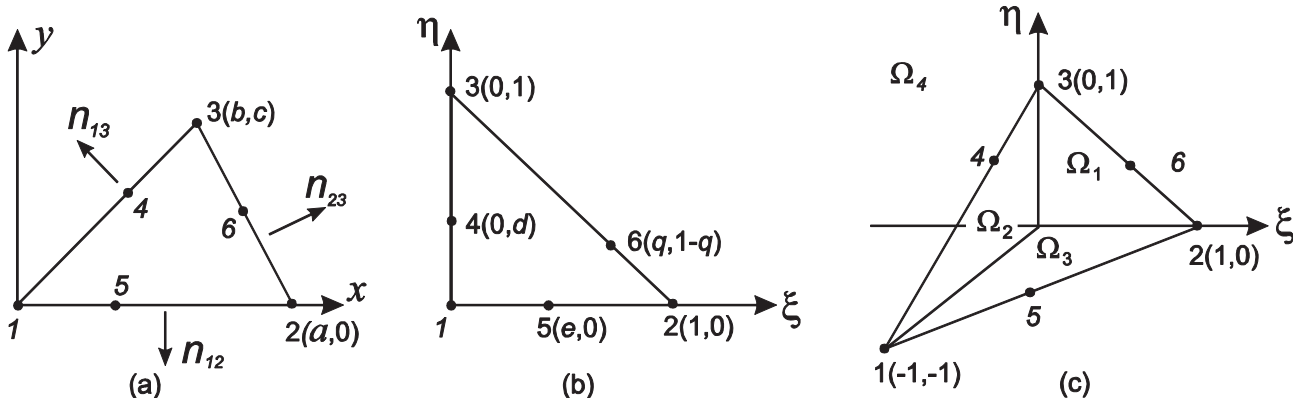


Figure 1. Triangular element.

$$\xi = \frac{1}{a} \left(x - \frac{b}{c} y \right), \quad \eta = \frac{1}{c} y \quad (20)$$

We will determine the degrees of freedom only at the vertices of the triangle.

Normal's to the element sides:

$$\mathbf{n}_{12} = \begin{Bmatrix} 0 \\ -1 \end{Bmatrix}, \quad \mathbf{n}_{13} = \frac{1}{a_{13}} \begin{Bmatrix} -c \\ b \end{Bmatrix}, \quad \mathbf{n}_{23} = \frac{1}{a_{23}} \begin{Bmatrix} c \\ a-b \end{Bmatrix}$$

The following approximation of displacements in the form (12) satisfies the conditions (5):

$$\boldsymbol{\varphi}_{i1}(\mathbf{x}) = \{\psi_i, 0\}^T, \quad \boldsymbol{\varphi}_{i2}(\mathbf{x}) = \{0, \psi_i\}^T \quad (21)$$

$$\psi_1 = 1 - \xi - \eta, \quad \psi_2 = \xi, \quad \psi_3 = \eta, \quad i=1,2,3$$

$$\chi_1 = \frac{1 - \xi - \eta}{2} \begin{Bmatrix} -c\eta \\ a\xi + b\eta \end{Bmatrix}, \quad \chi_2 = \frac{\xi}{2} \begin{Bmatrix} -c\eta \\ -a(1 - \xi) + b\eta \end{Bmatrix}$$

$$\chi_3 = \frac{\eta}{2} \begin{Bmatrix} c(1 - \eta) \\ a\xi - b(1 - \eta) \end{Bmatrix} \quad (22)$$

$$\zeta_1 = \frac{1 - \xi - \eta}{2} \begin{Bmatrix} -c\eta(\xi + 2\eta - 1) \\ -a\xi(1 - 2\xi - \eta) - b\eta(1 - \xi - 2\eta) \end{Bmatrix},$$

$$\zeta_2 = \frac{\xi}{2} \begin{Bmatrix} c\eta(\xi - \eta) \\ b\eta(\eta - \xi) - a(H - \xi) \end{Bmatrix},$$

$$\zeta_3 = \frac{\eta}{2} \begin{Bmatrix} c(H - \eta) \\ a\xi(\xi - \eta) - b(H - \eta) \end{Bmatrix}, \quad (23)$$

$$H(\xi, \eta) = 1 - 2\xi - 2\eta + 2\xi^2 + 2\xi\eta + 2\eta^2$$

Functions (22) – approximations [2].

b) Four-node Isoparametric Element

Let us consider a convex quadrangular finite element in the local coordinate system shown in Figure 2a. After an isoparametric transformation of the coordinate system (24), it is transformed into a unit square shown in Figure 2b.

$$\begin{aligned} x &= a\xi(1 - \eta) + b(1 - \xi)\eta + d\xi\eta, \\ y &= c(1 - \xi)\eta + e\xi\eta \end{aligned} \quad (24)$$

Normals to the sides:

$$\mathbf{n}_{12} = \begin{Bmatrix} 0 \\ -1 \end{Bmatrix}, \quad \mathbf{n}_{24} = \frac{1}{a_{24}} \begin{Bmatrix} e \\ a-d \end{Bmatrix},$$

$$\mathbf{n}_{34} = \frac{1}{a_{34}} \begin{Bmatrix} c-e \\ d-b \end{Bmatrix}, \quad \mathbf{n}_{13} = \frac{1}{a_{13}} \begin{Bmatrix} -c \\ b \end{Bmatrix}$$

We will determine the degrees of freedom only at the vertices of the quadrangle.

The following approximation of displacements in the form (12) satisfies the conditions (5):

$$\boldsymbol{\varphi}_{i1}(\mathbf{x}) = \begin{Bmatrix} 0 \\ \psi_i \end{Bmatrix}, \quad \boldsymbol{\varphi}_{i2}(\mathbf{x}) = \begin{Bmatrix} \psi_i \\ 0 \end{Bmatrix}, \quad i=1,2,3,4, \quad (25)$$

$$\begin{aligned} \psi_1 &= (1 - \xi)(1 - \eta), & \psi_2 &= \xi(1 - \eta), \\ \psi_3 &= (1 - \xi)\eta, & \psi_4 &= \xi\eta \end{aligned}$$

$$\boldsymbol{\varphi}_{13} = \frac{(1 - \eta)(1 - \xi)}{2} \begin{Bmatrix} -c\eta \\ b\eta + a\xi \end{Bmatrix},$$

$$\boldsymbol{\varphi}_{23} = \frac{\xi(1 - \eta)}{2} \begin{Bmatrix} -e\eta \\ -a(1 - \xi) + (d - a)\eta \end{Bmatrix},$$

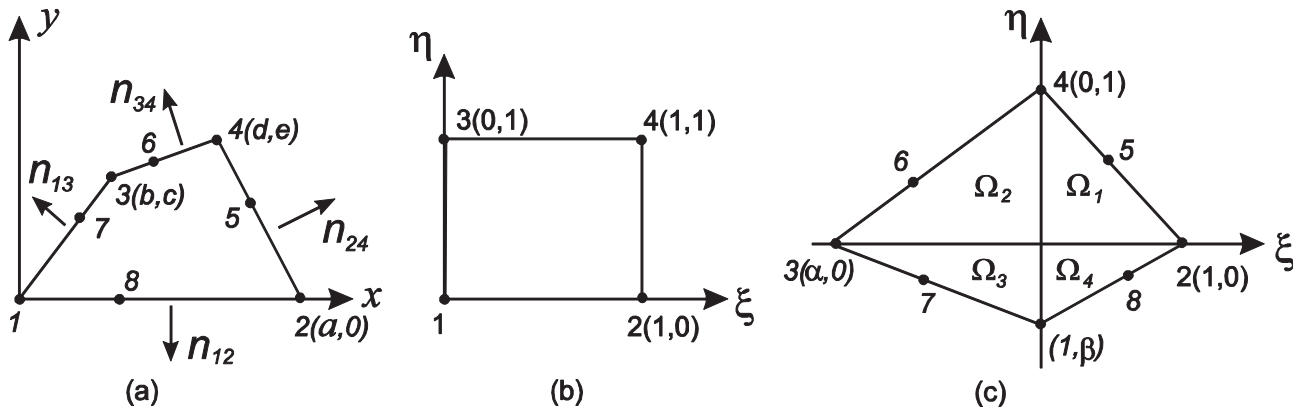


Figure 2. Quadrangular element.

$$\begin{aligned}\varphi_{33} &= \frac{(1-\xi)\eta}{2} \left\{ \frac{c(1-\eta) + (c-e)\xi}{(d-b)\xi - b(1-\eta)} \right\}, \\ \varphi_{43} &= \frac{\xi\eta}{2} \left\{ \frac{e(1-\eta) + (e-c)(1-\xi)}{(b-d)(1-\xi) + (a-d)(1-\eta)} \right\}\end{aligned}\quad (26)$$

Functions (26) – approximations [4].

$$\begin{aligned}\zeta_1(\mathbf{x}) &= \frac{(1-\xi)(1-\eta)}{2} \left\{ \frac{c\eta(1-2\eta)}{-b\eta(1-2\eta) - a\xi(1-2\xi)} \right\}, \\ \zeta_2(\mathbf{x}) &= \frac{\xi(1-\eta)}{2} \left\{ \frac{e\eta(1-2\eta)}{a(\xi-1)(1-2\xi) - (d-a)\eta(1-2\eta)} \right\}, \\ \zeta_3(\mathbf{x}) &= \frac{(1-\xi)\eta}{2} \left\{ \frac{c(1-\eta)(1-2\eta) - (c-e)\xi(1-2\xi)}{(b-d)\xi(1-2\xi) - b(1-\eta)(1-2\eta)} \right\}, \\ \zeta_4(\mathbf{x}) &= \frac{\xi\eta}{2} \left\{ \frac{e(1-\eta)(1-2\eta) + (e-c)(1-\xi)(1-2\xi)}{(b-d)(1-\xi)(1-2\xi) + (a-d)(1-\eta)(1-2\eta)} \right\}\end{aligned}\quad (27)$$

Two more functions are sometimes added which correspond to some internal degrees of freedom with their subsequent condensation:

$$\begin{aligned}\boldsymbol{\psi}_1 &= \left\{ \xi(1-\xi)\eta(1-\eta), 0 \right\}^T, \\ \boldsymbol{\psi}_2 &= \left\{ 0, \xi(1-\xi)\eta(1-\eta) \right\}^T\end{aligned}$$

$$\psi_1 = \frac{B_1}{2} \begin{cases} 1-2\eta-\xi^2+\eta^2, & \mathbf{x} \in \Omega_1 \\ 1-2\eta-A^2\xi^2+\eta^2, & \mathbf{x} \in \Omega_2 \\ 1-2\eta-A^2\xi^2+B^2\eta^2, & \mathbf{x} \in \Omega_3 \\ 1-2\eta-\xi^2+B^2\eta^2, & \mathbf{x} \in \Omega_4 \end{cases}, \quad \psi_2 = \frac{A_1}{2} \begin{cases} -\alpha+2\xi-\alpha\xi^2+\alpha\eta^2, & \mathbf{x} \in \Omega_1 \\ -\alpha+2\xi-A\xi^2+\alpha\eta^2, & \mathbf{x} \in \Omega_2 \\ -\alpha+2\xi-A\xi^2+\alpha B^2\eta^2, & \mathbf{x} \in \Omega_3 \\ -\alpha+2\xi-\alpha\xi^2+\alpha B^2\eta^2, & \mathbf{x} \in \Omega_4 \end{cases}$$

c) Four-node Element with a Piecewise Polynomial Approximation

Let us consider a quadrangular finite element in the local coordinate system shown in Figure 2a. It is transformed into a quadrangle shown in Figure 2c by replacing the coordinate system (28). A is the intersection point of the diagonals of the element.

$$\begin{cases} x = x_A + (a-x_A)\xi + (d-x_A)\eta, \\ y = y_A(1-\xi) + (e-y_A)\eta \end{cases}, \quad (28)$$

$$\begin{cases} \xi = p_{11}x + p_{12}y \\ \eta = p_{21}x + p_{22}y + \beta \end{cases}$$

$$\begin{aligned}p_{11} &= \frac{1}{a}, \quad p_{12} = -\frac{d}{ae}, \quad p_{21} = \frac{c}{\Delta}, \quad p_{22} = \frac{a-b}{\Delta}, \\ \alpha &= \frac{eb-dc}{ac}, \quad \beta = -\frac{ac}{\Delta}, \quad \Delta = c(d-a)(a-b)e, \\ A &= 1/\alpha, \quad B = 1/\beta, \\ A_1 &= 1/(1-\alpha), \quad B_1 = 1/(1-\beta)\end{aligned}$$

If the quadrangle is a rectangle, then $a=\beta=1$.

Let us consider functions (29) ψ_i , $i=1\div 8$, which are second-degree polynomials in each of the subareas Ω_i , $i=1,2,3,4$ and are continuous together with their first derivatives on the diagonals of the element:

$$\begin{aligned}
\psi_3 &= \frac{A_1}{2} \begin{cases} 1-2\xi+\xi^2-\eta^2, & \mathbf{x} \in \Omega_1 \\ 1-2\xi+A^2\xi^2-\eta^2, & \mathbf{x} \in \Omega_2 \\ 1-2\xi+A^2\xi^2-B^2\eta^2, & \mathbf{x} \in \Omega_3 \\ 1-2\xi+\xi^2-B^2\eta^2, & \mathbf{x} \in \Omega_4 \end{cases}, \quad \psi_4 = \frac{B_1}{2} \begin{cases} -\beta+2\eta+\beta\xi^2-\beta\eta^2, & \mathbf{x} \in \Omega_1 \\ -\beta+2\eta+A^2\beta\xi^2-\beta\eta^2, & \mathbf{x} \in \Omega_2 \\ -\beta+2\eta+A^2\beta\xi^2-B\eta^2, & \mathbf{x} \in \Omega_3 \\ -\beta+2\eta+\beta\xi^2-B\eta^2, & \mathbf{x} \in \Omega_4 \end{cases} \\
\psi_5 &= A_1 B_1 \begin{cases} 2\alpha\beta-4\beta\xi-4\alpha\eta+2\beta(2-\alpha)\xi^2+4\xi\eta+2\alpha(2-\beta)\eta^2, & \mathbf{x} \in \Omega_1 \\ 2\alpha\beta-4\beta\xi-4\alpha\eta+2A\beta\xi^2+4\xi\eta+2\alpha(2-\beta)\eta^2, & \mathbf{x} \in \Omega_2 \\ 2\alpha\beta-4\beta\xi-4\alpha\eta+2A\beta\xi^2+4\xi\eta+2\alpha B\eta^2, & \mathbf{x} \in \Omega_3 \\ 2\alpha\beta-4\beta\xi-4\alpha\eta+2\beta(2-\alpha)\xi^2+4\xi\eta+2\alpha B\eta^2, & \mathbf{x} \in \Omega_4 \end{cases} \\
\psi_6 &= A_1 B_1 \begin{cases} -2\beta+4\beta\xi+4\eta-2\beta\xi^2-4\xi\eta-(4-2\beta)\eta^2, & \mathbf{x} \in \Omega_1 \\ -2\beta+4\beta\xi+4\eta-A\beta(4-2A)\xi^2-4\xi\eta-(4-2\beta)\eta^2, & \mathbf{x} \in \Omega_2 \\ -2\beta+4\beta\xi+4\eta-A\beta(4-2A)\xi^2-4\xi\eta-2B\eta^2, & \mathbf{x} \in \Omega_3 \\ -2\beta+4\beta\xi+4\eta-2\beta\xi^2-4\xi\eta-4\xi\eta-2B\eta^2, & \mathbf{x} \in \Omega_4 \end{cases} \\
\psi_7 &= A_1 B_1 \begin{cases} -2-4\xi-4\eta+2\xi^2+4\xi\eta+2\eta^2, & \mathbf{x} \in \Omega_1 \\ -2-4\xi-4\eta-2A^2(1-2\alpha)\xi^2+4\xi\eta+2\eta^2, & \mathbf{x} \in \Omega_2 \\ -2-4\xi-4\eta-2A^2(1-2\alpha)\xi^2+4\xi\eta-2B^2(1-2\beta)\eta^2, & \mathbf{x} \in \Omega_3 \\ -2-4\xi-4\eta+2\xi^2+4\xi\eta-2B^2(1-2\beta)\eta^2, & \mathbf{x} \in \Omega_4 \end{cases} \\
\psi_8 &= A_1 B_1 \begin{cases} -2\alpha+4\xi+4\alpha\eta-(4-2\alpha)\xi^2-4\xi\eta-2\alpha\eta^2, & \mathbf{x} \in \Omega_1 \\ -2\alpha+4\xi+4\alpha\eta-2A\xi^2-4\xi\eta-2\alpha\eta^2, & \mathbf{x} \in \Omega_2 \\ -2\alpha+4\xi+4\alpha\eta-2A\xi^2-4\xi\eta-\alpha B(4-2B)\eta^2, & \mathbf{x} \in \Omega_3 \\ -2\alpha+4\xi+4\alpha\eta-(4-2\alpha)\xi^2-4\xi\eta-\alpha B(4-2B)\eta^2, & \mathbf{x} \in \Omega_4 \end{cases} \quad (29)
\end{aligned}$$

Since $\psi_i(\mathbf{x}_j) = \delta_i^j$, $i, j=1,2,3,4$, we can assign

$$\begin{aligned}
\boldsymbol{\varphi}_{i1}(\mathbf{x}) &= \begin{Bmatrix} \psi_i \\ 0 \end{Bmatrix}, \quad \boldsymbol{\varphi}_{i2}(\mathbf{x}) = \begin{Bmatrix} 0 \\ \psi_i \end{Bmatrix}, \quad i=1,2,3,4 \quad (30) \\
\boldsymbol{\chi}_3 &= \frac{1}{8} \begin{Bmatrix} c\psi_7 + (c-e)\psi_6 \\ (d-b)\psi_6 - b\psi_7 \end{Bmatrix}, \\
\boldsymbol{\chi}_4 &= \frac{1}{8} \begin{Bmatrix} e\psi_5 + (e-c)\psi_6 \\ (b-d)\psi_6 + (a-d)\psi_5 \end{Bmatrix} \quad (31)
\end{aligned}$$

The functions ψ_i , $i=5,6,7,8$ at the vertices of the quadrangle are equal to zero. They are nonzero at the middle of the sides and equal to one only at the node with a number matching that of the function. The following expression is obtained in (12) for functions corresponding to quasi-rotational degrees of freedom and satisfying conditions (5):

$$\begin{aligned}
\boldsymbol{\chi}_1 &= \frac{1}{8} \begin{Bmatrix} -c\psi_7 \\ b\psi_7 + a\psi_8 \end{Bmatrix}, \quad \boldsymbol{\chi}_2 = \frac{1}{8} \begin{Bmatrix} -e\psi_5 \\ -a\psi_8 + (d-a)\psi_5 \end{Bmatrix}, \\
\boldsymbol{\zeta}_1 &= \frac{1}{8} \begin{Bmatrix} -c\psi_7(A\xi - B\eta) \\ b\psi_7(A\xi - B\eta) - a\psi_8(B\eta - \xi) \end{Bmatrix}, \\
\boldsymbol{\zeta}_2 &= \frac{1}{8} \begin{Bmatrix} e\psi_5(\xi - \eta) \\ -a\psi_8(B\eta - \xi) - (d-a)\psi_5(\xi - \eta) \end{Bmatrix}, \\
\boldsymbol{\zeta}_3 &= \frac{1}{8} \begin{Bmatrix} -c\psi_7(A\xi - B\eta) + (c-e)\psi_6(\eta - A\xi) \\ (d-b)\psi_6(\eta - A\xi) + b\psi_7(A\xi - B\eta) \end{Bmatrix}, \\
\boldsymbol{\zeta}_4 &= \frac{1}{8} \begin{Bmatrix} e\psi_5(\xi - \eta) - (e-c)\psi_6(\eta - A\xi) \\ -(b-d)\psi_6(\eta - A\xi) + (a-d)\psi_5(\xi - \eta) \end{Bmatrix} \quad (32)
\end{aligned}$$

2.2. Incompatible Finite Elements (ω_z)

d) Triangle with Nodes at Vertices

Let us consider a triangle shown in Fig. 1a, which is transformed into a triangle in Fig. 1b by replacing the coordinates (20). The system of approximating functions of an element will be sought as third-degree polynomials in the finite element area. We will determine the degrees of freedom only at the vertices of the triangle.

Consider auxiliary functions corresponding to the rotational degrees of freedom obtained from $\zeta_i(\mathbf{x})$ in (27) and satisfying (14):

$$\begin{aligned}\lambda_i(\mathbf{x}) &= -4\zeta_i(\mathbf{x}) + \zeta(\mathbf{x}), \quad i=1,2,3, \\ \zeta(\mathbf{x}) &= \zeta_1(\mathbf{x}) + \zeta_2(\mathbf{x}) + \zeta_3(\mathbf{x})\end{aligned}\quad (33)$$

We adjust the functions (21) corresponding to the linear degrees of freedom of the classic element, so that the equalities (14) are satisfied:

$$\begin{aligned}\varphi_{11}(\mathbf{x}) &= \begin{Bmatrix} 1-\xi-\eta \\ 0 \end{Bmatrix} - \frac{a-b}{2ac}\zeta(\mathbf{x}), \\ \varphi_{12}(\mathbf{x}) &= \begin{Bmatrix} 0 \\ 1-\xi-\eta \end{Bmatrix} + \frac{1}{2a}\zeta(\mathbf{x}), \\ \varphi_{21}(\mathbf{x}) &= \begin{Bmatrix} \xi \\ 0 \end{Bmatrix} - \frac{b}{2ac}\zeta(\mathbf{x}), \quad \varphi_{22}(\mathbf{x}) = \begin{Bmatrix} 0 \\ \xi \end{Bmatrix} - \frac{1}{2a}\zeta(\mathbf{x}), \\ \varphi_{31}(\mathbf{x}) &= \begin{Bmatrix} \eta \\ 0 \end{Bmatrix} + \frac{1}{2c}\zeta(\mathbf{x}), \quad \varphi_{32}(\mathbf{x}) = \begin{Bmatrix} 0 \\ \eta \end{Bmatrix}\end{aligned}\quad (34)$$

The obtained approximations are incompatible now, because the equality of displacements on the sides of the element when it is connected to other elements of the design model is not provided. If in (18) we assume that

$$\varphi_{i3}(\mathbf{x}) = \lambda_i(\mathbf{x}), \quad i=1,2,3,$$

then the resulting system of functions already ensures the convergence of the method, since the equations (17) of the incompatibility criterion will be satisfied if we take the functions (21) of the classic element without rotational degrees of freedom (assuming they are zero) as the system of functions (16). But, as

shown by numerical experiments, there is no significant increase in calculation accuracy. Since the element with quasi-rotational degrees of freedom shows good accuracy, then in (18) we take $\mu_i(\mathbf{x})$, which are proportional to functions (22), as compatible functions, and $\zeta(\mathbf{x})$ – as incompatible ones. We obtain the only possible combination where the equalities of the completeness criterion (15) and the incompatibility criterion (17) are satisfied (If we use functions $\zeta_i(\mathbf{x})$, there can be alternative ways of representing functions $\varphi_{i3}(\mathbf{x})$, but (35) has shown the best results in the tests):

$$\varphi_{i3}(\mathbf{x}) = \frac{1}{3}(4\lambda_i(\mathbf{x}) + \zeta(\mathbf{x})), \quad i=1,2,3. \quad (35)$$

To increase calculation accuracy, it is reasonable to add five “internal” degrees of freedom with their subsequent condensation. They have corresponding approximations, which satisfy the conditions (19):

$$\psi_i(\mathbf{x}) = \Phi_i(\mathbf{x}) - \sum_{k=1}^3 \lambda_k(\mathbf{x}) L_{k3}(\Phi_i(\mathbf{x})),$$

$$\begin{aligned}\Phi_i &= \{\lambda_{i,v}, -\lambda_{i,u}\}^T, \quad \Psi_4 = \{H, 0\}^T, \quad \Psi_5 = \{0, H\}^T \\ H &= \xi\eta(1-\xi-\eta), \quad i=1,2,3\end{aligned}$$

e) Six-node Triangle

Let us consider an element in the local coordinate system, shown in Fig. 1a. After changing the coordinates (20), it is transformed into a triangle shown in Fig. 1b.

We will use fourth-degree polynomials.

Let us determine functions corresponding to the following degrees of freedom:

- rotation angles on the sides:

$$\begin{aligned}\varphi_{43} &= -\frac{2acp(\mathbf{x})(e(q-1)+(1-q)\xi+(e-q)\eta)}{a_{13}d(1-d)(e(1-q)+(q-e)d)} \begin{Bmatrix} b \\ c \end{Bmatrix}, \\ \varphi_{53} &= \frac{cp(\mathbf{x})(dq+(1-q-d)\xi-q\eta)}{e(1-e)(dq+(1-q-d)e)} \begin{Bmatrix} -2 \\ 0 \end{Bmatrix}, \\ \varphi_{63} &= \frac{2acp(\mathbf{x})(ed-d\xi-e\eta)}{a_{23}q(1-q)(ed-dq-e(1-q))} \begin{Bmatrix} a-b \\ c \end{Bmatrix},\end{aligned}\quad (36)$$

$$p(\mathbf{x}) = \xi\eta(1 - \xi - \eta)$$

- displacements on the sides:

$$\boldsymbol{\varphi}_{ij}(\mathbf{x}) = \mathbf{H}_{ij}(\mathbf{x}) - \boldsymbol{\varphi}_{i3}(\mathbf{x})L_{i3}(\mathbf{H}_{ij}(\mathbf{x})), \quad (37)$$

$$i=4,5,6, \quad j=1,2,$$

$$\mathbf{H}_{i1} = \begin{Bmatrix} P_{i-3} \\ 0 \end{Bmatrix}, \quad \mathbf{H}_{i2} = \begin{Bmatrix} 0 \\ P_{i-3} \end{Bmatrix}, \quad P_1 = \frac{(1 - \xi - \eta)^2 \eta^2}{d^2(1 - d)^2},$$

$$P_2 = \frac{\xi^2(1 - \xi - \eta)^2}{e^2(1 - e)^2}, \quad P_3 = \frac{\xi^2 \eta^2}{q^2(1 - q)^2}$$

- rotation angles at the vertices of the triangle, similarly to (35):

$$\boldsymbol{\varphi}_{i3}(\mathbf{x}) = \boldsymbol{\Phi}_i(\mathbf{x}) - \sum_{j=4}^6 \boldsymbol{\varphi}_{j3}L_{j3}(\boldsymbol{\Phi}_i(\mathbf{x})),$$

$$\boldsymbol{\Phi}_i(\mathbf{x}) = \frac{1}{3}(4\boldsymbol{\chi}_i(\mathbf{x}) + \boldsymbol{\zeta}(\mathbf{x})), \quad (38)$$

$$\boldsymbol{\chi}_1 = \frac{1 - \xi - \eta}{2} \begin{Bmatrix} c\eta(1 - d_1(1 - \xi - \eta)\eta) \\ a\xi(1 - e_1\xi(1 - \xi - \eta)) - \\ b\eta(1 - d_1(1 - \xi - \eta)\eta) \end{Bmatrix},$$

$$\boldsymbol{\chi}_2 = \frac{\xi}{2} \begin{Bmatrix} -c\xi\eta(1 - q_1\xi\eta) \\ -a\xi(1 - \xi - \eta)(1 - e_1\xi(1 - \xi - \eta)) - \\ (a - b)\xi\eta(1 - q_1\xi\eta) \end{Bmatrix},$$

$$\boldsymbol{\chi}_3 = \frac{\eta}{2} \begin{Bmatrix} c\xi(1 - q_1\xi\eta) - c(1 - \xi - \eta)(1 - d_1(1 - \xi - \eta)\eta) \\ (a - b)\xi(1 - q_1\xi\eta) + \\ b(1 - \xi - \eta)(1 - d_1(1 - \xi - \eta)\eta) \end{Bmatrix},$$

$$d_1 = \frac{1}{d(1 - d)}, \quad e_1 = \frac{1}{e(1 - e)}, \quad q_1 = \frac{1}{q(1 - q)}$$

Compatible functions $\boldsymbol{\chi}_i(\mathbf{x})$ are obtained from the condition that the tangential displacement u_t on the side ij varies quadratically, and the normal displacement u_n varies with θ_i according to the law:

$$u_n = \dots + a_{ij}\xi(1 - \xi)(1 - \frac{\xi(1 - \xi)}{a_{ik}(1 - a_{ik})})(\theta_j - \theta_i), \quad (39)$$

k – node on the side ij .

Formula (39) is an extension of the formula (4) taking into account the intermediate node.

$$\boldsymbol{\zeta}(\mathbf{x}) = r_1 \begin{Bmatrix} c \\ a - b \end{Bmatrix} H_1(\mathbf{x}) + r_2 \begin{Bmatrix} -c \\ b \end{Bmatrix} H_2(\mathbf{x}) + r_3 \begin{Bmatrix} 0 \\ -a \end{Bmatrix} H_3(\mathbf{x}) \quad (40)$$

$$H_1(\mathbf{x}) = \begin{cases} 0.5\xi\eta((\xi - \eta)), & q = 0.5 \\ 2\xi\eta((1 - q)\xi - q\eta) \\ ((5q - 2)\xi + (3 - 5q)\eta), & q \neq 0.5 \end{cases}$$

$$H_2(\mathbf{x}) = 2\eta(1 - \xi - \eta)(-d + d\xi + \eta) \\ ((3 - 5d) + (10d - 5)\eta)$$

$$H_3(\mathbf{x}) = 2\xi(1 - \xi - \eta)(e - \xi - e\eta) \\ ((3 - 5e) + (10e - 5)\xi)$$

The incompatible function $\boldsymbol{\zeta}(\mathbf{x})$ in (40) satisfies the equations (19), and the coefficients r_j , $j=1,2,3$, are found from the system of equations:

$$L_{i3}\boldsymbol{\zeta}(\mathbf{x}) = 1, \quad i=1,2,3. \quad (41)$$

- nodal displacements of the element:

$$\boldsymbol{\varphi}_{ij}(\mathbf{x}) = \boldsymbol{\Phi}_{ij}(\mathbf{x}) - \sum_{k=4}^6 \boldsymbol{\varphi}_{kj}L_{kj}(\boldsymbol{\Phi}_{ij}), \quad (42)$$

$$\boldsymbol{\Phi}_{ij}(\mathbf{x}) = \boldsymbol{\Psi}_{ij}(\mathbf{x}) - \sum_{k=1}^6 \boldsymbol{\varphi}_{k3}(\mathbf{x})L_{k3}(\boldsymbol{\Psi}_{ij}),$$

$i=1,2,3, \quad j=1,2, \quad \boldsymbol{\Psi}_{ij}(\mathbf{x})$ are linear functions (21).

The completeness criterion (15) and the incompatibility criterion (17) are satisfied.

The calculation accuracy can be increased by adding functions corresponding to the internal degrees of freedom:

$$\boldsymbol{\Psi}_i(\mathbf{x}) = \mathbf{Z}_i(\mathbf{x}) - \sum_{j=4}^6 \boldsymbol{\varphi}_{j3}L_{j3}(\mathbf{Z}_i(\mathbf{x})), \quad i=1,2.$$

$$\mathbf{Z}_1 = \{H, 0\}^T, \quad \mathbf{Z}_2 = \{0, H\}^T, \quad H = \xi\eta(1 - \xi - \eta)$$

f) Rectangle with Nodes at Vertices

Let us consider a rectangular finite element in the local coordinate system: $a_{12}=a$, $a_{13}=c$. The system of approximating functions of an element will be sought as fifth-degree

polynomials. Assuming $\xi=x/a$, $\eta=y/c$ we will display the element on that shown in Fig. 2b:

Determine the compatible functions φ_{i3} , $i=1,2,3$ in (12) with the help of (26) and (27) for $\varepsilon=-1$:

$$\begin{aligned}\varphi_{13} &= \begin{Bmatrix} -c\eta(1-\eta)^2(1-\xi) \\ a\xi(1-\xi)^2(1-\eta) \end{Bmatrix}, \\ \varphi_{23} &= \begin{Bmatrix} -c\eta(1-\eta)^2\xi \\ -a\xi^2(1-\xi)(1-\eta) \end{Bmatrix}, \\ \varphi_{33} &= \begin{Bmatrix} c\eta^2(1-\eta)(1-\xi) \\ a\xi(1-\xi)^2\eta \end{Bmatrix}, \\ \varphi_{43} &= \begin{Bmatrix} c\eta^2(1-\eta)\xi \\ -a\xi^2(1-\xi)\eta \end{Bmatrix}\end{aligned}\quad (43)$$

We adjust the functions of the linear degrees of freedom:

$$\begin{aligned}\varphi_{11} &= \Phi_{11} - \frac{1}{2c}(\lambda_1 + \lambda_3), \\ \varphi_{12} &= \Phi_{12} + \frac{1}{2a}(\lambda_1 + \lambda_2), \\ \varphi_{21} &= \Phi_{21} - \frac{1}{2c}(\lambda_2 + \lambda_4), \\ \varphi_{22} &= \Phi_{22} - \frac{1}{2a}(\lambda_1 + \lambda_2), \\ \varphi_{31} &= \Phi_{31} + \frac{1}{2c}(\lambda_1 + \lambda_3), \\ \varphi_{32} &= \Phi_{32} + \frac{1}{2a}(\lambda_3 + \lambda_4), \\ \varphi_{41} &= \Phi_{41} + \frac{1}{2c}(\lambda_2 + \lambda_4), \\ \varphi_{42} &= \Phi_{42} - \frac{1}{2a}(\lambda_3 + \lambda_4),\end{aligned}\quad (44)$$

where: $\Phi_{ij}(\mathbf{x})$ is a bilinear system of functions (25);

$$\begin{aligned}\lambda_1(\mathbf{x}) &= \varphi_{13}(\mathbf{x}) + H(\mathbf{x}), \\ \lambda_2(\mathbf{x}) &= \varphi_{23}(\mathbf{x}) - H(\mathbf{x}), \\ \lambda_3(\mathbf{x}) &= \varphi_{33}(\mathbf{x}) - H(\mathbf{x}), \\ \lambda_4(\mathbf{x}) &= \varphi_{43}(\mathbf{x}) + H(\mathbf{x}),\end{aligned}\quad (45)$$

$$H(\mathbf{x}) = \frac{5}{4} \begin{Bmatrix} c(1-2\xi)\eta^2(\eta-1)^2 \\ -a(1-2\eta)\xi^2(\xi-1)^2 \end{Bmatrix}$$

Functions λ_i , satisfy the equations (19) and ensure the fulfillment of the completeness criterion (15) and the incompatibility criterion (17).

g) Quadrangle

Let us consider a quadrangle shown in Figure 2a and perform the transformation of the coordinate system (28) into a quadrangle shown in Figure 2c. The system of approximating functions of an element will be sought as fourth-degree polynomials in each of the subareas Ω_i of the finite element.

Determine the compatible functions φ_{i3} , $i=1,2,3,4$ in (12) with the help of (31) and (32) for $\varepsilon=-1$. Functions $\lambda_i(\mathbf{x})$ for adjusting linear approximations can be represented as follows:

$$\lambda_i(\mathbf{x}) = \varphi_{i3}(\mathbf{x}) - \sum_{k=1}^4 r_{ik} \mathbf{Z}_k(\mathbf{x}) \quad (46)$$

$$\mathbf{Z}_i = \{\gamma_i(\mathbf{x}), 0\}^T, \quad \mathbf{Z}_{i+2} = \{0, \gamma_i(\mathbf{x})\}^T, \quad i=1,2,$$

$$\gamma_1 = \begin{cases} \alpha^2 \xi^2 \eta^2, & (\xi, \eta) \in \Omega_1 \cup \Omega_4, \\ -\xi^2 \eta^2, & (\xi, \eta) \in \Omega_2 \cup \Omega_3, \end{cases}$$

$$\gamma_2 = \begin{cases} \beta^2 \xi^2 \eta^2, & (\xi, \eta) \in \Omega_1 \cup \Omega_2, \\ -\xi^2 \eta^2, & (\xi, \eta) \in \Omega_3 \cup \Omega_4 \end{cases}$$

Coefficients r_{ij} in (46) are obtained as solutions of the systems of equations (19).

Functions corresponding to displacements:

$$\varphi_{ij}(\mathbf{x}) = \Psi_{ij}(\mathbf{x}) - \sum_{k=1}^3 \lambda_k(\mathbf{x}) L_{k3}(\Psi_{ij}(\mathbf{x})), \quad (47)$$

$$i=1,2,3,4, \quad j=1,2,$$

where $\Psi_{ij}(\mathbf{x})$ are approximations (30) of an element without rotational degrees of freedom.

The completeness criterion (15) is satisfied for the obtained approximations, since it follows from the properties of functions (31) and (32) that:

$$\sum_{i=1}^4 (\boldsymbol{\varphi}_{i3}(\mathbf{x}) - \boldsymbol{\lambda}_i(\mathbf{x})) = \sum_{i,k=1}^4 s_{ik} \mathbf{Z}_k(\mathbf{x}) \quad (48)$$

Functions $\boldsymbol{\zeta}_i(\mathbf{x})$ (32) satisfy the equations (19) and, therefore, we obtain a system of equations (19) in (48) for determining the coefficients s_{ik} with zero right-hand side.

h) Eight-node Quadrangle

Let us consider a quadrangle shown in Figure 2a and perform the transformation of the coordinate system (28) into a quadrangle shown in Figure 2c.

$$\omega_z = \frac{1}{2} \left(p_{11} \frac{\partial v}{\partial \xi} + p_{21} \frac{\partial v}{\partial \eta} - p_{12} \frac{\partial u}{\partial \xi} - p_{22} \frac{\partial u}{\partial \eta} \right) \quad (49)$$

The system of approximating functions will be sought as incomplete sixth-degree polynomials in the finite element subareas.

Determine functions for the nodes on the sides:

$$\boldsymbol{\varphi}_{i3} = \frac{\zeta_{i-4}(\mathbf{x})}{2f_{i-4}} \begin{Bmatrix} n_{yi} \\ -n_{xi} \end{Bmatrix}, \quad i=5,6,7,8, \quad (50)$$

$$\begin{Bmatrix} n_{xi} \\ n_{yi} \end{Bmatrix}^T$$

– normal to the side for the node i ;

$$f_{i-4} = -(n_{xi} \frac{\partial}{\partial x} + n_{yi} \frac{\partial}{\partial y}) \zeta_{i-4}(\mathbf{x})|_{x_i} =$$

$$-\left((n_{xi} r_{11} + n_{yi} r_{12}) \frac{\partial}{\partial \xi} + (n_{xi} r_{21} + n_{yi} r_{22}) \frac{\partial}{\partial \eta} \right) \zeta_{i-4}(\mathbf{x})|_{x_i}$$

$$\zeta_1 = \begin{cases} (1 - \xi - \eta) p(1, A, 1, B), & \mathbf{x} \in \Omega_1 \\ (1 - A\xi - \eta)^2 (1 - A\xi + (2 - 3B)\eta), & \mathbf{x} \in \Omega_2 \\ (1 - A\xi - B\eta)^3, & \mathbf{x} \in \Omega_3 \\ (1 - \xi - B\eta)^2 (1 + (2 - 3A)\xi - B\eta), & \mathbf{x} \in \Omega_4 \end{cases}$$

$$\zeta_2 = \begin{cases} (1 - \xi - \eta)^2 (1 - \xi + (2 - 3B)\eta), & \mathbf{x} \in \Omega_1 \\ (1 - A\xi - \eta) p(A, 1, 1, B), & \mathbf{x} \in \Omega_2 \\ (1 - A\xi - B\eta)^2 (1 + (2A - 3)\xi - B\eta), & \mathbf{x} \in \Omega_3 \\ (1 - \xi - B\eta)^3, & \mathbf{x} \in \Omega_4 \end{cases}$$

$$\zeta_3 = \begin{cases} (1 - \xi - \eta)^3, & \mathbf{x} \in \Omega_1 \\ (1 - A\xi - \eta)^2 (1 + (2A - 3)\xi - \eta), & \mathbf{x} \in \Omega_2 \\ (1 - A\xi - B\eta) p(A, 1, B, 1), & \mathbf{x} \in \Omega_3 \\ (1 - \xi - B\eta)^2 (1 - \xi + (2B - 3)\eta), & \mathbf{x} \in \Omega_4 \end{cases}$$

$$\zeta_4 = \begin{cases} (1 - \xi - \eta)^2 (1 + (2 - 3A)\xi - \eta), & \mathbf{x} \in \Omega_1 \\ (1 - A\xi - \eta)^3, & \mathbf{x} \in \Omega_2 \\ (1 - A\xi - B\eta)^2, & \mathbf{x} \in \Omega_3 \\ (1 - \xi - B\eta) p(1, A, B, 1), & \mathbf{x} \in \Omega_4 \end{cases} \quad (51)$$

$$p(z_1, z_2, z_3, z_4) = 1 + (z_1 - 3z_2)\xi + (z_3 - 3z_4)\eta + (3z_2 - 2z_1)\xi^2 + (3z_4 - 2z_3)\eta^2 + (2z_1z_3 - 3z_2 - 3z_4 + 6z_2z_4)\xi\eta$$

Let us determine functions corresponding to the rotational degrees of freedom in the nodes:

$$\boldsymbol{\varphi}_{i3}(\mathbf{x}) = \boldsymbol{\Phi}_i(\mathbf{x}) - \sum_{k=1}^4 r_{ik} \boldsymbol{\chi}_k(\mathbf{x}), \quad (52)$$

$$\boldsymbol{\Phi}_i(\mathbf{x}) = \mathbf{H}_i(\mathbf{x}) - \sum_{k=5}^8 \boldsymbol{\varphi}_{k3} L_{k3}(\mathbf{H}_i), \quad i=1,2,3,4,$$

where r_{ij} are solutions of the systems of equations (19),

$$\mathbf{H}_i(\mathbf{x}) = \boldsymbol{\psi}_{k3}(\mathbf{x}) T_i(\mathbf{x}),$$

$\boldsymbol{\psi}_{k3}(\mathbf{x})$ – are compatible functions of a quadrangular element with piecewise polynomial approximation (29-31) for $\varepsilon=-1$;

$$T_1 = P_{781}, T_2 = P_{582}, T_3 = P_{673}, T_4 = P_{564}, \quad (53)$$

$$P_{ijk}(\mathbf{x}) = \frac{(\xi - \xi_i)(\eta_j - \eta_i) - (\eta - \eta_i)(\xi_j - \xi_i)}{(\xi_k - \xi_i)(\eta_j - \eta_i) - (\eta_k - \eta_i)(\xi_j - \xi_i)}$$

$$\boldsymbol{\chi}_i(\mathbf{x}) = \mathbf{Z}_i - \sum_{j=1}^4 \sum_{k=5}^8 \boldsymbol{\varphi}_{kj} L_{kj}(\mathbf{Z}_i) \quad (54)$$

$$\mathbf{Z}_i = \{\gamma_i(\mathbf{x}), 0\}^T, \quad \mathbf{Z}_{i+2} = \{0, \gamma_i(\mathbf{x})\}^T, \quad i=1,2,$$

$$\gamma_1 = \xi^3 \eta^3 \begin{cases} \alpha^3 \beta^3, & \mathbf{x} \in \Omega_1 \\ \beta^3, & \mathbf{x} \in \Omega_2 \\ -1, & \mathbf{x} \in \Omega_3 \\ -\alpha^3, & \mathbf{x} \in \Omega_4 \end{cases}$$

$$\gamma_2 = \xi^3 \eta^3 \begin{cases} \alpha^3 \beta^3, & \mathbf{x} \in \Omega_1 \\ -\beta^3, & \mathbf{x} \in \Omega_2 \\ -1, & \mathbf{x} \in \Omega_3 \\ \alpha^3, & \mathbf{x} \in \Omega_4 \end{cases}$$

Adjust functions (29), ψ_i , $i=1 \div 8$:

$$\chi_i(\mathbf{x}) = \psi_i(\mathbf{x}) - \sum_{m=5}^8 \psi_i(\mathbf{x}_m) \chi_m(\mathbf{x}), \quad (55)$$

$$\chi_k(\mathbf{x}) = \frac{\psi_k(\mathbf{x})}{\psi_k(\mathbf{x}_k)}$$

$i=1,2,3,4$, $k=5,6,7,8$.

Functions corresponding to displacements are obtained using (55):

$$\varphi_{ij}(\mathbf{x}) = \psi_{ij}(\mathbf{x}) - \sum_{k=1}^8 \varphi_{k3}(\mathbf{x}) L_{k3}(\psi_{ij}), \quad (56)$$

$$\psi_{i1}(\mathbf{x}) = \begin{Bmatrix} \chi_i \\ 0 \end{Bmatrix}, \quad \psi_{i2}(\mathbf{x}) = \begin{Bmatrix} 0 \\ \chi_i \end{Bmatrix}, \quad i=1 \div 8, j=1,2$$

The obtained system of functions satisfies the completeness criterion (15) and the incompatibility criterion (17).

2.3. Compatible Elements (ω_z)

i) Triangle with Nodes at Vertices

Let us consider a triangle shown in Fig. 1a, and perform the transformation of the coordinate system (57) into a triangle shown in Fig. 1c, where point A is the intersection point of the medians of the triangle:

$$\begin{cases} \xi = p_{11}x + p_{12}y - 1 \\ \eta = p_{21}x + p_{22}y - 1 \end{cases} \quad (57)$$

$$p_{11} = \frac{2}{a}, \quad p_{12} = \frac{a-2b}{ac}, \quad p_{21} = \frac{1}{a}, \quad p_{22} = \frac{2a-b}{ac}$$

Let us write the functions $\lambda_i(\mathbf{x})$, $i=1,2,3$, which are second-degree polynomials in each of the subareas, are zero on the sides of the triangle, continuous within Ω and satisfy the conditions (14). We obtain the unique solution:

$$\lambda_1(\mathbf{x}) = \frac{2}{9} \begin{Bmatrix} c \\ -a-b \end{Bmatrix} \gamma_1(\mathbf{x}), \quad \lambda_3(\mathbf{x}) = \frac{2}{9} \begin{Bmatrix} -2c \\ 2b-a \end{Bmatrix} \gamma_3(\mathbf{x})$$

$$\lambda_2(\mathbf{x}) = \frac{2}{9} \begin{Bmatrix} c \\ 2a-b \end{Bmatrix} \gamma_2(\mathbf{x}), \quad (58)$$

$$\zeta = \begin{cases} 1-\xi-\eta, & \mathbf{x} \in \Omega_1 \\ 1+2\xi-\eta, & \mathbf{x} \in \Omega_2 \\ 1-\xi+2\eta, & \mathbf{x} \in \Omega_3 \end{cases} \quad \begin{cases} \gamma_1(\mathbf{x}) = (1-\xi-\eta)\zeta, \\ \gamma_2(\mathbf{x}) = (1-\xi+2\eta)\zeta, \\ \gamma_3(\mathbf{x}) = (1+2\xi-\eta)\zeta, \end{cases}$$

Functions λ_i , $i=1,2,3$ have discontinuities ω_z at the boundaries Ω_i (sides of connected elements, segments of medians), but $\omega_z(\lambda_i(\mathbf{x}))$ are continuous at the nodes of the element.

Compatible functions corresponding to the rotational degrees of freedom and satisfying the conditions (14), similarly to (35), can be represented as follows:

$$\varphi_{i3}(\mathbf{x}) = \frac{1}{3} (4\chi_i(\mathbf{x}) + \zeta(\mathbf{x})), \quad (59)$$

$$\zeta(\mathbf{x}) = \lambda_1(\mathbf{x}) + \lambda_2(\mathbf{x}) + \lambda_3(\mathbf{x})$$

where χ_i are functions (22) in the coordinate system (57).

The functions corresponding to displacements are obtained by substituting the functions $\zeta_i(\mathbf{x})$ from (59) and linear functions into (34):

$$\psi_1(\mathbf{x}) = \frac{1}{3}(1-\xi-\eta), \quad \psi_2(\mathbf{x}) = \frac{1}{3}(1+2\xi-\eta),$$

$$\psi_3(\mathbf{x}) = \frac{1}{3}(1-\xi+2\eta)$$

The calculation accuracy can be increased by adding functions equal to zero on the sides of the element as those corresponding to internal degrees of freedom:

$$\begin{aligned}\boldsymbol{\psi}_1(\mathbf{x}) &= \{R, 0\}^T, \quad \boldsymbol{\psi}_2(\mathbf{x}) = \{0, R\}^T, \\ R(\mathbf{x}) &= \begin{cases} (1 - \xi - \eta)^2, & \mathbf{x} \in \Omega_1 \\ (1 + 2\xi - \eta)^2, & \mathbf{x} \in \Omega_2 \\ (1 - \xi + 2\eta)^2, & \mathbf{x} \in \Omega_3 \end{cases}\end{aligned}$$

j) Six-node Triangle

Let us consider a triangle shown in Figure 1a, and perform the transformation of the coordinate system (57) into a triangle shown in Fig. 1c. The functions are sought as third-degree polynomials in each of the subareas.

Functions corresponding to the rotational degrees of freedom at the nodes are given by adjusting (58) (functions (36) can be applied, which will result in fourth-degree polynomials):

$$\boldsymbol{\varphi}_{i3}(\mathbf{x}) = \boldsymbol{\lambda}_i(\mathbf{x}) - \sum_{k=4}^6 \boldsymbol{\varphi}_{i3}(\mathbf{x}) L_{k3}(\boldsymbol{\lambda}_i(\mathbf{x})), \quad i=1,2,3, \quad (60)$$

$$\boldsymbol{\varphi}_{43}(\mathbf{x}) = \frac{c}{3\eta_4(\xi_4 - \eta_4)} \begin{Bmatrix} -1 \\ 0 \end{Bmatrix} H_1,$$

$$\boldsymbol{\varphi}_{53}(\mathbf{x}) = \frac{ac}{3a_{13}^2 \xi_5(\xi_5 - \eta_5)} \begin{Bmatrix} b \\ c \end{Bmatrix} H_2,$$

$$\boldsymbol{\varphi}_{63}(\mathbf{x}) = \frac{ac}{3a_{23}^2 \xi_6 \eta_6} \begin{Bmatrix} a-b \\ c \end{Bmatrix} H_3$$

$$H_1 = \begin{cases} \eta(\eta - \xi)(1 - \xi + 2\eta), & \mathbf{x} \in \Omega_3 \\ 0, & \mathbf{x} \in \Omega_1 \cup \Omega_2 \end{cases},$$

$$H_2 = \begin{cases} \xi(\xi - \eta)(1 + 2\xi - \eta), & \mathbf{x} \in \Omega_2 \\ 0, & \mathbf{x} \in \Omega_1 \cup \Omega_3 \end{cases},$$

$$H_3 = \begin{cases} \xi\eta(1 - \xi - \eta), & \mathbf{x} \in \Omega_1 \\ 0, & \mathbf{x} \in \Omega_2 \cup \Omega_3 \end{cases}$$

Functions corresponding to displacements are obtained from approximations of a classic element $\boldsymbol{\psi}_{ij}(\mathbf{x})$ without rotational degrees of freedom:

$$\boldsymbol{\varphi}_{ij}(\mathbf{x}) = \boldsymbol{\psi}_{ij}(\mathbf{x}) - \sum_{k=1}^6 \boldsymbol{\varphi}_{k3}(\mathbf{x}) L_{k3}(\boldsymbol{\psi}_{ij}(\mathbf{x})), \quad (61)$$

$$i=1 \div 6, j=1,2$$

The calculation accuracy can be increased by adding functions equal to zero on the sides of the element as those corresponding to eleven internal degrees of freedom:

$$\boldsymbol{\psi}_i(\mathbf{x}) = \mathbf{Z}_i(\mathbf{x}) - \sum_{k=4}^6 \boldsymbol{\varphi}_{i3}(\mathbf{x}) L_{k3}(\mathbf{Z}_i(\mathbf{x})), \quad i=1,2,3,$$

$$\mathbf{Z}_i(\mathbf{x}) = \{\varphi_{i+3,3,v}, -\varphi_{i+3,3,u}\}^T,$$

$$\boldsymbol{\psi}_4 = \begin{Bmatrix} R \\ 0 \end{Bmatrix}, \quad \boldsymbol{\psi}_5 = \begin{Bmatrix} 0 \\ R \end{Bmatrix}, \quad \boldsymbol{\psi}_6(\mathbf{x}) = \begin{Bmatrix} R_1 \\ 0 \end{Bmatrix}, \quad \boldsymbol{\psi}_7(\mathbf{x}) = \begin{Bmatrix} 0 \\ R_1 \end{Bmatrix}$$

$$\boldsymbol{\psi}_8 = \xi \boldsymbol{\psi}_4, \quad \boldsymbol{\psi}_9 = \xi \boldsymbol{\psi}_5, \quad \boldsymbol{\psi}_{10} = \eta \boldsymbol{\psi}_4, \quad \boldsymbol{\psi}_{11} = \eta \boldsymbol{\psi}_5$$

$$R_1(\mathbf{x}) = \begin{cases} 0, & \mathbf{x} \in \Omega_1 \\ \xi(1 + 2\xi - \eta)(1 - \eta), & \mathbf{x} \in \Omega_2 \\ \eta(1 - \xi + 2\eta)(1 - \xi), & \mathbf{x} \in \Omega_3 \end{cases}$$

k) Quadrangle with Nodes at Vertices

Let us consider a convex quadrangle shown in Figure 2a and perform the transformation of the coordinate system (28) into a quadrangle shown in Figure 2c.

The functions are sought as second-degree polynomials in each of the subareas.

Let us write the functions $\boldsymbol{\lambda}_i(\mathbf{x})$, $i=1,2,3,4$, which are second-degree polynomials in each of the subareas, are zero on the sides of the quadrangle, continuous within Ω and satisfy the conditions (14). We obtain the unique solution:

$$\begin{aligned}\boldsymbol{\lambda}_1(\mathbf{x}) &= \frac{2}{p} \begin{Bmatrix} p_{11} \\ p_{12} \end{Bmatrix} \gamma_1, \quad \boldsymbol{\lambda}_2(\mathbf{x}) = -\frac{2}{p} \begin{Bmatrix} p_{21} \\ p_{22} \end{Bmatrix} \gamma_2, \\ \boldsymbol{\lambda}_3(\mathbf{x}) &= \frac{2}{p} \begin{Bmatrix} p_{21} \\ p_{22} \end{Bmatrix} \gamma_3, \quad \boldsymbol{\lambda}_4(\mathbf{x}) = -\frac{2}{p} \begin{Bmatrix} p_{11} \\ p_{12} \end{Bmatrix} \gamma_4 \quad (62)\end{aligned}$$

$$p = p_{11}p_{22} - p_{12}p_{21},$$

$$\gamma_1 = \begin{cases} \eta(1 - A\xi - B\eta), & \mathbf{x} \in \Omega_3 \\ \eta(1 - \xi - B\eta), & \mathbf{x} \in \Omega_4 \\ 0, & \mathbf{x} \in \Omega_1 \cup \Omega_2 \end{cases}$$

$$\gamma_2 = \begin{cases} \xi(1 - \xi - \eta), & \mathbf{x} \in \Omega_1 \\ \xi(1 - \xi - B\eta), & \mathbf{x} \in \Omega_4 \\ 0, & \mathbf{x} \in \Omega_2 \cup \Omega_3 \end{cases}$$

$$\gamma_3 = \begin{cases} \eta(1 - A\xi - \eta), & \mathbf{x} \in \Omega_2 \\ \eta(1 - A\xi - B\eta), & \mathbf{x} \in \Omega_3 \\ 0, & \mathbf{x} \in \Omega_1 \cup \Omega_4 \end{cases}$$

$$\gamma_4 = \begin{cases} \xi(1-\xi-\eta), & \mathbf{x} \in \Omega_1 \\ \xi(1-A\xi-\eta), & \mathbf{x} \in \Omega_2 \\ 0, & \mathbf{x} \in \Omega_3 \cup \Omega_4 \end{cases}$$

Similarly to a triangular element, functions λ_i , $i=1,2,3,4$ have *discontinuities* ω_z at the boundaries Ω_i (sides of connected elements, segments of diagonals), but $\omega_z(\lambda_i(\mathbf{x}))$ is *continuous* at its nodes.

Compatible functions which correspond to rotational degrees of freedom, preserve equalities (15) and satisfy the equations of the incompatibility criterion (17) are given in the following form, taking into account the experience of creating triangular elements:

$$\begin{aligned} \boldsymbol{\varphi}_{i3}(\mathbf{x}) &= \frac{1}{3}(4\chi_i(\mathbf{x}) - \sum_{j=1}^4 \kappa(i,j)\lambda_j(\mathbf{x})), \\ \kappa(i,j) &= \begin{cases} 1, & ij - \text{side} \\ 0, & ij - \text{diagonal} \end{cases} \end{aligned} \quad (63)$$

where $\chi_i(\mathbf{x})$, $i=1,2,3,4$ are functions (31).

Functions corresponding to displacements are obtained from approximations (29) of an element without rotational degrees of freedom by adjusting them with the help of functions $\lambda_i(\mathbf{x})$ to satisfy the conditions (14):

$$\boldsymbol{\varphi}_{ij}(\mathbf{x}) = \boldsymbol{\psi}_{ij}(\mathbf{x}) - \sum_{k=1}^4 \lambda_k(\mathbf{x})L_{k3}(\boldsymbol{\psi}_{ij}), \quad (64)$$

The calculation accuracy can be increased by adding functions equal to zero on the sides of the element as those corresponding to internal degrees of freedom:

$$\begin{aligned} \boldsymbol{\psi}_4(\mathbf{x}) &= \{R, 0\}^T, \quad \boldsymbol{\psi}_5(\mathbf{x}) = \{0, R\}^T, \quad (65) \\ R(\mathbf{x}) &= \begin{cases} (1-\xi-\eta)^2, & \mathbf{x} \in \Omega_1 \\ (1-A\xi-\eta)^2, & \mathbf{x} \in \Omega_2 \\ (1-A\xi-B\eta)^2, & \mathbf{x} \in \Omega_3 \\ (1-\xi-B\eta)^2, & \mathbf{x} \in \Omega_4 \end{cases} \end{aligned}$$

l) Eight-node Quadrangle

Let us consider a convex quadrangle shown in Fig. 2a and perform the transformation of the coordinate system (28) into a quadrangle shown in Fig. 2c. The functions are sought as third-degree polynomials in each of the subareas. Functions corresponding to the rotational degrees of freedom can be given as follows:

$$\boldsymbol{\varphi}_{i3}(\mathbf{x}) = \lambda_i(\mathbf{x}) - \sum_{k=5}^8 \boldsymbol{\varphi}_{k3}(\mathbf{x})L_{k3}(\lambda_i(\mathbf{x})), \quad (66)$$

$$\boldsymbol{\varphi}_{k3}(\mathbf{x}) = \boldsymbol{\psi}_{k3}(\mathbf{x}), \quad i=1,2,3,4, k=5,6,7,8,$$

where $\boldsymbol{\psi}_{i3}(\mathbf{x})$ are functions (50), $\lambda_i(\mathbf{x})$ are functions (62).

Functions corresponding to displacements are obtained according to formula (56) by substituting functions (66).

The calculation accuracy can be increased by adding functions equal to zero on the sides of the element as those corresponding to eleven internal degrees of freedom functions (65).

2.4. Accuracy of Elements

The considered finite elements, except for the isoparametric ones, use polynomial or piecewise polynomial approximations of the displacement field over the entire area of the element.

Equalities of the completeness criterion (15) are satisfied for all elements including isoparametric ones. Let us add the equalities of the completeness criterion of the 2-nd order to them:

$$\begin{aligned} \sum_{i=1}^N x_i^2 \boldsymbol{\varphi}_{i1}(\mathbf{x}) &\equiv \begin{Bmatrix} x^2 \\ 0 \end{Bmatrix}, \quad \sum_{i=1}^N y_i^2 \boldsymbol{\varphi}_{i2}(\mathbf{x}) \equiv \begin{Bmatrix} 0 \\ y^2 \end{Bmatrix} \\ \sum_{i=1}^N x_i (y_i \boldsymbol{\varphi}_{i1}(\mathbf{x}) - \frac{1}{2} \boldsymbol{\varphi}_{i3}(\mathbf{x})) &\equiv \begin{Bmatrix} xy \\ 0 \end{Bmatrix}, \\ \sum_{i=1}^N y_i (y_i \boldsymbol{\varphi}_{i1}(\mathbf{x}) - \boldsymbol{\varphi}_{i3}(\mathbf{x})) &\equiv \begin{Bmatrix} y^2 \\ 0 \end{Bmatrix}, \\ \sum_{i=1}^N x_i (x_i \boldsymbol{\varphi}_{i2}(\mathbf{x}) + \boldsymbol{\varphi}_{i3}(\mathbf{x})) &\equiv \begin{Bmatrix} 0 \\ x^2 \end{Bmatrix}, \\ \sum_{i=1}^N y_i (x_i \boldsymbol{\varphi}_{i2}(\mathbf{x}) + \frac{1}{2} \boldsymbol{\varphi}_{i3}(\mathbf{x})) &\equiv \begin{Bmatrix} 0 \\ xy \end{Bmatrix}, \end{aligned} \quad (67)$$

They are satisfied only for compatible 6-node triangular and 8-node quadrangular elements whose functions are sought as second-degree polynomials. Despite a rather large number of degrees of freedom, the equalities (67) are *not satisfied* for elements with quasi-rotational degrees of freedom and all incompatible elements.

Considering that the equalities of the incompatibility criterion (17) are satisfied for all incompatible elements, we obtain the following minimum estimates of the order of the convergence rate according to [15] for regular partitions with sufficiently smooth boundary in the L_2 norm for elements:

- ***a-i, k*** – the first one in stresses and the second one in displacements;
- ***j, l*** (high-precision compatible elements) – the second one in stresses and the third one in displacements.

3. TESTS

All tests for elements with quasi-rotational degrees of freedom were performed with the value $\varepsilon=0.001$. Since the values of displacements and stresses calculated for these elements according to the hypothesis (4), and hypothesis (5) for the given ε *differ only in the fourth significant digit*, and only on the coarsest mesh, they are not provided.

All the approximations considered in this paper and corresponding to the “internal” degrees of freedom of the elements are applied.

The loads specified as uniformly distributed, trapezoidal and *parabolic* were reduced to nodal ones taking into account the condensation of “internal” degrees of freedom.

All calculations were performed in SCAD, which is a part of SCAD Office®.

3.1. Patch Tests

Patch tests [21] are performed in order to check whether the equalities of the completeness criterion (15) are satisfied for all considered elements:

- stiffness matrices of all considered finite elements each have three eigenvectors corresponding to their ***displacement as rigid bodies***;
- the results for plates under constant stresses were obtained with an accuracy up to a computational error.

These tests serve only as a correctness criterion of the program code.

3.2. Narrow Rectangular Plate

The plate of rectangular section shown in Fig. 3 is subjected to a trapezoidal load applied at its ends $P=\pm 2kEy$, $E=100\text{kPa}$, $\nu=0$, $h=1\text{m}$, $a=10\text{m}$, $b=1\text{m}$. Coefficient $k=0.06$ results in unit moments at the ends of the plate, when it is considered as a bar.

The problem has an analytical solution, known from the theory of elasticity:

$$u = -\frac{2}{b}kxy, \quad v = \frac{1}{b}k\left(y^2 + x^2 - \frac{1}{4}a^2\right) \quad (68)$$

The design models shown in Fig. 4 are taken from [7], where this problem was considered. Table 1 contains calculated vertical displacements at the point A(0,5), stresses σ_x at the point B(0,-5) and rotation angles ω at the point E(1.6(6),0). The following analytical solutions are obtained from (68):

$$v_A = -1.5\text{m}, \quad \sigma_{x,B} = 6\text{kPa}, \quad \omega_E = 0.4\text{rad}.$$

If the given plate is considered as a bar, then after applying a pair of moments at its ends

$$M_y = \pm 2kJ_y/h, \quad J_y = hb^3/12$$

(moment of inertia of the plate section), we obtain the same values of vertical deflection and rotation angle using rod theory.

A loading statically equivalent to the given load was considered to study moment loads, when the moments M_y are specified in the nodes C(-5,0) and D(5,0). Table 2 shows the results of experiments.

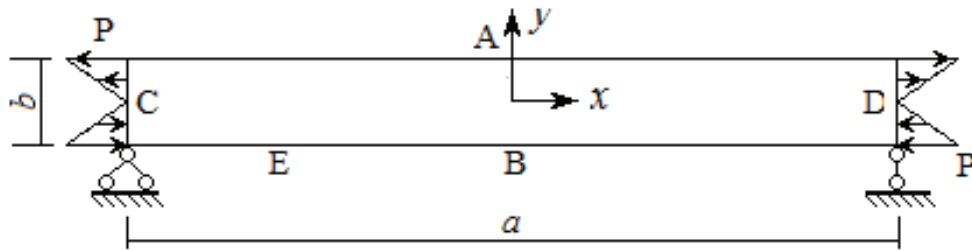


Figure 3. Narrow plate.

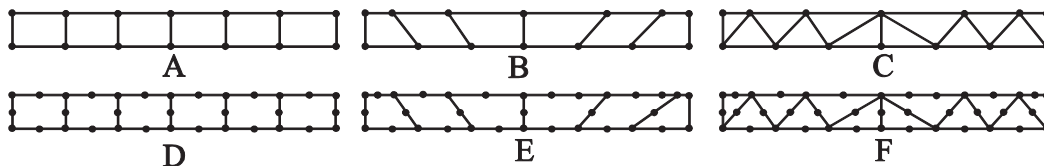


Figure 4. Design models 1x6 for a narrow rectangular plate.

Table 1. Displacements, stresses and rotation angles in a narrow plate.

Mesh type	Element	Displacements w_A (m)				Stresses σ_B (kPa)				Rotation angles ω_E (rad)			
		Mesh				Mesh				Mesh			
		1x6	2x12	4x24	8x48	1x6	2x12	4x24	8x48	1x6	2x12	4x24	8x48
A	b, c	-1.5				6				0.4			
	f	-1.231	-1.422	-1.480	-1.496	4.874	5.673	5.915	5.978	0.3255	0.3783	0.3943	0.3986
	g	-1.203	-1.412	-1.478	-1.495	4.775	5.639	5.905	5.976	0.3199	0.3761	0.3937	0.3984
	k	-0.923	-1.295	-1.442	-1.485	3.052	4.743	5.529	5.817	0.2430	0.3450	0.3846	0.3960
B	b	-1.298	-1.458	-1.490	-1.497	5.711	6.020	5.998	5.999	0.2945	0.3771	0.3933	0.3961
	c	-1.318	-1.458	-1.490	-1.497	5.686	6.027	6.001	6	0.3234	0.3838	0.3943	0.3964
	g	-0.777	-1.222	-1.418	-1.479	3.267	5.241	5.805	5.951	0.2005	0.3198	0.3758	0.3936
	k	-0.766	-1.200	-1.410	-1.476	2.332	4.088	5.280	5.747	0.2011	0.3193	0.3758	0.3936
C	a	-0.858	-1.261	-1.432	-1.482	3.318	5.026	5.741	5.939	0.2079	0.3750	0.4570	0.4780
	d	-0.920	-1.291	-1.440	-1.484	4.814	6.096	6.252	6.171	0.2323	0.3389	0.3823	0.3952
	i	-0.684	-1.118	-1.372	-1.464	1.779	3.412	4.894	5.635	0.1793	0.2991	0.3667	0.3908
D	h	-1.512	-1.502	-1.5		6.038	6.009	6.002	6.001	0.4012	0.3993	0.3998	0.4
	l	-1.5				6				0.4			
E	h	-1.511	-1.502	-1.5	-1.5	6.246	6.072	6.019	6.005	0.3934	0.3958	0.3983	0.3993
	l	-1.5				6				0.4			
F	e	-1.367	-1.461	-1.490	-1.497	5.318	5.754	5.914	5.970	0.3601	0.3897	0.3974	0.3993
	j	-1.5				6				0.4			

The obtained results slightly differ from those given in Table 2 only for elements with the degrees of freedom ω_z .

Numerical experiments show that the obtained rotation angles for the element with quasi-rotational degrees of freedom are *incorrect*.

3.3. Cantilever Plate under Simple Bending

Let us consider a plate shown in Figure 5: $E=3e7\text{ kPa}$, $\nu=0.25$, $h=1\text{ m}$, $a=48\text{ m}$, $b=12\text{ m}$. The plate is subjected to the following loads:

- on the side $x=a$:
 $f_y = -6ry(b-y)$ – parabolic load;
- on the side $x=0$: $f_x = 6ra(b-2y)$;
 $f_y = 6ry(b-y)$, $r = f/b^3/E$, $f = 40\text{ kN}$.

Table 2. Displacements, stresses and rotation angles in a narrow plate (loaded by a concentrated moment).

Mesh type	Element	Displacements w_A (m)				Stresses σ_B (kPa)				Rotation angles ω_E (rad)			
		Mesh				Mesh				Mesh			
		1x6	2x12	4x24	8x48	1x6	2x12	4x24	8x48	1x6	2x12	4x24	8x48
A	b	-1.499	-1.467	-1.457	-1.453	5.996	5.998	5.997	5.991	0.6877	1.5776	5.0046	18.805
	c	-1.499	-1.474	-1.464	-1.454	5.996	5.998	5.997	5.991	0.6877	1.5516	5.0064	18.803
	f	-1.286	-1.397	-1.449	-1.470	4.877	5.673	5.915	5.978	0.3178	0.3784	0.3943	0.3986
	g	-1.255	-1.403	-1.452	-1.470	4.775	5.639	5.905	5.976	0.3170	0.3749	0.3937	0.3984
	k	-0.938	-1.291	-1.431	-1.472	3.053	4.743	5.529	5.817	0.2409	0.3454	0.3846	0.3960
B	b	-1.225	-1.393	-1.456	-1.442	5.801	6.424	6.446	6.413	0.5241	0.9224	2.8121	10.096
	c	-1.295	-1.419	-1.441	-1.443	5.803	6.392	6.428	6.408	0.6074	1.2582	3.103	10.373
	g	-0.796	-1.208	-1.390	-1.455	3.264	5.241	5.805	5.951	0.1970	0.3207	0.3758	0.3936
	k	-0.780	-1.194	-1.396	-1.461	2.336	4.088	5.280	5.747	0.1999	0.3186	0.3758	0.3936
C	a	-1.029	-1.502	-1.700	-1.747	4.305	6.959	8.027	8.017	0.5514	0.6701	2.4418	9.1624
	d	-0.916	-1.279	-1.423	-1.467	4.801	6.097	6.252	6.171	0.2429	0.3447	0.3828	0.3952
	i	-0.697	-1.113	-1.359	-1.451	1.781	3.412	4.894	5.635	0.1785	0.2983	0.3668	0.3908
D	h	-1.528	-1.494	-1.494	-1.490	6.072	6.013	6.002	6.001	0.3897	0.4034	0.3953	0.3991
	l	-1.511	-1.496	-1.487	-1.483	6.003	6			0.3991	0.3996	0.4	
E	h	-1.521	-1.493	-1.495	-1.489	6.295	6.069	6.019	6.005	0.3703	0.4088	0.3976	0.3987
	l	-1.504	-1.490	-1.484	-1.484	5.998	6			0.3993	0.3974	0.4	
F	e	-1.372	-1.477	-1.490	-1.488	5.300	5.754	5.914	5.970	0.3788	0.3917	0.3974	0.3993
	j	-1.514	-1.519	-1.485	-1.482	6.001	6			0.3983	0.3994	0.3999	0.4

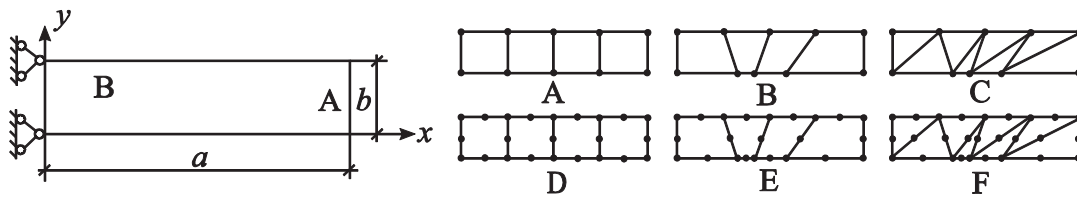


Figure 5. Cantilever plate and its design models.

This problem has an analytical solution:

$$\begin{aligned}
 u &= r(3(b-2y)(x-a)^2 - (v+2)(3by^2 - 2y^3)(6a^2 + (v+2)b^2)y - 3ba^2) \\
 v &= r(-6v(by - y^2)(x-a) + 2(x-a)^2 - (6a^2 + (v+2)b^2)x + 2a^3) \quad (69)
 \end{aligned}$$

The load on the side $x=0$ was ignored in many studies. In the case of the third degree of freedom it is an approximation even when there no additional nodes on the side of the cantilever. The design models shown in Figure 5 are taken from [2], where this problem was considered. Table 3 contains calculated vertical

displacements at the point A(48,6) and stresses σ_x at the point B(12,12). The following analytical solution is obtained from (69): $w_A = -0.353(3)m$, $\sigma_{x,B} = 60kPa$. $0.353(3)m$, $\sigma_{x,B} = 60kPa$.

3.4. Cook's Problem

Let us consider a wedge with a clamped left edge shown in Figure 6. A uniformly distributed load P is applied to its right edge. Following [4] we take:

$$\begin{aligned}
 E &= 1Pa, \quad v = 0.3(3), \quad h = 1m, \\
 P &= 0.0625 \text{ N/m}, \quad u|_{x=0}=0, \quad v|_{x=0}=0.
 \end{aligned}$$

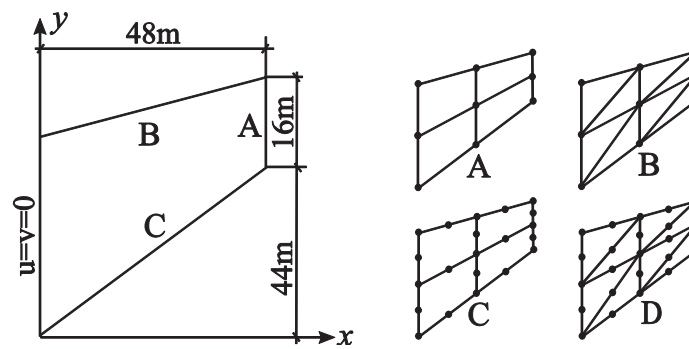


Figure 6. Wedge and its design models.

Table 3. Displacements and stresses in a cantilever plate.

Mesh type	Element	Displacements w_A (m)				Stresses σ_B (kPa)			
		Mesh				Mesh			
		1x4	2x8	4x16	8x32	1x4	2x8	4x16	8x32
A	<i>b</i>	-0.3283	-0.3456	-0.3511	-0.3527	59.988	60.998	60.746	60.438
	<i>c</i>	-0.3283	-0.3458	-0.3512	-0.3527	59.988	60.980	60.746	60.437
	<i>f</i>	-0.3541	-0.3583	-0.3586	-0.3572	64.969	61.874	61.028	60.509
	<i>g</i>	-0.3480	-0.3556	-0.3572	-0.3564	63.811	61.823	60.990	60.500
	<i>k</i>	-0.2742	-0.3264	-0.3451	-0.3510	43.205	54.035	57.923	59.226
B	<i>b</i>	-0.3342	-0.3465	-0.3513	-0.3527	61.512	61.304	60.945	60.501
	<i>c</i>	-0.3271	-0.3462	-0.3513	-0.3528	59.743	61.140	60.934	60.501
	<i>g</i>	-0.3227	-0.3487	-0.3544	-0.3553	61.805	62.292	61.366	60.725
	<i>k</i>	-0.2614	-0.3216	-0.3434	-0.3504	39.607	52.825	57.497	59.064
C	<i>a</i>	-0.2471	-0.3179	-0.3427	-0.3503	36.867	50.599	56.499	58.611
	<i>d</i>	-0.2673	-0.3236	-0.3440	-0.3505	44.407	52.306	57.177	59.052
	<i>i</i>	-0.2141	-0.2902	-0.3297	-0.3457	35.949	48.270	55.999	58.521
D	<i>h</i>	-0.3567	-0.3522	-0.3521	-0.3525	64.896	61.840	60.458	60.128
	<i>l</i>	-0.3540	-0.3534	-0.3533	-0.3533	60.004	60		
E	<i>h</i>	-0.3585	-0.3529	-0.3522	-0.3525	63.849	61.159	60.288	60.092
	<i>l</i>	-0.3533				59.328	59.804	59.960	59.991
F	<i>e</i>	-0.3398	-0.3488	-0.3519	-0.3529	41.195	52.981	57.554	58.844
	<i>j</i>	-0.3470	-0.3523	-0.3532	-0.3533	62.438	60.555	60.090	60.017

A statically equivalent stress was also considered when uniformly distributed moments were applied at the ends of the plate and reduced to a nodal load using the formula (8). No analytical solution is known for this problem. Stable numerical solution with an accuracy of up to 6 significant digits, obtained with various finite elements and mesh refinement up to 1024×1024 (3149825 nodes, 2^{20} elements):

- vertical displacement $w_A = -23.9677\text{m}$,
- principal stresses $\sigma_{1,B} = 0.203525\text{ Pa}$ and $\sigma_{3,C} = -0.23687\text{ Pa}$.

Table 4 shows the results of experiments. Some papers assume $\nu = 0.3$. The values are slightly different in this case:

$$w_A = -23.9119\text{m}, \sigma_{1,B} = 0.20353\text{Pa} \\ \text{and } \sigma_{3,C} = -0.23692\text{Pa}.$$

Table 4. Displacements and principal stresses in Cook's problem.

Mesh type	Element	Displacements w_A (m)				Pr. stresses $\sigma_{1,B}$ (kPa)				Pr. stresses $\sigma_{3,C}$ (kPa)			
		Mesh				Mesh				Mesh			
		2x2	4x4	8x8	16x16	2x2	4x4	8x8	16x16	2x2	4x4	8x8	16x16
A	<i>b</i>	-21.66	-23.23	-23.78	-23.92	0.1774	0.1977	0.2009	0.2032	-0.1730	-0.2197	-0.2322	-0.2354
	<i>c</i>	-21.56	-23.22	-23.78	-23.92	0.1747	0.1977	0.2007	0.2032	-0.1711	-0.2193	-0.2322	-0.2354
	<i>g</i>	-17.26	-21.92	-23.37	-23.79	0.1777	0.2013	0.2039	0.2049	-0.1760	-0.2279	-0.2388	-0.2395
	<i>k</i>	-17.55	-21.53	-23.13	-23.69	0.1430	0.1769	0.1953	0.2013	-0.1470	-0.1982	-0.2249	-0.2338
B	<i>a</i>	-17.46	-21.51	-23.23	-23.75	0.1196	0.1618	0.1873	0.1970	-0.1643	-0.2124	-0.2312	-0.2363
	<i>d</i>	-18.49	-22.00	-23.34	-23.76	0.1687	0.1693	0.1940	0.2018	-0.2011	-0.2382	-0.2485	-0.2482
	<i>i</i>	-15.36	-18.97	-21.60	-23.07	0.1486	0.1547	0.1838	0.1964	-0.1446	-0.1838	-0.2147	-0.2337
C	<i>h</i>	-23.24	-23.79	-23.90	-23.94	0.2051	0.2015	0.2042	0.2040	-0.2629	-0.2466	-0.2399	-0.2377
	<i>l</i>	-22.97	-23.76	-23.90	-23.94	0.2114	0.2023	0.2041	0.2037	-0.2557	-0.2430	-0.2392	-0.2375
D	<i>e</i>	-22.14	-23.57	-23.85	-23.93	0.1911	0.1903	0.1988	0.2014	-0.2110	-0.2301	-0.2369	-0.2376
	<i>j</i>	-21.21	-23.42	-23.85	-23.93	0.1305	0.1971	0.2020	0.2032	-0.1931	-0.2304	-0.2379	-0.2375

3.5. Bending of an Unlimited Wedge by a Concentrated Moment Applied to Its Vertex (Inglis Problem).

Let us consider an unlimited wedge with thickness $h=1\text{m}$ and moment M applied to its vertex shown in Figure 7a: r, β – polar coordinates of the point. This problem has an analytical solution [22]:

$$\begin{aligned}\sigma_r &= \frac{2M \sin(2\beta)}{r^2(2\alpha \cos(2\alpha) - \sin(2\alpha))}, \\ \tau_{r\beta} &= \frac{2M(\cos(2\alpha) - \cos(2\beta))}{r^2(2\alpha \cos(2\alpha) - \sin(2\alpha))}\end{aligned}\quad (70)$$

Let us consider the area $R \leq 24\text{m}$, $\alpha=22.5^\circ$ and specify the boundary conditions shown in Figure 7b. According to the Saint-Venant's principle these constraints will not have a significant effect on the results, since we will consider points A(4,-22°) and B(4,0°). Analytical solutions according to (70):

$$\sigma_{p,A} = 0.582474 \text{ kPa}, \tau_{r\beta,B} = 0.120634 \text{ kPa}.$$

We take:

$$E = 3.0 \cdot 10^7 \text{ kPa}, \nu = 0.2, h=1\text{m}, M=-1\text{kN}.$$

Radii of points in the design models in Figure 8: 0.5, 0.625, 1, 1.75, 2.5, 3.25, 4, 4.75, 5.5, 6.5, 7.75, 9.25, 11, 13, 15.5, 18, 21, 24.

Table 5 shows the results of calculations only for elements with degrees of freedom ω_z , since they are incorrect for elements with quasi-rotational degrees of freedom.

Let us consider the area $R \leq 24\text{m}$, $\alpha=22.5^\circ$ and specify the boundary conditions shown in Figure 7b. According to the Saint-Venant's principle these constraints will not have a significant effect on the results, since we will consider points A(4,-22°) and B(4,0°). Analytical solutions according to (70):

$$\sigma_{p,A} = 0.582474 \text{ kPa}, \tau_{r\beta,B} = 0.120634 \text{ kPa}.$$

We take:

$$E = 3.0 \cdot 10^7 \text{ kPa}, \nu = 0.2, h=1\text{m}, M=-1\text{kN}.$$

Radii of points in the design models in Figure 8: 0.5, 0.625, 1, 1.75, 2.5, 3.25, 4, 4.75, 5.5, 6.5, 7.75, 9.25, 11, 13, 15.5, 18, 21, 24.

Table 5 shows the results of calculations only for elements with degrees of freedom ω_z , since they are incorrect for elements with quasi-rotational degrees of freedom.

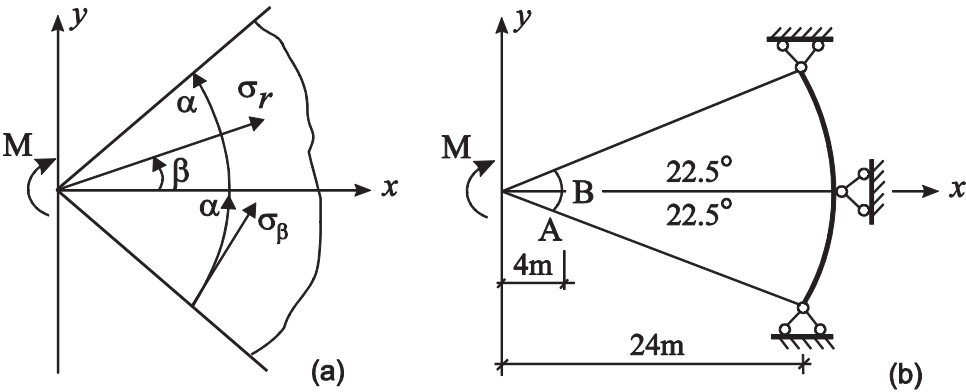


Figure 7. Inglis problem.

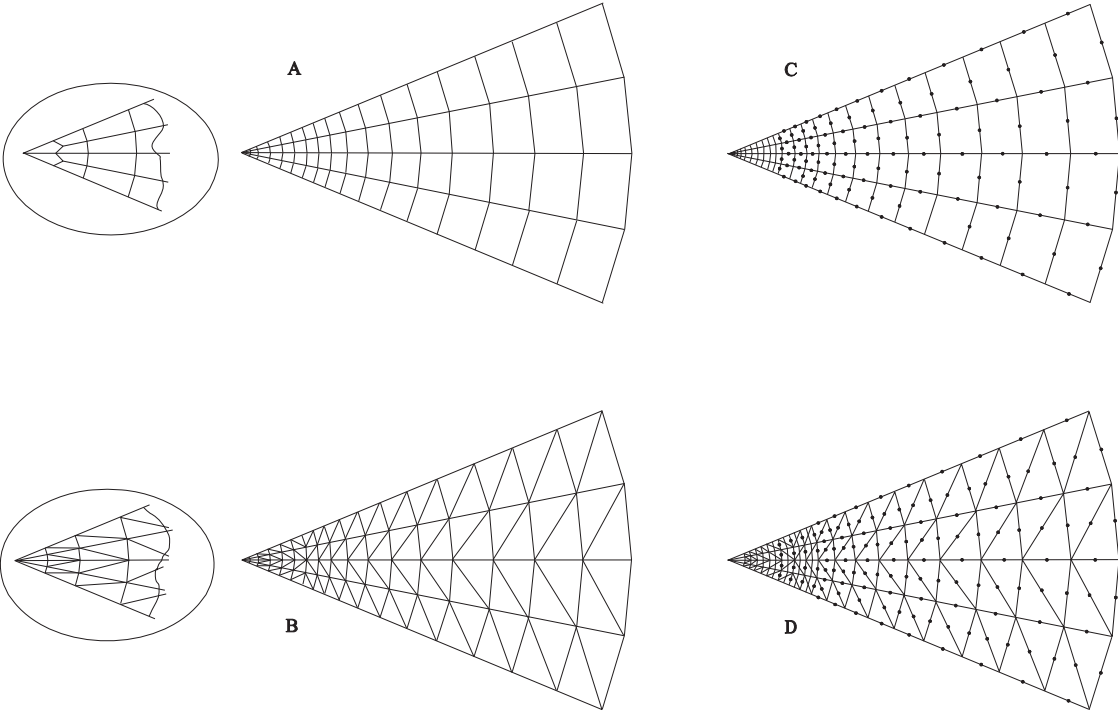


Figure 8. Wedge design models.

Table 5. Stresses in the Inglis problem.

Mesh type	Element	Stresses $\sigma_{r,A}$ (Pa)				Stresses $\tau_{t\beta,B}$ (Pa)			
		Mesh				Mesh			
		A	A2	A4	A8	A	A2	A4	A8
A	<i>g</i>	0.6108	0.5909	0.5851	0.5834	0.0914	0.1172	0.1216	0.1218
	<i>k</i>	0.5759	0.5781	0.5801	0.5812	0.1216	0.1208	0.1208	0.1207
C	<i>d</i>	0.6578	0.6108	0.5940	0.5875	0.1135	0.1121	0.1164	0.1185
	<i>i</i>	0.5541	0.5761	0.5811	0.5822	0.1043	0.1217	0.1232	0.1224
B	<i>h</i>	0.5637	0.5784	0.5816	0.5823	0.1522	0.1263	0.1220	0.1210
	<i>l</i>	0.5737	0.5809	0.5821	0.5824	0.1414	0.1259	0.1219	0.1210
D	<i>e</i>	0.6066	0.5892	0.5843	0.5830	0.1283	0.1244	0.1230	0.1220
	<i>j</i>	0.5418	0.5706	0.5791	0.5816	0.1220	0.1213	0.1209	0.1207

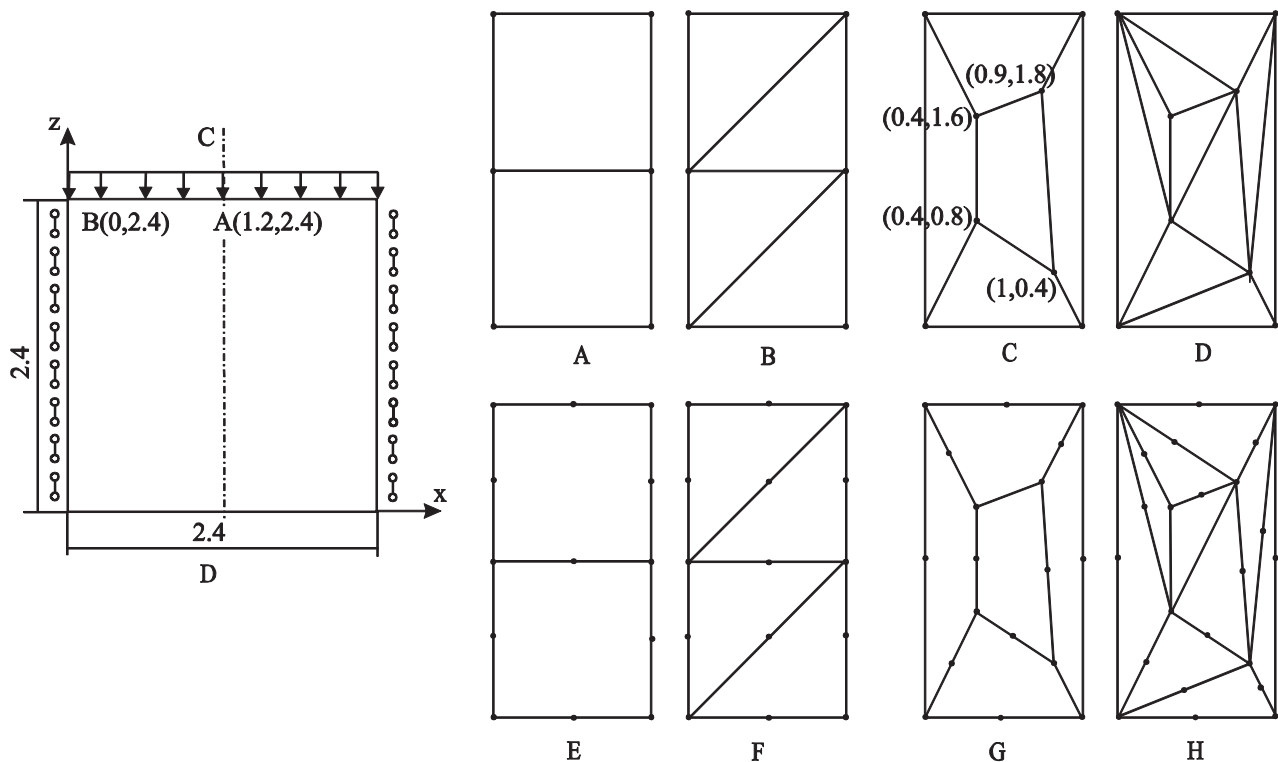


Figure 9. Deep beam and its design models.

3.6. Bending of a Rectangular Deep Beam.

Let us consider a square deep beam rigidly suspended on the sides $x=0$ and $x=2.4$ (Figure 9) and subjected to a uniformly distributed load p applied to its upper edge. This problem has an analytical solution in series, given in [23]. Displacement values are calculated with high accuracy in [24] for a square plate with the following characteristics: $E=2.65 \cdot \text{MPa}$, $\nu=0.15$, $h=0.1\text{m}$, $p=500\text{N/m}$: $w_A=-3.763392\text{mm}$, $u_B=2.210055\text{mm}$.

The calculation is performed only for the half of the deep beam taking into account the axis of symmetry CD and the following boundary conditions: $w|_{x=0}=u|_{x=1.2}=\omega/\theta|_{x=1.2}=0$. Design models are shown in Fig. 9. Models C and D are the same as those used for patch tests [20]. Calculation results are given in Table 6.

4. CONCLUSIONS

The conducted numerical experiments have confirmed theoretical foundations for creating finite elements:

- elements with quasi-rotational degrees of freedom **a,b,c** and incompatible elements **d,f,g** yield almost identical results in displacements and stresses;
- elements **a,b,c** can yield incorrect results in rotation angles;
- *compatible* elements **i,k** yield *slightly worse* results compared to elements **a,b,c,d,f,g**;
- as expected, elements with intermediate nodes on the sides **e,h,j,l** have yielded the best numerical results. And compatible elements **j,l** are unparallelled;
- all elements with degrees of freedom ω_z enable to calculate structures subjected to both concentrated and uniformly distributed moments.

It is now interesting to study the application of the given approximations when creating shell elements (especially in combined design models with bar elements).

Table 6. Displacements in the rigidly suspended deep beam.

Mesh type	Element	Displacements w_A (mm)				Displacements u_B (mm)			
		Mesh				Mesh			
		2x2	4x4	8x8	16x16	2x2	4x4	8x8	16x16
A	<i>b</i>	-3.4643	-3.6726	-3.7415	-3.7580	1.9846	2.1234	2.1739	2.1966
	<i>c</i>	-3.4603	-3.6686	-3.7414	-3.7580	1.8881	2.0835	2.1546	2.1870
	<i>f</i>	-3.5971	-3.6802	-3.7410	-3.7577	2.0216	2.0975	2.1564	2.1875
	<i>g</i>	-3.5344	-3.6762	-3.7395	-3.7573	1.8855	2.0341	2.1258	2.1725
	<i>k</i>	-3.3881	-3.6433	-3.7312	-3.7554	1.9479	2.0749	2.1505	2.1858
B	<i>a</i>	-3.2005	-3.6080	-3.7249	-3.7547	1.8805	2.0160	2.1214	2.1715
	<i>d</i>	-3.3494	-3.6562	-3.7377	-3.7582	2.1242	2.1274	2.1736	2.1967
	<i>i</i>	-3.0276	-3.5946	-3.7042	-3.7468	1.9472	2.0158	2.1133	2.1674
C	<i>b</i>	-3.1204	-3.6785	-3.7518	-3.7627	1.4033	1.9437	2.0779	2.1411
	<i>c</i>	-3.1483	-3.6716	-3.7507	-3.7626	1.5706	1.9523	2.0554	2.1257
	<i>g</i>	-3.1957	-3.6065	-3.7582	-3.7745	1.6774	1.6550	1.8636	2.0106
	<i>k</i>	-2.8401	-3.4950	-3.6285	-3.7053	1.8166	2.0413	2.1162	2.1461
D	<i>a</i>	-3.0684	-3.5233	-3.6936	-3.7464	1.7172	1.9280	2.0795	2.1497
	<i>d</i>	-3.2120	-3.5619	-3.7015	-3.7492	2.0067	2.0686	2.1351	2.1736
	<i>i</i>	-2.7636	-3.1829	-3.3407	-3.4860	1.8346	1.8803	1.9712	2.0734
E	<i>h</i>	-3.8112	-3.7866	-3.7752	-3.7677	1.9724	2.1122	2.1663	2.1923
	<i>l</i>	-3.7435	-3.7543	-3.7630	-3.7635	1.8486	2.0507	2.1359	2.1770
G	<i>h</i>	-3.8661	-3.8615	-3.8079	-3.7799	1.6800	1.9761	2.0908	2.1497
	<i>l</i>	-3.5164	-3.7586	-3.7651	-3.7639	1.3827	1.8735	2.0504	2.1316
F	<i>e</i>	-3.8582	-3.7694	-3.7593	-3.7621	1.7710	2.0022	2.1109	2.1648
	<i>j</i>	-3.4784	-3.7437	-3.7620	-3.7634	1.6815	1.9797	2.1015	2.1600
H	<i>e</i>	-3.6114	-3.7890	-3.8003	-3.7818	1.7490	1.9895	2.1021	2.1594
	<i>j</i>	-3.4959	-3.7713	-3.7742	-3.7665	1.4127	1.8596	2.0539	2.1392

REFERENCES

1. **Novozhilov V.V.** Osnovy nelineynoy teorii uprugosti [Foundations of the Nonlinear Theory of Elasticity]. Moscow, Gostekhteorizdat, 1948, 333 pages (in Russian).
2. **Allman D.J.** A compatible triangular element including vertex rotations for plane elasticity analysis. // *Computers and Structures*, 1984, Vol. 19(1-2), pp. 1-8.
3. **Allman D.J.** A quadrilateral finite element including vertex rotations for plane elasticity analysis. // *International Journal for Numerical Methods in Engineering*, 1988, Vol. 26(3), pp. 717-730.
4. **Cook R.D.** On the Allman triangle and a related quadrilateral element. // *Computers and Structures*, 1986, Volume 22(6), pp. 1065-1067.
5. **MacNeal R.H., Harder R.L.** A refined four-noded membrane element with rotational degrees of freedom. // *Computers and Structures*, 1988, Vol. 28(1), pp. 75-84.
6. **Karpilovskiy V.S.** Novyy sovместnyy chetyrehugolnyy konechnyy element balki-stenki s vrashchatelnymi stepenyami svobody [New compatible quadrangular deep beam finite element with rotational degrees of freedom]. // *Materials of the II International Scientific and Practical Conference "Suchasni` metodi i problemno-oriyintovani kompleksi rozrakhunku konstrukcij i yikh zastosuvannya u proyektuvanni i navchalnomu proczeni"* ["Modern Methods

- and Problem-Oriented Complexes for Structural Analysis and Their Application in Design and Educational Process*"]. Kyiv, September 2018, pp. 57-59 (in Russian)
7. **Wilson E.L., Ibrahimbegovic A.** Thick shell and solid elements with independent rotation fields. // *International Journal for Numerical Methods in Engineering*, 1991, Volume 31(7), pp. 1393-1414.
 8. **Zhang H., Kuong J.S.** Eight-node membrane element with drilling degrees of freedom for analysis of in-plane stiffness of thick floor plates. // *International Journal for Numerical Methods in Engineering*, 2008, Volume 76(13), pp. 2117-2136.
 9. **Yunus S., Saigal S., Cook R.** On improved hybrid finite elements with rotational degrees of freedom. // *International journal for numerical methods in engineering*, 1989, Vol. 28(4), pp. 785-800. DOI: 10.1002/nme.1620280405
 10. **Choo Y.S., Choi N., Lee B.C.** Quadrilateral and triangular plate elements with rotational degrees of freedom based on the hybrid Trefftz method. // *Finite Elements in Analysis and Design*, 2006, Volume 42(11), pp. 1002-1008.
 11. **Cook R.** A plane hybrid element with rotational d.o.f. and adjustable stiffness. // *International Journal for Numerical Methods in Engineering*, 1987, Volume 24(8), pp. 1499-1508.
 12. **Fellipa C.A.** A study of optimal membrane triangles with drilling freedoms. // *Computer Methods in Applied Mechanics and Engineering*, 2003, Volume 192(16-18), pp. 2125-2168.
 13. **Chen X.M., Cen S., Sun J.Y., Li Y.G.** Four-Node Generalized Conforming Membrane Elements with Drilling DOFs Using Quadrilateral Area Coordinate Methods. // *Mathematical Problems in Engineering*, 2015, Volumes 3-4, pp. 1-13.
 14. **Britvin E.I., Peysin A., Eisenberger M.** Deformiruyemyy v svoey ploskosti chetyrehugolnyy konechnyy element s vrashchatelnymi stepenyami svobody v uzlakh. Chast 2. Proizvolnyy chetyrehugolnik [Quadrangular finite element deformable in its plane with rotational degrees of freedom in the nodes. Part 2. Arbitrary quadrangle]. // *Structural Mechanics and Analysis of Constructions*, 2018, Volume 4, pp. 50-54 (in Russian).
 15. **Karpilovskyi V.S.** Issledovanie i konstruirovaniye nekotorykh tipov konechnykh elementov dlya zadach stroitel'noy mekhaniki. [Study and design of some types of finite elements for the structural mechanics problems]. // PhD Thesis, National transport university (KADI), Kyiv, 1982, 179 pages (in Russian)
 16. **Evzerov I.D.** Otsenki pogreshnosti po peremeshheniyam pri ispol'zovanii nesovmestny'kh konechny'kh e'lementov [Estimates of the error in displacements when using incompatible finite elements]. // *Chislennyye metody mekhaniki sploshnoy sredy [Numerical methods of continuum mechanics]*, Novosibirsk, 1983, Volume 14(5), pp. 24-31 (in Russian).
 17. **Gorodetsky A.S., Karpilovskyi V.S.** Metodicheskiye pekomentatsii po issledovaniyu i konstupipovaniyu konechnykh elementov [Methodological recommendations for the study and construction of finite elements]. Kyiv, NIIASS, 1981, 48 pages (in Russian).
 18. **Irons B.M., Razzaque A.** Experience with the path test. // In: *The Mathematical Foundations of the Finite Element Method with Application to Partial Differential Equations*, Academic Press, 1972, pp. 557-587.
 19. **Strang G., Fix G.** An Analysis of the Finite Element Method. Prentice Hall, Englewood Cliffs, N.J., 1973.
 20. **Aubin J.P.** Approximation of Elliptic Boundary-Value Problems. John Wiley & Sons, N.Y., 1972.
 21. **Macneal R.H., Harder R.L.** A proposed standard set of problems to test finite

element accuracy. // *Finite Elements in Analysis and Design*, 1985, Volume 1, pp. 3-20.

22. **Rekach V.G.** Rukovodstvo k resheniyu zadach po teorii uprugosti [Guide to Solving Problems of Elasticity]. Moscow, Vysha shkola, 1977, 216 pages (in Russian).
23. **Kalmanok A.S.** Raschet balok-stenok [Analysis of Deep Beams]. Moscow, Gosstroyizdat, 1956, 151 pages (in Russian).
24. **Gorodetsky A.S., Karpilovskyi V.S.** O svyazi metoda konechnykh elementov s variatsionno-raznostnymi metodami [On the relation between the finite element method and the variation difference methods]. // *Strength of Materials and Theory of Structures*, 1974, Volume 24, pp. 32-42. (in Russian).

СПИСОК ЛІТЕРАТУРИ

1. **Новожилов В.В.** Основы нелинейной теории упругости. – М.: Гостехтеориздат, 1948. – 333 с.
2. **Allman D.J.** A compatible triangular element including vertex rotations for plane elasticity analysis. // *Computers and Structures*, 1984, Vol. 19(1-2), pp. 1-8.
3. **Allman D.J.** A quadrilateral finite element including vertex rotations for plane elasticity analysis. // *International Journal for Numerical Methods in Engineering*, 1988, Vol. 26(3), pp. 717-730.
4. **Cook R.D.** On the Allman triangle and a related quadrilateral element. // *Computers and structures*, 1986, Volume 22(6), pp. 1065-1067.
5. **MacNeal R.H., Harder R.L.** A refined four-noded membrane element with rotational degrees of freedom. // *Computers and Structures*, 1988, Vol. 28(1), pp. 75-84.
6. **Карпиловский В.С.** Новый совместный четырехугольный конечный элемент балки-стенки с вращательными степенями свободы. // *Сборник трудов II Международной научно-практической конференции «Сучасні методи і проблемно-орієнтовані комплекси розрахунку конструкцій і їх застосування у проектуванні і навчальному процесі» [Современные методы и проблемно-ориентированные комплексы расчета конструкций и их применение в проектировании и учебном процессе]*. (г. Киев, 26-27 сентября 2018 года), Киев, 2018, с. 57-59.
7. **Wilson E.L., Ibrahimbegovic A.** Thick shell and solid elements with independent rotation fields. // *International Journal for Numerical Methods in Engineering*, 1991, Volume 31(7), pp. 1393-1414.
8. **Zhang H., Kuong J.S.** Eight-node membrane element with drilling degrees of freedom for analysis of in-plane stiffness of thick floor plates. // *International Journal for Numerical Methods in Engineering*, 2008, Volume 76(13), pp. 2117-2136.
9. **Yunus S., Saigal S., Cook R.** On improved hybrid finite elements with rotational degrees of freedom. // *International journal for numerical methods in engineering*, 1989, Vol. 28(4), pp. 785-800. DOI: 10.1002/nme.1620280405
10. **Choo Y.S., Choi N., Lee B.C.** Quadrilateral and triangular plate elements with rotational degrees of freedom based on the hybrid Trefftz method. // *Finite Elements in Analysis and Design*, 2006, Volume 42(11), pp. 1002-1008.
11. **Cook R.** A plane hybrid element with rotational d.o.f. and adjustable stiffness. // *International Journal for Numerical Methods in Engineering*, 1987, Volume 24(8), pp. 1499-1508.
12. **Fellipa C.A.** A study of optimal membrane triangles with drilling freedoms. // *Computer Methods in Applied Mechanics and Engineering*, 2003, Volume 192(16-18), pp. 2125-2168.
13. **Chen X.M., Cen S., Sun J.Y., Li Y.G.** Four-Node Generalized Conforming

- Membrane Elements with Drilling DOFs Using Quadrilateral Area Coordinate Methods. // *Mathematical Problems in Engineering*, 2015, Volumes 3-4, pp. 1-13.
14. **Бритвин Е.И., Пейсин А., Эйсенбергер М.** Деформируемый в своей плоскости четырехугольный конечный элемент с вращательными степенями свободы в узлах. Часть 2. Произвольный четырехугольник. // *Строительная механика и расчет сооружений*, 2018, №4, с. 50-54.
 15. **Карпиловский В.С.** Исследование и конструирование некоторых типов конечных элементов для задач строительной механики. Диссертация на соискание ученой степени кандидата технических наук по специальности 01.02.03 – «Строительная механика». – Киев: Национальный транспортный университет (КАДИ), 1982. – 179 с.
 16. **Евзеров И.Д.** Оценки погрешности по перемещениям при использовании несовместных конечных элементов // *Численные методы механики сплошной среды*, 1983, том 14, №5, с. 24-31.
 17. **Городецкий А.С., Карпиловский В.С.** Методические рекомендации по исследованию и конструированию конечных элементов. Киев: НИИАСС, 1981. – 48 с.
 18. **Irons B.M., Razzaque A.** Experience with the path test. // In: *The Mathematical Foundations of the Finite Element Method with Application to Partial Differential Equations*, Academic Press, 1972, pp. 557-587.
 19. **Стренг Г., Фикс Дж.** Теория метода конечных элементов – М.: Мир, 1977. – 349 с.
 20. **Обен Ж.-П.** Приближенное решение эллиптических краевых задач. – М.: Мир, 1977. – 384с.
 21. **Macneal R.H., Harder, R.L.** A proposed standard set of problems to test finite element accuracy. // *Finite Elements in Analysis and Design*, 1985, Volume 1, pp. 3-20.
 22. **Рекач В.Г.** Руководство к решению задач по теории упругости. – М.: Высшая школа, 1977. – 216 с.
 23. **Калманок А.С.** Расчет балок-стенок. – М.: Госстройиздат, 1956. – 151с.
 24. **Городецкий А.С., Карпиловский В.С.** О связи метода конечных элементов с вариационно-разностными методами. // *Сопротивление материалов и теория сооружений*, Выпуск 24, 1974, с. 32-42.

Viktor S. Karpilovskyi, PhD, Associated Professor, Director of IT Company ScadGroup Ltd.; 03037, 3A Osvity street, office 2, Kiev 03037, Ukraine; phone: +38(044)2497191(3); E-mail: kvs@scadsoft.com; <http://www.scadsoft.com>; ORCID: 0000-0002-9437-0373.

Карпиловский Виктор Семенович, кандидат технических наук, старший научный сотрудник, директор ООО ScadGroup; 03037, Украина, г.Киев, ул. Освіти(Просвещения), д.3а, оф. 2; тел: +38(044)2497191(3); E-mail: kvs@scadsoft.com; <http://www.scadsoft.com>; ORCID : 0000-0002-9437-0373.

TO ASSESS THE HORIZONTAL DISPLACEMENT OF PILES CAUSED BY EXCAVATION OF THE SOIL OF THE PIT

D.S. Kolesnik, Rashid A. Mangushev

Saint-Petersburg State University of Architecture and Civil Engineering, Saint-Petersburg, RUSSIA

Abstract: The article discusses and justifies the cases of horizontal movement of the top of the piles in the case of digging a pit of great depth. A statistical analysis of the results of executive documentation for completed pile fields at three construction sites in St. Petersburg was carried out, which made it possible to prove the causes of excess movements of the pile heads. A technique for assessing deformations depending on the depth of excavation of the pit and the characteristics of the soil base is proposed. The decrease in the modulus of subgrade reaction for calculating piles in the conditions of softened soils near the pile space is proved.

Keywords: piles, horizontal loading, excavation of the pit, deflection of the heads of piles, soft clay soils.

К ОЦЕНКИ ГОРИЗОНТАЛЬНОГО СМЕЩЕНИЯ СВАЙ ВЫЗВАННОГО ЭКСКАВАЦИЕЙ ГРУНТА КОТЛОВАНА

Д.С. Колесник, Р.А. Мангушев

Санкт-Петербургский государственный архитектурно-строительный университет,
г. Санкт-Петербург, РОССИЯ

Аннотация: В статье рассматриваются и обосновываются случаи горизонтального перемещения верха свай в случае рытья котлована значительной глубины. Был проведен статистический анализ результатов исполнительной документации по заполненным свайным полям на трех строительных площадках в Санкт-Петербурге, что позволило доказать причины избыточных перемещений свайных головок. Предложена методика оценки деформаций в зависимости от глубины выемки котлована и характеристик грунтового основания. Доказано уменьшение модуля реакции субстрата для расчета свай в условиях размягченных почв вблизи свайного пространства.

Ключевые слова: сваи, горизонтальная загрузка, выемка котлована, прогибы свай,
мягкие глинистые почвы

1. INTRODUCTION

In modern civil engineering, the organization of underground volumes is increasingly used with the placement of parking lots, used cellars, communications, etc.

In the conditions of the spread of large strata of weak clay soils, the arrangement of underground premises is fraught with difficulties and risks associated with the construction of a foundation pit fence. The most rational construction of the foundation in this case are piles made from the upper surface before the excavation.

The spread of pile foundations is associated, among other things, with a reduction in the duration of the zero-cycle work compared to footings on a natural foundation. The speed of the work is achieved due to the high technical characteristics of the equipment, as well as the combination of the processes of performing elements of the pile field and excavation of the pit.

As a rule, for the rational use of the underground space, a pit is usually performed with a depth of 5 to 8 m, with one or two basement floors, respectively. The installation of piles for buildings with an underground volume is usually

performed from the upper surface with the subsequent development of the pit to the design level. A driven or pressed-in pile can be put down with a mark of its head below the soil surface by 3 - 5 m, respectively, when using equipment for additional pressure to pile.

The mark of the top of piles made by drilling or ramming technology is usually combined with the horizon from which work is performed. The pile shaft above the assumed grillage is made unreinforced using the same concrete as the main section for piles of small diameter (up to 520 mm) or made of sand for larger piles, when it is economically viable.

Note that when performing elements of a pile field from the bottom of the pit, additional costs arise for the arrangement of ramps or the operation of cranes necessary to deliver construction equipment to the front of the work. In addition, in order to be able to carry out extreme piles, it is necessary to increase the dimensions of the pit compared to the first option. These measures are usually not economically feasible, and sometimes impossible if there is an existing dense building on the building site.

The excavation of foundation pits of basements in the conditions of the spread of soft soils is carried out after the organization the fencing under the protection of spacers or soil berm [1]. Excavation pits, spacer structures and soil berms are calculated according to their strength and stability to ensure mechanical safety of both the new construction project itself and the surrounding buildings. These calculations are performed on the condition that the permissible additional settlement of neighboring buildings is not exceeded.

On the other hand, maps of soils excavation and transport patterns during the excavation are reflected in the project of construction organization (PCO).

The sections of the documentation related to PCO do not suggest the possibility of serious errors or omissions in them, which, in turn, can lead to accidents or additional costs. These documents are developed from the experience of

construction and production facilities of the contractor. It is assumed that all the necessary analytical calculations and, especially, modeling in the FEM programs are carried out in the design of load-bearing and enclosing structures. In addition, a design organization is assigned a technique for performing pile field and loading on the of the pit boundaries.

Standard GOST 27751-2014 [2] prescribes to consider design transitional situations, that is, situations that have a short duration compared to the service life of a construction object. In particular, piles already completed, on which any external influence is exerted, must be calculated on it from the condition of limiting displacement, deflections, and moments. An example of such impacts is - loads on the soil caused by the operation of pile equipment, loads from moving or storing goods in the immediate vicinity of the pile or, loads caused by excavation of the pit.

When excavating a pit, the difference in elevations (from the layout to the bottom of the pit) causes horizontal pressures acting on the piles. If this factor is not taken into account, then at a significant pit depth (of the order of 5 m) in conditions of weak underlying soils, the pile heads receive significant deviations, reaching the order of several of their diameters and often exceeding the permissible ones (Figure 1).

As it is known, grillages are designed so that their contours overlap the contour of the pile field by $0.2d$, where d is the diameter or width of the pile. If the position of the goals in the plan exceeds these admissions, then we have to change the construction of the foundations, which entails the loss of time and material resources. In a number of cases, the question arises about the possibility of incorporating deviated piles into the work or their duplication.

Almost all federal or regional technical documents on the organization of work do not consider this aspect. An exception is one of the organization's standards [3], which limits the depth of cut during excavation by two meters, but this standard is based on practical experience in the manufacture of indentation piles in St. Petersburg, which of course cannot be extended to all possible cases.



Figure 1. Horizontal displacements of driven and bored piles.

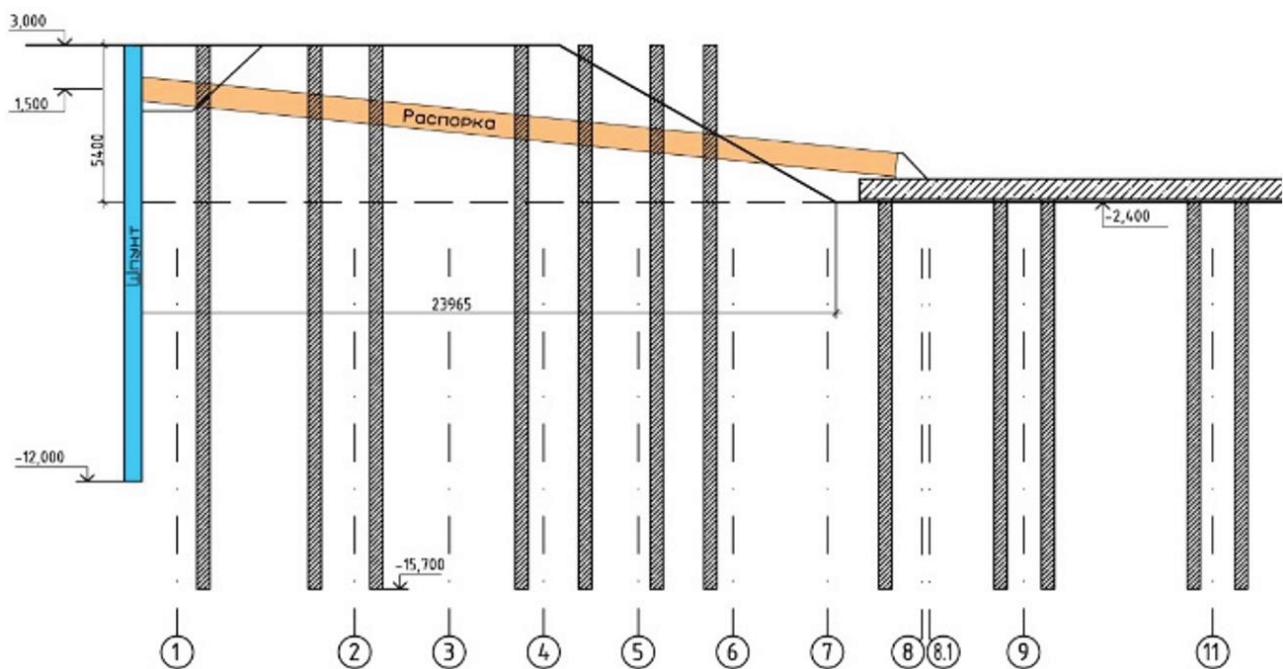


Figure 2. General scheme of the structural elements of the pit, spacer system, pile foundation.

On the other hand, forecasting and calculating such situations does not fall into the area of responsibility of specialized organizations, even if they carried out a geotechnical substantiation or design of enclosing structures. Relatively simple modeling of excavation in a two-

dimensional setting (a series of piles is presented in the form of a wall) gives underestimated values of forces in structures [4]. Thus, in the general case, highly qualified engineers and special software are required that allow three-dimensional modeling of the soil range [5,6].

2. EXAMPLES AND ANALYSIS OF THE HORIZONTAL DEVIATION OF THE UPPER PART OF THE PILES DURING THE EXCAVATION OF PITS

As an example of horizontal deviation of piles, we can consider the construction of a parking lot for a residential building under construction in one of the districts of St. Petersburg.

The foundation of the car park of one of the buildings is a grillage slab resting on a pile field of 216 bored piles with a diameter of $d = 520$ mm and a length of $L = 14.3$ m (after felling) made using the Fundex technology [7,8]. The point of the piles is entered into moraine glacial deposits lgIII, represented by dusty sandy loam and loam with gravel and pebbles). The calculated load on the pile adopted $N = 1500$ kN.

The arrangement of the underground space involved the excavation of a pit to a depth of 5.4 m. At the first stage of excavation of the pit, soil was extracted to the design level of the bottom of the pit with the arrangement of soil berm. On the following, a grillage slab and a strut system were carried out, after which the final excavation of the soil from the pit was carried out. Figure 2 shows a general diagram of the pit indicating the marks of structural elements of the fence, piles, grillage slabs.

Because of the first stage of work, previously manufactured piles received significant deviations in plan. As can be seen from Figure 3, measured in the process of geotechnical monitoring, the displacement of elements in a pile field is characterized by large values as they approach the pit edge (soil berm).

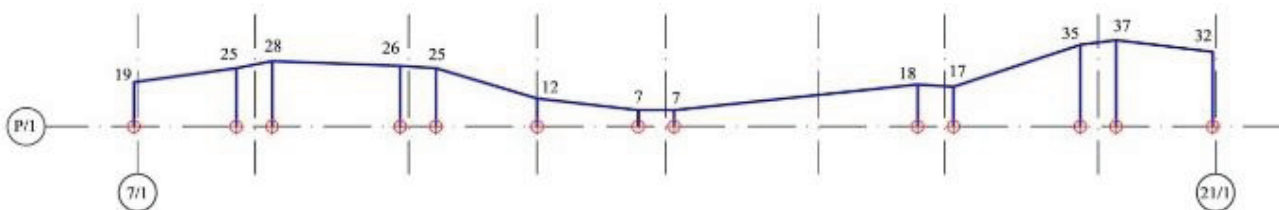


Figure 3. Diagram of the horizontal displacement of piles in cm (section along the P / 1 axis).

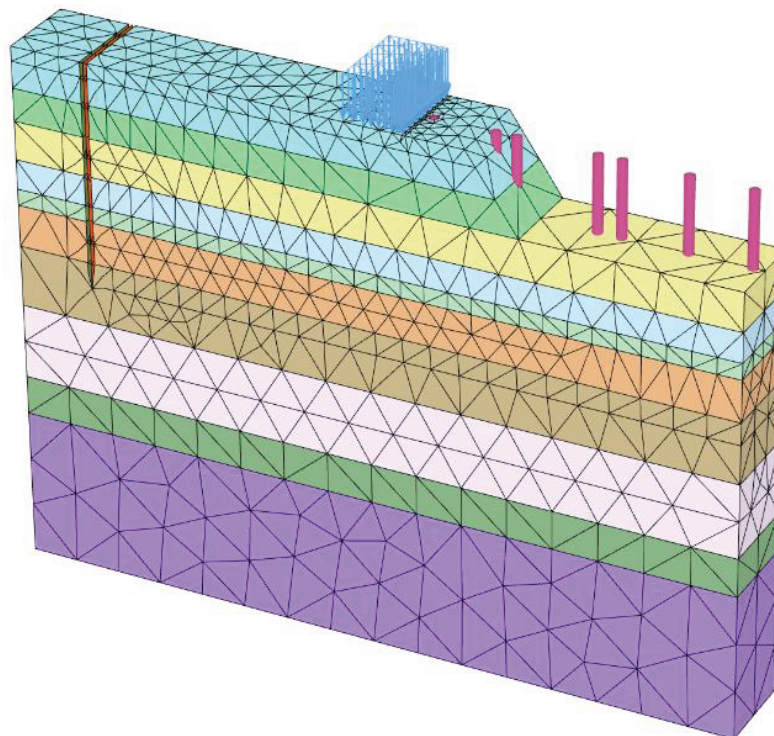


Figure 4. The design scheme of the simulated area.

The displacement of the heads of piles is associated with the horizontal pressure of the soil during the complete excavation of the excavation soil. The indicated effect is obvious from the point of view of soil mechanics and is confirmed by numerical calculation in the Plaxis 3D software package (Fig. 4). The simulation results showed that the deviation of the top of the piles can reach 46 cm or more. The horizontal movement of piles at an absolute mark of 1.780 (felling) reaches 25 cm.

Figures 4 and 5 show a design diagram including a series of piles along the "P / 1" axis and a soil mass limited by the "1" and "14/1" axes. On the edge of the slope, the load distributed over the area is simulated by pressure from the excavator. The calculation was carried out in several stages of soil excavation in the direction from the center of the pit (axis "14/1") to the sheet pile fence (axis "1"). Figure 6 shows plots of horizontal movements of piles during excavation of the central part of the pit in the axes "7" - "22" with the arrangement of soil berms. The implementation of such calculations for labor costs is comparable to the design of the capital construction objects themselves. Thus, for the described design case (a combination of weak clay soils and a large excavation depth), the need for expanding the set of design documentation with the geotechnical substantiation section related to the work below zero is obvious.

3. STATISTICAL ANALYSIS OF HORIZONTAL DEVIATIONS OF THE TOP OF THE PILES DURING THE CONSTRUCTION OF PITS

The situation when during the excavation of the pit piles get bent and horizontal movement is relatively new and is little reflected in both

technical documents and scientific publications. There is no justification of the necessary time from the moment of completion of piles to their excavation, which would allow the restoration of structural bonds in the soil near the pile space. For this case, the load on the edge of the excavation pit, for example, from a pile-pressing installation, the weight of which can reach up to 1200-1600kN, is also not taken into account.

As is known, Russian Building Code SP 45.13330.2017 [9] limits the horizontal movement of the heads at the tape and cluster piles to 0.2d (0.3d for deviations along the row). Obviously, these deviations take into account the geodetic error and production technology errors, but not horizontal movements of piles caused by excavation of the pit [10].

Based on the results of the consideration of technical as-built documentation for the completed work of the zero cycle, the materials were analyzed when installing pile foundations at sites with similar geological conditions at three sites in St. Petersburg. On all construction sites, factory-made piles were used, made before excavating the pit.

During statistical processing, a section with the number of piles of more than 150 pieces was selected (for object No. 2, two grips were selected that differ in the way the piles were grouped).

For all objects, the characteristic depth of excavation was 4.2 - 4.6 m. Clay soils underlying the bottom of the pit belonged to a fluid or fluid plastic consistency. The thickness of the underlying layer is comparable to the length of piles and amounted to 11-20 m.

Figure 7 shows the distribution of the number of piles with one or another deviation of the heads. The main characteristics of the considered objects are given in Table. 1.

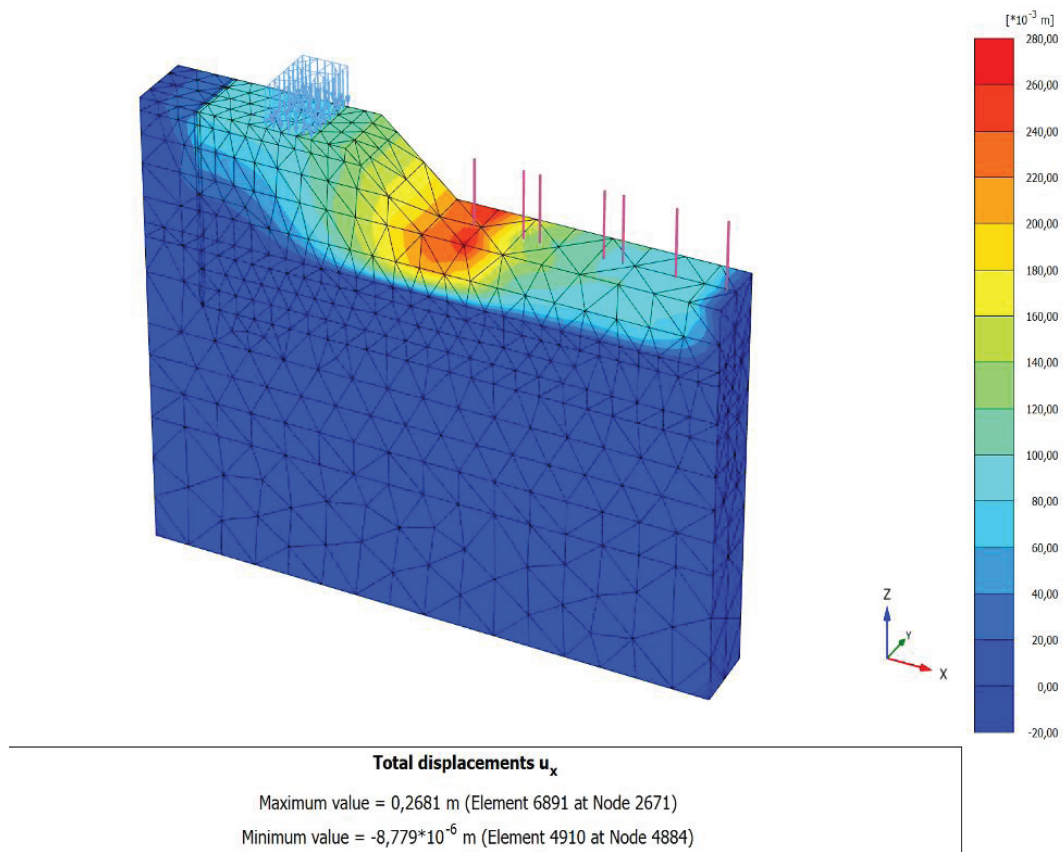


Figure 5. Horizontal movements of the soil mass during excavation.

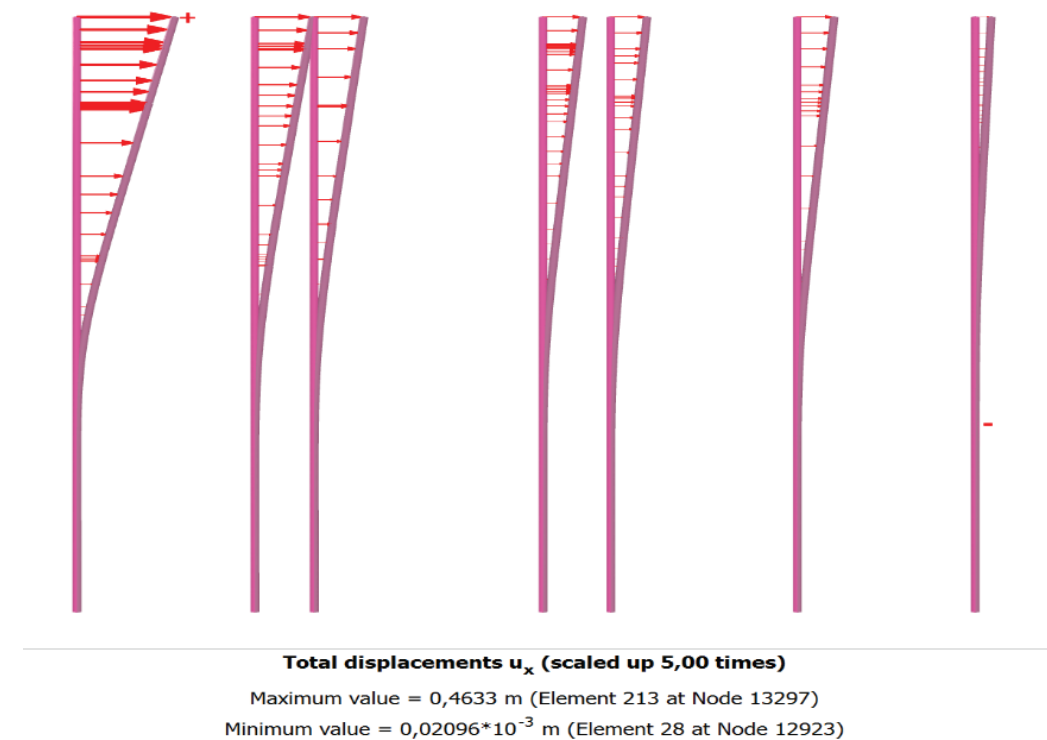


Figure 6. The calculated horizontal movements of piles during excavation of the central part of the pit with the device of soil berms.

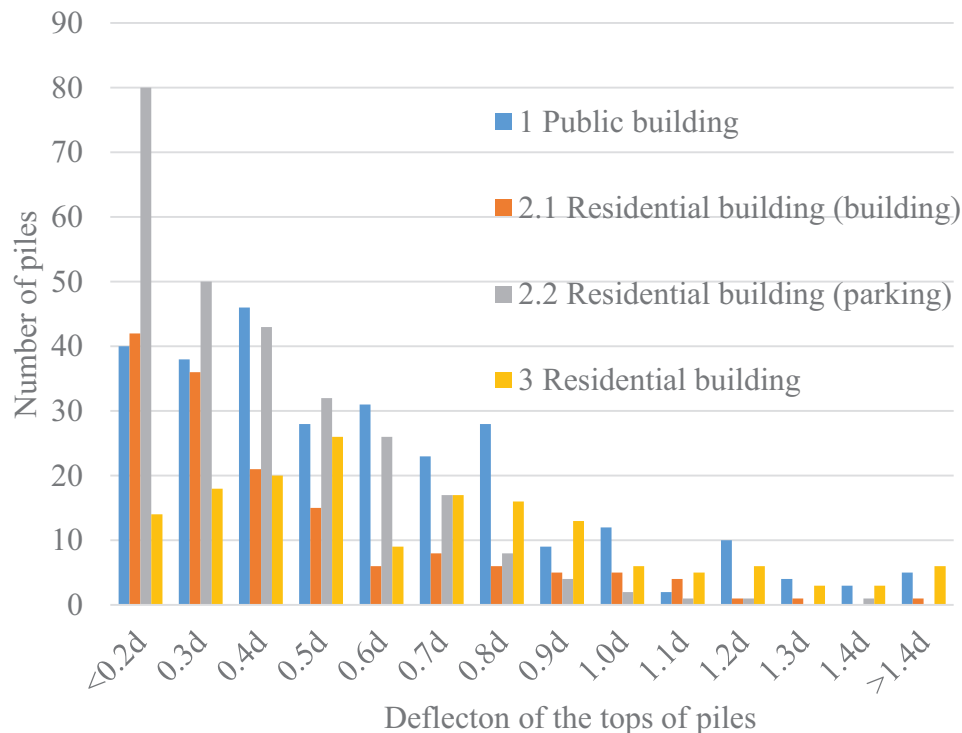


Figure 7. The distribution of the number of piles according to the deviation from the vertical.

Note that the values of deviations of piles after excavation is quite random. Basically, there is a deviation towards the excavation of the pit. On the other hand, the possibility of "accidental" movement, for example, across the slope or to each other for two adjacent piles, is not ruled out. Such their behavior can be caused by: excavation of neighboring elements from different sides, random loads along the edge of the pit, or piles being under load for a long time (during a break in work). In fig. 8 as an example, the value of the deviations of piles in the direction of excavation is presented, which amounted to: 18 25 cm (0.45d - 0.6d), across: 1-3 cm, which fits into the permissible error. Lines from the center of the piles indicate the movement of their head. At the same time, the maximum movements of piles reached 79 cm. As can be seen from the analysis of Figures 7, 8 and Table 1, in some cases, when digging pits of great depth in weak soils, horizontal deviations of the pile heads are observed, significantly exceeding the permissible values adopted in SP 45.13330.2017

[9], which in some cases required changes to the design of the pile field. Obviously, such movements should be predicted and appropriate amendments made in the design decisions of the zero cycle.

4. METHODOLOGY FOR ASSESSING THE DEVIATION OF PILES DURING EXCAVATION OF THE PIT

The method of calculating piles for horizontal loads was first formulated in the 1930s by Professor Urban [11], as a solution to a boundary problem. After 40 years, on the basis of field tests, the most generalized theory was developed, which was included in regulatory documents [12]. The main principles of the calculation are to consider the pile as a beam located on an elastic Winkler base, characterized by increasing depth of rigidity; force and moment are applied to one end of the beam, the other, in turn, has a fastening, depending on the soil.

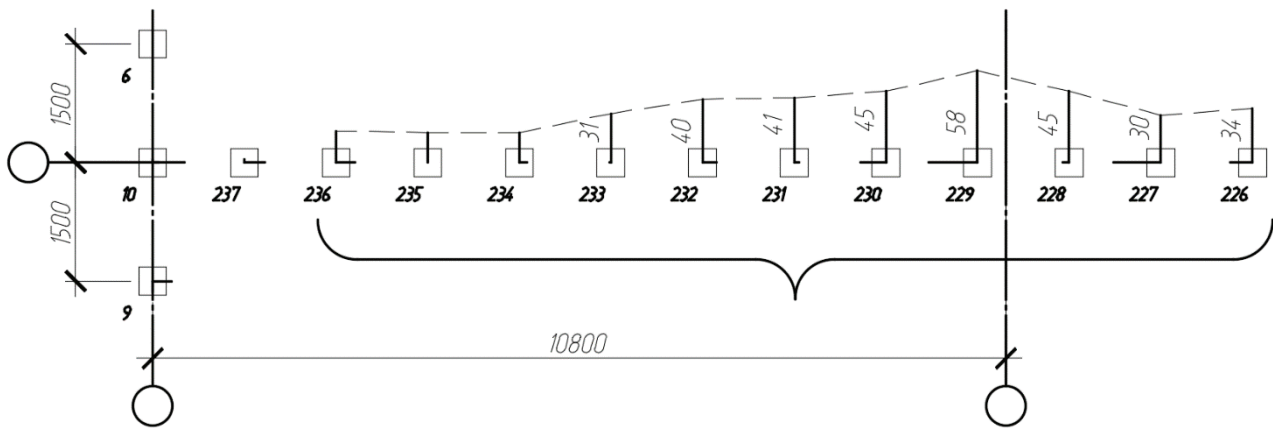


Figure 8. Fragment of the executive scheme of the pile field (object 1).

At present, instead of solving the laborious boundary value problem [13], displacement and force in piles can be determined by the finite element method [14] in a one-dimensional formulation. The described technique can be generalized to the case of a distributed load applied to a pile, since this does not contradict the formal logic.

We find linear loads on the pile from the solution of the Flaman problem [15]. This solution allows us to determine the horizontal stresses in the elastic half-space of the soil from an infinite band load applied to its face. The moment of excavation of a pile (Figure 4) located approximately at a distance of 1/3 of the length of the slope is considered, counting from its beginning. Soil located above the pile head is divided into elementary strips of width b_0 (0.2m). The slope angle is taken equal to 45 degrees. The expression for determining the stresses in the plane of the pile face is presented in the form:

$$\sigma_y = \sum_{i=1}^n \frac{2\gamma h_i b_0}{\pi} * \frac{|x| * x * z}{(x^2 + z^2)^2}$$

where σ_y is horizontal stress at the desired point, kPa; i – element band number; n – the number of elementary strips (60 pcs.); γ – specific gravity of soil, kN / m³; h_i – elementary strip height; b_0 – width of the elementary strip, m; x – distance from the considered point to the elementary strip, m; z – depth, m.

As you know, the basis of the Winkler model is customary to describe through the modulus of subgrade reaction, which depends on the depth and type of soil. It was experimentally established [16] that this modulus in clay soils increases linearly with depth. To maintain generality, we use the normative formula [14]:

$$c_z = \frac{Kz}{\gamma_c}$$

where c_z – the estimated value of the coefficient of bed soil, kN / m³; K – coefficient of proportionality depending on the type of soil, kN / m⁴; z – depth at which the section is located, m; γ_c – coefficient of working conditions (for a separate pile $\gamma_c = 3$).

The problem with this approach to assessing the movements of piles during their excavation is the difficulty of assigning a proportionality coefficient (K) for fluid clay and thixotropic soils. It is also obvious that the safety factor γ_c does not take into account the softening of the near-pile soil that occurs during its unloading and the introduction of piles [17]. We rewrite the formula as follows:

$$c_z = \frac{Kz}{\alpha\gamma_c}$$

where α is correction coefficient.

The basic calculation schemes for the example of object No. 1 are shown in Figure 5.

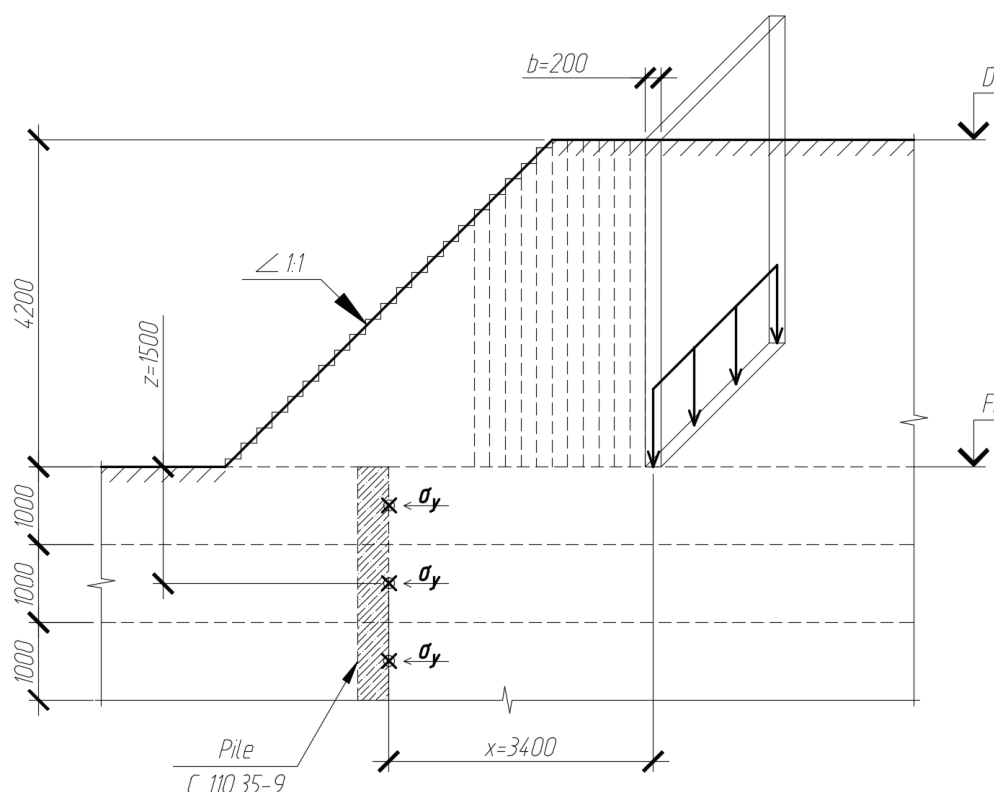


Figure 9. Scheme for determining horizontal stresses (object 1).

The proportionality coefficient K was taken equal to $4000 \text{ kN} / \text{m}^4$, the safety factor γ with equal to three, as for a single pile.

The conditional pile width for computer calculation is taken to be equal to the physical pile width d , and not $1.5d + 0.5\text{m}$, as is required in [14]. This conditional pile width is introduced into the calculation to take into account the influence of the size of the cross section of the pile on the soil resistance of the undisturbed structure [12]. It is likely that the soil in the near-pile zone will have large displacements along the slope, in comparison with the soil on which the pile “lies” and will not impede the movement of the pile.

The calculation of tasks for each object using the finite element method was carried out in LIRA SAPR 2015 software. The coefficient α was selected so that the resulting displacement of the column head coincided with the median value of deviations for the object. The results are summarized in Table 1.

The value of the correction coefficient α was 17–34, which corresponds to the movement of the

pile head by 17–24 cm under the given ground conditions. Thus, the value of the normative coefficient of bed decreases by several tens of times, which is associated with a violation of structural bonds in the soil during the execution and excavation of piles.

For the most problematic elements of the pile field, non-destructive continuity control was performed by the seismic-acoustic method. The calculated moment exceeded the moment of crack formation by 10-20% (Table 1), at depths corresponding to the jump of the reflectogram (5-10 diameters of piles).

It should be noted that the normative safety factor (γ_c) is taken to be equal to three only when calculating mono-pile foundations (support of lampposts, etc.). On the other hand, in the practice of domestic and foreign construction, there are cases of sliding piles into the foundation pit, united by grillage [4]. Thus, in these design cases, it is necessary to take the safety factor the same as when calculating a single pile.

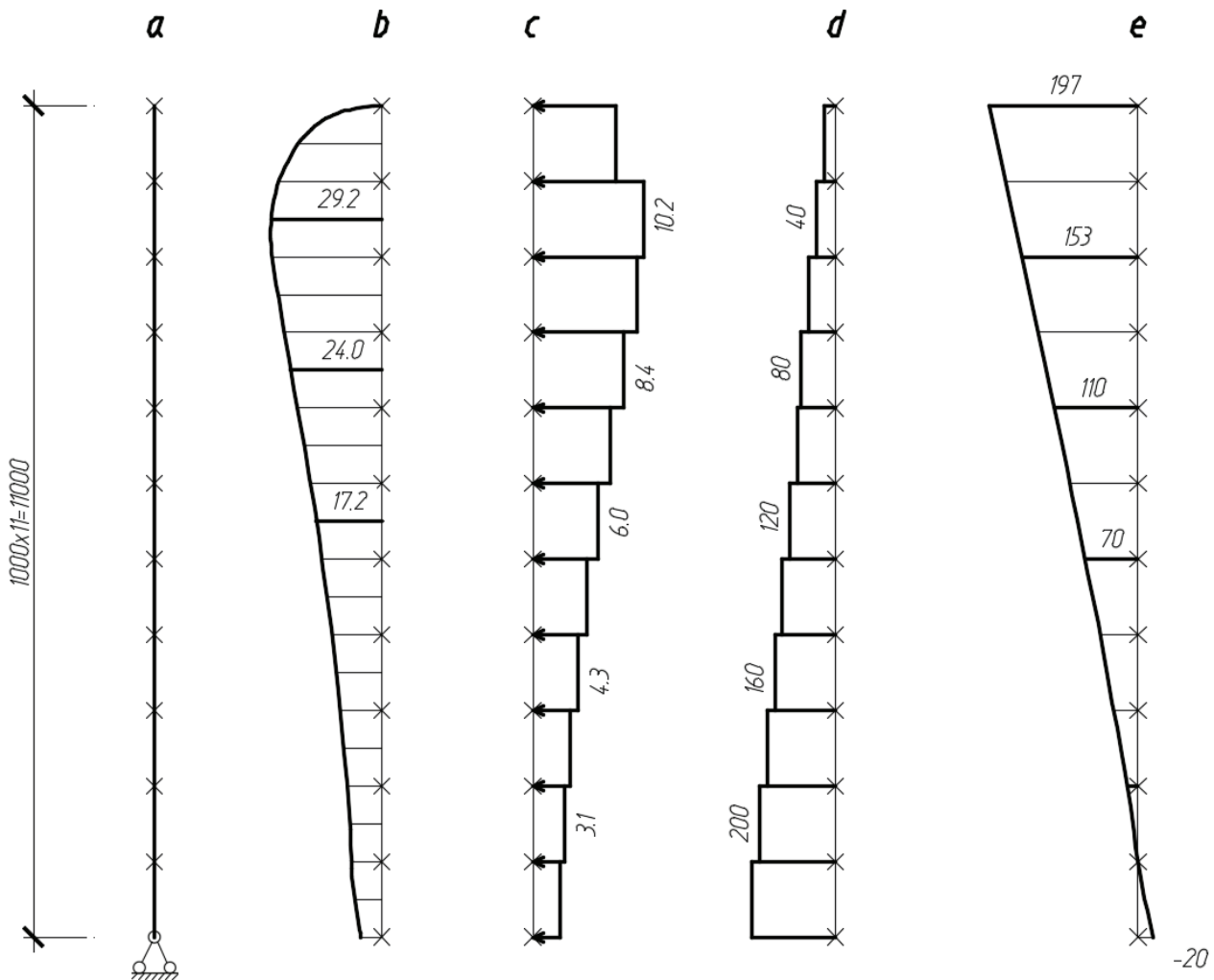


Figure 10. a) the geometric pattern of the pile; b) plot of stresses in the ground, kPa; c) linear loads on the beam, kN / m; d) the values of the coefficients of the bed of soil, kN / m³; e) resulting horizontal movement of the pile, mm (object 1).

Based on the construction experience and the provisions set forth in this article, the following conclusions can be drawn:

1. Obviously, the displacement of the heads of piles is associated with horizontal pressure and the movement of the soil of the slopes during the excavation of the pit.
2. The greatest influence on the deviation of the pile heads is exerted by the excavation depth of the pit and the presence of weak soils at the base.
3. To reduce the impact from the berms and slopes of the pit and to minimize the horizontal deviation of the completed piles,
4. In some cases, excavation of the pit should be carried out with captures of small depth (of the order of 1 m), so that the piles receive deviations in the other direction than at the previous stage of work.
5. It is necessary to assign a break between the implementation of piles and excavation of the soil during the excavation of the pit to restore its properties

Table 1. The main characteristics of the considered objects.

Number of object	1 Public building	2.1 Residential building (building)	2.2 Residential building (parking)	3 Residential building
A type of the pile	C 110.35-9	C 160.40-10	C 150.40-10	C 200.40-HCB.6
Absolute excavation mark, m	-4,200	-4,600	-4,600	-4,300
Recoverable soil	Dusty Sands	Bulk Peat		Bulk
Underlying soil	Loamy, dusty, light loams	Loamy, fluid-plastic loams		Plastic sandy loam, with flowing streaks, thixotropic
Characteristics of the underlying soil	$I_L=1.05..1.3$; $E=6..3\text{MIIa}$; $h=9.8\text{M}$	$I_L=0.91..1.21$; $E=5.5..8\text{MIIa}$; $h=10.8\text{M}$		$I_L=0.93$; $E=9\text{MIIa}$; $h=12.1\text{M}$
Technologies	Indentation	Indentation	Indentation	Driving
Type of grillages	band	band	field	band
Pile pitch in grillage, mm	1200	1200	1200	1200
Number of piles per grip	279	151	264	162
The number of piles with a deviation of more than 0.2d (% of the total)	239 (86%)	109 (72%)	185 (70%)	148 (91%)
The number of piles in the sample (% of the total)	159 (57%)	72 (48%)	132 (50%)	125 (77%)
Pile deviation towards the pit (median), cm	20	18	19	25
Pile deviation towards the pit (maximum), cm	39-51	37-49	29-53	50-79
Safety factor α (median value)	17	21	22	34
Deflection at accepted α , cm	19,7	17,0	17,5	23,3
Maximum moment, kNm	32,7	80,5	78,1	87,7

References

1. **Mangushev R.A., Nikiforova N.S., Konyushkov V.V., Osokin A.I., Sapin D.A.** Proektirovanie i ustrojstvo podzemnyh sooruzhenij v otkrytyh kotlovanah [Design and installation of underground structures in open pits]. Moscow, Saint-Petersburg, DIA Publishing House, 2013, 256 pages (in Russian).
2. GOST 27751-2014 Nadezhnost' stroitel'nyh konstrukcij i osnovanij. Osnovnye polozhenija [Reliability of building structures and foundations. The main provisions] (in Russian).
3. STO 38051320-001-2018 Sovremennye tehnologii pogruzhenija svaj vdavlivajushimi ustanovkami [Modern technologies for pile immersion with pressing units] (in Russian).
4. **Ong D.E.L., Lung C.F., Chow J.K.** Vlijanie predel'nogo davlenija na kust svaj privilegajushij k obrushivshemusja otkosu kotlovana [The effect of ultimate pressure on the pile bush adjacent to the collapsed slope of the pit]. // *Geotechnics*, 2011, No. 6, pp. 52-59 (in Russian).
5. **Paramonov V.N.** Gorizontaľnye smeshhenija svaj pri razrabotke kotlovana [Horizontal displacements of piles during the development of the pit] // *Geotechnics*, 2018., Volume 10, No. 4, pp. 45-57 (in Russian).
6. **Vershinin V.P., Gaido A.N., Sergeev Yu.O.** O smeshhenie jelementov v svajnom fundamente pri otkopke kotlovana [On the displacement of elements in the pile foundation during excavation of the pit]. // *Geotechnics*, 2016, No. 1, pp. 32-39 (in Russian).
7. **Mangushev R.A., Osokin A.I.** Geotekhnika Sankt-Peterburga [Geotechnics of St. Petersburg]. Moscow, ASV Publishing House, 2010, 264 pages (in Russian).
8. **Mangushev R.A., Gotman A.L., Znamensky V.V., Ponomarev A.B.** Svai i svajnye fundamenty. Konstrukcii, proektirovanie, i tehnologii [Piles and pile foundations. Constructions, design, and technology]. Moscow, ASV Publishing House, 2015, 320 pages (in Russian).
9. SP 45.13330.2017 Zemljanye sooruzhenija, osnovanija i fundamenty [Earthworks, footings and foundations] (in Russian).
10. **Ilyichev V.A., Mangushev R.A.** (Eds.) Spravochnik geotekhnika. Osnovanija, fundamenty i podzemnye sooruzhenija [Reference geotechnics. Foundations, foundations and underground structures]. Moscow, ASV Publishing House, 2016, 1040 pages (in Russian).
11. **Urban I.V.** Raschet tonkih stenok s uchetom uprugih svojstv grunta i stenki [Calculation of thin walls, taking into account the elastic properties of the soil and walls]. // *Transactions of MIIT*, 1939, Issue. 55 (in Russian).
12. **Zavriev K.S., Spyro G.S.** Raschety fundamentov i mostovyh opor glubokogo zalozhenija [Calculations of foundations and bridge supports deep laying]. Moscow, Transport Publishing House, 1970, 216 pages (in Russian).
13. SNiP 2.02.03-85 Svajnye fundamenty [Pile foundations] (in Russian),
14. SP 24.13330.2011 Svajnye fundamenty [Pile foundations] (in Russian).
15. **Lurie A.I.** Teorija uprugosti [Theory of elasticity]. Moscow, Publishing House of Science, 1970, 940 pages.
16. **Safonov A.P.** Nesushhaja sposobnost' svaj v glinistyh gruntah pri dejstvii gorizontaľnoj nagruzki [Bearing capacity of piles in clay soils under the action of horizontal load]. PhD Thesis. Sverdlovsk, 1984, 163 pages (in Russian).
17. **Mangushev R.A., Ershov A.V., Ershov S.V.** Ocenka vlijanija tehnologii izgotovlenija nabivnoj svai na sostojanie gruntovogo massiva [Evaluation of the impact of manufacturing technology of a printed pile on the state of the soil massif]. // *Bulletin of civil engineers*, 2009, No. 2, pp. 116-120 (in Russian).

СПИСОК ЛИТЕРАТУРЫ

1. Мангушев Р.А., Никифорова Н.С., Конюшков В.В., Осокин А.И., Сапин Д.А. Проектирование и устройство подземных сооружений в открытых котлованах. – М.: – СПб.: АСВ, 2013. – 256 с.
2. ГОСТ 27751-2014 Надежность строительных конструкций и оснований. Основные положения.
3. СТО 38051320-001-2018 Современные технологии погружения свай вдавливающими установками.
4. Онг Д.Э.Л., Люнг Ч.Ф., Чоу Й.К. Влияние предельного давления на куст свай прилегающий к обрушившемуся откошу котлована. // *Геотехника*, 2011, №6, с.52-59.
5. Парамонов В.Н. Горизонтальные смещения свай при разработке котлована. // *Геотехника*, 2018, том 10, №4, с. 45-57.
6. Вершинин В.П., Гайдо А.Н., Сергеев Ю.О. О смещение элементов в свайном фундаменте при откопке котлована. // *Геотехника*, 2016, №1, с. 32-39.
7. Мангушев Р.А., Осокин А.И. Геотехника Санкт-Петербурга. – М.: АСВ, 2010. – 264 с.
8. Мангушев Р.А., Готман А.Л., Знаменский В.В., Пономарев А.Б. Сваи и свайные фундаменты. Конструкции, проектирование, и технологии. – М.: АСВ, 2015. – 320 с.
9. СП 45.13330.2017 Земляные сооружения, основания и фундаменты.
10. Ильичев В.А., Мангушев Р.А. (ред.) Справочник геотехника. Основания, фундаменты и подземные сооружения. – М.: АСВ, 2016. – 1040 с.
11. Урбан И.В. Расчет тонких стенок с учетом упругих свойств грунта и стенки. // *Труды МИИТ*, 1939, Выпуск 55.
12. Завриев К.С., Шпиро Г.С. Расчеты фундаментов и мостовых опор глубокого заложения. – М.: Транспорт, 1970. – 216 с.
13. СНиП 2.02.03-85 Свайные фундаменты.
14. СП 24.13330.2011 Свайные фундаменты.
15. Лурье А.И. Теория упругости. – М.: Наука, 1970. – 940 с.
16. Сафонов А.П. Несущая способность свай в глинистых грунтах при действии горизонтальной нагрузки. Диссертация на соискание ученой степени кандидата технических наук по специальности 05.23.02 – «Подземные сооружения, основания и фундаменты». – Свердловск: Уральский Ордена Трудового Красного Знамени политехнический институт им. С.М. Кирова, 1984. – 163 с.
17. Мангушев Р.А., Ершов А.В., Ершов С.В. Оценка влияния технологии изготовления набивной сваи на состояние грунтового массива. // *Вестник гражданских инженеров*, 2009, №2, с. 116-120.

Rashid A. Mangushev, Corresponding Member of the Russian Academy of Architecture and Construction Sciences (RAACS), Professor, Dr.Sc.; Department of Geotechnics; Saint-Petersburg State University of Architecture and Civil Engineering; 5, Ulitsa Egorova, Saint-Petersburg, 190005, Russia; phones: +7 (812) 316-03-41; 316-48-36
E-mail geotechnica@spbgasu.ru.

D.S. Kolesnik, Ph.D. Student; Department of Geotechnics; Saint-Petersburg State University of Architecture and Civil Engineering; 5, Ulitsa Egorova, Saint-Petersburg, 190005, Russia; phones: +7 (812) 316-03-41; 316-48-36
E-mail geotechnica@spbgasu.ru.

Мангушев Рашид Абдуллович, член-корреспондент РААСН, профессор, доктор технических наук; заведующий кафедрой геотехники; Санкт-Петербургский государственный архитектурно-строительный университет; 190005, Россия, г. Санкт-Петербург, ул. Егорова 5; тел. +7 (812) 316-03-41; 316-48-36
E-mail geotechnica@spbgasu.ru.

Колесник Д.С., аспирант кафедры геотехники; Санкт-Петербургский государственный архитектурно-строительный университет; 190005, Россия, г. Санкт-Петербург, ул. Егорова 5; тел. +7 (812) 316-03-41; 316-48-36
E-mail geotechnica@spbgasu.ru.

USING THE CRITERION OF THE MINIMUM MATERIAL CAPACITY OF RODS UNDER STABILITY RESTRICTIONS FOR THE CASE OF MULTIPLE CRITICAL LOAD

Leonid S. Lyakhovich¹, Pavel A. Akimov^{1, 2, 3}, Anatoly P. Malinowski¹

¹ Tomsk State University of Architecture and Civil Engineering, Tomsk, RUSSIA

² National Research Moscow State University of Civil Engineering, Moscow, RUSSIA

³ Peoples' Friendship University of Russia, Moscow, RUSSIA

Abstract: As it is known, special criteria are formulated to evaluate the obtained solution of some optimization problems. In particular, we formulate a criterion that allows us to estimate the proximity of the decision on the rod of the lowest weight and the restrictions on the resistance to the minimum material-intensive for rectilinear rods for certain types of cross sections. The criterion is based on the analysis of stresses from bending moments arising from the loss of stability. If the least critical force is not a multiple, then the form of loss of stability and the corresponding diagram of moments are the only ones. At multiplicity of the least critical load there are multiple forms of loss of stability, and any of their linear combination is also its own form. To estimate the obtained solution, it is necessary to form a combination of multiple forms of buckling and the corresponding diagram of bending moments, which will serve as the basis for the use of the criterion. This paper proposes an approach that allows to determine such a combination of multiple forms, which will be the basis for the application of the criterion of proximity of the obtained solution to the minimum material-intensive.

Keywords: optimization, system minimal consumption of materials, stability, critical force, buckling, bending moments, multiplicity, tension, evaluation criteria for solutions of optimal problems

ИСПОЛЬЗОВАНИЕ КРИТЕРИЯ МИНИМАЛЬНОЙ МАТЕРИАЛОЕМКОСТИ СТЕРЖНЕЙ ПРИ ОГРАНИЧЕНИЯХ ПО УСТОЙЧИВОСТИ ДЛЯ СЛУЧАЯ КРАТНОЙ КРИТИЧЕСКОЙ НАГРУЗКИ

Л.С. Ляхович¹, П.А. Акимов^{1, 2, 3}, А.П. Малиновский¹

¹ Томский государственный архитектурно-строительный университет, г. Томск, РОССИЯ

² Национальный исследовательский Московский государственный строительный университет,
г. Москва, РОССИЯ

³ Российский университет дружбы народов, г. Москва, РОССИЯ

Аннотация: Как известно, для оценки полученного решения некоторых задач оптимизации сформулированы специальные критерии. В частности, сформулирован критерий, позволяющий оценить для прямолинейных стержней при определенных типах поперечных сечений близость решения о стержне наименьшего веса и ограничениях по устойчивости к минимально материалоемкому. Критерий основан на анализе напряжений от изгибающих моментов, возникающих при потере устойчивости. Если наименьшая критическая сила не кратная, то форма потери устойчивости и соответствующая ей эпюра моментов единственные. При кратности наименьшей критической нагрузки возникают кратные формы потери устойчивости, и любая их линейная комбинация также является собственной формой. Для оценки полученного решения необходимо сформировать комбинацию кратных форм потери устойчивости и соответствующую ей эпюру изгибающих моментов, которая и будет служить основой для использования критерия. В данной статье предлагается подход, позволяющий определять такую комбинацию кратных форм, которая станет основой для применения критерия близости полученного решения к минимально материалоемкому.

Ключевые слова: оптимизация, системы минимальной материалоемкости, устойчивость, критическая сила, формы потери устойчивости, изгибающие моменты, кратность, напряжения, критерии оценки решений оптимальных задач

The theoretical foundations of the creation of rods of the lowest weight, prone to buckling, originate from the research works of Lagrange [1], T. Clausen [2], E.L. Nikolai [2] and later N.G. Chentsova [4], J.L. Nudelman [5], A.F. Smirnov [6], A.I. Vinogradov [7], N. Olkhoff [8] and other authors.

In the contemporary literature, the considering problem is normally formulated in terms of non-linear mathematical programming.

Let us consider a centrally compressed straight line rod (for example, shown in Figure 1, although the boundary conditions in the planes of inertia may be different).

If $F(x)$ is the cross-sectional area of the rod, P is the acting force, $P1_{kp}[1]$ and $P2_{kp}[1]$ are the minimum critical forces in the main inertia planes of the section, then we need to find an expression $F(x)$ at which the rod would remain stable and the volume of the material of the rod V would be minimal. Thus, the objective function can be written as

$$V = \int_0^l F(x) dx, \quad (1)$$

Besides, we have the following restrictions

$$P \leq P1_{kp}[1] = P2_{kp}[1]. \quad (2)$$

There are a considerable number of methods for solving this problem. Most of them use finite-dimensional approaches. The process of optimization within the implementation of such methods most often stops at a stage when the objective function in the adjacent search steps decreases less than a predetermined value. Such a criterion for stopping the process of searching for a minimum in most cases gives an acceptable result. However, it does not allow researcher to confidently estimate the proximity of the so-

lution obtained to the solution of minimum material consumption (minimum material-intensive solution).

As a result of several research works [1, 2, 3] for rectilinear centrally compressed rods with certain types of cross sections (for example, those in which the moment of inertia is proportional to the square of the section area), a criterion was formulated to estimate the proximity of the solution to the solution of minimum material consumption.

In [3], it was shown that in the considering case, *the rod of the smallest volume will be a bar of equal resistance with respect to the moment diagram arising in the event of loss of stability*. Thus, with a loss of stability with a rod of the smallest volume, the normal stresses in the extreme fibers of the rod, found from the resulting moment diagrams, should be the same in all sections. That is, for the case when the loss of stability occurs in the two main planes of inertia, the criterion is written as

$$\sigma1(x) = const; \quad \sigma2(x) = const. \quad (3)$$

Under conditions (3), $\sigma1(x)$ and $\sigma2(x)$ are the absolute values of the normal stresses in the extreme fibers of the rod determined from the diagrams of the moments that occurred in the corresponding principal planes of inertia during loss of stability.

Since the buckling modes and the corresponding moment and stress diagrams are determined to within a constant factor, $\sigma1(x)$ and $\sigma2(x)$ are normalized. If the corresponding normalization is made so that the largest values of $\sigma1(x)$ and $\sigma2(x)$ would be equal to one, then the proximity of the obtained solution to the solution of minimum material consumption is estimated by the proximity of $\sigma1(x)$ and $\sigma2(x)$ to unity.

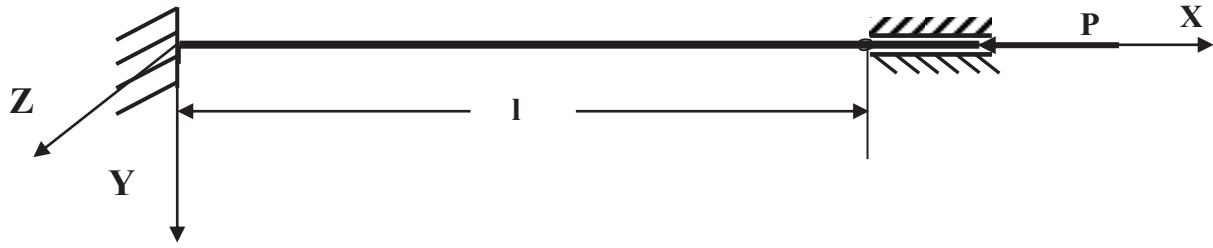


Figure 1. Considering centrally compressed straight line rod.

If the first critical force is not a multiple, then the moment diagram that occurs when stability is lost is unique. In this case, criterion (3) can be used on the basis of this diagram, including in combination with some other restrictions (see, for example, [9]).

If the first critical force is multiple, then multiple buckling modes and the corresponding moment diagrams appear. It is also known that any linear combination of multiple buckling modes will also be proper.

The multiplicity of critical forces that occurs when minimizing the volume of the rod for rigidly restrained rods was identified in [8]. However, the multiplicity of critical forces also occurs in other cases, for example, when optimizing the volume under constraints on the stability of some continuous beam schemes.

In these cases, it is necessary to establish a linear combination of bending moments diagrams corresponding to multiple buckling modes. This combination will serve as the basis for the use of the criterion (3).

Let us consider an approach to determination of such combination. We represent the approach for one main plane of inertia and threefold critical force. For the second plane and the other multiplicity of critical forces, all actions will be similar.

Let it be required to estimate the closeness of the search stage for the solution of the considering optimization problem to the minimum material-intensive one.

At the estimated stage of the search, in the considered main plane of inertia, the first critical forces in $P1_{cr}[1]$, $P1_{cr}[2]$ and $P1_{cr}[3]$ are found, the corresponding forms of buckling and

the estimated optimal cross-section sizes and their moments of resistance $w(x)$.

The following steps are performed in the following order:

1. Using the three first forms of buckling found at the estimated stage of the research, the corresponding diagrams of the absolute values of the bending moments $M_1(x)$, $M_2(x)$ and $M_3(x)$ are constructed. Plots are normalized, for example, so that

$$\int_0^l [M_1(x)]^2 dx = 1; \quad \int_0^l [M_2(x)]^2 dx = 1;$$

$$\int_0^l [M_3(x)]^2 dx = 1.$$

2. On the basis of the assumption about the optimality of the found dimensions of the cross-sections, a conditionally optimal diagram of the absolute values of the bending moments $M_0(x)$ is constructed, according to which relation (3), that is, the condition,

$$\sigma l(x) = \frac{M_0(x)}{w(x)} = 1$$

must be fulfilled. Thus, we have $M_0(x) = w(x)$. The plot is also normalized.

3. If the considering solution is optimal, then the combination of arising diagrams

$$M_{00}(x) = a * M_1(x) + b * M_2(x) + c * M_3(x)$$

should coincide with $M_0(x)$. The equations for finding the coefficients a , b and c will be obtained from the minimum condition of the quadratic deviation of the diagram $M_{00}(x)$ from $M_0(x)$. That is, from the minimum condition of the integral

$$\Delta M(a, b) = \int_0^l [M_0(x) - aM_1(x) - bM_2(x) - cM_2(x)]^2 dx,$$

we get three equations

$$\begin{aligned} \frac{\partial \Delta M(a, b, c)}{\partial a} &= 0; \quad \frac{\partial \Delta M(a, b, c)}{\partial b} = 0 \\ \frac{\partial \Delta M(a, b, c)}{\partial c} &= 0. \end{aligned}$$

After solution of the system, we can find the coefficients a , b and c .

4. From the

$$M_{00}(x) = aM_1(x) + bM_2(x) + cM_3(x)$$

plot, we can determine

$$\sigma l(x) = \frac{M_0(x)}{w(x)}$$

and normalize it, and by the proximity of the stress $\sigma l(x)$ in sections and its average value along the length of the rod

$$\Delta \sigma l = \left[\int_0^l \sigma l(x) dx \right] / l$$

to one, we estimate the optimality of the solution.

5. Besides, the optimality of the considering solution can also be evaluated by the proximity of the diagrams of $M_0(x)$ and $M_{00}(x)$. The proximity is estimated by the values of the differences

$$\Delta M_0(x) = M_0(x) - M_{00}(x)$$

in the sections and the average value of their absolute values along the length of the rod

$$\Delta M_{00} = \left\{ \int_0^l \text{sgn}[\Delta M_0(x)] \Delta M_0(x) dx \right\} / l.$$

6. If the multiplicity of critical forces for the considering system is not known in advance, then its presence or absence is revealed in the process of optimization. If the multiplicity is detected, then the differences

$$\begin{aligned} \Delta P1 &= \{P1_{kp}[2] - P1_{kp}[1]\} / P1_{kp}[1] \cdot 100\%; \\ \Delta P2 &= \{P1_{kp}[3] - P1_{kp}[1]\} / P1_{kp}[1] \cdot 100\% \end{aligned}$$

in the limit tend to zero. Let us give an illustration of the described approach with samples.

7. For a rod whose scheme is shown in Figure 1, the doubling of the critical force was considered in detail in [8]. Although the possibility of using of the criterion (3) was not considered in [8], taking into account the detailed analysis in [8] of the doubly critical load of a rigidly clamped rod, it seems appropriate to illustrate the proposed approach using other examples. Two numerical samples are considered. The first one deals with two-time critical force, and the second one deals with three-time critical force.

The first numerical sample. Let us consider a rectilinear square rod, compressed by a centrally applied longitudinal force with supporting conditions in both main planes of inertia of sections, shown in Figure 2.

A preliminary analysis showed that the critical force will be twofold.

Let $l = 9$ meters be width of span, $P = 3000000$ N be magnitude of force;

$E = 206000$ MPa be the modulus of elasticity of the material. The analysis was performed on the basis of a discrete model ([10]) of 41 fragments.



Figure 1. The first numerical sample.

For a discrete model, the objective function (1) is written as

$$V = \sum_1^n F[i](l/n) = \sum_1^n (b[i])^2 (l/n), \quad (4)$$

where $b[i]$ is the size of the square section of the rod; n is dimension of a discrete model.

Diagrams of $M_1(x)$, $M_2(x)$, $M_0(x)$, $M_{00}(x)$, $\Delta M_0(x)$ are represented by $M_1[i]$, $M_2[i]$, $M_3[i]$, $M_{00}[i]$, $\Delta M_0[i]$.

Since the boundary conditions in both main planes of inertia are the same, and the critical forces are assumed to be twofold, the stability constraints are written as

$$P \leq P_{1_{kp}}[1] = P_{1_{kp}}[2]. \quad (5)$$

Criterion (3) for the discrete model in this case takes the form

$$\sigma[i] = \text{const}. \quad (6)$$

Optimization was performed by one of the variants of the method of random search. The estimation of the proximity of the solution to the minimum material-based on criterion (6) was carried out at several stages of the computing (Tables 1 and 2).

Four stages were considered. The results of each stage are presented in the corresponding columns of Tables 1 and 2. Stage 0 corresponds to the results corresponding to the first access to the boundary of the allowable area for a rod of constant square cross-sectional length. The remaining columns show the results, respectively, at 300, 1300 and more than 40,000 tests of the

random search method. Table 1 shows the cross-section dimensions $b[i]$ for each stage. The bottom five lines show the values of the objective function – V , meters^3 ; the magnitudes of its decrease compared with stage 0 – ΔV , %; the difference between the first two critical forces – ΔP , %; the values of the coefficients a and b .

Table 2 shows the values of the differences

$$\Delta M_0[i] = M_0[i] - M_{00}[i]$$

and stresses $\sigma[i]$, and in the last line the average values for each stage are the values of these quantities ΔM_{00} and $\Delta \sigma$.

Analysis of the data in tables 1 and 2 shows that despite the small difference in the values of the objective function in the last two stages, the difference in cross sections between the values of differences $\Delta M_0[i]$ and stresses $\sigma[i]$ at these stages of the search is more significant. At the last stage, in almost all cross sections, the differences $\Delta M_0[i]$ are close to zero, and the stresses $\sigma[i]$ to unity.

The result obtained confirms that, even with a double critical force, criterion (3) can estimate the proximity of the obtained solution to the minimum material-intensive one.

Let us consider one more example, in which, according to preliminary calculations during optimization, the critical force turns out to be threefold.

Let us consider a rectilinear square rod, compressed by a centrally applied longitudinal force with supporting conditions in both main planes of inertia of sections, shown in Figure 3.

Table 1. Results of analysis.

	$b[i]$ by stages of search for optimum			
t	0	300	1300	>40000
1	2	3	4	5
1	0.0915	0.0626	0.0420	0.0426
2	0.0915	0.0655	0.0600	0.0596
3	0.0915	0.0789	0.0696	0.0692
4	0.0915	0.0784	0.0761	0.0761
5	0.0915	0.0835	0.0806	0.0813
6	0.0915	0.0821	0.0855	0.0854
7	0.0915	0.0927	0.0878	0.0888
8	0.0915	0.0883	0.0921	0.0916
9	0.0915	0.0949	0.0943	0.0938
10	0.0915	0.0984	0.0966	0.0957
11	0.0915	0.0949	0.0960	0.0971
12	0.0915	0.0924	0.0985	0.0982
13	0.0915	0.0944	0.0982	0.0990
14	0.0915	0.1110	0.0987	0.0995
15	0.0915	0.0975	0.1000	0.0997
16	0.0915	0.1010	0.0990	0.0997
17	0.0915	0.0995	0.1000	0.0993
18	0.0915	0.0929	0.0987	0.0986
19	0.0915	0.1189	0.0988	0.0977
20	0.0915	0.1021	0.0967	0.0964
21	0.0915	0.1053	0.0944	0.0948
22	0.0915	0.0833	0.0925	0.0927
23	0.0915	0.0998	0.0905	0.0902
24	0.0915	0.0799	0.0877	0.0872
25	0.0915	0.0857	0.0829	0.0834
26	0.0915	0.0787	0.0784	0.0787
27	0.0915	0.0806	0.0724	0.0728
28	0.0915	0.0654	0.0639	0.0647
29	0.0915	0.0743	0.0522	0.0523
30	0.0915	0.0701	0.0255	0.0049
31	0.0915	0.0730	0.0524	0.0518
32	0.0915	0.0603	0.0644	0.0640
33	0.0915	0.0636	0.0731	0.0719
34	0.0915	0.0793	0.0776	0.0777
35	0.0915	0.0736	0.0828	0.0823
36	0.0915	0.0834	0.0852	0.0859
37	0.0915	0.0966	0.0899	0.0888
38	0.0915	0.1000	0.0917	0.0912
39	0.0915	0.0911	0.0924	0.0931
40	0.0915	0.0889	0.0944	0.0946

1	2	3	4	5
41	0.0915	0.0852	0.0956	0.0957
V , meters ³	0.07539	0.06904	0.06492	0.06476
ΔV	0.00%	8.43%	13.89%	14.10%
ΔP	195.00%	130.49%	17.74%	0.03%
a	0.48987	0.83099	1.01063	1,02480
b	0.49986	0.13279	-0.01283	-0,02805

Table 2. Results of analysis.

	$\Delta M_0[i]$ by stages of search for optimum				σ by stages of search for optimum			
t	0	300	1300	>40000	0	300	1300	>40000
1	2	3	4	5	6	7	8	9
1	0.1396	0.0388	0.0008	0.0000	0.076842	0.135799	0.978754	0.9988
2	0.1070	0.0284	0.0019	0.0001	0.228466	0.301949	0.893968	0.9973
3	0.0757	0.0202	0.0024	0.0000	0.373973	0.476454	0.902065	0.9984
4	0.0465	0.0256	0.0019	0.0000	0.509501	0.441546	0.913346	0.9986
5	0.0202	0.0003	0.0010	0.0000	0.631502	0.597886	0.923345	0.9985
6	0.0025	0.0103	0.0032	0.0000	0.736850	0.541898	0.952999	0.9988
7	0.0210	0.0334	0.0064	0.0000	0.822944	0.718689	0.971152	0.9988
8	0.0350	0.0815	0.0001	0.0000	0.887779	0.941500	0.930939	0.9987
9	0.0441	0.0678	0.0041	0.0000	0.930011	0.827215	0.910997	0.9990
10	0.0481	0.0215	0.0091	0.0000	0.948989	0.662066	0.889453	0.9990
11	0.0472	0.0239	0.0144	0.0000	0.944770	0.514969	1.000000	0.9987
12	0.0415	0.0293	0.0056	0.0000	0.918104	0.487964	0.907040	0.9989
13	0.0312	0.0782	0.0094	0.0001	0.870409	0.867698	0.973216	0.9991
14	0.0169	0.1005	0.0105	0.0000	0.803706	0.381801	0.977651	0.9987
15	0.0010	0.0407	0.0069	0.0000	0.720548	0.468211	0.902845	0.9987
16	0.0218	0.0869	0.0025	0.0000	0.623928	0.350193	0.921093	0.9986
17	0.0448	0.0572	0.0006	0.0001	0.517169	0.765660	0.929211	0.9991
18	0.0347	0.0903	0.0021	0.0001	0.564413	0.924885	0.940865	0.9990
19	0.0191	0.1114	0.0039	0.0000	0.636604	0.402981	0.914728	0.9988
20	0.0061	0.1037	0.0092	0.0001	0.697070	0.312453	0.888763	0.9984
21	0.0038	0.0158	0.0016	0.0000	0.743026	0.556928	0.923710	0.9985
22	0.0101	0.0800	0.0006	0.0001	0.772075	1.000000	0.928379	0.9992
23	0.0123	0.0377	0.0066	0.0000	0.782309	0.485707	0.894467	0.9988
24	0.0101	0.0041	0.0022	0.0001	0.772383	0.572689	0.918233	0.9982
25	0.0035	0.0387	0.0057	0.0000	0.741573	0.416936	0.973638	0.9984
26	0.0077	0.0122	0.0055	0.0000	0.689821	0.669361	0.979892	0.9989
27	0.0232	0.0177	0.0015	0.0000	0.617743	0.497582	0.915495	0.9984
28	0.0428	0.0142	0.0031	0.0000	0.526627	0.744256	0.982150	0.9985
29	0.0661	0.0478	0.0002	0.0000	0.418400	0.256604	0.938477	0.9988
30	0.0723	0.0574	0.0035	0.0000	0.389795	0.110365	0.055568	-0.0546
31	0.0772	0.0454	0.0007	0.0000	0.366997	0.255342	0.910506	1.0000
32	0.0843	0.0037	0.0032	0.0000	0.333614	0.644771	0.880962	0.9992
33	0.0933	0.0282	0.0051	0.0000	0.292105	0.915174	0.876885	0.9992

1	2	3	4	5	6	7	8	9
34	0.0969	0.0431	0.0044	0.0000	0.275390	0.343807	0.971364	0.9987
35	0.0660	0.0390	0.0017	0.0000	0.418961	0.881604	0.919258	0.9988
36	0.1541	0.0365	0.0028	0.0001	0.554891	0.412768	0.950408	0.9995
37	0.1713	0.0655	0.0045	0.0000	0.679382	0.384630	0.905781	0.9986
38	0.1864	0.0676	0.0004	0.0001	0.788944	0.399366	0.929533	0.9985
39	0.1994	0.0502	0.0013	0.0001	0.880504	0.402443	0.938544	0.9992
40	0.2099	0.0156	0.0064	0.0000	0.951507	0.661024	0.899818	0.9987
41	0.2179	0.0131	0.0077	0.0001	1.000000	0.657937	0.968563	0.9983
Σ/n	0.0408	0.0435	0.0040	0.0000	0.6449	0.5461	0.9094	0.9731

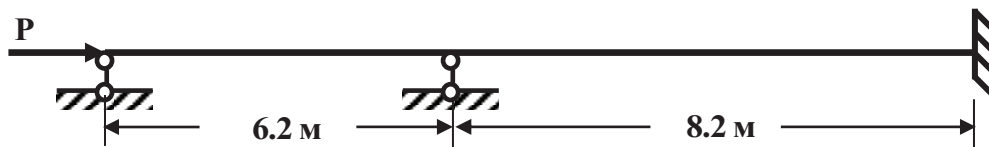


Figure 2. The second numerical sample.

The second numerical sample. Let us consider a rectilinear square rod, compressed by a centrally applied longitudinal force with supporting conditions in both main planes of inertia of sections, shown in Figure 3. The analysis was performed on the basis of a discrete model ([10]) of 41 fragments.

Since the boundary conditions in the two main planes of inertia are the same, and the critical forces are assumed to be threefold, the stability constraints are written as

$$P \leq P_{cr}[1] = P_{cr}[2] = P_{cr}[3]. \quad (7)$$

In the same way as in the first sample, optimization was performed by one of the variants of the random search method. The estimation of the proximity of the solution to the minimum material-based on criterion (6) was carried out at several stages of the calculation (Tables 3 and 4). Similarly to the first sample, four stages of finding the optimal solution were considered.

The results are presented in the corresponding columns of Tables 3 and 4. The designations in these tables are the same as in the first sample. In addition, Table 3 also lists the values of the coefficient c and the difference $\Delta P2$.

Analysis of the data in Tables 3 and 4 shows that in the last two stages of the search, the objective functions differ little.

However, at the same time, differences $\Delta M_0[i]$ and reduced stresses $\sigma[i]$ show that, despite the small difference in the values of the objective function in the last two stages, the difference between the values of differences $\Delta M_0[i]$ and stresses $\sigma[i]$ at these stages of the search is more significant. At the last stage, in almost all cross sections, the differences $\Delta M_0[i]$ are close to zero, and the stresses $\sigma[i]$ to unity. In sections 16 and 31, the stresses are far from unity. This is due to the significantly smaller compared with the other sizes of sections, which in such cases reduces the accuracy of the selected model.

From Table 3 it can be seen how the critical forces approach each other in stages. So, if at stage number 0 the difference $\Delta P1$ is 102.54%, and $\Delta P2$ – 236.62%, then at the last stage these differences are 0.01% and 0.03%.

Table 4 shows how the mean values of differences ΔM_{00} and stresses change $\Delta \sigma 1$.

Table 3. Results of analysis.

	$b[i]$ by stages of search for optimum			
t	0	300	1300	>40000
1	2	3	4	5
0.0893	0.0500	0.0503	0.0513	0.0893
0.0893	0.0724	0.0711	0.0705	0.0893
0.0893	0.0745	0.0818	0.0808	0.0893
0.0893	0.0865	0.0882	0.0875	0.0893
0.0893	0.0972	0.0925	0.0920	0.0893
0.0893	0.0936	0.0951	0.0950	0.0893
0.0893	0.1072	0.0967	0.0968	0.0893
0.0893	0.0991	0.0987	0.0976	0.0893
0.0893	0.0968	0.0950	0.0973	0.0893
0.0893	0.0980	0.0951	0.0960	0.0893
0.0893	0.0990	0.0930	0.0936	0.0893
0.0893	0.0901	0.0913	0.0898	0.0893
0.0893	0.0779	0.0848	0.0842	0.0893
0.0893	0.0807	0.0765	0.0759	0.0893
0.0893	0.0637	0.0631	0.0623	0.0893
0.0893	0.0477	0.0260	0.0057	0.0893
0.0893	0.0557	0.0609	0.0618	0.0893
0.0893	0.0748	0.0758	0.0753	0.0893
0.0893	0.0872	0.0832	0.0834	0.0893
0.0893	0.0881	0.0894	0.0889	0.0893
0.0893	0.0908	0.0925	0.0925	0.0893
0.0893	0.0879	0.0943	0.0947	0.0893
0.0893	0.0967	0.0959	0.0958	0.0893
0.0893	0.0898	0.0947	0.0958	0.0893
0.0893	0.0869	0.0941	0.0947	0.0893
0.0893	0.0963	0.0922	0.0925	0.0893
0.0893	0.0867	0.0888	0.0888	0.0893
0.0893	0.0811	0.0831	0.0834	0.0893
0.0893	0.0798	0.0757	0.0753	0.0893
0.0893	0.0604	0.0622	0.0618	0.0893
0.0893	0.0457	0.0242	0.0057	0.0893
0.0893	0.0676	0.0611	0.0602	0.0893
0.0893	0.0785	0.0733	0.0731	0.0893
0.0893	0.0807	0.0811	0.0806	0.0893
0.0893	0.0884	0.0849	0.0854	0.0893
0.0893	0.0957	0.0880	0.0883	0.0893
V , meters ³	0.1149	0.1003	0.0978	0.0973
ΔV	0.00	12.69	14.90	15.35
$\Delta P1$	102.54	31.20	5.72	0.01
$\Delta P2$	236.62	71.35	9.42	0.03

1	2	3	4	5
a	0.2813	0.8000	0.8283	0.5434
b	0.3571	0.1761	0.1846	0.4334
c	0.3932	0.0045	-0.0101	0.0516

Table 2. Results of analysis.

t	$\Delta M_0[i]$ by stages of search for optimum				σ by stages of search for optimum			
	0	300	1300	>40000	0	300	1300	>40000
1	2	3	4	5	6	7	8	9
1	0.1302	0.0087	0.0043	0.0000	0.1554	0.4562	0.9797	0.9995
2	0.0610	0.0332	0.0035	0.0000	0.4501	0.4111	0.8332	0.9992
3	0.0029	0.0161	0.0075	0.0000	0.6979	0.5343	0.8202	0.9991
4	0.0385	0.0139	0.0031	0.0002	0.8741	0.6878	0.8815	0.9974
5	0.0591	0.0696	0.0043	0.0002	0.9623	0.4408	0.8482	0.9998
6	0.0578	0.0032	0.0030	0.0000	0.9565	0.6429	0.8547	0.9988
7	0.0355	0.0852	0.0131	0.0000	0.8616	0.4575	0.9148	0.9988
8	0.0042	0.0033	0.0048	0.0000	0.6924	0.6418	0.8495	0.9987
9	0.0319	0.0418	0.0144	0.0001	0.5743	0.5161	0.9224	0.9984
10	0.0299	0.0824	0.0012	0.0001	0.5827	0.4106	0.8710	0.9992
11	0.0391	0.0502	0.0028	0.0001	0.5436	0.7646	0.8545	0.9995
12	0.0111	0.0683	0.0133	0.0001	0.6630	0.8699	0.8078	0.9984
13	0.0007	0.0358	0.0067	0.0000	0.7133	0.8247	0.8294	0.9985
14	0.0055	0.0431	0.0063	0.0000	0.6869	0.4253	0.8194	0.9989
15	0.0292	0.0192	0.0029	0.0000	0.5859	0.4439	0.8273	0.9990
16	0.0505	0.0094	0.0007	0.0000	0.4952	0.8522	1.0000	0.5329
17	0.0533	0.0249	0.0017	0.0000	0.4831	1.0000	0.8408	0.9987
18	0.0199	0.0160	0.0038	0.0000	0.6253	0.5361	0.8372	0.9989
19	0.0013	0.0875	0.0052	0.0002	0.7048	0.2975	0.8363	1.0000
20	0.0002	0.0171	0.0114	0.0000	0.7092	0.5696	0.8127	0.9988
21	0.0053	0.0234	0.0053	0.0001	0.6877	0.5537	0.8886	0.9984
22	0.0104	0.0662	0.0010	0.0000	0.7544	0.8805	0.8702	0.9989
23	0.0077	0.0523	0.0051	0.0000	0.7430	0.4862	0.8467	0.9988
24	0.0115	0.0459	0.0006	0.0000	0.6612	0.7939	0.8686	0.9986
25	0.0213	0.0236	0.0032	0.0001	0.6193	0.5421	0.8790	0.9983
26	0.0129	0.0406	0.0087	0.0000	0.7653	0.7485	0.9035	0.9990
27	0.0305	0.0474	0.0042	0.0001	0.8400	0.4487	0.8862	0.9996
28	0.0275	0.0163	0.0098	0.0001	0.8275	0.7107	0.9236	0.9993
29	0.0028	0.0230	0.0039	0.0001	0.7223	0.5182	0.8358	0.9979
30	0.0422	0.0090	0.0020	0.0000	0.5305	0.7365	0.8940	0.9990
31	0.0851	0.0091	0.0020	0.0000	0.3474	0.3901	0.3920	0.1702
32	0.0945	0.0139	0.0011	0.0000	0.3074	0.5187	0.8505	0.9981
33	0.0855	0.0221	0.0006	0.0000	0.3460	0.7489	0.8712	0.9984
34	0.0183	0.0742	0.0054	0.0000	0.6321	0.9912	0.8322	0.9989
35	0.0349	0.0245	0.0016	0.0001	0.8589	0.7232	0.8750	0.9993

1	2	3	4	5	6	7	8	9
36	0.0680	0.0961	0.0004	0.0000	1.0000	0.3548	0.8682	0.9987
Σ/n	0.0339	0.0366	0.0047	0.0001	0.6572	0.6091	0.8535	0.9629

So, if in the first three stages the average value of the differences ΔM_{00} is far from zero. Besides, the average stress $\Delta \sigma_1$ is far from one. Thus we have $\Delta M_{00} = 0.0001$ and $\Delta \sigma_1 = 0.9993$ at the last stage.

The result obtained in this sample confirms that with a triple critical force criterion (3) can estimate the closeness of the obtained solution to the minimum material-intensive one.

The approach proposed in this paper is based on using the criterion (3) of estimating the proximity of a solution for optimizing rods with constraints on resistance to the least material-intensive. This approach can be extended to cases of multiplicity of critical forces.

REFERENCES

1. **Lagrange J.-L.** Sur la Figure Des Colonnes. // *Mescellanea Taurinensia*, 1770-1773, Vol. 5, pp. 123.
2. **Clausen T.** Über die Form Architectonischer Säulen. // *Bull. cl. physico-math.* Acad. St.-Petersbourg, 1851, Vol. IX, pp. 371-380.
3. **Nikolay E.L.** Zadacha Lagranzha o Nivygodnejšem Ochertanii Kolonny [Lagrange's Problem About the Most Advantageous Outline of a Column]. // *News. Of St. Petersburg Polytechnic Institute*, 1907, Vol. VIII.
4. **Chentsov N.G.** Stojki Naimen'shego Vesa [Stands of a Minimum Weight]. // *Trudy TSAGI*, 1936, Vol. 265.
5. **Nudelman Ya.L.** Metody Opredelenija Sobstvennyh Chastot i Kriticheskikh Sil Dlja Sterzhnevnyh Sistem [Methods for Determining Natural Frequencies and Critical Forces for Rod Systems]. Moscow, Gostekhnizdat, 1949, 175 pages.
6. **Smirnov A.F.** Ustojchivost' i Kolebanija Sooruzhenij [Stability and Oscillations of Structures]. Moscow, Transzheldorizdat, 1958.
7. **Vinogradov A.I.** Problema Optimal'nogo Proektirovanija v Stroitel'noj Mehanike [The Problem of Optimal Design in Structural Mechanics]. Kyiv, Vyscha Shkola Publishing House in Kharkiv University, 1973, 167 pages.
8. **Olhoff, N., Rasmussen S.Kh.** O Prostyh i Dvukratnyh Optimal'nyh Kriticheskikh Nagruzkah Poteri Ustojchivosti Dlja Zashchennennyh Sterzhnej [On Simple and Two-Fold the Optimal Critical Load of Buckling for the Clamped Rods]. // *Mechanics. New in Foreign Science. Optimal Design of Structures*, 1981, Vol. 27, pp. 139-154.
9. **Lyakhovich L.S.** Osobyje Svojstva Optimal'nyh Sistem i Osnovnye Napravlenija ih Realizacii v Metodah Rascheta Sooruzhenij [Special Properties of Optimal Systems and the Main Directions of Their Implementation in the Methods of Calculation of Structures]. Tomsk, Tomsk State University of Architecture and Construction, 2009, 372 pages.
10. **Malinovsky A.P.** Chislennyj Metod Rascheta Sterzhnej na Prochnost', Ustojchivost' i Kolebanija [A Numerical Method of Calculation of the Stubs for Strength, Stability and Fluctuations]. // *Studies in Structures and Structural Mechanics*. Tomsk: Publishing House of TSU, 1978, pp. 85-96.

СПИСОК ПУБЛИКАЦИЙ

1. **Lagrange J.-L.** Sur la Figure Des Colonnes. // *Mescellanea Taurinensia*, 1770-1773, Vol. 5, pp. 123.
2. **Clausen T.** Über die Form Architectonischer Säulen. // *Bull. cl. physico-math.*

- Acad. St.-Petersbourg, 1851, Vol. IX, pp. 371-380.
3. **Николай Е.Л.** Задача Лагранжа о наивыгоднейшем очертании колонны. // Известия Санкт-Петербургского политехнического института, 1907, т. VIII.
 4. **Ченцов Н.Г.** Стойки наименьшего весаю // Труды ЦАГИ, 1936, Вып. 265.
 5. **Нудельман Я.Л.**, Методы определения собственных частот и критических сил для стержневых систем. – М.: Гостехиздат, 1949. – 175 с.
 6. **Смирнов А.Ф.** Устойчивость и колебания сооружений. – М.: Трансжелдориздат, 1958.
 7. **Виноградов А.И.** Проблема оптимального проектирования в строительной механике. – Харьков: Вища школа, Издательство при Харьковском университете, 1973. – 167 с.
 8. **Ольхофф Н, Расмуссен С.Х.** О простых и двухкратных оптимальных критических нагрузках потери устойчивости для защемленных стержней. // Механика. Новое в зарубежной науке. Оптимальное проектирование конструкций, 1981, №27, с. 139-154.
 9. **Ляхович Л.С.** Особые свойства оптимальных систем и основные направления их реализации в методах расчета сооружений. – Томск: Издательство Томского государственного архитектурно-строительного университета, 2009. – 372 с.
 10. **Малиновский А.П.** Численный метод расчета стержней на прочность, устойчивость и колебания. // Исследования по строительным конструкциям и строительной механике. – Томск: Издательство ТГУ, 1978, с. 85-96.

Акимов Павел Алексеевич, академик РААСН, профессор, доктор технических наук; временно исполняющий обязанности ректора Национального исследовательского Московского государственного строительного университета; профессор Департамента архитектуры и строительства Российского университета дружбы народов; профессор кафедры строительной механики Томского государственного архитектурно-строительного университета; 107031, г. Москва, ул. Большая Дмитровка, д. 24, стр. 1; тел. +7(495) 625-71-63; факс +7 (495) 650-27-31; Email: akimov@raasn.ru, pavel.akimov@gmail.com.

Малиновский Анатолий Павлович, доцент, кандидат технических наук, и.о. заведующего кафедрой строительной механики, Томский государственный архитектурно-строительный университет; 634003, Россия, г. Томск, Соляная пл. 2; e-mail: bat9203@gmail.com.

Leonid S. Lyakhovich, Full Member of the Russian Academy of Architecture and Construction Sciences, Professor, DSc, Head of Department of Structural Mechanics, Tomsk State University of Architecture and Building; 634003, Russia, Tomsk, Solyanaya St., 2; E-mail: lls@tsuab.ru

Pavel A. Akimov, Full Member of the Russian Academy of Architecture and Construction Sciences, Professor, Dr.Sc.; Acting Rector of National Research Moscow State University of Civil Engineering; Professor of Department of Architecture and Construction, Peoples' Friendship University of Russia; Professor of Department of Structural Mechanics, Tomsk State University of Architecture and Building; 24, Ul. Bolshaya Dmitrovka, 107031, Moscow, Russia; phone +7(495) 625-71-63; Fax: +7 (495) 650-27-31; E-mail: akimov@raasn.ru, pavel.akimov@gmail.com.

Anatoly P. Malinowski, Associate Professor, Ph.D, H.T. Head of Department of Structural Mechanics, Tomsk State University of Architecture and Building; 634003, Russia, Tomsk, Solyanaya St., 2; E-mail: bat9203@gmail.com.

Ляхович Леонид Семенович, академик РААСН, профессор, доктор технических наук, профессор кафедры строительной механики, Томский государственный архитектурно-строительный университет; 634003, Россия, г. Томск, Соляная пл. 2; E-mail: lls@tsuab.ru

A PROBABLISTIC APPROACH TO EVALUATION OF THE ULTIMATE LOAD ON FLEXURAL RC ELEMENT ON CRACK LENGTH

Sergey A. Solovyev

Vologda State University, Vologda, Russia

Abstract: The fracture mechanics of concrete and reinforced concrete is a promising direction in the development of methods for reinforced concrete structural elements design and inspection. At the same time, probabilistic methods of design and behavior analysis of structural elements are of particular interest. The article describes a probabilistic approach to load-bearing capacity and reliability analysis of flexural reinforced concrete elements based on the crack length criterion. The functional relationship between the critical stress intensity coefficient of concrete and the design compressive strength of concrete is given. The article presents a method for the reliability analysis of flexural reinforced concrete elements at the operational stage with limited statistical data about the critical stress intensity coefficient of concrete. The ultimate value of the failure probability (or reliability index) should be set for each object individually based on the value of the acceptable risk.

Key words: reliability theory, fracture mechanics, crack length, reinforced concrete beam, reinforced concrete slab, safety

ВЕРОЯТНОСТНЫЙ ПОДХОД К ОПРЕДЕЛЕНИЮ ДОПУСТИМОЙ НАГРУЗКИ НА ИЗГИБАЕМЫЙ ЖЕЛЕЗОБЕТОННЫЙ ЭЛЕМЕНТ ПО КРИТЕРИЮ ДЛИНЫ ТРЕЩИНЫ

С.А. Соловьев

Вологодский государственный университет, г. Вологда, РОССИЯ

Аннотация: Механика разрушения бетона и железобетона является перспективным направлением в развитии методов расчета железобетонных элементов конструкций. В то же время, особый интерес представляют вероятностные методы расчета и анализа работы несущих элементов строительных конструкций. В работе рассмотрен вероятностный подход к расчету несущей способности и надежности изгибаемых железобетонных элементов по критерию длины трещины. Приведена функциональная зависимость между критическим коэффициентом интенсивности напряжений бетона и расчетным сопротивлением бетона. В статье представлен метод расчета надежности изгибаемого железобетонного элемента на стадии эксплуатации при ограниченной статистической информации о критическом коэффициенте интенсивности напряжений бетона. Предельное значение вероятности безотказной работы (или индекса надежности) следует устанавливать для каждого объекта индивидуально, исходя из значения допустимого риска.

Ключевые слова: теория надежности, механика разрушения, длина трещины, железобетонная балка, железобетонная плита, безопасность

1. INTRODUCTION

Reinforced concrete flexural elements (beams and slabs) are common parts of different structures. The safety of a whole structure

depends from the reinforced concrete beams/slabs safety and reliability. By Eurocode 0 “Basis of structural design”, the reliability - the ability of a structure or a structural member to fulfill the specified requirements, including

the design working life, for which it has been designed. Reliability covers safety, serviceability and durability of a structure and is usually expressed in probabilistic terms. The measure of reliability is the failure probability or safety probability.

As noted in [1], for an adequate description of structural behavior, probabilistic methods must be resorted to. Properly speaking, an element of probability is embodied even in the deterministic approach, which claims to "simplify" the structure by eliminating all aspects of uncertainty. In practice structural reliability (or structural probabilistic design) increasingly is being applied, particularly for situations where quantitative, data-based risk assessment of non-elementary structural or other systems required [2].

Reinforced concrete (RC) flexural elements - beams and slabs are common structural elements in many buildings. Safety assessment of these elements is an important task. K.A. Piradov and N.V. Savickij [3] note that there is no theoretically justified approach for the design of reinforced concrete structural elements with cracks at the moment (reinforced concrete elements, especially without reinforcement prestressing, usually contain cracks at design loads), and current design method (safety factors method or limit state method from 1955) is based on a number of theoretically unsubstantiated empirical coefficients. Fracture mechanics [4, 5, 6] can be successfully applied for design of reinforced concrete elements with cracks. The relationship between fracture mechanics and reliability theory can be a powerful tool for evaluating the structural safety of reinforced concrete elements.

2. METHODS

There are different approaches to limiting the normal crack length in reinforced concrete beams. Some approaches limit the crack length to a percentage of the element's cross-section

height. The research [7] notes that the crack length must not exceed $0.3h_0$, where h_0 – distance from extreme compression fiber to centroid of longitudinal tension reinforcement. Gvozdev A.A. [8] proposed to limit crack length by value $0.5h$, where h – beam cross-section height. The research [9] offers next critical values: $0.7h$, if there is a crack in the middle of the beam span; $0.65h$, if in a third of the span and $0.3h$ if at the support points (shear area). More objective provisions for limiting the crack length can be obtained from the fracture mechanics equations for concrete and reinforced concrete. Thus, the following dependence is proposed in [10]:

$$l_{cr} = \frac{M^2 \cdot Y_1^2(a_1) \cdot ([2\pi - 1]/2\pi)}{(K_{IC}^b + K_{IC}^s)^2 b^2 h}, \quad (1)$$

where M – bending moment in the beam cross-section; K_{IC}^b – critical stress intensity coefficient of concrete; K_{IC}^s – critical stress intensity coefficient which characterizes the restraining effect of reinforcement on crack growth; b – width of the beam cross-section; h – height of the beam cross-section.

Function $Y_1(a_1)$ have the form

$$Y_1(a_1) = \sqrt{\pi} - a_1 - 1,$$

where $a_1 = a/h$; a – distance from extreme tensile fiber to centroid of longitudinal tension reinforcement.

The parameter K_{IC}^s have the form (for normal crack):

$$K_{IC}^s = \frac{60 A_s}{b \sqrt{\pi} \cdot a} \left[\frac{0.93}{\sqrt{1-a_1}} + \frac{1}{\sqrt{1-a_1^2}} - 0.93 \right]. \quad (2)$$

If we limit the crack length to a critical value $l_{cr,ult}$, then the following equation can be derived from equation (1) to evaluate the

bearing capacity (ultimate bending moment M_{ult}) of beam:

$$M_{ult} = \sqrt{\frac{l_{crc,ult} \cdot (K_{IC}^b + K_{IC}^s)^2 b^2 h}{\left(\sqrt{\pi} - \frac{a}{h} - 1\right) \cdot \left(\frac{2\pi - 1}{2\pi}\right)}}. \quad (3)$$

In accordance with the recommendations [10] and SP 63.13330.2018 "Concrete and reinforced concrete structures", the relationship between the critical stress intensity coefficient in concrete and the design compressive strength of concrete can be represented graphically (see Figure 1).

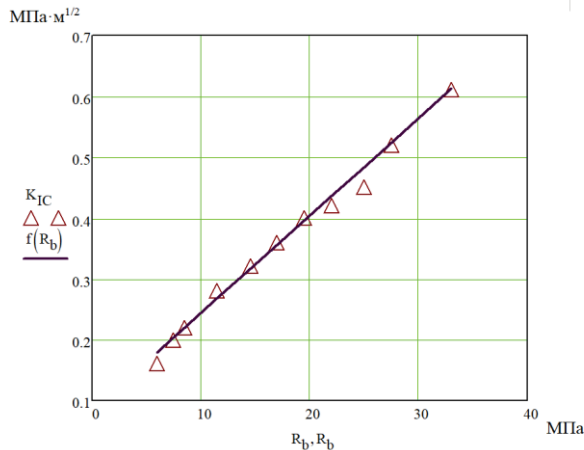


Figure 1. Functional relationship between the critical stress intensity coefficient in concrete and the design compressive strength of concrete.

This dependence also can be approximated as a linear function (in MPa):

$$K_{IC}^b(R_b) = 0.084 + 0.016 \cdot R_b.$$

Thus, having the functional relationship between the critical stress intensity coefficient in concrete and the design compressive strength of concrete it is possible to calculate critical stress intensity coefficient for the existing concrete by determining the compressive

strength (for example, by non-destructive testing).

The problem of assigning the ultimate crack length for a reinforced concrete beam also can be solved. If we take

$$M_{ult} = R_b b x (h_0 - 0.5x),$$

then the ultimate crack length can be expressed as:

$$l_{crc,ult} = \frac{[R_b b x (h_0 - 0.5x)]^2 \cdot [\sqrt{\pi} - a_1 - 1]^2}{(K_{IC}^b + K_{IC}^s)^2 b^2 h} \times \left(\frac{2\pi - 1}{2\pi}\right) \quad (4)$$

where

$$x = \frac{R_s A_s}{R_b b},$$

R_b and R_s – compressive strength of concrete and tensile strength of reinforcement; A_s – area of nonprestressed longitudinal tension reinforcement.

3. RESULTS AND DISCUSSION

Example 1. The reinforced concrete beam (without prestressed reinforcement) with cross-section dimensions $h=500$ mm and $b=250$ mm. Reinforcement: 5 bars with $\phi 12$ mm ($A_s = 1.231 \cdot 10^{-4}$ m²), with distance from extreme tensile fiber to centroid of longitudinal tension reinforcement $a=40$ mm. Then by eq. (2): $K_{IC}^s = 0.543$ MPa·m². Beam span $l=6$ m. If beam simply supported, then:

$$M = \frac{ql^2}{8}.$$

Figure 2 shows graph of the dependence of the ultimate load q on the required height h of cross section (with $K_{IC}^b = 0.32$ MPa·m²) for different approaches to limiting the crack length in

concrete – $0.3h$, $0.5h$ and $0.7h$ according to example 1 data.

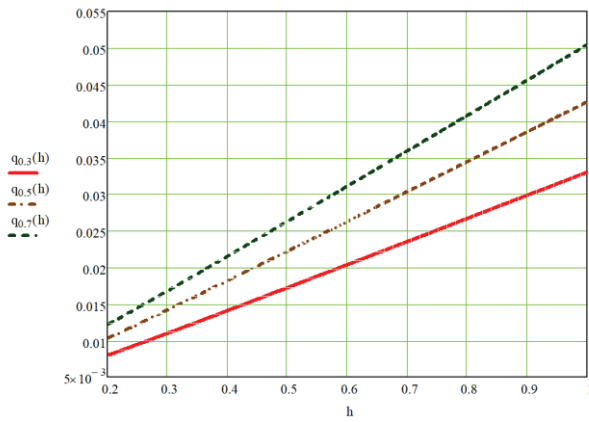


Figure 2. Graphs of dependence of the required height of beam cross-section h and the ultimate load q .

Figure 3 presents the dependence of the ultimate crack length in concrete l_{cr} and design compressive strength of concrete R_b .

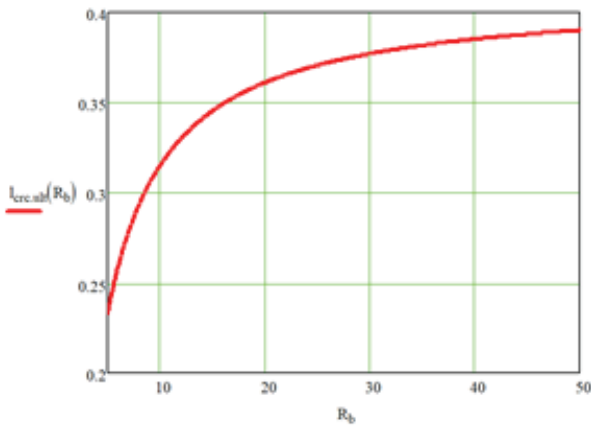


Figure 3. “Ultimate crack length – concrete resistance” diagram.

Figure 3 shows that with a small compressive strength of concrete (10 MPa), the ultimate crack length is 320 mm or $\sim 0.64h$ with an increasing of compressive strength, the ultimate crack length increases to the value $\sim 0.74h$ at 20 MPa and $\sim 0.76h$ at 30 MPa. The ultimate crack length is stabilized to a value of $\sim 0.78h$ next. Critical stress intensity coefficient determined by experimental methods for existing reinforced concrete structural elements. These methods are

often based on the correlation between critical stress intensity coefficient in concrete and the design compressive strength. Let's consider the problem of estimation the ultimate load q with a given confidence level if critical stress intensity coefficient is random variable with normal distribution. The problem is the simplest problem of the reliability theory [2] with a single random variable, so we present it without additional layouts.

Figure 4 shows the dependence of ultimate load q and K_{IC} variation coefficient C_x at the different significance levels. Data is taken from example 1.

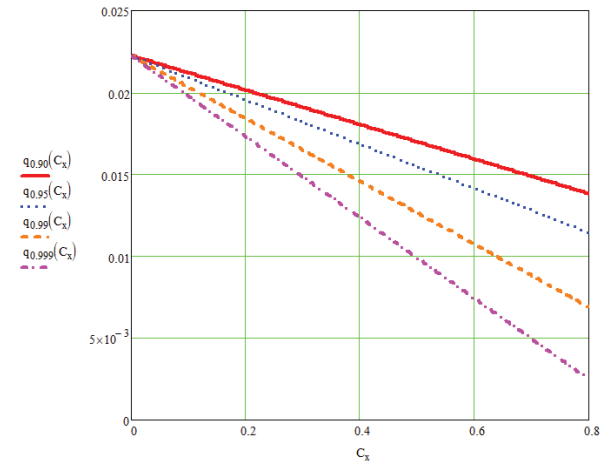


Figure 4. Dependence of ultimate load q and K_{IC} variation coefficient at the different significance levels.

Figure 4 shows that with the increase in the variability of the critical stress intensity coefficient, it is necessary to limit the ultimate load on the RC element to a greater extent in order to ensure the given level of reliability.

The inverse problem can also be solved –the reliability analysis of a reinforced concrete beam by the crack length criterion at the operation stage. A limit state mathematical model for reinforced concrete beam can be presented as:

$$\tilde{q} \leq \frac{l_{cr,ult} \cdot (\tilde{K}_{IC}^b + K_{IC}^s)^2 b^2 h}{\sqrt{\left(\sqrt{\pi} - \frac{a}{h} - 1\right) \cdot \left(\frac{2\pi - 1}{2\pi}\right)} l^2} \cdot \frac{8}{l^2},$$

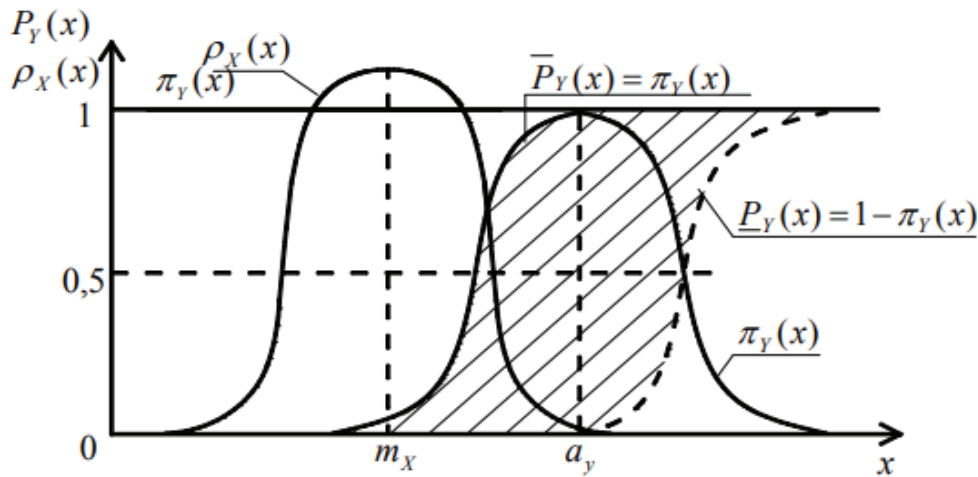


Figure 5. Probability density function of random variable X and distribution function of fuzzy variable Y graphs.

where the wavy line denotes random variables.

$$\text{Let } \tilde{q} = X, \sqrt{\frac{l_{crc,ult} \cdot (\tilde{K}_{IC}^b + K_{IC}^s)^2 b^2 h}{\left(\sqrt{\pi} - \frac{a}{h} - 1\right) \cdot \left(\frac{2\pi - 1}{2\pi}\right)}} \frac{8}{l^2} = Y.$$

Describing the load on the beam \tilde{q} and the critical stress intensity coefficient \tilde{K}_{IC}^b by the normal distribution, the probability of non-failure can be found as:

$$P = \Pr(X \leq Y) = \Phi(\beta) = \Phi\left(\frac{m_y - m_x}{\sqrt{S_x^2 + S_y^2}}\right), \quad (5)$$

where m_x and m_y – expected values of X and Y ; S_x and S_y – standard deviations of X and Y ; $\Phi()$ – value of the Laplace integral function; β – reliability index [11-13].

The function parameters are calculated by the follows equations: $m_x = m_q$, $S_x = S_q$,

$$m_y = \sqrt{\frac{l_{crc,ult} \cdot \left(m_{K_{IC}^b} + K_{IC}^s\right)^2 b^2 h}{\left(\sqrt{\pi} - \frac{a}{h} - 1\right) \cdot \left(\frac{2\pi - 1}{2\pi}\right)}} \frac{8}{l^2},$$

$$S_y = \sqrt{\frac{l_{crc,ult} \cdot \left(S_{K_{IC}^b}\right)^2 b^2 h}{\left(\sqrt{\pi} - \frac{a}{h} - 1\right) \cdot \left(\frac{2\pi - 1}{2\pi}\right)}} \frac{8}{l^2}.$$

If the reliability (probability of non-failure) requirements are not met, the design load value is reduced to the new value $m_x = m_q$ and the reliability value is recalculated.

However, it is not always possible to get a large amount of statistical data about the parameter \tilde{K}_{IC}^b . An approach based on a combination of probability theory and fuzzy set theory can be used in this case. Fuzzy set theory allows to model the variability of a random (fuzzy) variable with a small amount of statistical data. Figure 5 shows the probability density function of random variable X and the distribution function of fuzzy variable Y graphs

The reliability interval can be calculated using the following equations:

$$\begin{aligned} \underline{P} &= 1 - \int_0^{a_y} \frac{1}{\sqrt{2\pi}} \exp\left[-\frac{(x-m_x)^2}{2S_x^2}\right] \cdot \exp\left[-\left(\frac{x-a_y}{b_y}\right)^2\right] dx - \\ &- \int_{a_y}^{\infty} \exp\left[-\frac{(x-m_x)^2}{2S_x^2}\right] dx; \\ \bar{P} &= 1 - \int_0^{a_y} 0 dx - \\ &- \int_{a_y}^{\infty} \exp\left[-\frac{(x-m_x)^2}{2S_x^2}\right] \cdot \left[1 - \exp\left[-\left(\frac{x-a_y}{b_y}\right)^2\right]\right] dx \end{aligned}$$

where

$$a_y = \frac{Y_{\max} + Y_{\min}}{2}$$

– “mean” value;

$$b_y = \frac{Y_{\max} + Y_{\min}}{2 \cdot \sqrt{-\ln \alpha}}$$

– measure of variability; α - cut (risk) level [14-15]; Y_{\max} , Y_{\min} – minimum and maximum values based on test results and calculations. The reliability is described by the interval $[\underline{P}; \bar{P}]$.

For the above-described problem:

$$Y_{\max/\min} = \sqrt{\frac{l_{crc,ult} \cdot (K_{IC,max/\min}^b + K_{IC}^s)^2 b^2 h}{\left(\sqrt{\pi} - \frac{a}{h} - 1\right) \cdot \left(\frac{2\pi - 1}{2\pi}\right)}} \cdot \frac{8}{l^2}.$$

The optimal level of non-failure probability (or reliability index) should be set taking into account the acceptable risk [16-18].

4. CONCLUSIONS

1. The article presents probabilistic approach to evaluation the ultimate load on flexural reinforced concrete elements on crack length criterion based of fracture mechanics;
2. The functional relationship between the critical stress intensity coefficient of concrete and the design concrete resistance is given. It can be used in inspections and maintenances of RC elements;
3. An ultimate crack length should be set for reinforced concrete elements individually;
4. The article describes the reliability analysis method for reinforced concrete flexural elements on crack length with limited statistical data.

REFERENCES

1. **Elishakoff I.** Probabilistic Methods in the Theory of Structures: Strength of Materials, Random Vibrations, and Random Buckling. World Scientific Publishing Co, 2017, 400 pages.
2. **Melchers R.E., Beck A.T.** Structural reliability analysis and prediction. John Wiley & Sons, 2018, 497 pages.
3. **Piradov K.A., Savickij N.V.** Mekhanika razrusheniya i teoriya zhelezobetona [Fracture mechanics of concrete and reinforced concrete]. // *Beton i zhelezobeton*, 2014, No. 4, pp. 23-25 (in Russian)
4. **Tung N.D., Tue N.V.** A fracture mechanics-based approach to modeling the confinement effect in reinforced concrete columns. // *Construction and Building Materials*, 2016, Volume 102, pp. 893-903.
5. **Yehia N.A.B.** Fracture mechanics approach for flexural strengthening of reinforced concrete beams. // *Engineering Structures*, 2009, Volume 31, Issue 2, pp. 404-416.
6. **Sau N., Medina-Mendoza J., Borbon-Almada A.C.** Peridynamic modelling of

- reinforced concrete structures. // *Engineering Failure Analysis*, 2019, Volume 103, pp. 266-274.
7. **Zajcev Yu.V.** Mekhanika razrusheniya dlya stroitelej [Fracture mechanics for structural engineers]. Moscow, Vysshaya shkola, 1991, 287 pages (in Russian)
 8. **Gvozdev A.A.** Novoe v proektirovanii betonnyh i zhelezobetonnyh konstrukcij [New in concrete and reinforced concrete structures design]. Moscow, Strojizdat, 1978, 208 pages (in Russian).
 9. **Carpinteri A., Carmona J.R., Ventura G.** Propagation of flexural and shear cracks through RC beams by the bridged crack model. // *Magazine of concrete research*, 2007, No. 10, pp. 743-756.
 10. **Piradov K.A.** Teoreticheskie i eksperimental'nye osnovy mekhaniki razrusheniya betona i zhelezobetona [Theoretical and experimental foundations of concrete and reinforced concrete fracture mechanics]. Tbilisi, Energiya, 1998, 355 pages (in Russian)
 11. **Wang P., Zhang J., Zhai H., Qiu J.** A new structural reliability index based on uncertainty theory. // *Chinese Journal of Aeronautics*, 2017, Volume 30, Issue 4, pp. 1451-1458.
 12. **Van Coile R., Hopkin D., Bisby L., Caspeele R.** The meaning of Beta: background and applicability of the target reliability index for normal conditions to structural fire engineering. // *Procedia Engineering*, 2017, Volume 210, pp. 528-536.
 13. **Roudak M.A., Shayanfar M.A., Barkhordari M.A., Karamloo M.** A new three-phase algorithm for computation of reliability index and its application in structural mechanics. // *Mechanics Research Communications*, 2017, Volume 85, pp. 53-60
 14. **Li H., Nie X.** Structural reliability analysis with fuzzy random variables using error principle. // *Engineering Applications of Artificial Intelligence*, 2018, Volume 67, pp. 91-99.
 15. **Utkin V.S., Solovyev S.A., Kaberova A.A.** Znachenie urovnya sreza (riska) pri raschete nadezhnosti nesushchih elementov vozmozhnostnym metodom [Cut (risk) level in reliability analysis of structural elements by possibilistic methods]. // *Stroitel'naya mekhanika i raschet sooruzhenij*, 2015, No. 6, pp. 63-67. (in Russian)
 16. **Trbojevic V. M.** Another look at risk and structural reliability criteria. // *Structural Safety*, 2009, Volume 31, Issue 3, pp. 245-250.
 17. **Zhu B., Frangopol D.M.** Reliability, redundancy and risk as performance indicators of structural systems during their life-cycle. // *Engineering Structures*, 2012, Volume 41, pp. 34-49.
 18. **Crespo L.G., Kenny S.P., Giesy D.P.** Staircase predictor models for reliability and risk analysis. // *Structural Safety*, 2018, Volume 75, pp. 35-44.

СПИСОК ЛИТЕРАТУРЫ

1. **Elishakoff I.** Probabilistic Methods in the Theory of Structures: Strength of Materials, Random Vibrations, and Random Buckling. World Scientific Publishing Co, 2017, 400 pages.
2. **Melchers R.E., Beck A.T.** Structural reliability analysis and prediction. John Wiley & Sons, 2018, 497 pages.
3. **Пирадов К.А., Савицкий Н.В.** Механика разрушения и теория железобетона // *Бетон и железобетон*, 2014, №4, с. 23-25.
4. **Tung N.D., Tue N.V.** A fracture mechanics-based approach to modeling the confinement effect in reinforced concrete columns. // *Construction and Building Materials*, 2016, Volume 102, pp. 893-903.
5. **Yehia N.A.B.** Fracture mechanics approach for flexural strengthening of reinforced

- concrete beams. // *Engineering Structures*, 2009, Volume 31, Issue 2, pp. 404-416.
6. **Sau N., Medina-Mendoza J., Borbon-Almada A.C.** Peridynamic modelling of reinforced concrete structures. // *Engineering Failure Analysis*, 2019, Volume 103, pp. 266-274.
7. **Зайцев Ю.В.** Механика разрушения для строителей. – М.: Высшая школа, 1991. – 287 с.
8. **Гвоздев А.А.** Новое в проектировании бетонных и железобетонных конструкций. – М.: Стройиздат, 1978. – 208 с.
9. **Carpinteri A., Carmona J.R., Ventura G.** Propagation of flexural and shear cracks through RC beams by the bridged crack model. // *Magazine of concrete research*, 2007, No. 10, pp. 743-756.
10. **Пирадов К.А.** Теоретические и экспериментальные основы механики разрушения бетона и железобетона. – Тбилиси: Энергия, 1998. – 355 с.
11. **Wang P., Zhang J., Zhai H., Qiu J.** A new structural reliability index based on uncertainty theory. // *Chinese Journal of Aeronautics*, 2017, Volume 30, Issue 4, pp. 1451-1458.
12. **Van Coile R., Hopkin D., Bisby L., Caspeele R.** The meaning of Beta: background and applicability of the target reliability index for normal conditions to structural fire engineering. // *Procedia Engineering*, 2017, Volume 210, pp. 528-536.
13. **Roudak M.A., Shayanfar M.A., Barkhordari M.A., Karamloo M.** A new three-phase algorithm for computation of reliability index and its application in structural mechanics. // *Mechanics Research Communications*, 2017, Volume 85, pp. 53-60
14. **Li H., Nie X.** Structural reliability analysis with fuzzy random variables using error principle. // *Engineering Applications of Artificial Intelligence*, 2018, Volume 67, pp. 91-99.
15. **Уткин В.С., Соловьев С.А., Каберова А.А.** Значение уровня среза (риска) при расчете надежности несущих элементов возможным методом. // *Строительная механика и расчет сооружений*, 2015, №6, с. 63-67.
16. **Trbojevic V. M.** Another look at risk and structural reliability criteria. // *Structural Safety*, 2009, Volume 31, Issue 3, pp. 245-250.
17. **Zhu B., Frangopol D.M.** Reliability, redundancy and risk as performance indicators of structural systems during their life-cycle. // *Engineering Structures*, 2012, Volume 41, pp. 34-49.
18. **Crespo L.G., Kenny S.P., Giesy D.P.** Staircase predictor models for reliability and risk analysis. // *Structural Safety*, 2018, Volume 75, pp. 35-44.

Sergey A. Solovyev, Candidate of Technical Sciences, Associated Professor, Industrial and Civil Department, Vologda State University, 15, Lenin str., Vologda, 160000, Russia.

E-mail: ser6sol@yandex.ru.

Соловьев Сергей Александрович, кандидат технических наук, доцент кафедры «Промышленное и гражданское строительство», Вологодский государственный университет; 160000, Россия, г. Вологда, ул. Ленина, д. 15;

E-mail: ser6sol@yandex.ru.

A.A. ILYUSHIN'S FINAL RELATION, ALTERNATIVE EQUIVALENT RELATIONS AND VERSIONS OF ITS APPROXIMATION IN PROBLEMS OF PLASTIC DEFORMATION OF PLATES AND SHELLS

PART 1: A.A. ILYUSHIN'S FINAL RELATION

Aleksandr V. Starov, Sergei .JU. Kalashnikov

Volgograd state technical university, Volgograd, RUSSIA

Abstract: The finite relationship between the forces and moments of plates and shells in the parametric form of the theory of small elastoplastic deformations is investigated of A.A. Ilyushin, to determine the load-bearing capacity of structures from a material without hardening. A geometric image of the exact yield surface in the space of generalized stresses is obtained. In the first part of the article the conclusion of the final relation is given. In the second and third parts, by introducing other parameters, alternative equivalent dependences of the final relationship have been developed and variants of its approximation for application in computational practice are considered. In the fourth part, additional properties of the final relationship are considered, the possibility and necessity of its use in problems of plastic deformation of plates and shells is shown.

Keywords: the plasticity theory, plastic deformation of plates and shells, surface of fluidity, plasticity condition

КОНЕЧНОЕ СООТНОШЕНИЕ А.А. ИЛЮШИНА, АЛЬТЕРНАТИВНЫЕ ЭКВИВАЛЕНТНЫЕ ЗАВИСИМОСТИ И ВАРИАНТЫ ЕГО АППРОКСИМАЦИИ В ЗАДАЧАХ ПЛАСТИЧЕСКОГО ДЕФОРМИРОВАНИЯ ПЛАСТИН И ОБОЛОЧЕК

ЧАСТЬ 1: КОНЕЧНОЕ СООТНОШЕНИЕ А.А. ИЛЮШИНА

А.В. Старов, С.Ю. Калашников

Волгоградский государственный технический университет, г. Волгоград, РОССИЯ

Аннотация: Выполнено исследование конечного соотношения между силами и моментами пластин и оболочек в параметрическом виде теории малых упругопластических деформаций А.А. Ильюшина, для определения несущей способности конструкций из материала без упрочнения. Получен геометрический образ точной поверхности текучести в пространстве обобщенных напряжений. В первой части статьи приводится вывод конечного соотношения. Во второй и третьей частях введением других параметров разработаны альтернативные эквивалентные зависимости конечного соотношения и рассмотрены варианты его аппроксимации для применения в расчетной практике. В четвертой части рассмотрены дополнительные свойства конечного соотношения, показана возможность и необходимость его использования в задачах пластического деформирования пластин и оболочек.

Ключевые слова: теория пластичности, пластическое деформирование пластин и оболочек, поверхность текучести, условия пластичности

INTRODUCTION

Theory of small elastoplastic deformations Ilyushin was created in connection with the problem of the strength of the projectile while moving in the barrel of the gun. All calculations were carried out by the methods of the theory of elasticity, although a small residual plastic deformation was allowed by normative documents. Together with theorems on simple loading, unloading, and the method of elastic solutions, the theory of A.A. Ilyushin was a powerful apparatus for investigating the strength, deformability and stability of structural elements, structures and machine parts beyond the elastic limit. [1-8]

The theory of elastoplastic deformations of plates and shells is presented by A.A. Ilyushin in [9-14], where on the basis of the methods of the theory of plasticity a finite relationship between forces and moments was obtained to determine the load-bearing capacity of structures from a material without hardening and the limiting state is characterized by the propagation of fluidity throughout the volume.

Since the equations of the theory of plates and shells are formulated in generalized forces and generalized displacements, the conditions of strength and plasticity must also be represented in generalized forces. The transformation of the condition of strength and plasticity from the stress space into the space of generalized stresses is one of the most important and complex problems of the theory of limiting equilibrium of plates and shells [15-16].

The parametric equation of the limiting hypersurface in generalized stresses for thin plates and shells on the basis of the Mises condition of plasticity and the relations of the theory of small elastoplastic deformations was first obtained by A.A. Ilyushin [9,13]. The traditional Kirchhoff-Love hypotheses and the incompressibility of the material are used. Received A.A. Ilyushin's relations are not expressed in explicit form and are complex for solving practical problems. The geometrical image of the exact yield surface in

the literature is absent.

Similar relations with the introduction of other parameters were obtained in the works of V.V. Rozhdestvensky [17], G.S. Shapiro [18], P.G. Hodge [19-22], D.C. Drucker, H.G. Hopkins [23], D.C. Drucker [24], D.C. Drucker, R.T. Shield [25], E.T. Onat [26,28], E.T. Onat, W. Prager [27] and other authors. Detailed reviews of literature on this topic can be found in [15-16], as well as in the works of N. Jones [29-30] and Yu.V. Nemirovsky, TP Romanova [31].

In the works of M.I. Erhov [32-33], on the basis of the two-layer cross section model and the flow conditions of R. Mises, a finite relationship between the internal forces and the moments of ideally plastic plates and shells is obtained on the assumption that the strain intensity within the layer is constant in the plastic region. Here is a schematic model of the exact yield surface and the proposed version of its approximation. A similar model of the approximation of the cross-section of a homogeneous shell by a two-layered cross section was used by V.I. Rosenblum [34-37], Yu.N. Rabotnov [38]. This approach and its various variants were used by other authors.

If the shell material is ideally plastic and satisfies to a condition of fluidity of Mises, for a plastic condition $\sigma_i = \sigma_s = \text{const}$. In this case in purely plastic areas of a shell the right parts of determining relations for the generalised pressure will be uniform functions of a zero order concerning six parameters ε_i, χ_i .

From this necessity of existence of a final relation which plays a role of a condition of fluidity follows and connects values of efforts and the moments in purely plastic areas of a shell [9,39]. Owing to noted property of uniformity of the equations in purely plastic areas ε_i, χ_i it is possible to replace deformation components ε_i, χ_i in the corresponding speeds $\dot{\varepsilon}_i, \dot{\chi}_i$.

The definition of the ultimate load reduces to the construction of internal stress fields, moments, displacements, and velocities of dis-

placements of the middle surface that satisfy equilibrium equations in the plastic regions, the final relationship, the dependencies between the velocities of displacements of the middle surface and the deformation rates that determine the relations for generalized stresses. In rigid regions, the velocities must vanish or correspond with the rigid displacement with joints, and the forces and moments must satisfy the equilibrium conditions and do not contradict the final relation. The specified static and kinematic boundary conditions must also be satisfied [9, 39].

The final relation corresponding to the defining equations [9] has a very complex structure and is not explicitly expressed. For an approximate analysis, it is approximated by a quadratic dependence [9-10,32-37], which corresponds to the particular case [9], while the bilinear form

$$P_{\varepsilon\chi} = \varepsilon_1\chi_1 + \varepsilon_2\chi_2 + \frac{1}{2}\varepsilon_1\chi_2 + \frac{1}{2}\varepsilon_2\chi_1 + \varepsilon_{11}\chi_{12} = 0 :$$

$$\frac{1}{N_s^2} \left(N_1^2 - N_1 N_2 + N_2^2 + 3N_{12}^2 \right) +$$

$$+ \frac{1}{N_s^2} \left(M_1^2 - M_1 M_2 + M_2^2 + 3M_{12}^2 \right) = 1,$$

$$N_s = \sigma_s h, \quad M_s = \frac{\sigma_s h^2}{4}.$$

For the axisymmetric problem, the following approximations are also used.

1. *A semilinear final relation* [19, 32-37], which corresponds to the linearization of the previous relation

$$n^2 + m^2 = 1, \quad n = \max \left\{ \left| \frac{N_1}{N_s} \right|, \left| \frac{N_2}{N_s} \right|, \left| \frac{N_1 - N_2}{N_s} \right| \right\},$$

$$m = \max \left\{ \left| \frac{M_1}{M_s} \right|, \left| \frac{M_2}{M_s} \right|, \left| \frac{M_1 - M_2}{M_s} \right| \right\}.$$

2. *The final relationship with a limited interaction of forces and moments* [19, 32-37], which

does not take into account the interaction of membrane and bending force factors, and others. The degree of approximation of these relations to the exact one [9] depends on the ratio $0 \leq P_{\varepsilon\chi}^2 \leq P_\varepsilon \cdot P_\chi$. Meanwhile, elementary analysis shows that in the center of a flexible circular plate or a slender axisymmetric shell is always satisfied $P_{\varepsilon\chi}^2 = P_\varepsilon \cdot P_\chi \neq 0$.

In the works of V.I. Korolev [40] and P.M. Ogibalov [41] deduces the derivation of the finite relation AA. Ilyushin and solve the problem for the simplest complex stress state of shells at $P_\chi \neq 0, P_\varepsilon \neq 0, P_{\varepsilon\chi} = 0$.

The purpose of this article is to investigate the final relationship of AA. Ilyushin, obtaining a geometric image of the exact yield surface, alternative dependencies and variants of its approximation.

In the first part of the paper, with some abbreviations, the derivation of the final relation presented in §24-26 [9] is given. In contrast to [9], the designations of stresses, forces and shear forces in the shell sections have been changed

$$\sigma_x, \sigma_y, \sigma_z, \tau_{xy}, \tau_{zx}, \tau_{zy}$$

$N_1, N_2, N_{12}, n_1, n_2, n_{12}, Q_1, Q_2$, while the numbering of formulas, tables, graphs and references to formulas are completely preserved. In the second and third parts, alternative equivalent dependencies of the final relationship are developed and variants of its approximation are considered for application in computational practice. In the fourth part, additional properties of the final relationship are considered, the possibility and necessity of its use in problems of plastic deformation of plates and shells is shown.

1.1. The connection between internal forces, moments and deformations of the shell on the basis of the theory of small elastoplastic deformations

Intensity of deformations, according to (4.7):

$$e_i = \frac{2}{\sqrt{3}} \sqrt{P_\varepsilon - 2zP_{\varepsilon\chi} + z^2P_\chi},$$

$$P_\varepsilon = \varepsilon_1^2 + \varepsilon_1\varepsilon_2 + \varepsilon_2^2 + \varepsilon_{12}^2, \quad P_\chi = \chi_1^2 + \chi_1\chi_2 + \chi_2^2 + \chi_{12}^2,$$

$$P_{\varepsilon\chi} = \varepsilon_1\chi_1 + \varepsilon_2\chi_2 + \frac{1}{2}\varepsilon_1\chi_2 + \frac{1}{2}\varepsilon_2\chi_1 + \varepsilon_{11}\chi_{12}. \quad (4.19)$$

The stresses according to (4.2):

$$S_x = \sigma_x - \frac{1}{2}\sigma_y = \frac{\sigma_i}{e_i}(\varepsilon_1 - z\chi_1),$$

$$S_y = \sigma_y - \frac{1}{2}\sigma_x = \frac{\sigma_i}{e_i}(\varepsilon_2 - z\chi_2), \quad (4.20)$$

$$S_{xy} = \tau_{xy} = \frac{2\sigma_i}{3e_i}(\varepsilon_{12} - z\chi_{12}),$$

And σ_i there is a certain function e_i , the voltage τ_{xz} , τ_{yz} , σ_z is small in comparison with the main ones. If the shell is thin enough and the ratio of its thickness to the characteristic radius of curvature can be neglected, we obtain the following five expressions for the forces:

$$N_1 = \int_{-\frac{h}{2}}^{\frac{h}{2}} \sigma_x dz, \quad N_2 = \int_{-\frac{h}{2}}^{\frac{h}{2}} \sigma_y dz, \quad N_{12} = \int_{-\frac{h}{2}}^{\frac{h}{2}} \tau_{xy} dz,$$

$$Q_1 = \int_{-\frac{h}{2}}^{\frac{h}{2}} \tau_{zx} dz, \quad Q_2 = \int_{-\frac{h}{2}}^{\frac{h}{2}} \tau_{zy} dz. \quad (4.21)$$

The shearing forces Q_1 , Q_2 , despite the small stresses τ_{zx} , τ_{zy} , are not equal to zero, and are determined from the equilibrium equations. Similarly, one can write formulas for bending and twisting moments

$$M_1 = \int_{-\frac{h}{2}}^{\frac{h}{2}} \sigma_x z dz, \quad M_2 = \int_{-\frac{h}{2}}^{\frac{h}{2}} \sigma_y z dz, \quad M_{12} = \int_{-\frac{h}{2}}^{\frac{h}{2}} \tau_{xy} z dz. \quad (4.22)$$

For simplification of calculations instead of forces N_1 , N_2 , N_{12} it is convenient to enter their linear combinations

$$S_1 = N_1 - \frac{1}{2}N_2 = \int_{-\frac{h}{2}}^{\frac{h}{2}} S_x dz, \quad S_2 = N_2 - \frac{1}{2}N_1 = \int_{-\frac{h}{2}}^{\frac{h}{2}} S_y dz,$$

$$\frac{2}{3}S_{12} = N_{12} = \int_{-\frac{h}{2}}^{\frac{h}{2}} S_{xy} dz, \quad (4.23)$$

And instead of the moments M_1 , M_2 , M_{12} of their combination

$$H_1 = M_1 - \frac{1}{2}M_2 = \int_{-\frac{h}{2}}^{\frac{h}{2}} S_x z dz,$$

$$H_2 = M_2 - \frac{1}{2}M_1 = \int_{-\frac{h}{2}}^{\frac{h}{2}} S_y z dz, \quad (4.24)$$

$$\frac{2}{3}H_{12} = M_{12} = \int_{-\frac{h}{2}}^{\frac{h}{2}} S_{xy} z dz.$$

From (4.23) and (4.20) we have:

$$\begin{aligned}
S_1 &= \varepsilon_1 \int_{-\frac{h}{2}}^{\frac{h}{2}} \frac{\sigma_i}{e_i} dz - \chi_1 \int_{-\frac{h}{2}}^{\frac{h}{2}} \frac{\sigma_i}{e_i} z dz, \\
S_2 &= \varepsilon_2 \int_{-\frac{h}{2}}^{\frac{h}{2}} \frac{\sigma_i}{e_i} dz - \chi_2 \int_{-\frac{h}{2}}^{\frac{h}{2}} \frac{\sigma_i}{e_i} z dz, \\
S_{12} &= \varepsilon_{12} \int_{-\frac{h}{2}}^{\frac{h}{2}} \frac{\sigma_i}{e_i} dz - \chi_{12} \int_{-\frac{h}{2}}^{\frac{h}{2}} \frac{\sigma_i}{e_i} z dz,
\end{aligned} \quad (4.23')$$

And from (4.24) we have:

$$\begin{aligned}
H_1 &= \varepsilon_1 \int_{-\frac{h}{2}}^{\frac{h}{2}} \frac{\sigma_i}{e_i} z dz - \chi_1 \int_{-\frac{h}{2}}^{\frac{h}{2}} \frac{\sigma_i}{e_i} z^2 dz, \\
H_2 &= \varepsilon_2 \int_{-\frac{h}{2}}^{\frac{h}{2}} \frac{\sigma_i}{e_i} z dz - \chi_2 \int_{-\frac{h}{2}}^{\frac{h}{2}} \frac{\sigma_i}{e_i} z^2 dz, \\
H_{12} &= \varepsilon_{12} \int_{-\frac{h}{2}}^{\frac{h}{2}} \frac{\sigma_i}{e_i} z dz - \chi_{12} \int_{-\frac{h}{2}}^{\frac{h}{2}} \frac{\sigma_i}{e_i} z^2 dz.
\end{aligned} \quad (4.24')$$

In formulas (4.23') and (4.24'), there are three types of integrals that are common in shell thickness:

$$J_1 = \int_{-\frac{h}{2}}^{\frac{h}{2}} \frac{\sigma_i}{e_i} dz, \quad J_2 = \int_{-\frac{h}{2}}^{\frac{h}{2}} \frac{\sigma_i}{e_i} z dz, \quad J_3 = \int_{-\frac{h}{2}}^{\frac{h}{2}} \frac{\sigma_i}{e_i} z^2 dz. \quad (4.25)$$

Through them the forces and moments are expressed:

$$\begin{aligned}
\frac{3}{4} N_1 &= \left(\varepsilon_1 + \frac{1}{2} \varepsilon_2 \right) J_1 - \left(\chi_1 + \frac{1}{2} \chi_2 \right) J_2, \\
\frac{3}{4} N_2 &= \left(\varepsilon_2 + \frac{1}{2} \varepsilon_1 \right) J_1 - \left(\chi_2 + \frac{1}{2} \chi_1 \right) J_2, \\
\frac{3}{2} N_{12} &= \varepsilon_{12} J_1 - \chi_{12} J_2, \\
\frac{3}{4} M_1 &= \left(\varepsilon_1 + \frac{1}{2} \varepsilon_2 \right) J_2 - \left(\chi_1 + \frac{1}{2} \chi_2 \right) J_3, \\
\frac{3}{4} M_2 &= \left(\varepsilon_2 + \frac{1}{2} \varepsilon_1 \right) J_2 - \left(\chi_2 + \frac{1}{2} \chi_1 \right) J_3, \\
\frac{3}{2} M_{12} &= \varepsilon_{12} J_2 - \chi_{12} J_3.
\end{aligned} \quad (4.26)$$

Since in (4.25) σ_i there is a given function of e_i , and its form for each material becomes known in particular problems, it is natural to get rid of integration with respect to z and proceed from (4.19) to integrate over e_i .

Multiplying J_1 by P_ε , J_2 by $-2P_{\varepsilon\chi}$, J_3 by J_χ and by adding the results, we get:

$$J_1 P_\varepsilon - 2J_2 P_{\varepsilon\chi} + J_3 P_\chi = \frac{3}{4} \int_{-\frac{h}{2}}^{\frac{h}{2}} \sigma_i e_i dz. \quad (4.28)$$

Differentiating (4.19) with respect to z , we find:

$$\frac{3}{4} e_i de_i = (z P_\chi - P_{\varepsilon\chi}) dz. \quad (4.29)$$

Multiply no J_1 by $-2P_{\varepsilon\chi}$ and J_2 on P_χ and add the results, then we get:

$$-J_1 P_{\varepsilon\chi} + J_2 P_\chi = \frac{3}{4} \int \sigma_i de_i. \quad (4.30)$$

We find the expression z^2 by e_i , for this it is necessary to solve the quadratic equation (4.19)

$$z^2 P_\chi - 2zP_{\varepsilon\chi} + P_\varepsilon = \frac{3}{4}e_i^2,$$

Which root which is not contradicting a relation (4.29), is

$$z = \frac{P_{\varepsilon\chi}}{P_\chi} + \frac{\sqrt{3}}{2\sqrt{P_\chi}} \sqrt{e_i^2 - \frac{4}{3} \frac{P_\varepsilon P_\chi - P_{\varepsilon\chi}^2}{P_\chi}} \cdot \text{sign}(zP_\chi - P_{\varepsilon\chi}), \quad (4.31)$$

And it is always necessary to take a positive value of the square root. Differentiating (4.31), we obtain:

$$dz = \frac{\sqrt{3}}{2\sqrt{P_\chi}} \frac{e_i de_i \cdot \text{sign} de_i}{\sqrt{e_i^2 - \frac{4}{3} \frac{P_\varepsilon P_\chi - P_{\varepsilon\chi}^2}{P_\chi}}}. \quad (4.32)$$

The value $\text{sign } zP_\chi - P_{\varepsilon\chi}$, according to (4.29), coincides with a sign $\frac{de_i}{dz}$ and as in intervals interesting us dz always it is positive at change z

$$\text{from } -\frac{h}{2} \text{ to } +\frac{h}{2}$$

integration on de_i should be executed so that de_i too increased, i.e. it is necessary to integrate on $de_i \cdot \text{sign} de_i$.

Let's consider values of intensity of deformations in three points on an axis z :

$$z = -\frac{h}{2}, \quad z = +\frac{h}{2}, \quad z = z_0, \quad z_0 = \frac{P_{\varepsilon\chi}}{P_\chi}. \quad (4.33)$$

Let's designate them accordingly:

$$e_{i1} = \frac{2}{\sqrt{3}} \sqrt{P_\varepsilon + hP_{\varepsilon\chi} + \frac{h^2}{4}P_\chi} \quad \left(z = -\frac{h}{2} \right),$$

$$e_{i2} = \frac{2}{\sqrt{3}} \sqrt{P_\varepsilon - hP_{\varepsilon\chi} + \frac{h^2}{4}P_\chi} \quad \left(z = +\frac{h}{2} \right),$$

$$e_{i0} = \frac{2}{\sqrt{3}\sqrt{P_\chi}} \sqrt{P_\varepsilon P_\chi - P_{\varepsilon\chi}^2} \quad (z = z_0).$$

(4.34)

Apparently from (4.29), the point $z = z_0$ is a minimum point e_i . Hence, inequalities always take place

$$e_{i1} \geq e_{i0}, \quad e_{i2} \geq e_{i0}. \quad (4.34')$$

We shall say that the deformations of the stretching and the shift of the middle surface $\varepsilon_1, \varepsilon_2, \varepsilon_{12}$ are commensurable or small in comparison with deformations of the bending of the shell

$$\pm \frac{h}{2} \chi_1, \quad \pm \frac{h}{2} \chi_2, \quad \pm \frac{h}{2} \chi_{12}$$

or that the latter are dominant if the point z_0 does not exceed the thickness of the shell

$$-\frac{h}{2} \leq z_0 = \frac{P_{\varepsilon\chi}}{P_\chi} \leq \frac{h}{2}. \quad (4.35)$$

Deformations of the middle surface will be called large or dominant as compared with deformation of the bend if the point is located outside the thickness of the shell, that is, if one of the inequalities holds

$$z_0 = \frac{P_{\varepsilon\chi}}{P_\chi} > \frac{h}{2}, \quad z_0 = \frac{P_{\varepsilon\chi}}{P_\chi} < -\frac{h}{2}. \quad (4.36)$$

In case of commensurable tensile deformations and a bending, the integral from any positive

value R on a thickness of a shell is necessary for calculating under the formula:

$$\int_{-\frac{h}{2}}^{\frac{h}{2}} R dz = \frac{\sqrt{3}}{2\sqrt{P_\chi}} \left[\int_{e_{i0}}^{e_{i1}} \frac{Re_i de_i}{\sqrt{e_i^2 - e_{i0}^2}} + \int_{e_{i0}}^{e_{i2}} \frac{Re_i de_i}{\sqrt{e_i^2 - e_{i0}^2}} \right]. \quad (4.35')$$

In case of incommensurable or large tensile deformations such integral should be calculated under the formula:

$$\int_{-\frac{h}{2}}^{\frac{h}{2}} R dz = \frac{\sqrt{3} \cdot \text{sign}(e_{i2} - e_{i1})}{2\sqrt{P_\chi}} \int_{e_{i1}}^{e_{i2}} \frac{Re_i de_i}{\sqrt{e_i^2 - e_{i0}^2}}. \quad (4.36')$$

We introduce the notation of the principal quantities in the theory of shells:

$$\begin{aligned} A = A_0, \quad B = B_0, \quad C = C_0 \quad \left(-\frac{h}{2} \leq z_0 \leq \frac{h}{2} \right), \\ A = A_1, \quad B = B_1, \quad C = C_1 \quad \left(|z_0| > \frac{h}{2} \right), \end{aligned} \quad (4.37)$$

Where the values A_0, B_0, C_0 refer to the case of the dominant deformation of the bending and are equal to:

$$\begin{aligned} A_0 &= - \int_{e_{i0}}^{e_{i1}} \sigma_i de_i + \int_{e_{i0}}^{e_{i2}} \sigma_i de_i = \int_{e_{i1}}^{e_{i2}} \sigma_i de_i, \\ B_0 &= \int_{e_{i0}}^{e_{i1}} \frac{\sigma_i de_i}{\sqrt{e_i^2 - e_{i0}^2}} + \int_{e_{i0}}^{e_{i2}} \frac{\sigma_i de_i}{\sqrt{e_i^2 - e_{i0}^2}}, \\ C_0 &= \int_{e_{i0}}^{e_{i1}} \sigma_i \sqrt{e_i^2 - e_{i0}^2} de_i + \int_{e_{i0}}^{e_{i2}} \sigma_i \sqrt{e_i^2 - e_{i0}^2} de_i. \end{aligned} \quad (4.37')$$

And A_1, B_1, C_1 concern to a case of a dominating stretching of a median surface and are equal:

$$\begin{aligned} A_0 = A_1 = \int_{e_{i1}}^{e_{i2}} \sigma_i de_i, \quad B_1 = \int_{e_{i1}}^{e_{i2}} \frac{\sigma_i de_i}{\sqrt{e_i^2 - e_{i0}^2}} \cdot \text{sign}(e_{i2} - e_{i1}), \\ C_1 = \int_{e_{i1}}^{e_{i2}} \sigma_i \sqrt{e_i^2 - e_{i0}^2} de_i \cdot \text{sign}(e_{i2} - e_{i1}). \end{aligned} \quad (4.37'')$$

J_1, J_2, J_3 (4.23'), (4.24'), (4.26) and (4.27), it is possible to express the integrals J_1, J_2, J_3 entering in the formulas through the basic values A, B, C depending on the basic quadratic forms $P_\varepsilon, P_\chi, P_{\varepsilon\chi}$, according to formulas (4.37). For this purpose we notice that the integral J_1 on the basis of formulas (4.25) and (4.35')-(4.36') is directly expressed through function B then from (4.30) it is found J_2 through A and B , after from (4.28) is received J_3 through A, B, C . Thus we find following formulas:

$$\begin{aligned} J_1 &= \frac{\sqrt{3}}{2P_\chi^{\frac{1}{2}}} B, \quad J_2 = \frac{\sqrt{3}P_{\varepsilon\chi}}{2P_\chi^{\frac{3}{2}}} B + \frac{3}{4P_\chi} A, \\ J_3 &= \frac{3\sqrt{3}}{8P_\chi^{\frac{3}{2}}} C + \frac{\sqrt{3}P_{\varepsilon\chi}^2}{2P_\chi^{\frac{5}{2}}} B + \frac{3P_{\varepsilon\chi}}{2P_\chi^2} A. \end{aligned} \quad (4.38)$$

Values A, B, C need to attribute an index «0» and to calculate them under formulas (4.37') if bending strain dominates or to attribute an index «1» and to calculate according to (4.37'') if the stretching-compression of a middle surface dominates.

The formula (4.32) and all subsequent calculations lose their meaning when the momentless state is stressful, when the quantities e_i and σ_i are constant in thickness. In this case

$$P_\chi = P_{\varepsilon\chi} = 0, \quad e_i = \frac{2}{\sqrt{3}} \sqrt{P_\varepsilon}, \quad (4.39)$$

And the integrals J_1, J_2, J_3 can be calculated directly. From the formulas (4.25) we have:

$$J_1 = h \frac{\sigma_i}{e_i}, \quad J_2 = 0, \quad J_3 = \frac{h^3}{12} \frac{\sigma_i}{e_i}, \quad (4.40)$$

As equality

$$P_\chi = 0$$

is possible only at

$$\chi_1 = \chi_2 = \chi_{12} = 0$$

all bending moments are equal to zero.

The relations (4.23'), (4.24') or (4.26), (4.27) give the expressions for the forces and moments acting on the shell element through three quadratic forms $P_\varepsilon, P_\chi, P_{\varepsilon\chi}$:

$$\begin{aligned} P_\varepsilon &= \varepsilon_1^2 + \varepsilon_1 \varepsilon_2 + \varepsilon_2^2 + \varepsilon_{12}^2, \quad P_\chi = \chi_1^2 + \chi_1 \chi_2 + \chi_2^2 + \chi_{12}^2, \\ P_{\varepsilon\chi} &= \varepsilon_1 \chi_1 + \varepsilon_2 \chi_2 + \frac{1}{2} \varepsilon_1 \chi_2 + \frac{1}{2} \varepsilon_2 \chi_1 + \varepsilon_{12} \chi_{12} \end{aligned} \quad (4.43)$$

And six components of deformations and distortions $\varepsilon_1, \varepsilon_2, \varepsilon_{12}, \chi_1, \chi_2, \chi_{12}$, hence through the three components of the displacement vector of the point of the middle surface, since deformations and curvatures have differential expressions through u, v, w .

We show that all deformations and curvatures can be expressed in terms of forces and moments. To do this, we find the expressions for the quadratic forms (4.43) in terms of analogous quadratic forms of forces and moments. According to the expressions S, H , through T, M (4.23)-(4.24) we have the identities:

$$\begin{aligned} P_S &= S_1^2 + S_1 S_2 + S_2^2 + 3S_{12}^2 = \\ &= \frac{3}{4} (N_1^2 - N_1 N_2 + N_2^2 + 3N_{12}^2), \\ P_H &= H_1^2 + H_1 H_2 + H_2^2 + 3H_{12}^2 = \\ &= \frac{3}{4} (M_1^2 - M_1 M_2 + M_2^2 + 3M_{12}^2), \\ P_{SH} &= S_1 H_1 + S_2 H_2 + \frac{1}{2} S_1 H_2 + \frac{1}{2} S_2 H_1 + \\ &+ 3S_{12} H_{12} = \\ &= \frac{3}{4} \left(N_1 M_1 + N_2 M_2 - \frac{1}{2} N_1 M_2 - \frac{1}{2} N_2 M_1 + \right. \\ &\quad \left. + 3N_{12} M_{12} \right). \end{aligned} \quad (4.44)$$

We form the quadratic forms P_S, P_H, P_{SH} according to relations (4.23') and (4.24'), replacing the integrals entering them by the notation (4.25) by J_1, J_2, J_3 .

From the group of equations (4.23') we have:

$$P_S = J_1^2 P_\varepsilon - 2J_1 J_2 P_{\varepsilon\chi} + J_2^2 P_\chi. \quad (4.45')$$

Similarly, from the group of equations (4.24') we find:

$$P_H = J_2^2 P_\varepsilon - 2J_2 J_3 P_{\varepsilon\chi} + J_3^2 P_\chi. \quad (4.45'')$$

Constructing from both groups of equations (4.23'), (4.24') a bilinear form P_{SH} and collecting the coefficients of the products J_1, J_2 and J_2, J_3 , we obtain:

$$P_{SH} = J_1 J_2 P_\varepsilon - (J_1 J_3 + J_2^2) P_{\varepsilon\chi} + J_2 J_3 P_\chi. \quad (4.45''')$$

As the left parts of relation (4.45) are known functions (4.44) forces and the moments, and right depend only from $P_\varepsilon, P_\chi, P_{\varepsilon\chi}$ as J_1, J_2, J_3 are expressed under formulas (4.38), (4.37), (4.34) relation (4.45) represent three algebraic

equations from which it is possible to express forms $P_\varepsilon, P_\chi, P_{\varepsilon\chi}$ through P_S, P_H, P_{SH} :

$$\begin{aligned} P_\varepsilon &= f_1(P_S, P_H, P_{SH}), \quad P_\chi = f_2(P_S, P_H, P_{SH}), \\ P_{\varepsilon\chi} &= f_3(P_S, P_H, P_{SH}) \end{aligned} \quad (4.46)$$

Actually it can be executed after the particular characteristic of a material of a shell is given, i.e. the function kind is set $\sigma_i = \Phi(e_i)$.

Assuming that expressions (4.46) are found, we can find expressions of deformations ε, χ through forces T, M or S, H . For this purpose it is necessary to substitute (4.46) in (4.38), to express J_1, J_2, J_3 through P_S, P_H, P_{SH} and to decide the equations (4.23'), (4.24') rather ε, χ . Thus, we receive definitive formulas:

$$\begin{aligned} \varepsilon_1 &= \frac{1}{\Delta}(S_1 J_3 - H_1 J_2), \quad \chi_1 = \frac{1}{\Delta}(S_1 J_2 - H_1 J_1), \\ \varepsilon_2 &= \frac{1}{\Delta}(S_2 J_3 - H_2 J_2), \quad \chi_2 = \frac{1}{\Delta}(S_2 J_2 - H_2 J_1), \\ \varepsilon_{12} &= \frac{1}{\Delta}(S_{12} J_3 - H_{12} J_2), \quad \chi_{12} = \frac{1}{\Delta}(S_{12} J_2 - H_{12} J_1), \\ \Delta &= (J_1 J_3 - J_2^2). \end{aligned} \quad (4.47)$$

1.2. The final relationship between forces and moments and the formulation of the problem of the load-carrying capacity of shells

If intensity of deformations e_i (4.19) any layers of a shell is great enough in comparison with yield strength e_s , i.e.

$$\frac{2}{\sqrt{3}} \sqrt{P_\varepsilon - 2zP_{\varepsilon\chi} + z^2 P_\chi} = e_i \gg e_s, \quad (4.56)$$

and its material does not possess hardening the law $\sigma_i = \Phi(e_i)$ coincides with a condition of

plasticity of Mizes:

$$\sigma_i = \sigma_s = \text{const.}, \quad (4.57)$$

Or can be approximately replaced by a condition of plasticity of Sen-Venan-Kulon:

$$\tau_{\max} = \frac{\sigma_s}{\sqrt{3}} = \text{const.} \quad (4.58)$$

We show that in this case there exists a finite (not differential) relation between the forces and the moments. Using formulas (4.37), taking the integral sign as a constant σ_i , we can calculate the values of the functions A, B, C .

In the case of dominant bending deformations, the formulas (4.37') take the form:

$$\begin{aligned} A_0 &= \sigma_s (e_{i2} - e_{i1}), \\ B_0 &= \sigma_s \ln \frac{(e_{i1} + \sqrt{e_{i1}^2 - e_{i0}^2})(e_{i2} + \sqrt{e_{i2}^2 - e_{i0}^2})}{e_{i0}^2}, \\ C_0 &= \frac{\sigma_s}{2} (e_{i1} \sqrt{e_{i1}^2 - e_{i0}^2} + e_{i2} \sqrt{e_{i2}^2 - e_{i0}^2}) - \frac{1}{2} e_{i0}^2 B_0, \end{aligned} \quad (4.59')$$

and in case of dominating lengthening of a middle surface from formulas (4.37 ") it is found:

$$\begin{aligned} A_1 &= \sigma_s (e_{i2} - e_{i1}), \quad B_1 = \sigma_s \left| \ln \frac{(e_{i2} + \sqrt{e_{i2}^2 - e_{i0}^2})}{(e_{i1} + \sqrt{e_{i1}^2 - e_{i0}^2})} \right|, \\ C_1 &= \frac{\sigma_s}{2} |e_{i2} \sqrt{e_{i2}^2 - e_{i0}^2} - e_{i1} \sqrt{e_{i1}^2 - e_{i0}^2}| - \frac{e_{i0}^2}{2} B_1. \end{aligned} \quad (4.59'')$$

In both cases of value e_{i1}, e_{i2}, e_{i0} are expressed by formulas (4.34). Considering the last as the equations concerning three quadratic forms $P_\chi, P_{\varepsilon\chi}, P_\varepsilon$, we copy them in a kind:

$$P_{\varepsilon} + hP_{\varepsilon\chi} + \frac{h^2}{4}P_{\chi} = \frac{3}{4}e_{i1}^2, \quad P_{\varepsilon} - hP_{\varepsilon\chi} + \frac{h^2}{4}P_{\chi} = \frac{3}{4}e_{i2}^2,$$

$$P_{\varepsilon}P_{\chi} - P_{\varepsilon\chi}^2 = \frac{3}{4}e_{i0}^2P_{\chi}.$$

Solving them with respect to quadratic forms leads to the following results:

$$\begin{aligned} hP_{\varepsilon\chi} &= \frac{3}{8}(e_{i1}^2 - e_{i2}^2), \quad P_{\varepsilon} = \frac{3}{8}(e_{i1}^2 + e_{i2}^2) - \frac{h^2}{4}P_{\chi}, \\ \frac{h^2}{4}P_{\chi} &= \frac{3}{16}\left(\sqrt{e_{i1}^2 - e_{i0}^2} \pm \sqrt{e_{i2}^2 - e_{i0}^2}\right)^2. \end{aligned} \quad (4.60)$$

To determine the sign in the last formula, we use inequalities (4.35) and (4.36). In the case of the dominant bending strain from (4.35), we have:

$$-2 \cdot \frac{h^2}{4}P_{\chi} \leq hP_{\varepsilon\chi} \leq 2 \cdot \frac{h^2}{4}P_{\chi}.$$

This inequality will take place, if in the formula (4.60) for P_{χ} in brackets to take a sign (+). The inequality (4.36) will take place, if for P_{χ} in brackets to take a sign (-).

Below, in all formulas with two signs, the upper sign will refer to the case of the dominant bending of the shell, and the lower sign to the case of the dominant extension-compression.

We introduce two basic parameters λ and μ :

$$\lambda = \frac{e_{i2}}{e_{i1}}, \quad \mu = \frac{e_{i0}}{e_{i1}}. \quad (4.61)$$

These parameters satisfy the following conditions:

$$0 \leq \lambda \geq \mu \leq 1, \quad (4.61')$$

Since e_{i0} - is the minimum value of the strain

intensity at a given point of the shell. Then the formulas (4.60) can be rewritten in the form:

$$P_{\chi} = \frac{3e_{i1}^2}{4h^2}\Delta_1^2, \quad P_{\varepsilon\chi} = \frac{3e_{i1}^2}{8h}\Delta\Delta_1, \quad P_{\varepsilon} = \frac{3e_{i1}^2}{16}(4\mu^2 + \Delta^2), \quad (4.62)$$

where Δ_1 and Δ designate following functions:

$$\Delta_1 = \left| \sqrt{1-\mu^2} \pm \sqrt{\lambda^2-\mu^2} \right|, \quad \Delta = \frac{1-\lambda^2}{\Delta_1}. \quad (4.63)$$

The kind of the formula (4.62) for P_{ε} becomes clear if to take into consideration identity:

$$4\mu^2 + \Delta^2 = 1 + \lambda^2 + 2\mu^2 \mp 2\sqrt{(1-\mu^2)(\lambda^2-\mu^2)}.$$

Using the notation λ , μ and the established rule for applying two-valued formulas, we can rewrite the expressions for the functions A , B , C (4.59) in the form:

$$\begin{aligned} A &= \sigma_s e_{i1} \varphi(\lambda, \mu), \quad B = \sigma_s \psi(\lambda, \mu), \\ C &= \frac{\sigma_s}{2} e_{i1}^2 [\chi(\lambda, \mu) - \mu^2 \psi(\lambda, \mu)], \end{aligned} \quad (4.64)$$

Functions φ , ψ also χ are determined so:

$$\begin{aligned} \varphi &= \lambda - 1, \quad \psi = \left| \ln \frac{1 + \sqrt{1-\mu^2}}{\mu} \pm \ln \frac{\lambda + \sqrt{\lambda^2-\mu^2}}{\mu} \right|, \\ \chi &= \left| \sqrt{1-\mu^2} \pm \lambda \sqrt{\lambda^2-\mu^2} \right|. \end{aligned} \quad (4.65)$$

Using formulas (4.62) and (4.64), we can be convinced that quadratic forms P_S , P_H , P_{SH} , according to formulas (4.45) and (4.38), do not depend on value e_{i1} and are functions only parameters λ , μ .

In this connection it is natural to introduce the

notation for the characteristic value of forces N_1, N_2, N_{12} and moments M_1, M_2, M_{12} :

$$N_s = \sigma_s h, \quad M_s = \frac{\sigma_s h^2}{4}. \quad (4.66)$$

The quantities N_s, M_s in the problems of momentless deformations of shells and problems of purely moment deformations play the same role as the yield stress σ_s in the plane stress problem. Therefore, it is useful to introduce the notation for dimensionless forces and moments:

$$\begin{aligned} n_1 &= \frac{N_1}{N_s}, & n_2 &= \frac{N_2}{N_s}, & n_{12} &= \frac{N_{12}}{N_s}, \\ m_1 &= \frac{M_1}{M_s}, & m_2 &= \frac{M_2}{M_s}, & m_{12} &= \frac{M_{12}}{M_s}, \end{aligned} \quad (4.67)$$

and instead of quadratic forms (4.44), consider quadratic forms of dimensionless forces and moments:

$$\begin{aligned} Q_n &= n_1^2 - n_1 n_2 + n_2^2 + 3n_{12}^2, \\ Q_m &= m_1^2 - m_1 m_2 + m_2^2 + 3m_{12}^2, \\ Q_{nm} &= n_1 m_1 + n_2 m_2 - \frac{1}{2} n_1 m_2 - \frac{1}{2} n_2 m_1 + 3n_{12} m_{12}. \end{aligned} \quad (4.68)$$

The last are connected with P_S, P_H, P_{SH} obvious relation:

$$Q_n = \frac{4P_S}{3N_s^2}, \quad Q_m = \frac{4P_H}{3M_s^2}, \quad Q_{nm} = \frac{4P_{SH}}{3N_s M_s}. \quad (4.69)$$

Performing rather cumbersome transformations of the right-hand sides of equations (4.45), namely squaring polynomials and multiplying, and then collecting the coefficients for $\psi^2, \phi^2, \phi\psi, \chi\psi, \phi\chi, \chi^2$, we obtain the follow-

ing equations:

$$\begin{aligned} Q_n &= \frac{1}{\Delta_1^2} (\mu^2 \psi^2 + \phi^2), \\ Q_{nm} &= \frac{2}{\Delta_1^3} (\mu^2 \Delta \psi^2 + \Delta \phi^2 + \mu^2 \phi \psi + \phi \chi), \\ Q_m &= \frac{4}{\Delta_1^4} \left[\mu^2 (\mu^2 + \Delta^2) \psi^2 + (4\mu^2 + \Delta^2) \phi^2 + \right. \\ &\quad \left. + 2\mu^2 \Delta \phi \psi - 2\mu^2 \psi \chi + 2\Delta \phi \chi + \chi^2 \right]. \end{aligned} \quad (4.70')$$

Since the right-hand sides of equations (4.70'), according to (4.63) and (4.65), are functions of two parameters λ, μ , in a three-dimensional space with variables Q_n, Q_m, Q_{nm} they represent a surface

$$F(Q_n, Q_m, Q_{nm}) = 0, \quad (4.70)$$

and (4.70') is the parametric equation of this surface. The relation between the quadratic forms (4.68) obtained in this way is called the final relation between the forces and moments acting in the shells. The final relationship was obtained from the Mizes hypothesis $\sigma_i = \sigma_s$ and therefore it is a generalization of the Mizes condition. The final relation derived from the equations of the theory of small elastic-plastic deformations will have the same form, according to the theory of flow the Sen-Venan- Mizes.

Existence of a final relation between forces N and the moments M in case of ideal plasticity, i.e. under condition of Mizes and at small elastic deformations, follows and is direct from formulas (4.23') and (4.24') as thus they are uniform zero degree concerning six values $\varepsilon_1, \varepsilon_2, \varepsilon_{12}, \chi_1, \chi_2, \chi_{12}$.

The surface (4.70) represents a three-dimensional image of the indicated surface of the six-measurement space.

We pass to more in-depth study of a final relation (4.70'). We note three special cases of a final relation.

1. The momentless state of stress takes place at

$$\chi_1 = \chi_2 = \chi_{12} = 0, \text{ with } P_{\varepsilon\chi} = 0 \quad (4.68).$$

The final relation is obtained from (4.70') if we assume that the deformations of the fibers along the thickness of the shell are the same

$$e_{i1} = e_{i2} = e_{i0}, \quad \lambda = \mu = 1.$$

In formulas (4.63), (4.65), one should take the lower sign and then uncover the uncertainties in formulas (4.70'). Then we find, obviously, the Mizes condition:

$$Q_m = Q_{nm} = 0, \quad Q_n = 1, \quad (4.71')$$

Or in expanded form:

$$N_1^2 - N_1 N_2 + N_2^2 + 3N_{12}^2 = N_s^2. \quad (4.71)$$

2. *Purely moments the tension* takes place in the absence of lengthening of a middle surface. The quadratic form

$$P_\varepsilon = 0,$$

that is why

$$P_{\varepsilon\chi} = 0.$$

As appears from the formula (4.19), intensity of deformations e_i is even function z and, according to (4.34), we have

$$e_{i1} = e_{i2}, \quad e_{i0} = 0, \quad \lambda = 1, \quad \mu = 0.$$

In formulas (4.63), (4.65) it is necessary to take the upper sign as from (4.33) it is had $z_0 = 0$, thus we receive

$$\Delta_1 = 2, \quad \Delta = 0, \quad \varphi = 0, \quad \mu\psi = 0, \quad \chi = 2.$$

The final relation (4.70') becomes:

$$Q_n = Q_{nm} = 0, \quad Q_m = 1, \quad (4.72')$$

Or in expanded form:

$$M_1^2 - M_1 M_2 + M_2^2 + 3M_{12}^2 = M_s^2. \quad (4.72)$$

3. The elementary difficult tension of shells at

$$P_\chi \neq 0, \quad P_\varepsilon \neq 0$$

takes place, if the bilinear form $P_{\varepsilon\chi}$ addresses in zero:

$$P_{\varepsilon\chi} = \chi_1 \left(\varepsilon_1 + \frac{1}{2} \varepsilon_2 \right) + \chi_2 \left(\varepsilon_2 + \frac{1}{2} \varepsilon_1 \right) + \chi_{12} \varepsilon_{12} = 0. \quad (4.73)$$

It can take place in cases

$$\begin{aligned} a) \quad & \chi_1 \neq 0, \quad \chi_{12} = \chi_2 = 0, \quad \varepsilon_1 + \frac{1}{2} \varepsilon_2 = 0, \\ b) \quad & \varepsilon_1 \neq 0, \quad \varepsilon_{12} = \varepsilon_2 = 0, \quad \chi_1 + \frac{1}{2} \chi_2 = 0 \end{aligned}$$

And many other things. From (4.60) it is thus had $e_{i1} = e_{i2} > e_{i0}$, $\lambda = 1$, $\mu < 1$, i.e. dominating bending strain is available. We find:

$$\begin{aligned} \Delta = \varphi = 0, \quad \Delta_1 = \chi = 2\sqrt{1-\mu^2}, \\ \psi = 2 \ln \frac{1+\sqrt{1-\mu^2}}{\mu}, \end{aligned}$$

and after simple transformations the final relation becomes:

$$Q_n = \frac{\mu^2}{1-\mu^2} \ln^2 \frac{1+\sqrt{1-\mu^2}}{\mu}, \quad Q_{nm} = 0, \\ Q_m = \left(\frac{\mu^2}{1-\mu^2} \ln \frac{1+\sqrt{1-\mu^2}}{\mu} - \frac{1}{\sqrt{1-\mu^2}} \right)^2. \quad (4.74)$$

It gives a line of interception of a surface (4.70) with a plane $Q_{nm} = 0$. As Q_n , Q_m are essentially positive, all surface is disposed between planes

$$Q_n = 0 \text{ and } Q_m = 0,$$

and a line (4.74) between positive directions of axes Q_n , Q_m , i.e. in the first quadrant of a plane

$$Q_{nm} = 0.$$

The point

$$Q_m = 0, \quad Q_n = 1$$

corresponding to a non-propulsive condition of a shell, is received from (4.74) at $\mu = 1$, and the point

$$Q_n = 0, \quad Q_m = 1$$

corresponding purely moment to a condition of a shell, is received at

$$\mu = 0, \text{ as } \mu \ln \mu = 0 \text{ at } \mu = 0.$$

The curve Q_n , Q_m can be constructed on the points which coordinates are introduced in table 4 [9] (the expanded version of the table it is resulted in 2 parts of the article). On Figure 53 [9] coordinates (it is resulted in 2 parts of the article) the curve (4.74) and a straight line is represented

$$Q_n + Q_m = 1, \quad (4.75)$$

which well enough approximates it. The maxi-

mum deviation of a straight line makes about 9 %. The surface (4.70) is symmetric concerning a plane

$$Q_{nm} = 0.$$

Thus, it is enough to know about a surface (4.70), only in the first octant of co-ordinate system Q_n , Q_m , Q_{nm} . It is possible to be convinced that on a line $\lambda = 1$ in a value plane (Q_n, Q_m) Q_n , Q_m have a maximum. If to use Schwarz's inequality concerning quadratic forms Q_n , Q_m , Q_{nm} $Q_{nm}^2 \leq Q_n \cdot Q_m$, it is possible to conclude that the value Q_{nm} on the module also is limited.

Table 5 [9] (the expanded version of the table is resulted in 2 parts of the article) gives coordinates of some points of a surface on lines $\lambda = const$, and against each value λ are given: in the first line - Q_n in the second - Q_m and in the third - Q_{nm} .

The greatest values Q_{nm} will be, when Schwarz's inequality is transformed into equality

$$Q_{nm}^2 = Q_n \cdot Q_m, \quad (4.77)$$

and it is possible only when values n and m are proportional:

$$\frac{n_1}{m_1} = \frac{n_2}{m_2} = \frac{n_{12}}{m_{12}}. \quad (4.77')$$

Let's show that the hyperbolic paraboloid (4.77) is crossed with a surface (4.70) on a line $\mu = 0$.

From (4.65) at $\mu = 0$ it is had:

$$\varphi = \lambda - 1, \quad \chi = 1 \pm \lambda^2, \quad \mu\psi = 0, \\ \Delta_1 = 1 \pm \lambda, \quad \Delta = \frac{1 - \lambda^2}{1 \pm \lambda}. \quad (4.77'')$$

Introducing these values to the equations (4.70), we receive:

$$Q_n = \frac{\varphi^2}{\Delta_1^2}, \quad Q_{nm} = \frac{2\varphi}{\Delta_1^3}(\Delta\varphi + \chi), \quad Q_m = \frac{4}{\Delta_1^4}(\Delta\varphi + \chi)^2. \quad (4.78)$$

From here in case of a dominating stretching of a shell at the lower sign in (4.77 ") it is had:

$$Q_n = 1, \quad Q_{nm} = Q_m = 0,$$

I.e. the line $\mu = 0$ degenerates in a point.

In case of a dominating bending of a shell it is received:

$$Q_n = \left(\frac{1-\lambda}{1+\lambda}\right)^2, \quad Q_{nm} = -\frac{4\lambda(1-\lambda)}{(1+\lambda)^3}, \quad Q_m = \frac{16\lambda^2}{(1+\lambda)^4}, \quad (4.79')$$

whence follows (4.77). Besides, from last equations it is found other relation

$$Q_m = (1 - Q_n)^2, \quad (4.79)$$

Combining it with (4.77), we find:

$$|Q_{nm}| = (1 - Q_n)\sqrt{Q_n}. \quad (4.80)$$

From here we conclude that the line $\mu = 0$ determining greatest on the module of value of the bilinear form Q_{nm} , represents a line of interception of two parabolic cylinders from which the cylinder (4.79) passes through points:

$$\begin{aligned} Q_n = 1, \quad Q_m = 0, \quad Q_{nm} = 0, \\ Q_n = 0, \quad Q_m = 1, \quad Q_{nm} = 0, \end{aligned}$$

Having forming, parallel to co-ordinate Q_{nm} , the cylinder (4.80) has forming, parallel to co-ordinate Q_m , and passes through the same

points. The line $\mu = 0$ limiting a piece of a surface (4.70) for dominating bending on which values Q_n , Q_{nm} , Q_m have mechanical sense, is shown on fig. 54 (it is resulted in 2 parts of the article).

The maximum value of ordinate Q_{nm} on the module will be at

$$Q_n = \frac{1}{3}, \quad Q_m = \frac{4}{9}$$

and

$$|Q_{nm}|_{\max} = \frac{2}{3\sqrt{3}}.$$

The final relation between forces and the moments in case of a dominating bending matters

$$|Q_{nm}|_{\max} = \frac{2}{3\sqrt{3}}.$$

can be approximately presented, as pair of the planes passing through a line (4.75) and through points

$$Q_n = \frac{1}{3}, \quad Q_m = \frac{4}{9}, \quad Q_{nm} = \pm \frac{2}{3\sqrt{3}}.$$

They have the equation:

$$Q_n + Q_m + \frac{1}{\sqrt{3}}|Q_{nm}| = 1. \quad (4.81)$$

As six components of deformations and bendings are expressed by means of differential operations on curvilinear coordinates through three components of a displacement vector u , v , w of a middle surface, they should satisfy to the equations of compatibility of deformations.

Generally it is possible to express the compatibility equations through forces N and the moments M , but they will contain one more func-

tion of coordinates e_{i1} . The differential equations of equilibrium and conditions of compatibility of deformations will be insufficiently for definition of forces N_1, N_2, N_{12} , the moments M_1, M_2, M_{12} and unknown function e_{i1} .

The final relation (4.70') between forces and the moments will be the missing equation also. In a kind of that this relation not differential and from it follows that forces and the moments and their quadratic forms Q_n, Q_m, Q_{nm} are limited on value, at any external forces equilibrium of a shell is impossible.

As lift capability of a shell is called limiting value of external forces at which internal forces N and the moments M satisfy to a final relation (4.70'), to the equilibrium equations, conditions of compatibility of deformations and boundary conditions.

In special cases thanks to a final relation the problem about equilibrium becomes statically definable and does not demand conditions of compatibility of deformations. Then the question on lift capability of a shell is decided rather simply.

It more becomes simpler, if forces and the moments can be expressed through external forces only by means of the equilibrium equations that takes place, for example, in the non-propulsive theory of shells, in that case the final relation (4.70') determines lift capability.

Conditions of compatibility of deformations do a problem about definition of lift capability rather difficult and consequently the approximate methods of its solution have great value.

The energy method of the solution consists in the following: are set by the suitable form of the deformed surface of shells and, making expressions of a variation of activity of internal forces and activity of external forces on variations of movings, compare them. Approximate limiting value of external forces can be received, if material hardening to put equal to zero, and deformations beyond all bounds to increase or saving constants yield strength

$$\sigma_s = 3Ge_s,$$

G to aim to infinity, and e_s - to zero.

On Figures 2.1-2.4 the fluidity surface

$$F(Q_n, Q_m, Q_{nm}) = 0$$

in three-dimensional space with variables is presented Q_n, Q_m, Q_{nm} . A black line – section of a surface a plane

$$Q_{nm} = 0,$$

formulas (4.74), a red line - a line of a maximum $|Q_{nm}|$ (4.79)-4.80).

1.3. The relationship between internal forces, moments and deformations of the shell on the basis of flow theory for an ideal plastic material

We show that the relations (4.26-4.27) remain valid also in the framework of the flow theory. Specific power dissipation of energy per unit volume:

$$D = \sigma_x \dot{\epsilon}_x + \sigma_y \dot{\epsilon}_y + \sigma_z \dot{\epsilon}_z + \tau_{xy} \dot{\gamma}_{xy} + \tau_{zx} \dot{\gamma}_{zx} + \tau_{zy} \dot{\gamma}_{zy}. \quad (1.3.1)$$

The plasticity condition of R. Mizes:

$$F = (\sigma_x - \sigma_y)^2 + (\sigma_x - \sigma_z)^2 + (\sigma_y - \sigma_z)^2 + 6(\tau_{xy}^2 + \tau_{zx}^2 + \tau_{zy}^2) - 2\sigma_s^2. \quad (1.3.2)$$

On the basis of the associate law of flow and a postulate of Druker for true fields of speeds of movings power of a dissipation of energy receives the maximum value, speeds of deformations are determined from a condition of a maximum of function

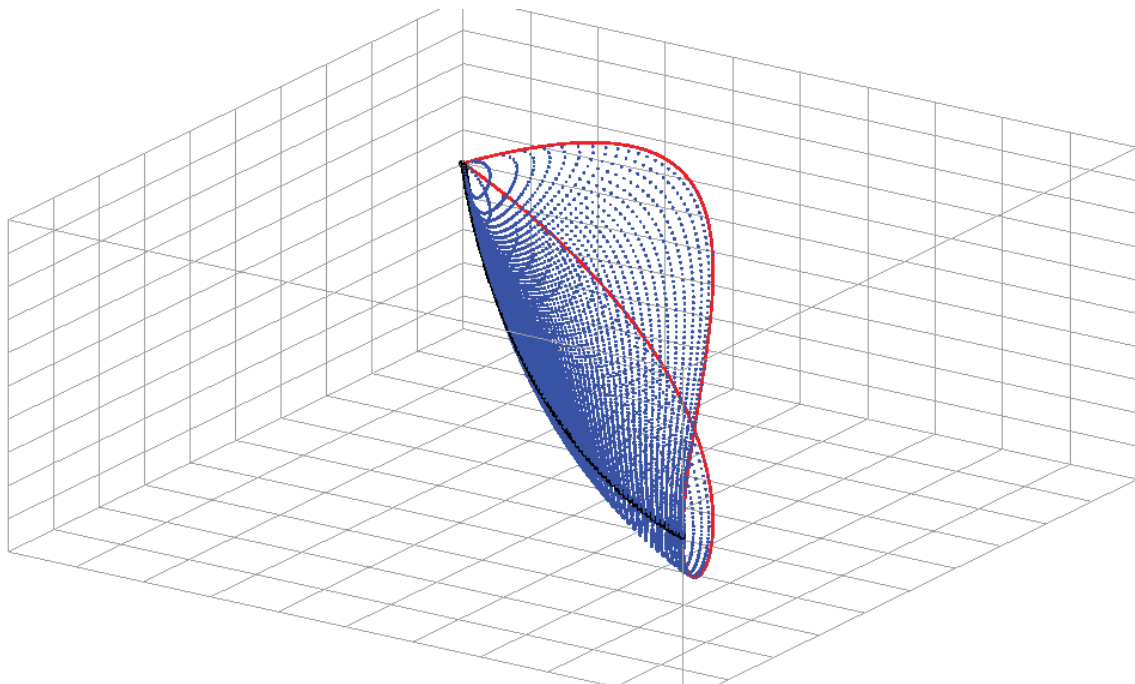


Figure 2.1. A fluidity surface $F(Q_n, Q_m, Q_{nm}) = 0$ in three-dimensional space with variables Q_n, Q_m, Q_{nm} .

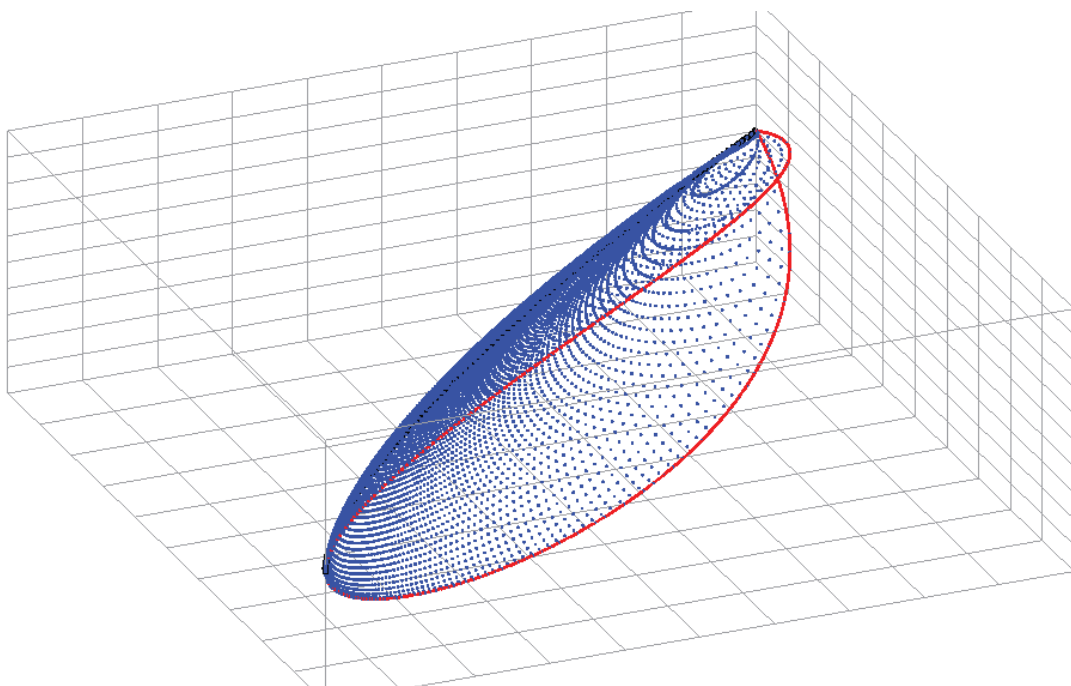


Figure 2.2. A fluidity surface $F(Q_n, Q_m, Q_{nm}) = 0$ in three-dimensional space with variables Q_n, Q_m, Q_{nm} .

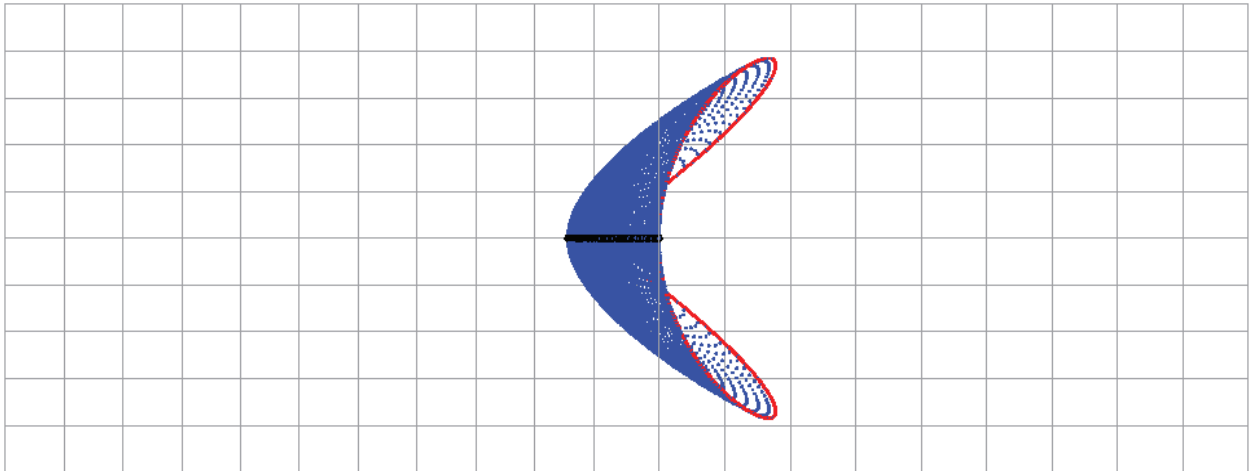


Figure 2.3. A fluidity surface $F(Q_n, Q_m, Q_{nm}) = 0$ in three-dimensional space with variables Q_n, Q_m, Q_{nm} .

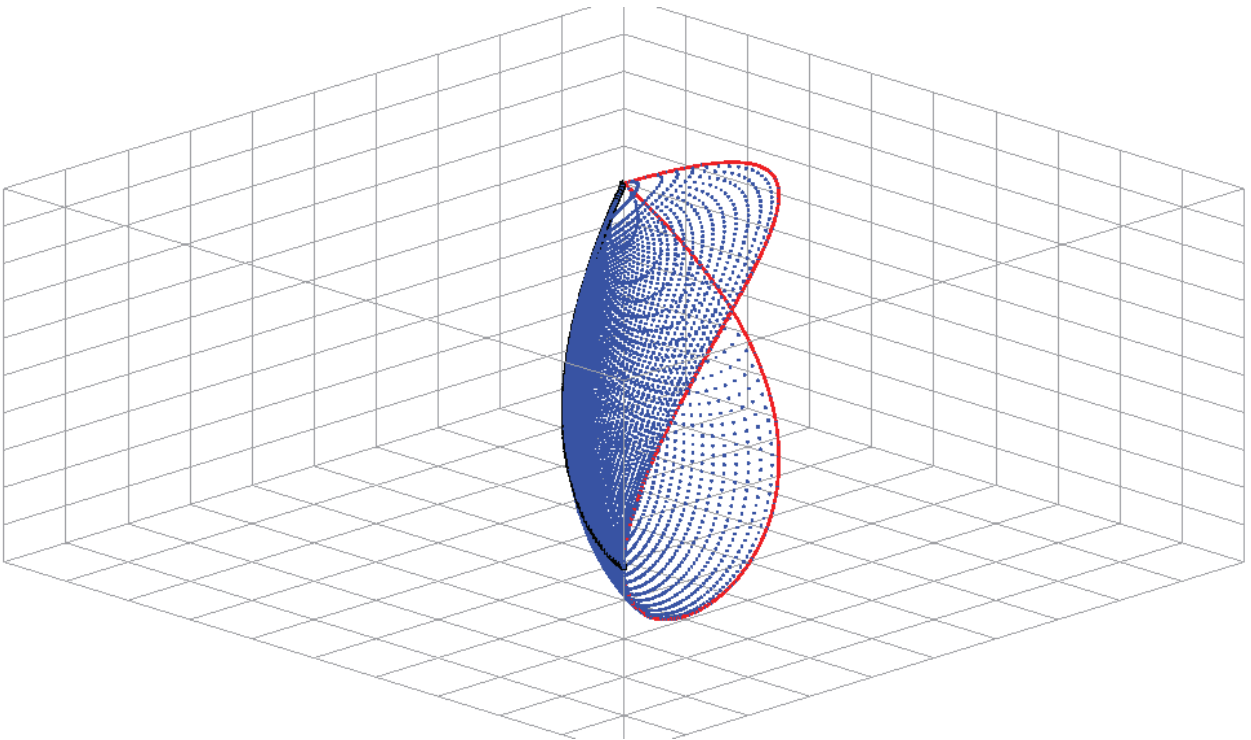


Figure 2.4. A fluidity surface $F(Q_n, Q_m, Q_{nm}) = 0$ in three-dimensional space with variables Q_n, Q_m, Q_{nm} .

$$\Phi = D - \lambda F,$$

where D and F according to (1.3.1)-(1.3.2):

$$\begin{aligned}\dot{\varepsilon}_x &= 6\lambda(\sigma_x - \sigma_0), \quad \dot{\varepsilon}_y = 6\lambda(\sigma_y - \sigma_0), \\ \dot{\varepsilon}_z &= 6\lambda(\sigma_z - \sigma_0), \quad \frac{1}{2}\dot{\gamma}_{xy} = 6\lambda\tau_{xy}, \quad \frac{1}{2}\dot{\gamma}_{xz} = 6\lambda\tau_{xz}, \\ \frac{1}{2}\dot{\gamma}_{zy} &= 6\lambda\tau_{zy}, \quad \sigma_0 = \frac{\sigma_x + \sigma_y + \sigma_z}{3}.\end{aligned}\quad (1.3.3)$$

Excluding λ by means of (1.3.2), we receive relation of flow of Sen-Venan-Mizes-Levi-Ishlinsky

$$\begin{aligned}\sigma_x - \sigma_0 &= \frac{2\sigma_s}{3\dot{\varepsilon}_i} \cdot \dot{\varepsilon}_x, \quad \sigma_y - \sigma_0 = \frac{2\sigma_s}{3\dot{\varepsilon}_i} \cdot \dot{\varepsilon}_y, \\ \sigma_z - \sigma_0 &= \frac{2\sigma_s}{3\dot{\varepsilon}_i} \cdot \dot{\varepsilon}_z, \quad \tau_{xy} = \frac{2\sigma_s}{3\dot{\varepsilon}_i} \cdot \frac{1}{2}\dot{\gamma}_{xy}, \\ \tau_{zx} &= \frac{2\sigma_s}{3\dot{\varepsilon}_i} \cdot \frac{1}{2}\dot{\gamma}_{zx}, \quad \tau_{zy} = \frac{2\sigma_s}{3\dot{\varepsilon}_i} \cdot \frac{1}{2}\dot{\gamma}_{zy},\end{aligned}\quad (1.3.4)$$

where intensity of speeds of deformations

$$\dot{\varepsilon}_i = \frac{\sqrt{2}}{3} \sqrt{(\dot{\varepsilon}_x - \dot{\varepsilon}_y)^2 + (\dot{\varepsilon}_x - \dot{\varepsilon}_z)^2 + (\dot{\varepsilon}_y - \dot{\varepsilon}_z)^2 + \frac{6}{4}(\dot{\gamma}_{xy}^2 + \dot{\gamma}_{zx}^2 + \dot{\gamma}_{zy}^2)}.\quad (1.3.5)$$

For a flat tension and problems of a bending of plates and shells it agree hypotheses of Kirhgof-fa-Ljava

$$\sigma_z = 0, \quad \tau_{zx} = \tau_{zy} = 0$$

and a condition of an incompressibility of a material

$$\dot{\varepsilon}_x + \dot{\varepsilon}_y + \dot{\varepsilon}_z = 0:$$

$$\dot{\varepsilon}_x = \dot{\varepsilon}_1 - \dot{\chi}_1 z, \quad \dot{\varepsilon}_y = \dot{\varepsilon}_2 - \dot{\chi}_2 z, \quad \frac{1}{2}\dot{\gamma}_{xy} = \dot{\varepsilon}_{12} - \dot{\chi}_{12} z,$$

$$\dot{\varepsilon}_1 = \dot{\varepsilon}_x|_{z=0}, \quad \dot{\varepsilon}_2 = \dot{\varepsilon}_y|_{z=0}, \quad \dot{\varepsilon}_{12} = \frac{1}{2}\dot{\gamma}_{xy}|_{z=0},\quad (1.3.6)$$

The equations (1.3.4) and (1.3.5) taking into account (1.3.5) become

$$\begin{aligned}\sigma_x &= \frac{4\sigma_s}{3\dot{\varepsilon}_i} \left(\dot{\varepsilon}_x + \frac{1}{2}\dot{\varepsilon}_y \right) = \\ &= \frac{4\sigma_s}{3\dot{\varepsilon}_i} \left[\left(\dot{\varepsilon}_1 + \frac{1}{2}\dot{\varepsilon}_2 \right) - \left(\dot{\chi}_1 + \frac{1}{2}\dot{\chi}_2 \right) z \right], \\ \sigma_y &= \sigma_x = \frac{4\sigma_s}{3\dot{\varepsilon}_i} \left(\dot{\varepsilon}_y + \frac{1}{2}\dot{\varepsilon}_x \right) =\end{aligned}\quad (1.3.7)$$

$$\begin{aligned}&= \frac{4\sigma_s}{3\dot{\varepsilon}_i} \left[\left(\dot{\varepsilon}_2 + \frac{1}{2}\dot{\varepsilon}_1 \right) - \left(\dot{\chi}_2 + \frac{1}{2}\dot{\chi}_1 \right) z \right], \\ \tau_{xy} &= \frac{2\sigma_s}{3\dot{\varepsilon}_i} \cdot \frac{1}{2}\dot{\gamma}_{xy} = (\dot{\varepsilon}_{12} - \dot{\chi}_{12} z), \\ \dot{\varepsilon}_i &= \frac{2}{\sqrt{3}} \sqrt{\dot{\varepsilon}_x^2 + \dot{\varepsilon}_x \dot{\varepsilon}_y + \dot{\varepsilon}_y^2 + \frac{1}{4}\dot{\gamma}_{xy}^2}.\end{aligned}\quad (1.3.8)$$

Longitudinal and shearing forces, bending and twisting moments according to (4.21)-(4.22)

$$\begin{aligned}\frac{3}{4}N_1 &= \left(\dot{\varepsilon}_1 + \frac{1}{2}\dot{\varepsilon}_2 \right) J_1 - \left(\dot{\chi}_1 + \frac{1}{2}\dot{\chi}_2 \right) J_2, \\ \frac{3}{4}N_2 &= \left(\dot{\varepsilon}_2 + \frac{1}{2}\dot{\varepsilon}_1 \right) J_1 - \left(\dot{\chi}_2 + \frac{1}{2}\dot{\chi}_1 \right) J_2,\end{aligned}\quad (1.3.9)$$

$$\begin{aligned}\frac{3}{2}N_{12} &= \dot{\varepsilon}_{12} J_1 - \dot{\chi}_{12} J_2, \\ \frac{3}{4}M_1 &= \left(\dot{\varepsilon}_1 + \frac{1}{2}\dot{\varepsilon}_2 \right) J_2 - \left(\dot{\chi}_1 + \frac{1}{2}\dot{\chi}_2 \right) J_3, \\ \frac{3}{4}M_2 &= \left(\dot{\varepsilon}_2 + \frac{1}{2}\dot{\varepsilon}_1 \right) J_2 - \left(\dot{\chi}_2 + \frac{1}{2}\dot{\chi}_1 \right) J_3,\end{aligned}\quad (1.3.10)$$

$$\frac{3}{2}M_{12} = \dot{\varepsilon}_{12} J_2 - \dot{\chi}_{12} J_3,$$

where integrals J_1, J_2, J_3 :

$$J_1 = \int_{-\frac{h}{2}}^{\frac{h}{2}} \frac{\sigma_s}{\dot{e}_i} dz, \quad J_2 = \int_{-\frac{h}{2}}^{\frac{h}{2}} \frac{\sigma_s}{\dot{e}_i} z dz, \quad J_3 = \int_{-\frac{h}{2}}^{\frac{h}{2}} \frac{\sigma_s}{\dot{e}_i} z^2 dz, \quad (1.3.11)$$

and intensity of speeds of deformations:

$$\begin{aligned} \dot{e}_i &= \frac{2}{\sqrt{3}} \sqrt{\dot{P}_\varepsilon - 2z\dot{P}_{\varepsilon\chi} + z^2\dot{P}_\chi}, \\ \dot{P}_\varepsilon &= \dot{\varepsilon}_1^2 + \dot{\varepsilon}_1\dot{\varepsilon}_2 + \dot{\varepsilon}_2^2 + \dot{\varepsilon}_{12}^2, \quad \dot{P}_\chi = \dot{\chi}_1^2 + \dot{\chi}_1\dot{\chi}_2 + \dot{\chi}_2^2 + \dot{\chi}_{12}^2, \\ \dot{P}_{\varepsilon\chi} &= \dot{\varepsilon}_1\dot{\chi}_1 + \dot{\varepsilon}_2\dot{\chi}_2 + \frac{1}{2}\dot{\varepsilon}_1\dot{\chi}_2 + \frac{1}{2}\dot{\varepsilon}_2\dot{\chi}_1 + \dot{\varepsilon}_{11}\dot{\chi}_{12}. \end{aligned} \quad (1.3.12)$$

Thus the final relation remains fair and within the limits of the flow theory if in all formulas of sections 1.1-1.2 to replace deformations $\varepsilon_1, \varepsilon_2, \varepsilon_{12}$ and changes of curvature of a median surface $\chi_1, \chi_2, \chi_{12}$ with speeds of deformations $\dot{\varepsilon}_1, \dot{\varepsilon}_2, \dot{\varepsilon}_{12}$ and speed of change of curvature of a median surface $\dot{\chi}_1, \dot{\chi}_2, \dot{\chi}_{12}$. For the hardening account in formulas it is necessary to consider (1.3.11) yield strength as function of intensity of deformations and intensity of speeds of deformations $\sigma_s = \sigma_s(e_i, \dot{e}_i)$.

CONCLUSIONS

The geometrical image of an exact surface of fluidity in space of the generalised pressure which A.A. Ilyushin in the works and in references is absent that allows to execute its approximation for the solution of practical problems is received. It is shown that a final relation remain fair and within the limits of the theory of flow for ideally plastic material.

REFERENCES

1. **Kijko I.A., Brovko G.L., Vasin R.A.** (Eds.) K 100-letiju so dnja rozhdenija A.A. Il'ju-shina (20.01.1911-31.05.1998) // Up-rugost' i neuprugost' [To the 100 anniversary from the date of A.A. Ilyushin's birth (20.01.1911-31.05.1998) Elasticity and inelasticity]. // Materials of the International scientific symposium on problems of mechanics of the deformable bodies, devoted to the 100 anniversary from the date of A.A. Ilyushin's birth. Moscow, Publishing house of the Moscow university, 2011, pp. 9-12 (in Russian).
2. Aleksej Antonovich Il'jushin: k 100-letiju so dnja rozhdenija [Alexey Antonovich Ilyushin: to the 100 anniversary from the date of a birth]. // *Bulletin of the Tyumen state university. Physical and mathematical modelling. Oil, gas, power*, 2010, No. 6, pp. 198-203 (in Russian).
3. K 100-letiju so dnja rozhdenija A.A. Il'jushina [To the 100 anniversary from the date of A.A. Ilyushin's birth]. // *News of the Russian Academy of Sciences. Mechanics of a firm body*, 2011, No. 1, pp. 3-4 (in Russian).
4. K 100-letiju so dnja rozhdenija Alekseja Antonovicha Il'jushina (20.01.1911-31.05.1998) [To the 100 anniversary from the date of Alexey Antonovich Ilyushin's birth (20.01.1911-31.05.1998)]. // *The Bulletin of the Moscow university. Series 1: Mathematics. Mechanics*, 2011, No. 1, pp. 77-79 (in Russian).
5. **Ilyushina E.A.** Nadjozhnost' v nauke i zhizni (k 95-letiju so dnja rozhdenija A.A. Il'jushina) [Reliability in a science and life (to the 95 anniversary from the date of A.A. Ilyushin's birth)]. // *News of the Russian Academy of Sciences. Mechanics of a firm body*, 2005, No. 6, pp. 3 (in Russian).
6. **Brovko G.L., Bykov D.L., Vasin R.A., Georgievsky D.V., Kijko I.A., Molodsov I.N., Pobedrja B.E.** Nauchnoe nasledie

- A.A. Il'yushina i razvitie ego idej v mehanike [A.A.Ilyushin's scientific heritage and development of its ideas in the mechanic]. // *News of the Russian Academy of Sciences. Mechanics of a firm body*, 2011, No. 1, pp. 5-18 (in Russian).
7. **Kadymov V.A., Nutsbidze D.V.** Tvorcheskoe nasledie professora A.A. Il'yushina i ego vklad v pobedu v Velikoj Otechestvennoj vojne [The Creative heritage of professor A.A.Ilyushin and its contribution to a victory in the Great Patriotic War]. // *Human. Society. Inclusion*, 2015, No. 2(22), pp. 10-13 (in Russian).
 8. **Bondar V.S., Vasin R.A., Kijko I.A.** Shkola-seminar "A.A. Il'yushin - vydajushhij mehanik sovremennosti" v MGTU "MAMI" [School-seminar "A.A.Ilyushin - the outstanding mechanic of the present" in MGTU "MAMI"]. // *Problems of engineering and automation*, 2011, No. 3, pp. 136-139 (in Russian).
 9. **Ilyushin A.A.** Plastichnost'. Chast' pervaja. Uprugo-plasticheskie deformacii [Plasticity. Part 1. Elasto-plastic deformations]. Moscow, Gostehizdat, 1948, 376 pages (in Russian).
 10. **Ilyushin A.A., Shemjakina E.I., Kijko I.A., Vasin R.A.** Plastichnost'. Chast' 1. Uprugo-plasticheskie deformacii [Plasticity. Part 1. Elasto-plastic deformations]. Moscow, Publishing house Logos, Moscow, 2004, 388 pages (in Russian).
 11. **Ilyushin A.A.** Trudy. T. 1 (1935-1945) [Works. P.1 (1935-1945)] / Composers: E.A. Ilyushin, N.R. Korotkina. Moscow, Publishing house of the physical and mathematical literature, 2003, 352 pages (in Russian).
 12. **Ilyushin A.A.** Trudy (1946-1966) Chast' 2 Plastichnost' [Works (1946-1966). P.2. Plasticity] / Composers E.A. Ilyushin, M.R. Korotkina. Moscow Publishing house of the physical and mathematical literature, 2004, 480 pages (in Russian).
 13. **Ilyushin A.A.** Konechnoe sootnoshenie mezhdur silami i momentami i ih svyazi s deformacijami v teorii obolochek [Final a ratio between forces and the moments and their communications with deformations in the theory of shells]. // *Applied mathematics and mechanics*, 1945, No. 1, pp. 101-110 (in Russian).
 14. **Ilyushin A.A.** Priblizhennaja teorija uprugoplasticheskikh deformacij osesimmetrichnykh obolochek [Approach the theory of elasto-plastic deformations of axisymmetrical shells]. // *Applied mathematics and mechanics*, 1944, No. 8, pp. 15-24 (in Russian).
 15. **Olshak V., Savchuk A.** Neuprugoe povedenie obolochek [Not Elastic behaviour of shells]. Moscow, Mir, 1969, 144 pages (in Russian).
 16. **Olshak V., Mruz Z., Pezhina P.** Sovremennoe sostojanie teorii plastichnosti [The current state of the theory of plasticity]. Moscow, Mir, 1964, 243 pages (in Russian).
 17. **Rozhdestvensky V.V.** K voprosu o predel'nykh sostojanijah sechenij tonkih obolochek [To a question on limiting conditions of sections of the thin shells]. // *Researches concerning the building mechanics and the plasticity theory*, Moscow, 1956, pp. 223-233 (in Russian).
 18. **Shapiro G.S.** O poverhnostjah tekuchestv dlja ideal'no plasticheskikh obolochek [About surfaces of fluidity for ideally plastic shells]. // *Continuum Problems, to the 70 anniversary of academician N.I. Muskhelishvili*. Moscow, Publishing house AN of the USSR, 1961, pp. 504-507 (in Russian).
 19. **Hodge P.G.** Yield conditions for rotationally symmetric shells under axisymmetric loading. // *J. Appl. Mech.*, 1960, No. 2, 27, pp. 323-331.
 20. **Hodge P.G.** The Mises yield conditions for rotationally symmetric shells. // *Quart. Appl. Math.*, 1961, Vol. 18, pp. 305-311.
 21. **Hodge P.G.** A comparison of yield conditions in the theory of plastic shells. // *Prob-*

- lems in continuum mechanics*, SIAM, Philadelphia, 1961, pp. 165-177.
22. **Hodge P.G.** The theory of rotationally symmetric plastic shells. // *Non-classical shell problems*. Amsterdam, North-Holland Publishing Company, 1964, pp. 621-648.
 23. **Drucker D.C., Hopkins H.G.** Combined Concentrated and Distributed Load on Ideally – Plastic Circular Plates. // *Proc. 2nd U.S. Nat. Cong. App. Mech.*, 1954, pp. 517-520 (in Russian).
 24. **Drucker D.C.** Plastic design methods - advantages and limitations. // *Trans. Soc. Nav., Eng.*, 1957, Vol. 65, pp. 172-196.
 25. **Drucker D.C., Shield R.T.** Limit analysis of symmetrically loaded thin shells of revolution. // *Appl. Mech.*, 1959, Vol. 26, pp. 61-68.
 26. **Onat E.T.** The plastic collapse of cylindrical shells under axially symmetrical loading. // *Quart. Appl. Math.*, 1955, Vol. 13, pp. 68-72.
 27. **Onat E.T., Prager W.** Limit analysis of shells of revolution. // *Proc. Ned. Akad. Wetensch.*, 1954, Vol. 57, Ser. B, pp. 534-548.
 28. **Onat E.T.** Plastic shells, Non-classical shell problems. // Amsterdam, North-Holland Publishing Company, 1967, pp. 649-659.
 29. **Jones N.** Plasticity Methods in Protection and Safety of Industrial Plant and Structural Systems Against Extreme Dynamic Loading. // *Defence Science Journal*, 2008, Vol. 58, No. 2, pp. 181-193.
 30. **Jones N.** Structural impact. United Kingdom, Cambridge University Press, 2003, 591 pages.
 31. **Nemirovsky JU.V., Romanova T.P.** Dinamicheskoe soprotivlenie ploskih plasticheskikh pregrad [Dynamic resistance of flat plastic barriers]. Novosibirsk, Publishing house Geo, 2009, 312 pages (in Russian).
 32. **Erhov M.I.** Teorija ideal'no plasticheskikh tel i konstrukcij [The theory of ideally plastic bodies and designs]. Moscow, The Science, 1978, 352 pages (in Russian).
 33. **Erhov M.I.** Konechnoe sootnoshenie mezhdu silami i momentami pri plasticheskoy deformacii obolochek [Between forces and the moments at plastic deformation of shells]. // *The building mechanics and calculation of facilities*, 1959, No. 3, pp. 38-41 (in Russian).
 34. **Rozenbljum V.I.** Ob uslovii plastichnosti dlja tonkostennyh obolochek [About a condition of plasticity for thin-walled shells]. // *Applied mathematics and mechanics*, 1960, Vol. 24, pp. 364-366 (in Russian).
 35. **Rozenbljum V.I.** O polnoj sisteme uravnenij plasticheskogo ravnovesija tonkostennyh obolochek [About full system of the equations of plastic equilibrium of thin-walled shells]. // *The engineering Magazine. Mechanics of a solid body*, 1966, No. 3, pp. 483-492.
 36. **Rozenbljum V.I.** O raschete nesushhej sposobnosti ideal'no plasticheskikh osesimmetrichnyh obolochek [About calculation of lift capability of ideally plastic axisymmetrical shells]. // *Questions of the theory of elasticity and plasticity*. Leningrad, Publishing house of the Leningrad state university, 1965, pp. 67-75 (in Russian).
 37. **Rozenbljum V.I.** O raschete nesushhej sposobnosti ideal'no plasticheskikh osesimmetrichnyh obolochek [About calculation of lift capability of ideally plastic axisymmetrical shells]. // *Researches on elasticity and plasticity*. Leningrad, Publishing house of the Leningrad state university, 1965, pp. 207-218 (in Russian).
 38. **Rozenbljum V.I.** Priblizhennaja teorija ravnovesija plasticheskikh obolochek [The approximate theory of equilibrium of plastic shells]. // *Applied mathematics and mechanics*, 1954, Volume 18, 3, pp. 289-302 (in Russian).
 39. **Rabotnov JU.N.** Priblizhennaja tehnickeskaja teorija uprugoplasticheskikh ob-

- olochek [Approach the technical theory of elastic and plastic shells]. // *Applied mathematics and mechanics*, 1951, Volume 15, Issue 2, pp. 167-174 (in Russian).
40. **Birger I.A., Panovko J.G.** (Eds.) Prochnost', ustojchivost', kolebanija. Spravochnik v treh tomah. Tom 2 [Strength, stability, oscillations. A directory in three volumes. Volume 2]. Moscow, Engineering, 1968. 463 pages (in Russian).
 41. **Korolev V.I.** Uprugo-plasticheskie deformacii obolochek [Elasto-plastic deformations of shells]. Moscow, Engineering, 1971, 304 pages.
 42. **Ogibalov P.M.** Voprosy dinamiki i ustojchivosti obolochek [Questions of dynamics and stability of shells]. Moscow, Publishing house of the Moscow university, 1963, 420 pages.
 43. **Dvajt G.B.** Tablicy integralov i drugie matematicheskie formuly [Tables of integrals and other mathematical formulas]. Moscow, Science, 1966, 228 pages (in Russian).
 44. **Vygodsky M.Ja.** Spravochnik po vysshej matematike [The Directory on higher mathematics]. Moscow, Science, 1977, 872 pages (in Russian).
 45. **Starov A.V.** Polnaja sistema uravnenij dinamicheskogo udarnogo nagruzhenija zhestkoplasticheskih pologih obolochek vrashhenija s uchetom bol'shih progibov [Full system of the equations of dynamic impact loading rigidly plastic shallow shells of rotation taking into account large deflections]. // *Building mechanics of engineering designs and facilities*, 2011, No. 4, pp. 26-31 (in Russian).
- по проблемам механики деформируемых тел, посвященного 100-летию со дня рождения А.А. Ильюшина. – М: Издательство Московского университета, 2011, с. 9-12.
2. Алексей Антонович Ильюшин: к 100-летию со дня рождения. // *Вестник Тюменского государственного университета. Физико-математическое моделирование. Нефть, газ, энергетика*, 2010, №6, с. 198-203.
 3. К 100-летию со дня рождения А.А. Ильюшина. // *Известия Российской академии наук. Механика твердого тела*, 2011, №1, с. 3-4.
 4. К 100-летию со дня рождения Алексея Антоновича Ильюшина (20.01.1911-31.05.1998). // *Вестник Московского университета. Серия 1: Математика. Механика*, 2011, №1, с. 77-79.
 5. **Ильюшина Е.А.** Надёжность в науке и жизни (к 95-летию со дня рождения А.А. Ильюшина). *Известия Российской академии наук. Механика твердого тела*, 2005, №6, с. 3.
 6. **Бровко Г.Л., Быков Д.Л., Васин Р.А., Георгиевский Д.В., Кийко И.А., Молодцов И.Н., Победря Б.Е.** Научное наследие А.А. Ильюшина и развитие его идей в механике. // *Известия Российской академии наук. Механика твердого тела*, 2011, №1, с. 5-18.
 7. **Кадымов В.А., Нуцубидзе Д.В.** Творческое наследие профессора А.А. Ильюшина и его вклад в победу в Великой Отечественной войне. // *Человек. Общество. Инклюзия*, 2015, №2(22), с. 10-13.
 8. **Бондарь В.С., Васин Р.А., Кийко И.А.** Школа-семинар «А.А. Ильюшин - выдающийся механик современности» в МГТУ «МАМИ». // *Проблемы машиностроения и автоматизации*, 2011, №3, с. 136-139.
 9. **Ильюшин А.А.** Пластичность. Часть первая. Упруго-пластические деформации. – М: Гостехиздат, 1948. – 376 с.

СПИСОК ЛИТЕРАТУРЫ

1. **Кийко И.А., Бровко Г.Л., Васин Р.А.** (ред.) К 100-летию со дня рождения А.А. Ильюшина (20.01.1911-31.05.1998) // *Упругость и неупругость / Материалы Международного научного симпозиума*

10. **Ильюшин А.А.** Пластичность. Часть первая. Упруго-пластические деформации / Науч. предисл. Е.И. Шемякина, И.А. Кийко, Р.А. Васина. Репр. воспр. текста изд. 1948 г. – М: Логос, 2004. – 388 с..
11. **Ильюшин А.А.** Труды. Том 1 (1935-1945). / Составители: Е.А. Ильюшина, Н.Р. Короткина. – М.: Физматлит, 2003. – 352 с.
12. **Ильюшин А.А.** Труды (1946-1966). Том 2. Пластичность. / Составители Е.А. Ильюшина, М.Р. Короткина. – М.: Физматлит, 2004. – 480 с.
13. **Ильюшин А.А.** Конечное соотношение между силами и моментами и их связи с деформациями в теории оболочек. // *ПММ*, 1945, №1, с. 101-110.
14. **Ильюшин А.А.** Приближенная теория упруго-пластических деформаций осесимметричных оболочек. // *ПММ*, 1944, №8, с. 15-24.
15. **Ольшак В., Савчук А.** Неупругое поведение оболочек. – М: Мир, 1969. – 144 с.
16. **Ольшак В., Мруз З., Пежина П.** Современное состояние теории пластичности. – М: Мир, 1964. – 243 с.
17. **Рождественский В.В.** К вопросу о предельных состояниях сечений тонких оболочек. // *Исследования по вопросам строительной механики и теории пластичности*. – М: ЦНИПС, 1956, с. 223-233.
18. **Шапиро Г.С.** О поверхностях текучести для идеально пластических оболочек. // *Проблемы сплошной среды, к 70-летию академика Н. И. Мухелишвили*. – М: Изд-во АН СССР, 1961, с. 504-507.
19. **Hodge P.G.** Yield conditions for rotationally symmetric shells under axisymmetric loading. // *J. Appl. Mech.*, 1960, No. 2, 27, pp. 323-331.
20. **Hodge P.G.** The Mises yield conditions for rotationally symmetric shells. // *Quart. Appl. Math.*, 1961, Vol. 18, pp. 305-311.
21. **Hodge P.G.** A comparison of yield conditions in the theory of plastic shells. // *Problems in continuum mechanics*, SIAM, Philadelphia, 1961, pp. 165-177.
22. **Hodge P.G.** The theory of rotationally symmetric plastic shells. // *Non-classical shell problems*. Amsterdam, North-Holland Publishing Company, 1964, pp. 621-648.
23. **Drucker D.C., Hopkins H.G.** Combined Concentrated and Distributed Load on Ideally – Plastic Circular Plates. // *Proc. 2nd U.S. Nat. Cong. App. Mech.*, 1954, pp. 517-520 (in Russian).
24. **Drucker D.C.** Plastic design methods - advantages and limitations. // *Trans. Soc. Nav., Eng.*, 1957, Vol. 65, pp. 172-196.
25. **Drucker D.C., Shield R.T.** Limit analysis of symmetrically loaded thin shells of revolution. // *Appl. Mech.*, 1959, Vol. 26, pp. 61-68.
26. **Onat E.T.** The plastic collapse of cylindrical shells under axially symmetrical loading. // *Quart. Appl. Math.*, 1955, Vol. 13, pp. 68-72.
27. **Onat E.T., Prager W.** Limit analysis of shells of revolution. // *Proc. Ned. Akad. Wetensch.*, 1954, Vol. 57, Ser. B, pp. 534-548.
28. **Onat E.T.** Plastic shells, Non-classical shell problems. // Amsterdam, North-Holland Publishing Company, 1967, pp. 649-659.
29. **Jones N.** Plasticity Methods in Protection and Safety of Industrial Plant and Structural Systems Against Extreme Dynamic Loading. // *Defence Science Journal*, 2008, Vol. 58, No. 2, pp. 181-193.
30. **Jones N.** Structural impact. United Kingdom, Cambridge University Press, 2003, 591 pages.
31. **Немировский Ю.В., Романова Т.П.** Динамическое сопротивление плоских пластических преград. – Новосибирск: Издательство Гео, 2009. – 312 с.
32. **Ерхов М.И.** Теория идеально пластических тел и конструкций. – М: Наука, 1978. – 352 с.

33. **Ерхов М.И.** Конечное соотношение между силами и моментами при пластической деформации оболочек. // *Строительная механика и расчет сооружений*, 1959, №3, с. 38-41.
34. **Розенблюм В.И.** Об условии пластичности для тонкостенных оболочек. // *ПММ*, 1960, том 24, с. 364-366.
35. **Розенблюм В.И.** О полной системе уравнений пластического равновесия тонкостенных оболочек. // *Инж. журнал. МТТ*, 1966, №3, с. 483-492.
36. **Розенблюм В.И.** О расчете несущей способности идеально пластических осесимметричных оболочек. // *Вопросы теории упругости и пластичности*. – Л.: ЛГУ, 1965, с. 67-75.
1. **Розенблюм В.И.** О расчете несущей способности идеально пластических осесимметричных оболочек. // *Исследования по упругости и пластичности*. – М.: – Л.: ЛГУ, 1965, с. 207-218.
37. **Розенблюм В.И.** Приближенная теория равновесия пластических оболочек / В.И. Розенблюм // *ПММ*, 1954, Том 18, Выпуск 3, с. 289-302.
38. **Работнов Ю.Н.** Приближенная техническая теория упругопластических оболочек. // *ПММ*, 1951, Том 15, Выпуск 2, с. 167-174.
39. **Биргер И.А., Пановко Я.Г.** (ред.) Прочность, устойчивость, колебания. Справочник в трех томах. Том 2. – М: Машиностроение, 1968. – 463 с.
40. **Королев В.И.** Упруго-пластические деформации оболочек. – М: Машиностроение, 1971. – 304 с.
41. **Огибалов П.М.** Вопросы динамики и устойчивости оболочек. – М: Издательство Московского университета, 1963. – 420 с.
42. **Двайт Г.Б.** Таблицы интегралов и другие математические формулы. – М.: Наука, 1966. – 228 с.
43. **Выгодский М.Я.** Справочник по высшей математике. – М.: Наука, 1977. – 872 с.
44. **Старов А.В.** Полная система уравнений динамического ударного нагружения жесткопластических пологих оболочек вращения с учетом больших прогибов / А.В. Старов. // *Строительная механика инженерных конструкций и сооружений*, 2011, №4, с. 26-31.

Starov Aleksandr Vasil'evich, Associate Professor, Doctor of Engineering Science, Associate Professor of Structural Mechanics Department, Volgograd State Technical University. 1, Akademicheskaya St., Volgograd, 400074, Russian Federation; e-mail: starov1954@mail.ru.

Kalashnikov Sergey Yur'evich, Advisor of the Russian Academy of Architecture and Construction Sciences (RAACS), Professor, Doctor of Engineering Science, Professor, Academician of the International Higher Education Academy of Sciences, Vice-Rector, Volgograd State Technical University. 1, Akademicheskaya St., Volgograd, 400074, Russian Federation; E-mail: kalashnikov@vstu.ru.

Старов Александр Васильевич, доцент, доктор технических наук, доцент кафедры строительной механики, Волгоградский государственный технический университет (ВолГТУ); 400074, Россия, г. Волгоград, ул. Академическая, 1; e-mail: starov1954@mail.ru.

Калашников Сергей Юрьевич, советник Российской академии архитектуры и строительных наук (РААСН), профессор, доктор технических наук, проректор, Волгоградский государственный технический университет (ВолГТУ); 400074, Россия, г. Волгоград, ул. Академическая, 1; e-mail: kalashnikov@vstu.ru.

BENDING OF RING PLATES, PERFORMED FROM AN ORTHOTROPIC NONLINEAR DIFFERENTLY RESISTANT MATERIAL

Alexandr A. Treschev, Evgeniy A. Zhurin

Tula State University, Tula, RUSSIA

Abstract. This article proposes a mathematical model of axisymmetric transverse bending of an annular plate of average thickness, the loading of which is assumed to be on the upper surface of a transverse uniformly distributed load. An orthotropic plate made of a material whose mechanical characteristics nonlinearly depend on the type of stress state is considered. The most universal, built in the normalized tensor space of stresses associated with the main axes of anisotropy of the material are taken as defining relations. The loads were taken in such a way that the deflections of the middle surface of the plate could be considered small compared to its thickness. Fastening plates are presented in two versions: 1) rigid fastening on the outer and inner contours; 2) hinge bearing on the outer and inner contours. As a result of the formulation of the boundary value problem, a mathematical model was developed for the class of problems in question, implemented as a numerical algorithm integrated into the application package of the MatLAB environment. To solve the system of resolving differential equations of plate bending, the method of variable parameters of elasticity was used with a finite-difference approximation of the second order of accuracy.

Key words: transverse bending, axisymmetric deformation, ring plate, orthotropic material, nonlinear dissociation, small deflections

ИЗГИБ КОЛЬЦЕВЫХ ПЛАСТИН, ВЫПОЛНЕННЫХ ИЗ ОРТОТРОПНОГО НЕЛИНЕЙНО РАЗНОСОПРОТИВЛЯЮЩЕГОСЯ МАТЕРИАЛА

А.А. Трещев, Е.А. Жури

Тульский государственный университет, г. Тула, РОССИЯ

Аннотация. В представленной статье предлагается математическая модель осесимметричного поперечного изгиба кольцевой пластины средней толщины, нагружение которой предполагается по верхней поверхности поперечной равномерной распределённой нагрузкой. Рассматривается ортотропная пластина, выполненная из материала, механические характеристики которого нелинейно зависят от вида напряженного состояния. В качестве определяющих соотношений приняты наиболее универсальные, построенные в нормированном тензорном пространстве напряжений, связанном с главными осями анизотропии материала. Величины нагрузок принимались с таким расчетом, чтобы прогибы срединной поверхности пластины могли считаться малыми по сравнению с ее толщиной. Закрепления пластин представлены в двух вариантах: 1) жёсткое закрепление по внешнему и внутреннему контурам; 2) шарнирное опирание по внешнему и внутреннему контурам. В результате постановки краевой задачи была разработана математическая модель для рассматриваемого класса задач, реализованная в виде численного алгоритма интегрированного в пакет прикладных программ среды MatLAB. Для решения системы разрешающих дифференциальных уравнений изгиба пластин использовался метод переменных параметров упругости с конечно-разностной аппроксимацией второго порядка точности.

Ключевые слова: поперечный изгиб, осесимметричное деформирование, кольцевая пластина, ортотропный материал, нелинейная разносопротивляемость, малые прогибы

1. INTRODUCTION

Currently, more and more often designed and built buildings, manufactured parts of machines and devices, which until recently had no analogues. These objects require deformation-strength calculation of high accuracy, as the slightest error at the initial stage of design can lead to serious accidents.

Over time, more and more technological materials are created for which the theory of calculation of traditional (classical) materials is not acceptable. That is why the development of new and modernization of old models is an urgent task of modern construction and engineering.

It is obvious that researchers need not only to develop a mathematical model, but also to test it experimentally, and compare it with other models for similar designs. With a deeper study of the materials it will be possible to calculate the components and structural elements with minimal errors. This will allow you to develop a design without waste of material.

In this paper we consider the axisymmetric deformation of the annular plate of medium thickness. The plate material is adopted orthotropic. The nonlinear properties of the material appear already in the early stages of deformation and strongly affect the subsequent stress distribution. It is not possible to reliably describe the deformation of such a plate by conventional linear functions.

The development of the theory of calculation of plates of resistive anisotropic materials have been studied by many scholars such as S.A. Ambartsumyan, R.M. Jones, C.W. Bert, A.V. Berezin, A.A. Zolochovsky, N.M. Matchenko, A.A. Treshchev and others [1-33].

S.A. Ambartsumyan in his works [1, 2, 3] proposed the simplest variants of defining relations in the form of equations of state. In the framework of the theory of small elastic deformations, piecewise linear relations between the principal stresses and strains were established, and the question of the relations between shear stresses and shear was not

discussed. In S. A. Ambartsumyan's model [1, 2, 3] the field of principal stresses is divided into regions of the first and second genera [3, 4, 5]. This model is similar in form to the classical generalized Hooke's law of orthotropic matter, but the elastic moduli and the coefficients of transverse deformation in the directions of the principal axes are determined separately from the experiments on axial tension (E_k^+ , ν_{km}^+) and compression (E_k^- , ν_{km}^-). The direct application of the proposed relations is possible only in cases when the distribution of the principal stresses by their signs at different points of the body is known in advance, and also if the model constraints on the constants arising from the symmetry condition of the compliance tensor are observed.

Model R.M. Jones [6, 7, 8, 9] it is based on the construction of a matrix of weighted malleability, the symmetry of which in areas with different signs of the main stresses is achieved by introducing weight coefficients into the non-diagonal components. The weights represent the pairwise correlation of modules in the principal stresses

$$k_1 = |\sigma_1| / (|\sigma_1| + |\sigma_2|), \quad k_2 = |\sigma_2| / (|\sigma_1| + |\sigma_2|).$$

The simplest model of equations of state for anisotropic multimodule bodies is proposed by C.W. Bert [10, 11, 12, 13]. This model is applicable to fibrous materials when it is considered that the components of the compliance matrix depend on the sign of normal stresses arising in the direction of the fibers, that is, when stretching along the fibers, one symmetric matrix of compliance is used, when compressing – another. The rigor of this model is violated when the normal stresses along the fibers are equal to zero.

A more complex, but no less controversial model is proposed by A.A. Zolochovsky [14, 15, 16, 17, 18, 19, 20, 21], which introduced an equivalent stress, the second degree of which is determined by the potential of deformation. Potential constants are "hidden" in expressions that make up the equivalent voltage. The

equivalent stress is determined by the sum of the linear and quadratic joint in-stress variants. Due to the presence of irrationality in the stress-strain coupling equations, it is not possible to distinguish the compliance matrix in General. The obtained nonlinear relations are sufficiently complex and contain a large number of constants to be experimentally determined. In particular, for an orthotropic material in a quasilinear approximation, it is necessary to determine thirty-two constants, and only 18 of the simplest reference experiments (uniaxial tension and contraction in the direction of the main axes of orthotropy and at an angle of 45° to them) can be established.

2. METHODS

It is obvious that even a detailed analysis of the most well-known models of determining ratios of anisotropic materials of different resistances indicates that these models are not free from serious shortcomings and are based on separate hypotheses, often unfounded by experimental facts. In particular, E.V. Lomakin in [22, 23] formulates the strain potential for anisotropic materials in the form of an energy function from the ratio of the mean stress to the stress intensity

$$\xi = \sigma / \sigma_i$$

(where

$$\sigma = \sigma_{ij} \cdot \delta_{ij} / 3$$

– average stress,

$$\sigma_i = \sqrt{1,5 S_{ij} S_{ij}}$$

– stress intensity;

$$S_{ij} = \sigma_{ij} - \delta_{ij} \sigma$$

– stress deviator components; δ_{ij} – Kronecker symbol) multiplied by the convolution of the

fourth rank compliance tensor with the second rank stress tensors in the principal axes of the anisotropy of the material. A serious drawback of the introduced relations is the discontinuity of the functional parameter ξ , which leads to uncertainties of an infinite nature, which has been repeatedly pointed out in [24, 25].

In the works of Matchenko N.M. and Treschev A.A. [25, 26] are the deformation potentials for anisotropic dissolving materials allowing the quasilinear approximation, normalized vector in nine-dimensional space of stresses. In these works the equations of state of two levels of accuracy are obtained. Despite the rationality of this approach, the obtained relations are also not free from significant drawbacks, which for the equations of the first level of accuracy are complex functional dependencies between uncorrelated constants of materials, and for the equations of the second level – an excessively large number of constants to be experimentally determined, which requires the involvement of experiments on complex stress States.

In subsequent works [27, 28, 29] Treschev A.A. carried out a corrective formulation of the equations of state for different classes of anisotropic materials, both in quasi-linear and in non-linear formulations. The nonlinear model [31] uses equations of state represented by the type of generalized Hooke's law for anisotropic materials by type:

$$e_{km} = H_{kmpq}(\sigma_i, \alpha_{st}) \cdot \sigma_{pq}; \quad H_{kmpq} = H_{pqkm}; \\ k, m, q, p, s, t, = 1, 2, 3, \dots$$

In particular, for orthotropic material, these dependences are presented as follows:

$$e_{11} = (A_{1111} + B_{1111} \cdot \alpha_{11}) \cdot \sigma_{11} + \\ + [A_{1122} + B_{1122} \cdot (\alpha_{11} + \alpha_{22})] \cdot \sigma_{22} + \\ + [A_{1133} + B_{1133} \cdot (\alpha_{11} + \alpha_{33})] \cdot \sigma_{33}; \\ e_{22} = [A_{1122} + B_{1122} \cdot (\alpha_{11} + \alpha_{22})] \cdot \sigma_{11} + \\ + (A_{2222} + B_{2222} \cdot \alpha_{22}) \cdot \sigma_{22} + \\ + [A_{2233} + B_{2233} \cdot (\alpha_{22} + \alpha_{33})] \cdot \sigma_{33};$$

$$\begin{aligned}
 e_{33} &= [A_{1133} + B_{1133} \cdot (\alpha_{11} + \alpha_{33})] \cdot \sigma_{11} + \\
 &+ [A_{2233} + B_{2233} \cdot (\alpha_{22} + \alpha_{33})] \cdot \sigma_{22} + \\
 &+ (A_{3333} + B_{3333} \cdot \alpha_{33}) \cdot \sigma_{33}; \\
 2e_{12} &= C_{1212}(\sigma_i) \cdot \tau_{12}; \\
 2e_{23} &= C_{2323}(\sigma_i) \cdot \tau_{23}; \\
 2e_{13} &= C_{1313}(\sigma_i) \cdot \tau_{13}.
 \end{aligned} \quad (1)$$

where

$$a_{ij} = \sigma_{ij} / S;$$

– normalized stresses in the principal anisotropy axes of the material;

$$S = (\sigma_{ij} \cdot \sigma_{ij})^{0.5} = \sqrt{\sigma_{11}^2 + \sigma_{22}^2 + \sigma_{33}^2 + 2(\tau_{12}^2 + \tau_{23}^2 + \tau_{31}^2)}$$

– module full voltage (norm of the space of stresses); $A_{ijkm}, B_{ijkm}, C_{ijkm}$ – nonlinear functions that determine the mechanical properties of a material.

For orthotropic bodies the number of independent material functions reaches fifteen [29, 30, 31]. The presentation of these functions, which determine the properties of the material, is carried out by approximating the experimental diagrams of deformation under uniaxial tension and compression along the main axes of anisotropy and diagrams obtained for shear in the three main planes of orthotropies by processing them in the program Microcal Origin Pro 8.0 (Microcal Software Inc.). In this case, for structural orthotropic nonlinearly resistive composite material AVCO Mod 3a [29, 30] are presented as follows:

$$\begin{aligned}
 A_{kkkk}(\sigma_i) &= 0.5 \cdot [1/E_k^+(\sigma_i) + 1/E_k^-(\sigma_i)]; \\
 B_{kkkk}(\sigma_i) &= 0.5 \cdot [1/E_k^+(\sigma_i) - 1/E_k^-(\sigma_i)]; \\
 A_{kkmm}(\sigma_i) &= -0.5 \cdot \left[\frac{\nu_{km}^+(\sigma_i)}{E_m^+(\sigma_i)} + \frac{\nu_{km}^-(\sigma_i)}{E_m^-(\sigma_i)} \right]; \\
 B_{kkmm}(\sigma_i) &= -0.5 \cdot \left[\frac{\nu_{km}^+(\sigma_i)}{E_m^+(\sigma_i)} - \frac{\nu_{km}^-(\sigma_i)}{E_m^-(\sigma_i)} \right];
 \end{aligned} \quad (2)$$

$$\begin{aligned}
 C_{kmkm}(\sigma_i) &= 1/G_{km}(\sigma_i); \\
 E_k^\pm(\sigma_i) &= a_k^\pm + m_k^\pm \cdot \sigma_i + n_k^\pm \cdot \sigma_i^2; \\
 \nu_{km}^\pm(\sigma_i) &= \lambda_{km}^\pm + \beta_{km}^\pm \cdot \sigma_i + \mu_{km}^\pm \cdot \sigma_i^2; \\
 G_{km}(\sigma_i) &= g_{km} + p_{km} \cdot \sigma_i + q_{km} \cdot \sigma_i^2.
 \end{aligned}$$

where $a_k^\pm, m_k^\pm, n_k^\pm, \lambda_{km}^\pm, \beta_{km}^\pm, \mu_{km}^\pm, g_{km}, p_{km}, q_{km}$ – the constants of nonlinear material functions determined by processing of experimental diagrams of deformation by the method of least squares and presented in table 1.

This model of nonlinear orthotropic resistive material [29, 30, 31] is currently the least controversial, gives the results as close as possible to the experimental data and therefore is the basis for the construction of the method of calculating the plates.

Consider the stress-strain state of the annular plate under loading by a transverse uniformly distributed load of intensity “ q ” (MPa). Material of plates taken with non-linear characteristic having cylindrical orthotropy and properties of resistivity. In this case, we focus on two options for the support of the object of study:

- plate with rigidly clamped contours according to Figure 1a;
- the plate is hinged on the contours in accordance with Figure 1b.

Due to the axial symmetry, the problems are considered taking into account the cylindrical coordinate system (r, θ, z) . In this case, the traditional model assumptions [30] are considered to be valid in the following form: 1) the normal to the median plane after deformation is rotated by an angle ψ_θ relative to the circumferential coordinate axis θ ; 2) when determining the parameters of the stress state, the influence of normal stresses σ_z is neglected due to their smallness.

Based on the above assumptions, for deformations at the points of the plate we have:

$$\begin{aligned}
 e_r &= u_{,r} + z \cdot \psi_{\theta,r}; \\
 e_\theta &= u/r + z \cdot \psi_\theta / r; \\
 \gamma_{rz} &= w_{,r} + \psi_\theta
 \end{aligned} \quad (3)$$

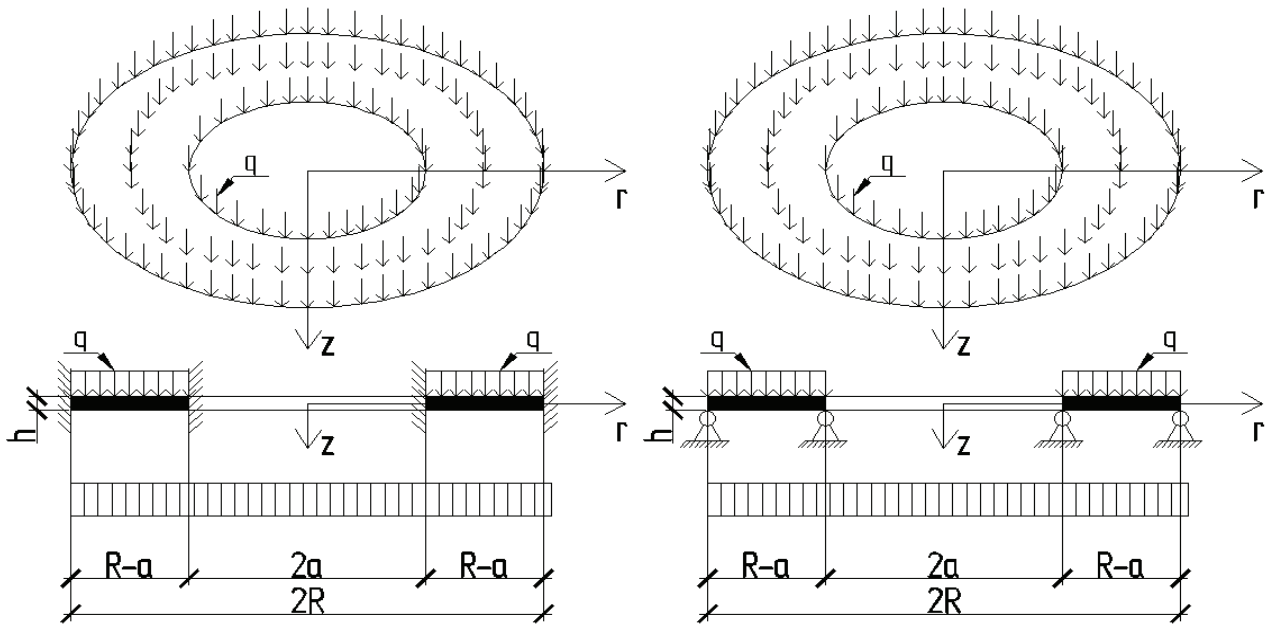


Figure 1. Design scheme of the ring plate with two types of support:
a) rigidly clamped circuits; b) pivotally supported circuits.

where u – radial movements in the middle surface; ψ_θ – rotation angle of the plate section relative to the axis; θ ; w – deflection of the middle surface of the plate.

Taking into account the accepted hypotheses of equation (1) we transform to the form:

$$\begin{aligned} e_r &= (A_{1111}(\sigma_i) + B_{1111}(\sigma_i) \cdot \alpha_r) \cdot \sigma_r + \\ &+ [A_{1122}(\sigma_i) + B_{1122}(\sigma_i) \cdot (\alpha_r + \alpha_\theta)] \cdot \sigma_\theta; \\ e_\theta &= [A_{1122}(\sigma_i) + B_{1122}(\sigma_i) \cdot (\alpha_r + \alpha_\theta)] \cdot \sigma_r + \\ &+ (A_{2222}(\sigma_i) + B_{2222}(\sigma_i) \cdot \alpha_\theta) \cdot \sigma_\theta; \\ e_z &= [A_{1133}(\sigma_i) + B_{1133}(\sigma_i) \cdot \alpha_r] \cdot \sigma_r + \\ &+ [A_{2233}(\sigma_i) + B_{2233}(\sigma_i) \cdot \alpha_\theta] \cdot \sigma_\theta; \\ e_{rz} &= C_{1313}(\sigma_i) \cdot \tau_{rz}; \end{aligned} \quad (4)$$

where

$$\begin{aligned} \alpha_r &= \sigma_r / S; \\ \alpha_\theta &= \sigma_\theta / S; \\ \alpha_{rz} &= \sigma_{rz} / S; \\ S &= \sqrt{\sigma_r^2 + \sigma_\theta^2 + \tau_{rz}^2}; \\ \sigma_i &= \sqrt{\sigma_r^2 - \sigma_r \cdot \sigma_\theta + \sigma_\theta^2 + 3\tau_{rz}^2}. \end{aligned}$$

For the convenience of further presentation, we introduce the following designations:

$$\begin{aligned} C_{1111} &= A_{1111}(\sigma_i) + B_{1111}(\sigma_i) \cdot \alpha_r; \\ C_{1122} &= A_{1122}(\sigma_i) + B_{1122}(\sigma_i) \cdot (\alpha_r + \alpha_\theta); \\ C_{1133} &= A_{1133}(\sigma_i) + B_{1133}(\sigma_i) \cdot \alpha_r; \\ C_{2222} &= A_{2222}(\sigma_i) + B_{2222}(\sigma_i) \cdot \alpha_\theta; \\ C_{2233} &= A_{2233}(\sigma_i) + B_{2233}(\sigma_i) \cdot \alpha_\theta; \\ C_{1313} &= C_{1313}(\sigma_i); \end{aligned} \quad (5)$$

Having expressed stresses through deformations taking into account the simplifying equations (3)-(5), after simple mathematical manipulations we come to the following dependences:

$$\begin{aligned} \sigma_r &= \Delta_{1111}(u_{,r} - z \cdot \psi_{\theta,r}) + \Delta_{1122}(u/r - z \cdot \psi_\theta / r); \\ \sigma_\theta &= \Delta_{1122}(u_{,r} - z \cdot \psi_{\theta,r}) + \Delta_{2222}(u/r - z \cdot \psi_\theta / r); \\ \tau_{rz} &= \frac{(\psi_\theta + w_{,1})}{\Delta_{1313}}; \end{aligned} \quad (6)$$

$$\begin{aligned} \Delta_{1111} &= C_{2222} / (C_{1111} \cdot C_{2222} - C_{1122}^2); \\ \Delta_{1122} &= C_{1122} / (C_{1111} \cdot C_{2222} - C_{1122}^2); \\ \Delta_{2222} &= C_{1111} / (C_{1111} \cdot C_{2222} - C_{1122}^2); \\ \Delta_{1313} &= C_{1313}; \end{aligned} \quad (7)$$

Table 1. AVCO Mod 3a composite material constants [29, 30].

Type of prototype test	Technical parameter	The first element of a nonlinear function	The second element of the nonlinear function	The third element of the nonlinear function
1	2	3	4	5
Uniaxial tension along the main axes of orthotropy	$E_k^+(\sigma_i), \text{Pa}$	α_1^+	m_1^+	n_1^+
		$1.058 \cdot 10^{-10}$	62.829	$1.535 \cdot 10^{-6}$
		α_2^+	m_2^+	n_2^+
		$2.864 \cdot 10^{-10}$	-105.476	$5.893 \cdot 10^{-7}$
		α_3^+	m_3^+	n_3^+
		$2.301 \cdot 10^{-10}$	88.349	$3.711 \cdot 10^{-6}$
	$\nu_{km}^+(\sigma_i)$	λ_{12}^+	β_{12}^+	μ_{12}^+
		0.158	$-3.106 \cdot 10^{-9}$	$2.192 \cdot 10^{-17}$
		λ_{21}^+	β_{21}^+	μ_{21}^+
		0.103	$-1.79 \cdot 10^{-9}$	$9.106 \cdot 10^{-18}$
		λ_{13}^+	β_{13}^+	μ_{13}^+
		0.203	$2.15 \cdot 10^{-9}$	$6.148 \cdot 10^{-17}$
		λ_{23}^+	β_{23}^+	μ_{23}^+
		0.104	$0.87 \cdot 10^{-10}$	$6.741 \cdot 10^{-17}$
		λ_{31}^+	β_{31}^+	μ_{31}^+
		0.146	$-0.146 \cdot 10^{-10}$	$6.971 \cdot 10^{-17}$
Uniaxial compression along the main axes of orthotropy	$E_k^-(\sigma_i), \text{Pa}$	α_1^-	m_1^-	n_1^-
		$9.988 \cdot 10^9$	-12.943	$6.71 \cdot 10^{-7}$
		α_2^-	m_2^-	n_2^-
		$2.326 \cdot 10^{10}$	-436.81	$-6.077 \cdot 10^{-7}$
		α_3^-	m_3^-	n_3^-
		$5.14 \cdot 10^9$	-129.15	$-78.31 \cdot 10^{-6}$
	$\nu_{km}^-(\sigma_i)$	λ_{12}^-	β_{12}^-	μ_{12}^-
		0.118	$-1.457 \cdot 10^{-9}$	$2.136 \cdot 10^{-17}$
		λ_{21}^-	β_{21}^-	μ_{21}^-
		0.06	$1.77 \cdot 10^{-9}$	$2.947 \cdot 10^{-17}$
		λ_{13}^-	β_{13}^-	μ_{13}^-
		0.264	$-1.118 \cdot 10^{-9}$	$3.01 \cdot 10^{-17}$
		λ_{23}^-	β_{23}^-	μ_{23}^-
		0.189	$2.156 \cdot 10^{-9}$	$2.104 \cdot 10^{-17}$
		λ_{31}^-	β_{31}^-	μ_{31}^-
		0.134	$-0.457 \cdot 10^{-10}$	$5.819 \cdot 10^{-17}$

1	2	3	4	5
A shift in the principal planes of orthotropy	$G_{km}(\sigma_i), \text{ Pa}$	g_{12}	p_{12}	q_{12}
		$4.07 \cdot 10^9$	$-1,6$	$-8.38 \cdot 10^{-6}$
		g_{23}	p_{23}	q_{23}
		$1.723 \cdot 10^9$	16.899	$-1.1 \cdot 10^{-5}$
		g_{31}	p_{31}	q_{31}
		$2.43 \cdot 10^9$	-54.455	$-1.97 \cdot 10^{-5}$

Deformations e_z are not explicitly included here, but they are easily computed from the third equation of the system (4).

Taking as a basis the new physical equations, we thus do not make changes in the dependence of the static-geometric nature, and therefore the static conditions for the annular plates in a cylindrical coordinate system will be presented in the traditional form [29, 30]

$$\begin{aligned} N_{r,r} + (N_r - N_\theta) / r &= 0; \\ Q_{r,r} + Q_r / r &= -q; \\ M_{r,r} + (M_r - M_\theta) / r - Q_r &= 0; \end{aligned} \quad (8)$$

where $N_r, N_\theta, Q_r, M_r, M_\theta$ – forces and moments in cross sections of plate.

Forces and moments are determined by integrating expressions for stresses (6) over the plate thickness:

$$\begin{aligned} N_r &= \int_{-h/2}^{h/2} \sigma_r dz; \quad N_\theta = \int_{-h/2}^{h/2} \sigma_\theta dz; \\ Q_r &= \int_{-h/2}^{h/2} \tau_{rz} dz; \\ M_r &= \int_{-h/2}^{h/2} \sigma_r \cdot z dz; \quad M_\theta = \int_{-h/2}^{h/2} \sigma_\theta \cdot z dz; \end{aligned} \quad (9)$$

From the joint consideration of dependences (6) – (9), the resolving equations of axisymmetric bending of plates of average thickness having cylindrical orthotropy and nonlinear dependence of mechanical characteristics of the material on the type of stress state follow:

$$\begin{aligned} D_{11,r} \cdot u_{,rr} + K_{11,r} \cdot \psi_{\theta,rr} + D_{12,r} \cdot u_{,r} / r + \\ + K_{12,r} \cdot \psi_{\theta,r} / r + (D_{11} \cdot u_{,r} + K_{11} \cdot \psi_{\theta,r} + \\ + D_{12} \cdot u / r + K_{12} \cdot \psi_{\theta} / r - D_{12} \cdot u_{,r} + \\ + K_{12} \psi_{\theta,r} + D_{22} \cdot u / r + K_{22} \cdot \psi_{\theta} / r) / r = 0; \\ D_{13,r} \cdot (w_{,rr} + \psi_{\theta,r}) + D_{13} (w_{,r} + \psi_{\theta}) / r = -q; \end{aligned} \quad (10)$$

$$\left(\begin{aligned} &K_{11} \cdot u_{,r} + R_{11} \cdot \psi_{\theta,r} + K_{12} \cdot u / r + \\ &+ R_{12} \cdot \psi_{\theta} / r - K_{12} u_{,r} + R_{12} \cdot \psi_{\theta,r} + \\ &6K_{22} u / r + R_{22} \cdot \psi_{\theta} / r \\ &- D_{13} \cdot (w_{,r} + \psi_{\theta}) = 0. \end{aligned} \right) / r -$$

where $D_{11}, D_{12}, D_{22}, D_{13}, K_{11}, K_{12}, K_{22}, R_{11}, R_{12}, R_{22}$ – the integral of the function on the plate thickness, resulting after integration by formulas (9); $D_{11,r}, D_{12,r}, D_{33,r}, K_{11,r}, K_{12,r}, R_{11,r}, R_{12,r}$ – derivatives of integral functions on the radial coordinate.

To solve the obtained equations (10) we use the finite-difference method with the second-order approximation of accuracy [32, 33].

3. RESULTS AND DISCUSSION

To solve this class of problems the program is developed in MatLAB. Considered 2 options for fixing the plate: hinge and rigid clamping at the edges. Also, 3 variants of the decision were considered. For clarity, each of the solutions is indicated by its own, different from the other line:

— considered model [27, 28, 29];

— solutions without taking into account the properties of resistivity taking into account the stiffness of the material only in axial tension;

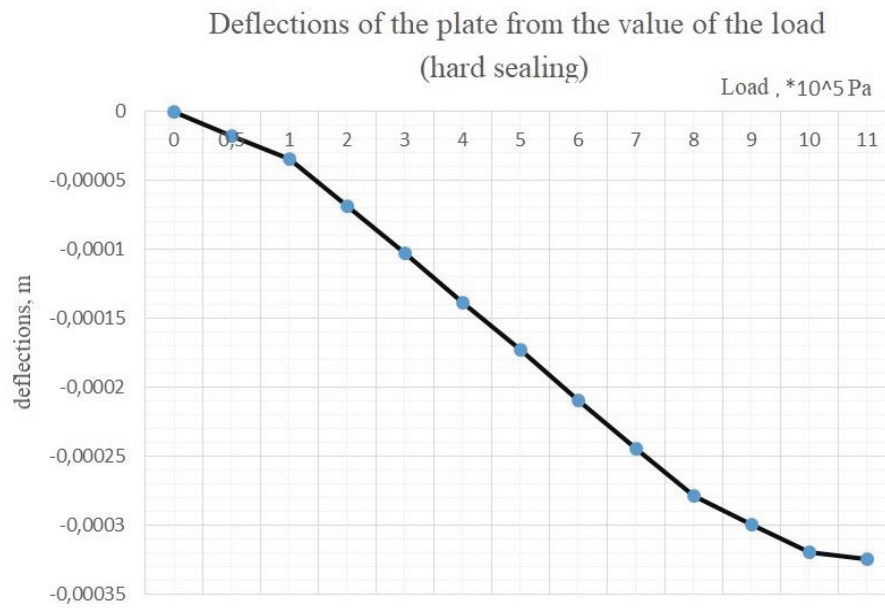


Figure 2. Deflections of the plate from the load.

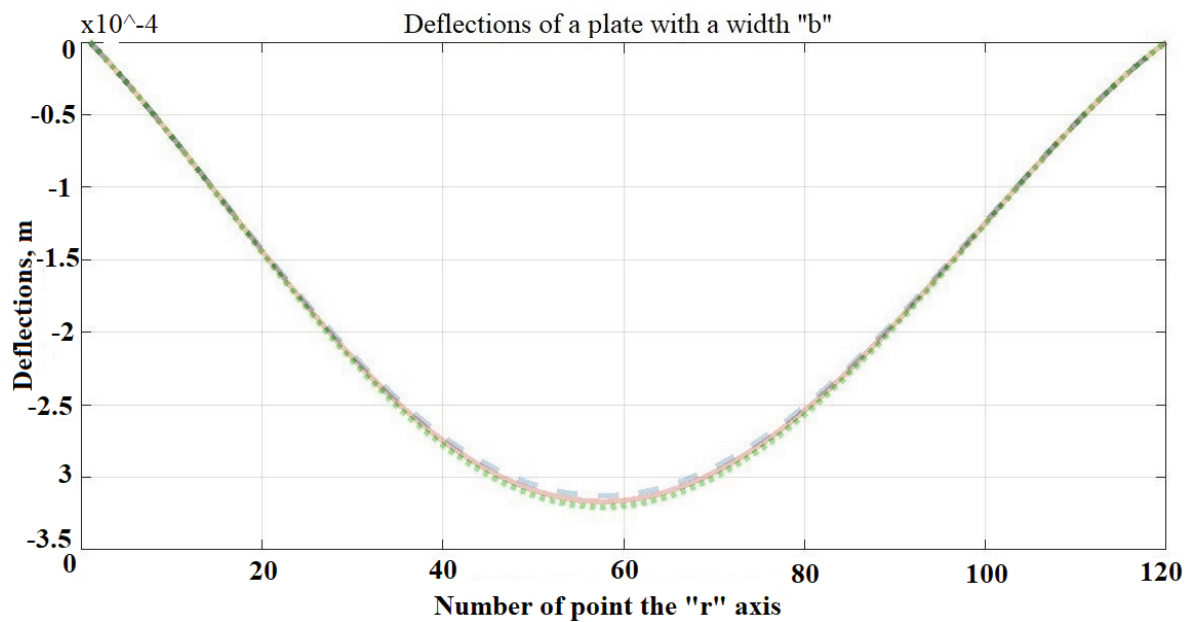


Figure 3. Deflection of the plate along the coordinate r.

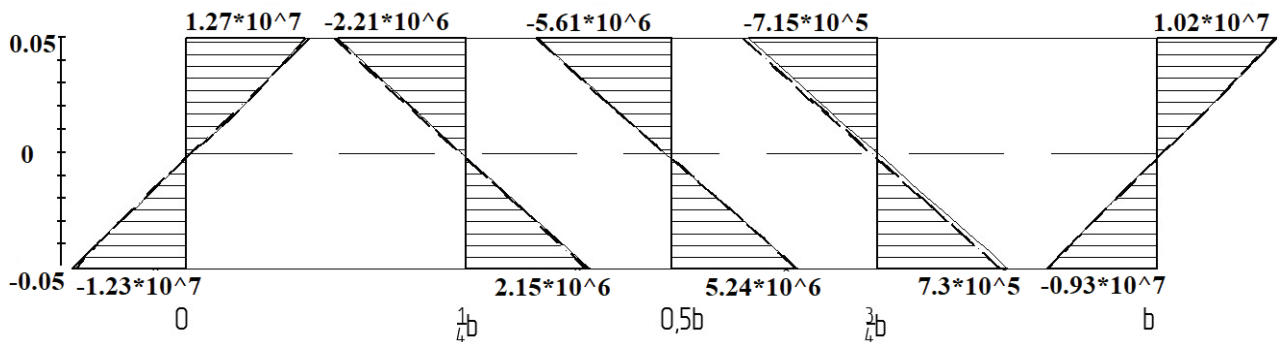


Figure 4. Stress distribution σ_r over the thickness of the annular plate in typical cross-sections, PA.

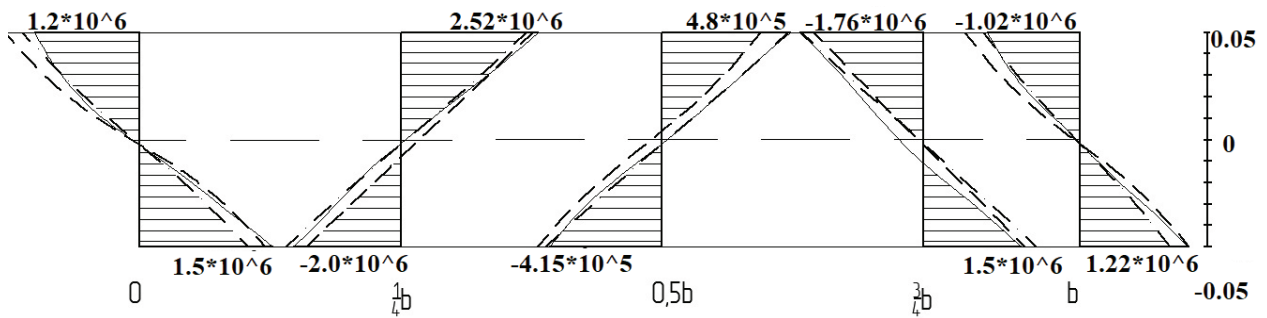


Figure 5. Stress distribution σ_θ over the thickness of the annular plate in typical cross-sections, PA.

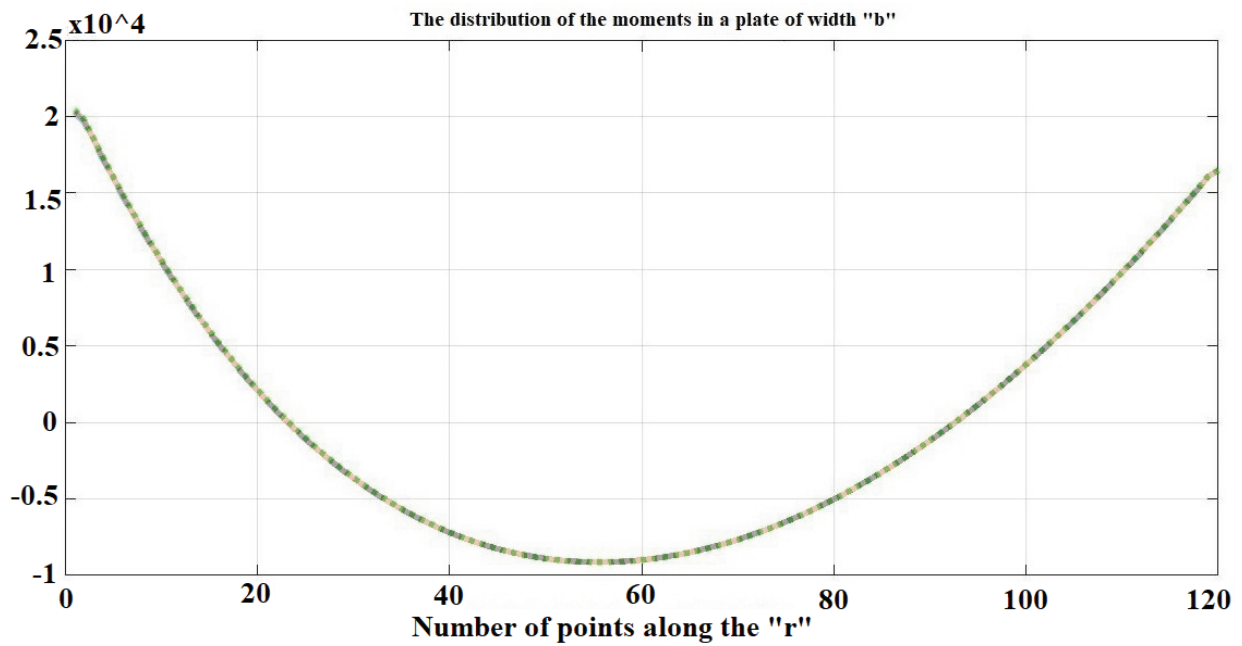


Figure 6. Distribution of M_r moments on the annular plate.

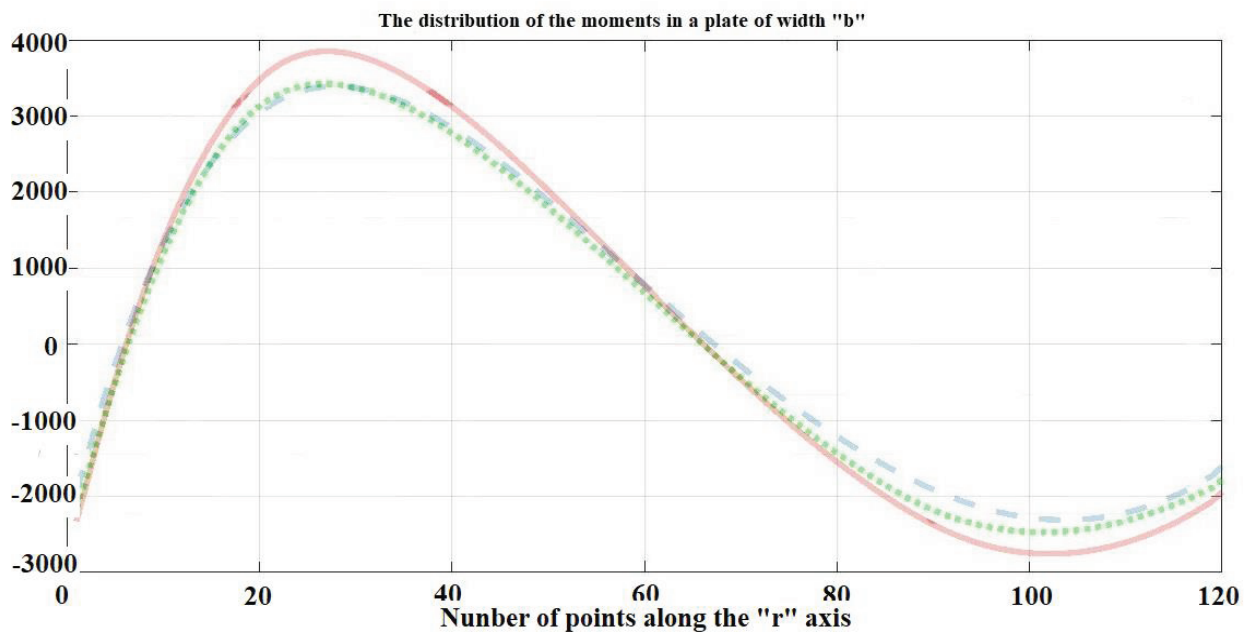


Figure 7. Distribution of moments M_θ on the annular plate.

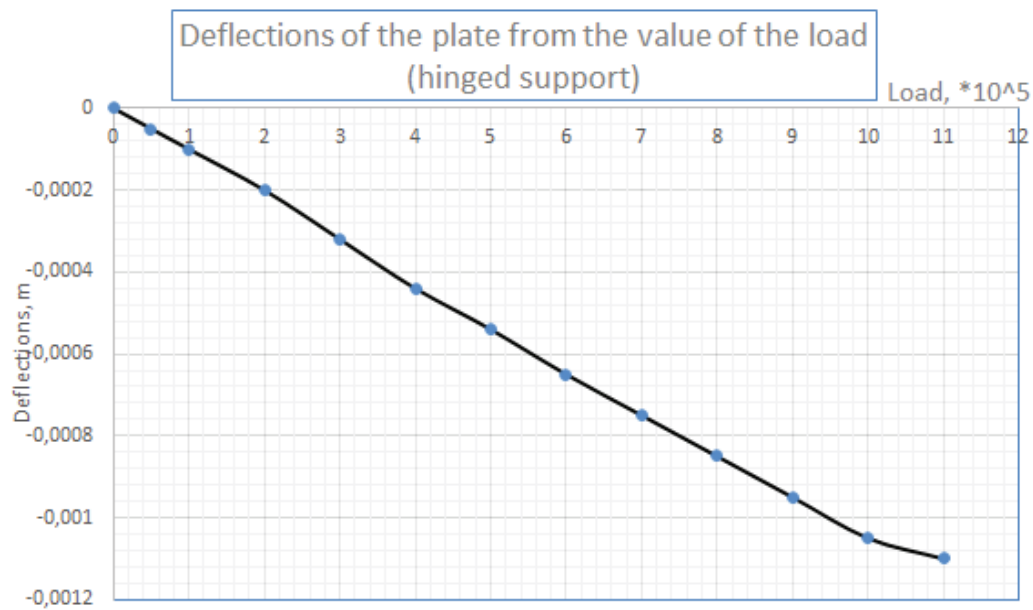


Figure 8. Deflections of the plate from the load.

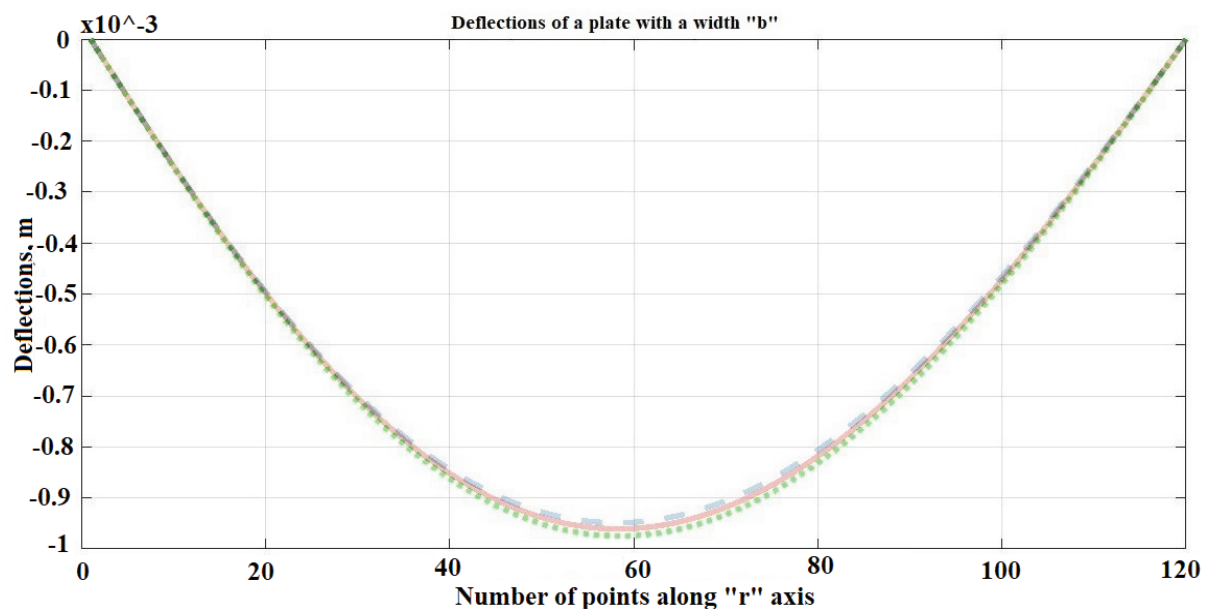


Figure 9. Deflection of the plate along the coordinate r .

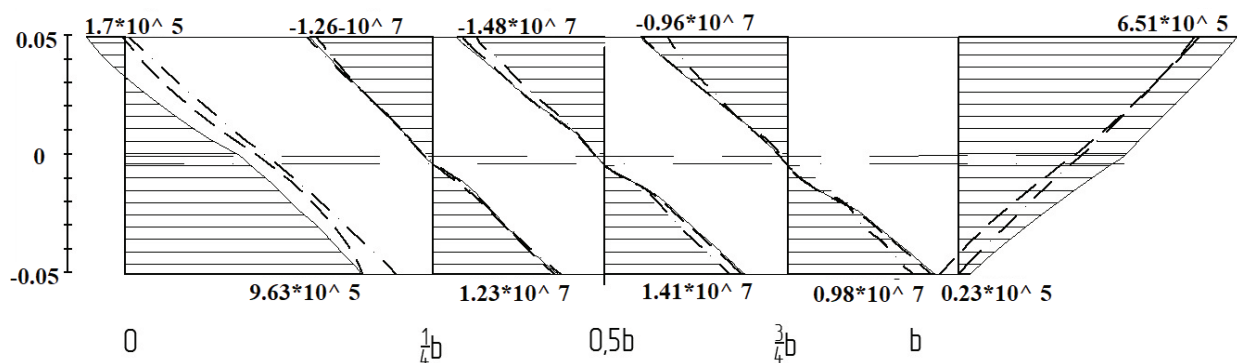


Figure 10. Stress distribution σ_r over the thickness of the annular plate in typical cross-sections, PA

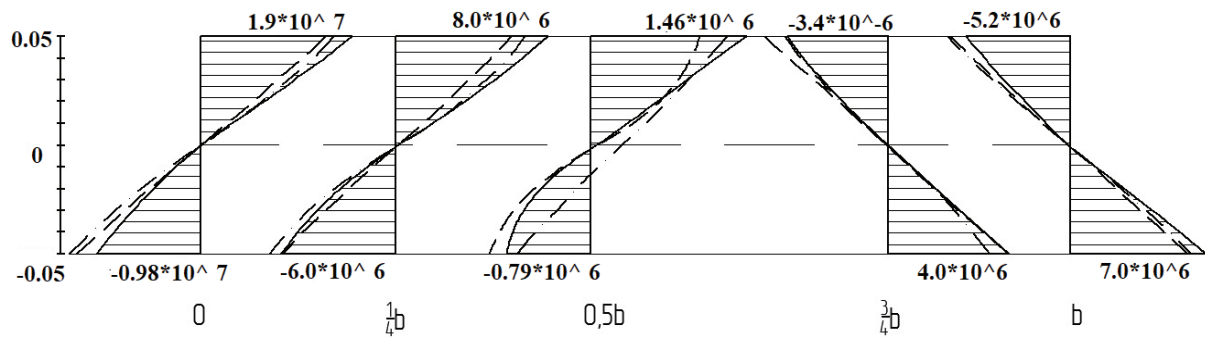


Figure 11. Stress distribution σ_θ over the thickness of the annular plate in typical cross-sections, PA

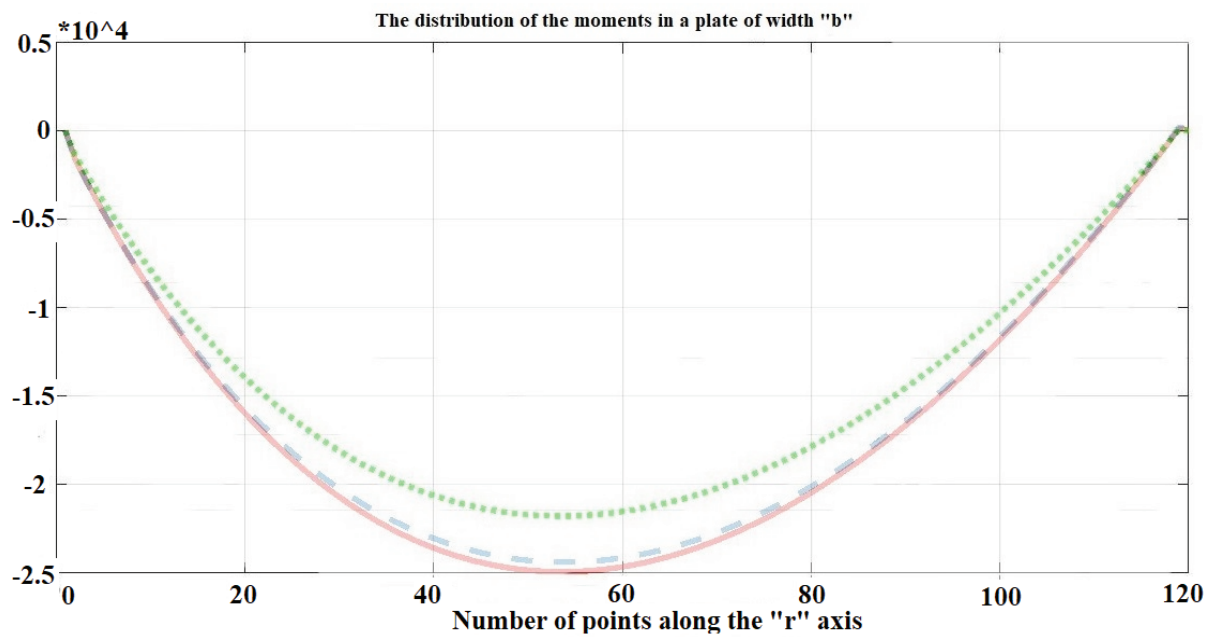


Figure 12. Distribution of M_r moments on the annular plate.

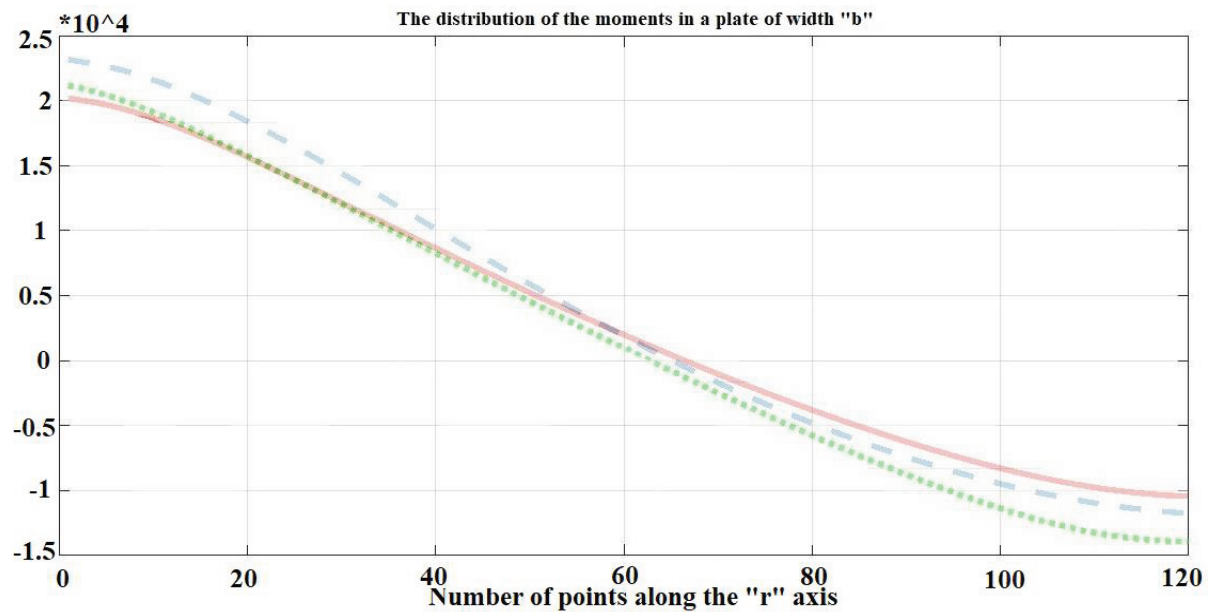


Figure 13. Distribution of moments M_θ on the annular plate.

..... – solutions without taking into account the properties of resistivity, taking into account the stiffness of the material only in axial compression.

After processing the calculation results, the following graphs and charts were obtained:

- deflections from the load value;
- deflections on the coordinate "r";
- distribution of stresses in the plate in different sections;
- horizontal movement and rotation angles of the middle surface of the plate;
- distribution of moments in the plate.

The main results are given on the graphs for the section of the ring plate "R-a". From 2 to 11 figure shows the results of the calculation of the plate with a rigid clamping, and from 14 to 21 figure – with a hinge support.

4. SUMMARY

During the implementation of the model of deformation of ring plates under the action of uniformly distributed loads, the basic values of the parameters characterizing their stress-strain states are obtained.

As a result of comparison of the solutions of the considered problems on the presented deformation model with the data of the traditional nonlinear theory without taking into account the properties of the resistivity, the following features characterizing the differences in the stress-strain state parameters are noted:

1) A rigidly fixed plate:

- the difference in deflections is 1.3%;
- the difference in the values of forces in different sections of the annular plate varies in the range of 1.5-3% for σ_r ; 13-17% for σ_{rz} ; 5-7% for σ_θ ;
- c. the difference in horizontal displacement values is 6%;
- d. the difference in the values of the angles of rotation is 4%;
- e. the difference in the values of the moment of M_r is 0.5-1%; and M_θ – 10-15%.

2) Hinged plate:

- a. the difference in deflections is 1.5-2%;
- b. the difference in the stress values in different sections of the annular plate varies in the range of 7-15% for σ_r ; 5-19% for σ_{rz} ; 10-14% for σ_θ ;
- c. the difference in the values of horizontal displacements is 2-4%;
- d. the difference in the values of the angles of rotation is 15-17%;
- e. the difference in the moment M_r is 15%; and M_θ - 25%.

Thus, it is established that the non-linear material resistivity is not taken into account when considering the deformation parameters of various structures made of such materials, which leads to noticeable errors.

5. CONCLUSIONS

As a result of the study, a model of deformation of orthotropic materials was concretized and applied, which most accurately and adequately describes most of the currently known nonlinear materials. The model is based on the processed results of experiments on deformation of materials with different resistance, material nonlinear functions and constants [30].

To solve the problem of deformation of a ring plate from a nonlinear orthotropic material according to the developed model, the method of variable parameters of elasticity with a finite-difference approximation of the second order of accuracy was used. Developed the algorithm of decision of task "calculation of axisymmetric deformation of circular plates, the average thickness of the non-linear orthotropic resistive materials with small deflections". Practical application of the algorithm and evaluation of iterative methods of the solution were implemented with the help of "MatLAB" software package.

As a result of the work done, a number of test problems on the topic of deformation of plates of average thickness from nonlinear orthotropic materials were solved, the parameters of the state of the plates at different stages of loading

by a transverse uniformly distributed load were determined, two options for fixing the ring plates were considered, the results of comparing three.

REFERENCES

1. **Ambartsumyan S.A.** Teorija anizotropnyh plastin: prochnost', ustojchivost', kolebanija [Theory of anisotropic plates: strength, stability, vibrations]. Moscow, Nauka, 1967, 266 pages (in Russian).
2. **Ambartsumyan S.A.** Osnovnye uravnenija i sootnoshenija raznomodul'noj teorii uprugosti anizotropnogo tela [Basic equations and ratios of the multi-modular theory of elasticity of an anisotropic body]. // *Izv. Academy of Sciences of the USSR. MTT*, 1969, Vol. 3, pp. 51–61 (in Russian).
3. **Ambartsumyan S.A.** Raznomodul'naja teorija uprugosti [Multi-modular theory of elasticity]. Moscow, Nauka, 1982, 320 pages (in Russian).
4. **Ambartsumyan S.A., Khachatryan A.A.** Osnovnye uravnenija teorii uprugosti dlja materialov, raznosoprotivljajushhihsja rastjazheniju i szhatiju [The basic equations of the theory of elasticity for materials of different resistance to tension and compression]. // *Inzh. journals MTT*, 1966, Vol. 2, pp. 44–53 (in Russian).
5. **Ambartsumyan S.A., Khachatryan A.A.** K raznomodul'noj teorii uprugosti [Towards a multimodular theory of elasticity]. // *Ing. journals MTT*, 1966, Vol. 6, pp. 64–67 (in Russian).
6. **Jones R.M.** A Nonsystemmetric Compliance Matrix Approach to Nonlinear Multimoduls Ortotropic Materials. // *AIAA Journal*, 1977, Vol. 15, Issue 10, pp. 1436–1443.
7. **Jones R.M., Nelson D.A.R.** Material for nonlinear Deformation. // *AIAA Journal*, 1976, Vol. 14, Issue 6, pp. 709–716.
8. **Jones R.M.** Modeling Nonlinear Deformation of the Carbon-Carbon Composite Materials. // *AIAA Journal*, 1980, Vol. 18, Issue 8, pp. 995–1001.
9. **Jones R.M.** Stress-Strain Relations for Materials with Moduli in Tension and Compression. // *AIAA Journal*, 1977, Vol. 15, Issue 1, pp. 16–25.
10. **Bert C.W.** Models for Fibrous Composites. // *Transaction of the ASME*, 1977, Vol. 99 H. - Ser. D., Issue 4, pp. 344–349.
11. **Bert C.W.** Micromechanics of the different elastic behavior of filamentary composite in tension and compression. Mechanics of bimodulus materials. New York, ASME, 1979, pp. 17–28.
12. **Bert C.W., Gordaninejad F.** Multimodular Materials. // *International Journal for Numerical Methods in Engineering*, 1984, Vol. 20, pp. 479–503.
13. **Bert C.W., Reddy J.N., Chao W.C.** Bending of Thick Rectangular Plates Laminated of Bimodulus Composite Materials. // *AIAA Journal*, 1981, Vol. 19, Issue 10, pp. 1342–1349.
14. **Zolochovsky A.A.** K tenzornoj svjazi v teorijah uprugosti i plastichnosti anizotropnyh kompozitnyh materialov, raznosoprotivljajushhihsja rastjazheniju i szhatiju [To tensor coupling in the theories of elasticity and plasticity of anisotropic composite materials that are differently opposed to tension and compression]. // *Mechanics of composite materials*, 1985, Vol. 1, pp. 53–58 (in Russian).
15. **Zolochovsky A.A.** Opredejajushhie uravnenija i nekotorye zadachi raznomodul'noj teorii uprugosti anizotropnyh materialov [Determining equations and some problems of the multimodular theory of elasticity of anisotropic materials]. // *PMTF*, 1985, Issue 4, pp. 131–138 (in Russian).
16. **Zolochovsky A.A.** K teorii plastichnosti materialov razlichno soprotivljajushhihsja rastjazheniju i szhatiju [On the theory of plasticity of materials differently resisting tension and compression]. // *Izv. universi-*

- ties. *Engineering*, 1986, Vol. 6, pp. 13-16 (in Russian).
17. **Zolochovsky A.A.** O sootnoshenijah teorii uprugosti anizotropnyh raznomodul'nyh materialov [On the relations of the theory of elasticity of anisotropic multi-modular materials]. // *Dynamics and durability of machines*. Kharkov, High school, 1981, Vol. 34, pp. 3-8 (in Russian).
18. **Zolochovsky A.A.** Sootnoshenija raznomodul'noj teorii uprugosti anizotropnyh materialov na osnove treh smeshannyh invariantov. // *Dynamics and Strength of Machines*. Kharkov, High school, 1987, Vol. 46, pp. 85-89 (in Russian).
19. **Zolochovsky A.A., Morachkovsky O.K.** Napravlenija razvitija modelej i metodov rascheta nelinejnogo deformirovanija tel i jelementov mashinostroitel'nyh konstrukcij [The directions of development of models and methods for calculating the nonlinear deformation of bodies and elements of engineering structures]. // *Dynamics and strength of machines*. Kharkov, High school, 1989, Vol. 50, pp. 3-9 (in Russian).
20. **Zolochovsky A.A., Sklepus S.N.** K teorii plastichnosti s tremja invariantami naprjazhennogo sostojanija [On the theory of plasticity with three invariants of the stress state]. // *Izv. universities. Engineering*, 1987, Vol. 5, pp. 7-10 (in Russian).
21. **Zolochovsky A.A.** Ob uchete raznosoprotivljaemosti v teorii polzuchesti izotropnyh i anizotropnyh materialov [Concerning consideration of the multiresistance in the theory of creep of isotropic and anisotropic materials]. // *PMTF*, 1982, Vol. 4, pp. 140-144 (in Russian).
22. **Lomakin E.V.** Raznomodul'nost' kompozitnyh materialov [Multi-modularity of composite materials]. // *Mechanics of composite materials*, 1981, Vol. 1, pp. 23-29 (in Russian).
23. **Lomakin E.V.** Sootnoshenija teorii uprugosti dlja anizotropnogo tela, deformacionnye harakteristiki kotoryh zavisjat ot vida naprjazhennogo sostojanija [Relations of the theory of elasticity for an anisotropic body, the deformation characteristics of which depend on the type of stress state]. // *Izv. Academy of Sciences of the USSR. MTT*, 1983, Issue 3, pp. 63-69.
24. **Berezin I.S., Zhidkov N.P.** Metody vychislenij [Calculation methods]. Volumes 1, 2. Moscow, State. publishing house physical. lit-ry, 1959, 464 pages (in Russian).
25. **Matchenko N.M., Treshchev A.A.** Uchet vlijanija vida naprjazhennogo sostojanija na uprugie i plasticheskie sostojanija nachal'no izotropnyh deformiruemyh sred [Accounting for the influence of the type of stress state on elastic and plastic states of initially isotropic deformable media]. // *Abstracts of the reports of the International Scientific and Technical Symposium, "Modeling and similarity criteria in the processes of developed plastic form change"*. Orel, OPT, 1996, pp. 11-12 (in Russian).
26. **Matchenko N.M., Treshchev A.A.** Teorija deformirovanija raznosoprotivljajushhihsja materialov. Tonkie plastiny i obolochki [Theory of deformation of materials with different resistance. Thin plates and shells]. Moscow, Tula: RAACS, TSU, 2005, 187 pages (in Russian).
27. **Treshchev A.A.** Opisanie nelinejnogo deformirovanija anizotropnyh materialov [Description of non-linear deformation of anisotropic materials]. // *Actual problems of the construction and construction industry: a collection of materials of the International Conference*. Tula, TSU, 2001, pp. 107-108 (in Russian).
28. **Treshchev A.A.** Opisanie deformirovanija nelinejnyh anizotropnyh materialov [Description of the deformation of nonlinear anisotropic materials]. // *Architectural and building materials science at the turn of the century: materials of reports of the International Conference*. Belgorod, BelGTASM, 2002, pp. 86 (in Russian).
29. **Treshchev A.A.** Teorija deformirovanija i prochnosti materialov s iznachal'noj

navedjonnogo chuvstvitel'nost'ju k vidu naprjazhjonno-go sostojanija. Opredelja-jushhie sootnoshenija [The theory of de-formation and strength of materials with in-ital induced sensitivity to the type of stress state. Defining relationships]. Moscow, Tu-la, RAACS, TulSU, 2016, 328 pages (in Russian).

30. **Treschev A.A.** Anizotropnye plastiny i ob-olochki iz raznosoprotivljajushhihsja mate-riakov [Anisotropic plates and shells from materials of different resistance]. Moscow, Tula, RAACS, TSU, 2007, 160 pages (in Russian).
31. **Jones R.M., Nelson D.A.R.** Theoretical-experimental correlation of material models for non-linear deformation of graphite. // *AIAA Journal*, 1976, Vol. 14, No. 10, pp. 1427-1435.
32. **Birger I.A., Mavlyutov R.R.** Soprotivlenie materialov [Resistance materials]. Moscow, Science. Ch. ed. Phys.-Mat. lit., 1986, 560 pages (in Russian).
33. **Pisarenko G. S., Mozharovsky N. S.** Uravnenija i kraevye zadachi teorii plas-tichnosti i polzuchesti [Equations and boundary value problems of the theory of plasticity and creep]. Kiev, Science Dumka, 1981, 496 pages (in Russian).

СПИСОК ЛИТЕРАТУРЫ

1. **Амбарцумян С.А.** Теория анизотропных пластин: прочность, устойчивость, колебания. – М.: Наука, 1967. – 266 с.
2. **Амбарцумян С.А.** Основные уравнения и соотношения разномодульной теории упругости анизотропного тела. // Изв. АН СССР. МТТ, 1969, №3, с. 51-61.
3. **Амбарцумян С.А.** Разномодульная теория упругости. – М.: Наука, 1982. – 320 с.
4. **Амбарцумян С.А., Хачатрян А.А.** Основные уравнения теории упругости для материалов, разностойчивляющихся растяжению и сжатию. // *Инж. журн. МТТ*, 1966, №2, с. 44-53.
5. **Амбарцумян С.А., Хачатрян А.А.** К разномодульной теории упругости. // *Инж. журн. МТТ*, 1966, №6, с. 64-67.
6. **Jones R.M.** A Nonsystemmetric Compliance Matrix Approach to Nonlinear Multimoduls Ortotropic Materials. // *AIAA Journal*, 1977, Vol. 15, Issue 10, pp. 1436-1443.
7. **Jones R.M., Nelson D.A.R.** Material for nonlinear Deformation. // *AIAA Journal*, 1976, Vol. 14, Issue 6, pp. 709-716.
8. **Jones R.M.** Modeling Nonlinear Deformation of the Carbon-Carbon Composite Materials. // *AIAA Journal*, 1980, Vol. 18, Issue 8, pp. 995-1001.
9. **Jones R.M.** Stress-Strain Relations for Materials with Moduli in Tension and Compression. // *AIAA Journal*, 1977, Vol. 15, Issue 1, pp. 16-25.
10. **Bert C.W.** Models for Fibrous Composites. // *Transaction of the ASME*, 1977, Vol. 99 H. - Ser. D., Issue 4, pp. 344-349.
11. **Bert C.W.** Micromechanics of the different elastic behavior of filamentary composite in tension and compression. Mechanics of bi-modulus materials. New York, ASME, 1979, pp. 17-28.
12. **Bert C.W., Gordaninejad F.** Multi-modular Materials. // *International Journal for Numerical Methods in Engineering*, 1984, Vol. 20, pp. 479-503.
13. **Bert C.W., Reddy J.N., Chao W.C.** Bending of Thick Rectanqular Plates Laminated of Bimodulus Composite Materials. // *AIAA Journal*, 1981, Vol. 19, Issue 10, pp. 1342-1349.
14. **Золочевский А.А.** К тензорной связи в теориях упругости и пластичности анизотропных композитных материалов, разностойчивляющихся растяжению и сжатию. // *Механика композитных материалов*, 1985, №1, с. 53-58.
15. **Золочевский А.А.** Определяющие уравнения и некоторые задачи разномодульной теории упругости

- анизотропных материалов. // *ПМТФ*, 1985, №4, с. 131-138.
16. **Золочевский А.А.** К теории пластичности материалов различно сопротивляющихся растяжению и сжатию. // *Известия вузов. Машиностроение*, 1986, №6, с. 13-16.
 17. **Золочевский А.А.** О соотношениях теории упругости анизотропных разномодульных материалов. // *Динамика и прочность машин*. – Харьков: Вища школа, 1981, Выпуск 34, с. 3-8.
 18. **Золочевский А.А.** Соотношения разномодульной теории упругости анизотропных материалов на основе трех смешанных инвариантов. // *Динамика и прочность машин*. – Харьков: Вища школа, 1987, Выпуск 46, с. 85-89.
 19. **Золочевский А.А., Морачковский А.А.** Направления развития моделей и методов расчета нелинейного деформирования тел и элементов машиностроительных конструкций. // *Динамика и прочность машин*. – Харьков: Вища школа, 1989, Выпуск 50, с. 3-9.
 20. **Золочевский А.А., Склепус С.Н.** К теории пластичности с тремя инвариантами напряженного состояния. // *Известия вузов. Машиностроение*, 1987, №5, с. 7-10.
 21. **Золочевский А.А.** Об учете разнсопротивляемости в теории ползучести изотропных и анизотропных материалов. // *ПМТФ*, 1982, №4, с. 140-144.
 22. **Ломакин Е.В.** Разномодульность композитных материалов. // *Механика композитных материалов*, 1981, №1, с. 23-29.
 23. **Ломакин Е.В.** Соотношения теории упругости для анизотропного тела, деформационные характеристики которых зависят от вида напряженного состояния. // *Известия АН СССР. МТТ*, 1983, №3, с. 63-69.
 24. **Березин И.С., Жидков Н.П.** Методы вычислений. В двух томах. Том 1. – М.: Государственное издательство физико-математической литературы, 1959. – 464 с.
 25. **Матченко Н.М., Трещев А.А.** Учет влияния вида напряженного состояния на упругие и пластические состояния начально изотропных деформируемых сред. // *Тезисы докладов Международного научно-технического симпозиума, «Моделирование и критерии подобия в процессах развитого пластического формоизменения»*. – Орел: ОПТУ, 1996, с. 11-12.
 26. **Матченко Н.М., Трещев А.А.** Теория деформирования разнсопротивляющихся материалов. Тонкие пластины и оболочки. – М.; Тула: РААСН; ТулГУ, 2005. – 187 с.
 27. **Трещев А.А.** Описание нелинейного деформирования анизотропных материалов. // *Актуальные проблемы строительства и строительной индустрии: сборник материалов Международной конференции*. – Тула: ТулГУ, 2001, с. 107–108.
 28. **Трещев А.А.** Описание деформирования нелинейных анизотропных материалов. // *Архитектурно-строительное материаловедение на рубеже веков: материалы докладов Международной конференции*. – Белгород: БелГТАСМ, 2002, с. 86.
 29. **Трещев А.А.** Теория деформирования и прочности материалов с изначальной наведённого чувствительностью к виду напряжённого состояния. Определяющие соотношения. – М.: – Тула: РААСН, ТулГУ, 2016. – 328 с.
 30. **Трещев А.А.** Анизотропные пластины и оболочки из разнсопротивляющихся материалов. – М.: – Тула: РААСН, ТулГУ, 2007. – 160 с.

31. **Jones R.M., Nelson D.A.R.** Theoretical-experimental correlation of material models for non-linear deformation of graphite. // *AIAA Journal*, 1976, Vol. 14, Issue 10, pp. 1427-1435.
32. **Биргер И.А., Мавлютов Р.Р.** Сопротивление материалов. – М.: Наука. Главная редакция физико-математической литературы, 1986 – 560 с.
33. **Писаренко Г.С., Можаровский Н.С.** Уравнения и краевые задачи теории пластичности и ползучести. – Киев: Наук. думка, 1981 – 496 с.

Трещев Александр Анатольевич, член-корреспондент Российской академии архитектуры и строительных наук (РААСН), профессор, доктор технических наук; заведующий кафедрой «Строительство, строительные материалы и конструкции», Тульский государственный университет; 300012, Россия, г. Тула, пр. Ленина, 92; тел. +7 (905) 622-90-58; E-mail: taa58@yandex.ru.

Журин Евгений Андреевич, аспирант кафедры «Строительство, строительные материалы и конструкции», Тульский государственный университет; 300012, Россия, г. Тула, пр. Ленина, 92; тел. +7 (920) 276-01-46; e-mail: eazhurin@mail.ru.

Alexander A. Treschev, Corresponding Member of the Russian Academy of Architecture and Construction Sciences (RAACS), Professor, Doctor of Technical Sciences, Head of Department of Construction, Building Materials and Structures, Tula State University; 300012, Russia, Tula, Lenin Ave. 92; phone: +7 (905) 622-90-58; E-mail: taa58@yandex.ru.

Evgeniy A. Zhurin, Graduate student of the department "Construction, building materials and structures", Tula State University; 300012, Russia, Tula, Lenin Ave. 92; phone: +7 (920) 276-01-46; e-mail: eazhurin@mail.ru.

INVESTIGATIONS OF HISTORICAL CITIES OF UZBEKISTAN AND KAZAKHSTAN AS OBJECTS OF THE SILK WAY

A.Zh. Zhussupbekov¹, F.S. Temirova², A.A. Riskulov³, A.R. Omarov¹

¹ L.N. Gumilyov Eurasian National University, Nur-Sultan city, KAZAKHSTAN

² Karshi Engineering-Economics Institute, Karshi city, UZBEKISTAN

³ Tashkent Institute of Design, Construction and of Automobile Roads, Tashkent, UZBEKISTAN

Abstract: Since ancient times, the cities of Uzbekistan and Kazakhstan have gained worldwide fame, like pearls scattered along the Great Silk Road, they sparkle under the bright sun. Cities of modern Uzbekistan have existed for thousands of years - Tashkent (2200 years), Termez, Bukhara, Khiva (2500 years), Shakhrisabz and Karshi (2700 years), Samarkand (2750 years), Margilan (2000 years), Almaty (1000 years), Turkestan (2000 years), Chimgent (2200 years) and Taraz (2000 years). In Uzbekistan and Kazakhstan, numerous collections, repositories, archives and libraries preserve the richest collections of manuscripts collected over many centuries. And all thanks to its favorable location in a picturesque oasis, almost in the center of the network of roads of the Great Silk Road.

Keywords: Central Asia, historical monuments, Hodge Ahmed Yassavi, Arystan-Bab, Palace Ak-Sarai

ИССЛЕДОВАНИЯ ИСТОРИЧЕСКИХ ГОРОДОВ УЗБЕКИСТАНА И КАЗАХСТАНА КАК ОБЪЕКТОВ ШЕЛКОВОГО ПУТИ

А.Ж. Жусупбеков¹, Ф.С. Темирова², А.А. Рискулов³, А.Р. Омарова¹

¹ Евразийский национальный университет им. Л.Н. Гумилева, город Нур-Султан, КАЗАХСТАН

² Каршинский инженерно-экономический институт, г. Карши, УЗБЕКИСТАН

³ Ташкентский институт по проектированию, строительству и эксплуатации автомобильных дорог, Ташкент, УЗБЕКИСТАН

Аннотация: С древних времен города Узбекистана и Казахстана приобрели всемирную известность: жемчужины, разбросанные по Великому шелковому пути, сверкают под ярким солнцем. Города современного Узбекистана существуют тысячи лет – Ташкент (2200 лет), Термез, Бухара, Хива (2500 лет), Шахрисабз и Карши (2700 лет), Самарканд (2750 лет), Маргилан (2000 лет), Алматы (1000 лет), Туркестан (2000 лет), Чимкент (2200 лет) и Тараз (2000 лет). В Узбекистане и Казахстане многочисленные коллекции, хранилища, архивы и библиотеки хранят самые богатые собрания рукописей, формировавшиеся многие столетия. И все это благодаря его выгодному расположению в живописном оазисе, практически в центре сети дорог Великого шелкового пути.

Ключевые слова: Центральная Азия, исторические памятники, Ходж Ахмеда Яссави, Арыстан-Баб, Дворец Ак-Сарай

1. INTRODUCTION

The history of our ancient land leaves deep into the millennia. Holding an advantageous geographical position, the connecting North with the South, the East with the West, Central Asia was the important center on the road of a caravan which became history under the name

of the Great Silk Way. On branches of this ancient transcontinental highway not only trade developed – there was an active process of mutual enrichment of ideas, cultures, traditions, religions, crafts and technologies. One of the types of the works directly concerning cultural heritage, demanding greater financial influences, but which aren't receiving

the due amount of financing is carrying out engineering-geological and geotechnological researches of historical monuments of architecture of Central Asia.

Environmental problems are connected with changes of historically developed geological and hydrogeological mode. In particular is a raising of ground waters and increase in their structure of concentration of salts, increase in moisture content and salt in the soil. These phenomena started promoting actively deformation of designs and an intensive erosion of walls and bases of monuments of architecture. Especially strongly historical buildings of the cities located in low territories of Central Asia (Bukhara, Khiva) suffer. Now the listed above negative facts negatively influence and the architecture monuments which are in rather favorable foothill territories of Central Asia: in such as Samarkand, Shakhrisabz, Shymkent, etc. however here increase in humidity in soil and raising of ground waters is generally connected with a human factor: urbanization and development of communication systems. For this reason studying of this problem needs to be conducted in two directions: in the global - change of a geoecological situation of Central Asia, in local scale - to look for evidence-based ways of decrease in level of its influence for the purpose of preservation of masterpieces of world famous monuments of architecture. We will begin with the main thing: a geoecological situation in the region. Central Asia is located between two large rivers: Amu Darya and Syr-Darya which rivers use Uzbekistan, Kazakhstan, Turkmenistan, Tajikistan and Kyrgyzstan (Figure 1).

The territory has a various and difficult relief: from the East ridges of Gissar – Scarlet and Tien Shan, from the West extensive desert plains of Kizilkum and Kara Kum. Both rivers in the northwest flow into the Aral Sea adjoining from the North and the West of a plateau Ustyurt and from Kyzylkumami's southeast. The Aral Sea on a map appears as a third largest inland reservoir of the planet and is after the North American lake Top and the Caspian Sea.



Figure 1. Map of the Central Asian Republics (Kazakhstan, Uzbekistan, Turkmenistan, Tajikistan and Kyrgyzstan).

The questions of geotechnical researches and also the reasons resulting in need of strengthening of the foundations of monuments of architecture were considered in the works by B.I. Dalmatov, R.A. Mangushev, V.M. Ulitsky, Y. Iwasaki, E.M. Pashkin, V.A. Vasenin, A.I. Polishchuk, A.Z. Khasanov, I.I. Usmankhodzhayev, C.Viggiani, C. Tsatsanifos, T.O. Zhunissoy, A.G. Shashkin, M.B. Lisyuk, R.E. Dashko and other scientists. Considerable interest in questions of restoration of monuments of architecture of Central Asia was shown by K. Tuyakbayev, S. S. Agitayev, A. B. Seydaliyeva. Materials on memorial architecture of Kazakhstan and Central Asia were considered in various aspects in works of A.Kh.Margulan, K. A. Akishev, T.N. Senigova, A. G. Maximova, K. M. Baypakov, V.Olkhovskiy, V. L. Voronina, G. A. Pugachenkova, M. M. Mendikulov, E.M. Baitenov, G.G. Gerasimova, V. V. Konstantinova, T.D. Dzhanyzbekov, M. B. Hodzhayev, S. S. Dzhambulatov, B. T. Tuyakbayeva, S. I. Adzhigaliyeva, B. A. Gludinov, K. S. Abdurashidov, etc.

We will provide some statistical data. Development of droughty lands began from 30th years of the XX century. In 10 years only in the territory of Uzbekistan, more than 250 km of channels with a total area of irrigation of 420

thousand hectares were laid. Since 1960, the irrigating network increased by 874 km, and the area – by 690 thousand hectares. Now the total length of irrigation canals makes over 160 thousand km only across Uzbekistan, which select from sources more than 50 km³ waters in a year, and across Central Asia in general to 100 km³/year. For this period, the area of the irrigated lands increased by four times and made more than 3.5 million hectares. Since this period, inflow of water to the Aral Sea is reduced: 1970 - to 36 km³, 1980 - to 10 km³/year, and in 1990 practically to zero.

As a result of it Aral's level decreased more than 15 m, the volume of water was reduced more than 70% (600 km³), and the area – more than a third. In deep Arale it was possible to catch to 1.5 million centners of fish a year. Since 1960 salinity of water reached 30% that led to death of fresh-water fishes, such as a sazan, the bream, the zherekh. From a bottom of the drained Aral annually norths rise in the atmosphere of 15-75 million t of dust. In Priaralye on each hectare settles to 520 kg of dust, sand and salts.

In the course of accumulation of drainage and washing waters in lowlands of deserts lakes which sizes increase since 1960 were formed. For example, borders of Arnosay (Syr-Darya) reached the menacing sizes. Such new growth leads to local change of a climatic situation. In particular to flooding of natural pastures, bogging of territories and a sharp raising of the horizon of ground waters. The same situation arose in lower reaches of Amu Darya (the lake Sarikamysh).

If to consider that the average consumption of water on watering of the irrigated lands makes 9-10 thousand m³ on hectare (optimum 6-7 thousand m³ on hectare the rest on evaporation), the remained 5-6 thousand m³/hectare resupply ground waters. For this reason the level and a mineralization of ground waters in Central Asia increases practically everywhere.

It should be noted especially that the developed hydrogeological situation causes extensive

damage to the geoecological environment of the historical cities of Central Asia. It is known that in the course of a raising of ground waters there is a deformation of a surface of the earth. It leads to uneven rainfall of civil and industrial buildings, constructions, and also historical monuments of architecture.

For the last decade there were serious problems connected with preservation of world famous masterpieces of architecture. In particular, the salted ground waters owing to the aggression in relation to construction materials as a result of difficult physical and chemical processes start erodirovat intensively underground and elevated designs of monuments therefore often there are deformations, and in certain cases and their final fracture. As an example, it is possible to bring catastrophic destruction of one of minarets of the Chor-Minor complex, strong deformations of a complex Tim Abdulkhana, a complex ARC and an inclination of minarets in Bukhara (Figure 2) or deformations of some monuments in Samarkand, the Ichang-Kala complex in Khiva.

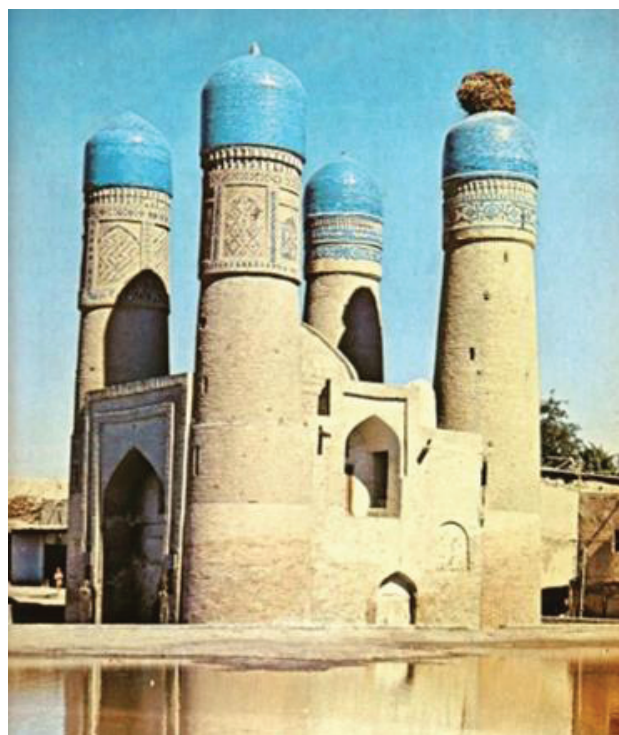


Figure 2. The Chor-Minor Complex in Bukhara.

Influence of the mineralized ground waters on

the historic centers located in low territories of an oasis, such as Bukhara and Khiva is most notable. Both of these cities are located in the valley of Amu Darya. The large-scale irrigational works described above led to sharp increase of ground waters that respectively worsened historically developed geological situation in the region. For example, the construction of the Tashauzsky branch of the channel 180 km long begun 1982 with a capacity of 400 m³/sec. (the channel is laid in 12 km from the city of Khiva) worsened a condition of 175 thousand hectares of the old irrigated arable lands of Khwarezm and led to an aggravation of the hydrogeological mode of the ancient city of Khiva. Process of bogging and secondary salinization affected fauna and flora. So as a result of change of habitat aggression of termites which started destroying intensively structures and especially materials of elements of designs of historical monuments increased.

At construction of monuments of architecture in the IX-X centuries it was applied (a ceramic square brick Muslim) to construction of walls, a flooring of floors of rooms and the yards by the sizes: 23x23x3 cm; 12x12x3 cm; 60x63x6,5 cm. In the X-XI centuries also applied a brick of 21x21x2,5 cm; 24x24x4 cm; in the XII-XVI centuries also applied a brick the sizes of the parties of 24-28 cm and 4,5-7 cm thick. Water absorption of wall ceramics fluctuates ranging from 18 to 30% depending on material. The compressive strength of 50-300 kg / cm (5-30 MPa). Frost over 50 cycles (Voronina V.L. 1953).

2. THE SHORT DESCRIPTION OF HISTORICAL MONUMENTS OF ARCHITECTURE OF CENTRAL ASIA

2.1 The mausoleum of Hodge Ahmed Yassavi (XIV-XV cen.).

Architectural complex of Hodge Ahmed Yassavi in Turkestan - the bright example of architecture of timurids time which united

different rooms, various on function, in the walls: dzhamaatkhana, gurkhana (tomb), big and small aksara, kitapkhana, askhana, kudukhana and numerous hudzhra. Because of such variety of functions of the building scientists can't come to a consensus concerning its name in any way, and therefore call it differently: mausoleum, mosque, memorial complex, hanaka. Each of names characterizes only one of functions of this grandiose complex and doesn't reflect all services and rituals provided in it. Recently in a circle of experts it most often call "hanaka" - the term which it is accepted to call hospices (monasteries) of dervishes (Akishev K.A., Ageyeva Ye.I. 1958).

The Hanaka was built according to instructions of the emir Timur in 1399 on a place of burial of Hodge Ahmed Yassavi who died in the XII century. The official history of Timur "The book of victories" ("Zafar-name") connects a narration about a laying of the building with events of the end of 1397 when Timur solemnly made ziarat (worship) on Ahmed Yasavi's grave. According to "The book of victories", during stay in the Yassy city Timur instructed in creation here, on the suburb of its possession, a grandiose construction, worthy to Hodge Ahmed Yassavi's memory. It had to glorify Islam, promote its further distribution, facilitate government of extensive edge.

Timur's instructions on construction were executed strictly. According to the legend when erected the mausoleum, from a humdan (b rick-works) which was in Sauran city workers who handed over a brick for construction were placed. In 1405 Timur died, and works on Ahmed Yassavi's mausoleum stopped. Remained incomplete portal part (peshtak) and finishing of interiors of some rooms of the building.

As it was told earlier, Ahmed Yassavi's hanaka - the multipurpose construction including a number of rooms: to a dzhamaatkhana - the hall for meetings, a tomb - a place of burial of Ahmed Yassavi, a mosque, big and small aksarai - rooms for meetings, debates; to a kitabkhana - the room for census of papers,

storage of books and documents; to an askhana - the room where ritual food prepared; to a kudukhana- the room with a well; hudzhra - rooms for attendants of a hanaka and pilgrims. All rooms of a hanaka are grouped in composition in a rectangle about 50 in size (60 m and 15 m high. Domes and arches of a portal tower to 38 m (Figure 3).

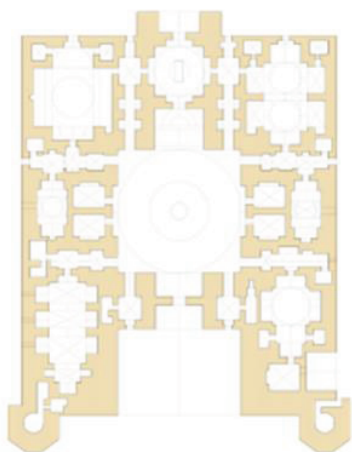


Figure 3. Schematic plan and general view of the mausoleum of Hodge Ahmed of Yassavi.

The connecting link of all rooms - a dzhamaatkhana is a smart room of a complex, square in the plan with the parties, equal 18,2 meters, is covered by the largest of remained in Central Asia a sphere and conic dome with an unary cover. Here passed meetings and group meeting (zikra) of dervishes. In the center of the hall there is a ritual cauldron (from here another,

more used name of the hall - Kazanlyk) cast according to the legend, from an alloy of seven metals. A cauldron is a symbol of a unification and hospitality. Diameter its 2.2 meters, weight is two tons. The exaggerated sizes of a cauldron are dictated by ancient beliefs of Turkic tribes: the edge of a cauldron has to be at height of a mouth of the person which to it goes. The surface of a cauldron is decorated with three belts of relief inscriptions against a vegetable ornament.

Top says that this cauldron for water - Timur's gift to the construction erected in memory of Hodge Ahmed Yassavi. In average of the word: "Be blessed", year of production of a cauldron - 1399 and a name of the master - Abdulgazizibn Sharafutdin from Tabriz. In the lower it is told: "Kingdom to Allah". Handles of a copper have an appearance of flowers of a lotus and alternate with round ledges (Tuyakbayeva B., Proskurin A. 1989).

The Hanaka of Ahmed Yassavi played a significant role in formation of the Turkestan necropolis, which developed on a place of the early medieval cemetery presented by several over sepulchral constructions and mausoleums with traditional orientation of their entrances to the southwest - in the direction to Mecca (Figure 4).

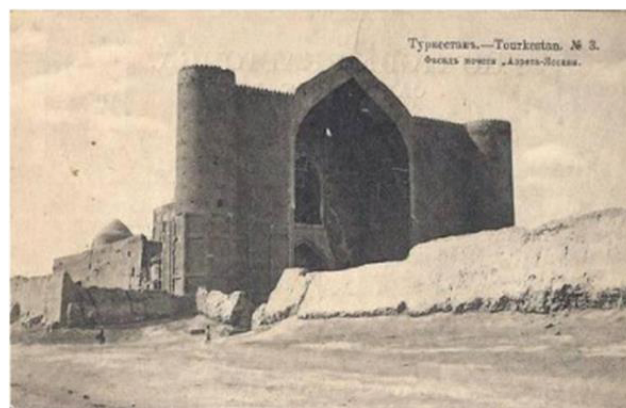


Figure 4. Old photos of the mausoleum of Hodge Ahmed Yassav.

2.2 The mausoleum of Arystan-Bab (XIV-XV cen.).

The mausoleum was built over a grave of the famous religious mystic ArystanBab, living in

the XII century in the Southern Kazakhstan region. The first construction of the mausoleum belongs to the XIV-XV centuries. From it carved wooden columns of an ayvan remained. In the XVIII century on a place of the ancient mazar destroyed by an earthquake two dome construction with ayvan, leaning on two carved wooden columns was constructed. The building of the XVIII century collapsed and in 1909 was built up a new about what the inscription on one of frieze cartouches says. Now above Arystan-Bab's grave there is a mausoleum of 3 0x13 m (Figure 5).

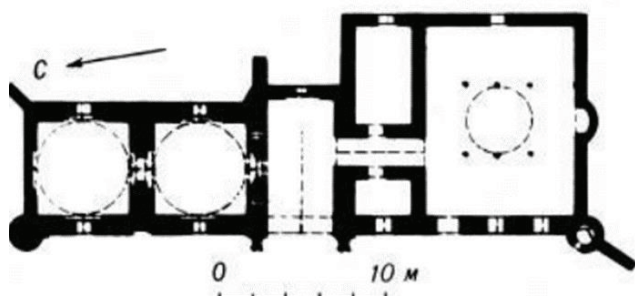


Figure 5. Schematic plan of the mausoleum Arystan-Bab.

In 1971 because of the high level of the ground waters which led it to a critical condition, the mosque was taken down and built up anew. The building is built of a zhzhenny brick on alabaster solution, in a front laying of walls (Figure 6). The building behind little change in an azimuth is focused from the East to the west. Two square rooms of tombs adjoin to each other and form the extended rectangle. From the West the square of the room of a mosque with hotel and taratkhanly for ablution adjoins. Tombs and a mosque connect the ayvan.

The main facade is solved simply and at the same time impressively. It consists of a portal, two walls and angular towers. Instead of massive medieval portals, here the easy portal which is decoratively processed with a lancet arch, leaning on walls of an ayvan. The arch has from two parties of a frame in the form of columns buttresses with sockets on the center of the planes of buttresses.



Figure 6. The modern view of the mausoleum Arystan-Bab and two remained columns of the XIV-XV century.

The lancet arch is executed by a wedge-shaped laying where the strelchatost is reached by wedge-shaped wedged bricks (Margulan A.KH., Basenov T.K., Mendikulov M.M. 1959). Tombs have dome overlapping. Domes are based upon low deaf drums. Transition from a plan square to domes is carried out by means of angular tromp without stalactite decorative fillings.

2.3. The Palace Ak-Sarai (XV cen.).

At Amir Timur time in northwest part of Shakhrisabz the huge palace Ak-Sarai surpassing in scale even the government residence Kuk-Sarai in Samarkand ("Ak" in translation - white, majestic, noble was built; "sarai" - the palace). The main construction works were carried out in 1380-1396. Along with local masters, masters were involved in construction and finishing of the palace from Khwarezm and other subdued countries. The building of the palace was destroyed already in the second half of the XVI century. At Sheybanids, seeking to rub memory of greatness Timurids.

On a legend a cause of destruction was rage Abdullah khan II who, come nearer to the city, saw in the distance high structures of Ak-Sarai. Having considered that it is already close to the city, the khan rushed off at a gallop, but, having tired out a horse to death, didn't reach to Shakhrisabz. Up to now only ruins of a grandiose portal remained (Figure 7).



Figure 7. The portal of the Palace Ak-Sarai.

Test time was passed by its lateral tower foundations. Long ago the arch between lateral towers which had flight in 22 m collapsed. Modern height of towers about 38 m, and in the past it reached 50 m. In them there were spiral staircases conducting on the top part of a portal which according to messages of contemporaries was trimmed by a gear parapet. Descriptions of Palace Ak-Sarai are available in the diary of the Spanish ambassador Klavikho who visited here in 1404 and also in work "Baburnam" of the beginning of the XVI century. All grandiose

construction of the Palace Ak-Sarai differed in skillful decorative finishing. On a portal of the Palace Ak-Sarai heraldic images of a lion and the sun, and also Amir Timur's sign in the form of three rings were laid out by a mosaic. One of texts of palace inscriptions says: "If you doubt our greatness – look at our constructions". On a mosaic plait of a portal the name of the Iranian master of facing Mahomed Yusuf Tebrizi remained.

In the past behind a huge portal of the palace there was an extensive yard with the pool from which the set of mosaic tiles remained. From the South the palace was adjoined by a garden in which the pavilion for receptions and feasts which vaulted portal was on the main axis opposite to an entrance was built. As Klavikho reports, the reception halls "were painted with gold and an azure, and are revetted with tiles, and the ceiling all is gilded". On a cross axis from two parties also there were small portals rooms for which served for work of "divan" - the State Council. The yard was covered by two-storeyed building (Zasytkin B.N. 1931).

2.4. The complex Poi-Kalyan (XII-XVI cen.).

Minaret Kalyan (Great) is the main symbol of sacred Bukhara. The minaret served not only to convoke Muslims to a prayer, but was a symbol of the power and power of spiritual governors. The bottom of a minaret had the central ensemble of Bukhara – Poi-Kalyan – literally "The bottom great". A minaret — one of the highest buildings of Bukhara, its height of 46,5 meters with the lower diameter of 9 meters, a construction of a conic form with a lamp above (Figure 8). The minaret is ornated —the cylindrical body is laid out by strips of a flat and relief laying, revealing rotundity of a construction at any lighting. The lamp dome, unfortunately, didn't remain. It is possible to get to a minaret from a roof of a cathedral mosque to which it is connected by transition. In a tower there is a helicoid ladder with 140 steps. On eaves there is an inscription about its construction in 1127. Also the name of the architect – Bako is mentioned.



Figure 8. View of a minaret and a mosque Kalyan in Bukhara.

The mosque Kalyan in a modern look was constructed at the beginning of the XVI century. At the first Sheybanids time. Since then five centuries, excepting decades of Soviet period, it acts as the main cathedral mosque of Bukhara. The mosque replaced with itself the old karakhanids mosque of the XII century built along with a minaret Kalyan. The scale of this sheybanids mosque is comparable to temurids cathedral mosques in Samarkand and Herat. It concedes to Bibi-Hanym mosque in Smarkanda on the volume of structures, but, having dimensions of 130x80 m, surpasses it in the area.

3. CONCLUSION

For the last decade there were serious problems connected with preservation of world famous masterpieces of architecture. In particular, the salted ground waters owing to the aggression in relation to construction materials as a result of difficult physical and chemical processes start erodirovat intensively underground and elevated designs of monuments therefore often there are deformations, and in certain cases and their final fracture.

Ancient technologies of construction of the bases are studied. According to tests follows that during the summer period of time process of natural drying of clay takes place rather intensively and makes about 10% in days. During t his period the average size of density of soil reached $\rho_d=16,5 \text{ g/cm}^3$ that is rather high. As showed laboratory researches, at such density soil becomes almost not collapsible.

Thus, ancient masters easily reached the high density of soil which in modern conditions is reached thanks to use of heavy machinery.

At the construction time of monuments of architecture in the IX-X centuries the ceramic square brick (Muslim) was applied to construction of walls, a flooring of floors of rooms and the yards by the sizes: 23x23x3 cm; 12x12x3 cm; 60x63x6,5 cm.

In the X-XI centuries also applied a brick of 21x21x2,5 cm; 24x24x4 cm; in the XIXVI centuries also applied a brick the sizes of the parties of 24-28 cm and 4,5-7 cm thick. Water absorption of wall ceramics fluctuates ranging from 18 to 30% depending on material. Strength at compression is 50-300 kg/cm² (5-30 MPa). Frost resistance is over 50 cycles.

The mosques, the madrasah, mausoleums and other monumental buildings which remained up to now give a complete idea of engineering, constructive and planning and decorative features of construction and architecture of an era of Amir Timur and Timuridov. Century achievements of the past were enriched with new receptions and perfect system.

REFERENCES

1. **Voronina V.L.** Drevnjaja stroitel'naja tehnika Srednej Azii [Ancient construction equipment of Central Asia]. // *Arhitekturnoe nasledstvo*, 1953, Vol. 4, pp. 3-35 (in Russian).
2. **Akishev K.A., Ageyeva Ye.I.** Drevniye pamyatniki Kazakhstana [Ancient monuments of Kazakhstan]. Alma-Ata, "Kazgosizdat", 1958, 60 pages (in Russian).
3. **Tuyakbayeva B., Proskurin A.** (1989). Mirovozzrencheskiye osnovy funktsional'no-planirovochnoy struktury khanaki Akhmeda Yasavi [Worldviews of the functional planning structure of Hanaki Ahmed Yawashi]. // *Pamyatniki istorii i kul'tury Kazakhstana*, 1989, Vol. 4, pp. 106-116 (in Russian).

4. **Margulan A.Kh., Basenov T.K., Mendikulov M.M.** (1959). *Arkitektura Kazakhstana* [Architecture of Kazakhstan]. Alma-Ata, "Kazgosizdat", 1959, 173 pages (in Russian).
5. **Zasyarkin B.N.** *Pamyatniki monumental'nogo iskusstva Vostoka* [Monuments of monumental art of the East]. // *Khudozhestvennaya kul'tura Sovetskogo Vostoka*. Moscow, Leningrad, 1931, pp. 21-49 (in Russian).

REFERENCES

1. **Воронина В.Л.** Древняя строительная техника Средней Азии. // *Архитектурное наследие*, Выпуск 4. – М.: Госиздат лит. по строительству и архитектуре, 1953, с. 3-35.
2. **Акишев К.А., Агеева Е.И.** Древние памятники Казахстана. – Алма-Ата: Казгосиздат, 1958. – 60 с.
3. **Туякбаева В., Проскурин А.** Мировоззренческие основы функционально-планировочной структуры ханаки Ахмеда Йаваси. // *Памятники истории и культуры Казахстана*, 1989, Выпуск 4, с. 106-116.
4. **Маргулан А.Х., Басенов Т.К., Мендикулов М.М.** Архитектура Казахстана. – Алма-Ата: Казгосиздат, 1959. 170 с.
5. **Засуркин Б.Н.** Памятники монументального искусства Востока. // *Художественная культура Советского Востока*. – М.: – Л., 1931, с. 21-49.

phone: 0(375) 221-09-23; e-mail: atm@qmii.uz.

A.A. Riskulov; Tashkent Institute of Design, Construction and of Automobile Roads; 20, Prospekt A. Timura, Tashkent, 100600, Uzbekistan; phone (fax): +998712321439; E-mail: devonxona@tayi.uz

A.R. Omarov; Department of Civil Engineering, L.N.Gumilyov Eurasian National University, Kazhimukan street, 13a, NurSultan city, 010000, Kazakhstan; phone: +7 (7172) 709500; e-mail: enu@enu.kz.

Жусупбеков А.Ж., профессор, доктор технических наук; Евразийский национальный университет им. Л.Н. Гумилева; 010008, Республика Казахстан, г. Астана, ул. Сатпаева, д. 2, Тел: +7 (7172) 709500; E-mail: enu@enu.kz.

Темирова Ф.С.; Каршинский инженерно-экономический институт; 180100, Узбекистан, г. Карши Кашкадарьинской области, ул. Мустакиллик, д. 225; тел. 0(375) 221-09-23; e-mail: atm@qmii.uz.

Рискулов А.А., Ташкентский институт по проектированию, строительству и эксплуатации автомобильных дорог; Республика Узбекистан, город 100060, Ташкент, проспект А. Тимура, дом 20; тел. (факс): +998712321439; E-mail: devonxona@tayi.uz

Омарова А.Р.; Евразийский национальный университет им. Л.Н. Гумилева; 010008, Республика Казахстан, г. Астана, ул. Сатпаева, д. 2, тел: +7 (7172) 709500; e-mail: enu@enu.kz.

A.Zh. Zhussupbekov, Professor, Dr.Sc.; Department of Civil Engineering, L.N. Gumilyov Eurasian National University, Kazhimukan street, 13a, NurSultan city, 010000, Kazakhstan; phone: +7 (7172) 709500; E-mail: enu@enu.kz.

F.S. Temirova; Department of Economics, Karshi Engineering-Economics Institute / Mustaqillikstreet, 225 (office), Karshi city, 180100, Uzbekistan;

OPTIMIZATION PROBLEMS OF MATHEMATICAL MODELLING OF A BUILDING AS A UNIFIED HEAT AND POWER SYSTEM

Yuri A. Tabunshchikov, Marianna M. Brodach

Moscow Architectural Institute (State Academy), Moscow, RUSSIA

Abstract: The mathematical model of a building as a single heat energy system by the decomposition method is represented by three interconnected mathematical models: the first is a mathematical model of the energy interaction of a building's shell with an outdoor climate; the second is a mathematical model of energy flows through the shell of a building; the third is a mathematical model of optimal control of energy consumption to ensure the required microclimate. Optimization problems for three mathematical models with objective functions are formulated. Methods for solving these problems are determined on the basis of the calculus of variations and the Pontryagin maximum principle. A method for assessing the skill of an architect and engineer in the design of a building as a single heat energy system is proposed.

Keywords: building as a single heat power system, mathematical model, heat consumption optimization, outdoor climate, building envelope, maximum principle

ОПТИМИЗАЦИОННЫЕ ЗАДАЧИ МАТЕМАТИЧЕСКОГО МОДЕЛИРОВАНИЯ ЗДАНИЯ КАК ЕДИНОЙ ТЕПЛОЭНЕРГЕТИЧЕСКОЙ СИСТЕМЫ

Ю.А. Табунициков, М.М. Бродач

Московский архитектурный институт (государственная академия), г. Москва, РОССИЯ

Аннотация: Математическая модель здания как единой теплоэнергетической системы методом декомпозиции представлена тремя взаимосвязанными математическими моделями: первая – математическая модель энергетического взаимодействия оболочки здания с наружным климатом; вторая – математическая модель энергетических потоков через оболочку здания; третья – математическая модель оптимального управления расходом энергии на обеспечения требуемого микроклимата. Сформулированы оптимизационные задачи для трех математических моделей с целевыми функциями. Определены методы решения этих задач на основе вариационного исчисления и принципа максимума Понтрягина. Предложен метод оценки мастерства архитектора и инженера при проектировании здания как единой теплоэнергетической системы.

Ключевые слова: здание как единая теплоэнергетическая система, математическая модель, оптимизация теплопотребления, наружный климат, оболочка здания, принцип максимума

Thermal engineering design of the building is based on the tasks of determining the consumption of thermal energy required to maintain optimal or permissible thermal conditions in the room. This problem can be considered as optimization, if we take as the objective function the minimization of the energy expenditure spent on

ensuring the optimal or permissible thermal regime, i.e. as finding a minimum of the following equation:

$$Q = \int_{\tau_1}^{\tau_2} C_H Q_H d\tau + \int_{\tau_3}^{\tau_4} C_x Q_x d\tau \rightarrow \min, (1)$$

where Q_h, Q_x are the consumption of thermal energy for heating and cooling buildings, W ; C_h, C_x are the cost of a unit of heat and a unit of cold, *rubles/W*; $(\tau_2 - \tau_1), (\tau_4 - \tau_3)$ are building heating and cooling periods, *hours*.

When minimizing energy costs, it is necessary to understand that these costs are part of the reduced costs related to the operational component of the reduced costs. The criterion for choosing one or another technical solution can be only a minimum of the costs presented.

At the same time, minimizing operating costs is a critical energy challenge. A typical situation is this: organizing heating or cooling of a building and considering the building as a single energy system, we get that the required energy consumption will vary greatly depending on the shape of the building, the indicators of heat and sun protection, the type of heating or cooling system, etc. Each option has some advantages and some disadvantages, and, due to the complexity of the situation, it is not immediately obvious which of them is preferable finally and why. In order to clarify the situation and help the decision maker, a series of mass calculations is carried out, which can be replaced by the solution of optimization problems.

The mathematical model of the building as a single heat energy system was considered in detail in [1]. In accordance with the principles of system analysis and decomposition, we will present the mathematical model of the building as a single heat energy system with the following three mathematical models.

The first is a mathematical model of the energy interaction of the building envelope with the directed energy impact of the outdoor climate. The heat and power characteristics of an external climate acting on a building can be expressed by the following equations:

$$\begin{aligned} Q_t &= c\rho V m(t_e - t_h), & W \\ Q_v &= c\rho(t_e - t_h) \sum F_i v_i, & W, \\ Q_I &= \sum J_i F_i, & W \end{aligned} \quad (2)$$

where Q_t, Q_v, Q_I are energy exposure to outside air, wind and solar radiation; $c\rho$ is volumetric heat capacity of outdoor air, $kJ / (m^3 \cdot ^\circ C)$; V is building volume, m^3 ; F_i is area of i -th outer surface, m^2 ; t_e, t_h are temperatures of the internal and external air, $^\circ C$; m is air exchange rate, $1/hour$; v_i is air speed, m/s ; J_i is the intensity of the solar radiation incident on the surface of the i -th fence, W/m^2 ;

The second mathematical model is a mathematical model that describes heat flows through the shell of a building.

The third mathematical model is a mathematical model that describes the energy contained in the volume of a building.

In accordance with the presentation of the mathematical model of the building as a single energy system and its presentation by three interconnected mathematical models, we formulate the following three optimization problems.

Here we dwell in more detail on the solution of the first optimization problem; the solution of the second and third optimization problems can be found in [1].

The first task of optimally taking into account the energy impact of the external climate on the building envelope can be formulated as follows: to determine the shape of the building envelope so that the positive impact of the outdoor climate on it can be maximized and its negative impact can be neutralized as much as possible.

The objective function is to optimize the accounting for the heat and energy impact of the external climate in the heat balance of the building.

Optimization of the shape of the building can be performed for various climatic periods of the year: for the coldest five-day period in order to reduce the estimated capacity of the heating system; for the heating period in order to reduce energy costs for heating; for the hottest month in order to reduce the installation capacity of the air conditioning system; for the cooling period of the building in order to reduce energy costs for cooling; for the accounting year in order to reduce energy costs for heating and cooling the building. There may be other climatic periods, depending on the problem being solved.

The obtained optimization problem, which reduces to finding the equation of the directrix and the height of a curved cylindrical surface, relates to isoparametric problems of the calculus of variations [2, 3]. In accordance with the methodology of isoparametric problems [2], we need to determine the extremum of a function that describes the heat balance of a building with a curved surface:

$$\begin{aligned}
 Q &= \\
 &= ZH \int_0^{2\pi} [q_{Enc}(\varphi)(1 - P_W) \\
 &+ q_W(\varphi)P_W] \sqrt{r^2(\varphi) + r'^2(\varphi)} d\varphi \\
 &+ + \frac{1}{2} [q_{roof}(1 - P_{roof}) \\
 &+ q_{roof}^{gl} P_{roof}] \int_0^{2\pi} r^2(\varphi) d\varphi \\
 &+ + \frac{1}{2} q_{fl} \int_0^{2\pi} r^2(\varphi) d\varphi \\
 &= ZH \int_0^{2\pi} q_1(\varphi) \sqrt{r^2(\varphi) + r'^2(\varphi)} d\varphi \\
 &+ q_2 \int_0^{2\pi} r^2(\varphi) d\varphi, (3)
 \end{aligned}$$

where we have

$$\begin{aligned}
 q_1(\varphi) &= q_{Enc}(\varphi)(1 - P_W) + q_W(\varphi)P_W; \\
 q_2 &= \frac{1}{2} [q_{roof}(1 - P_{roof}) + q_{roof}^{gl} P_{roof} + q_{fl}];
 \end{aligned} \quad (4)$$

Q is the amount of heat required to maintain a given room temperature, W ; $q_{Enc}(\varphi)$, $q_W(\varphi)$ are specific heat fluxes passing respectively through the external vertical glazed and glazed enclosing structures, calculated taking into account the directed influence of solar radiation and wind (air filtration) in polar coordinates, W/m^2 ; q_{roof} , q_{roof}^{gl} are specific heat fluxes, respectively, through the

unglazed and glazed parts of the coating, calculated taking into account the effect of solar radiation, W/m^2 ; q_{fl} is specific heat flow through the building envelope of the first floor, W/m^2 ; P_W is glazing coefficient of the vertical building envelope; P_{roof} is glazing coefficient; F_0 is total floor area of the building, m^2 ; H is floor height, m ; Z is the number of floors; $r(\varphi)$ is radius (directrix equation), m ; φ is angle.

We determine the extremum of function (3) from the equation:

$$F_0 = \frac{1}{2} Z \int_0^{2\pi} r^2(\varphi) d\varphi. \quad (5)$$

Here F_0 , H , $q_1(\varphi)$, q are given values; $r(\varphi)$, Z are unknown variables that need to be determined.

In order to determine the necessary initial condition in the isoparametric problem by finding the extremum of the function from the equation, we present an additional function [2]:

$$J^* \int_0^{2\pi} (Q_1 + \lambda Q_2) d\varphi = \int_0^{2\pi} Q d\varphi, \quad (6)$$

where we have

$$\begin{aligned}
 Q &= Q_1 + \lambda Q_2 \\
 Q_1 &= ZH q_1(\varphi) \sqrt{r^2(\varphi) + r'^2(\varphi)} + \frac{1}{2} q_2 r^2(\varphi) \\
 Q_2 &= Z r^2(\varphi)
 \end{aligned} \quad (7)$$

λ is some constant to be defined.

For the additional function (6), we write the Euler equation for the variable $r(\varphi)$:

$$\frac{\partial Q}{\partial r} - \frac{d}{d\varphi} \left(\frac{\partial Q}{\partial r'} \right) = 0 \quad (8)$$

and differential equation (6) through Z :

$$\frac{dJ^*}{dZ} = 0 \quad (9)$$

As a result, we get the system of equations:

$$\begin{aligned} & ZHq_1(\varphi) \left[\frac{r}{\sqrt{r^2+r'^2}} + \frac{r''(r^2+r'^2)-r'^2(r+r'')}{r^2} \right] + ZHq'_1(\varphi) \frac{r}{\sqrt{r^2+r'^2}} + \\ & (q_2 + 2\lambda Z)r = 0 \quad (10) \\ & \int_0^{2\pi} \left[Hq_1(\varphi) \sqrt{r^2+r'^2} + \lambda r^2 \right] d\varphi = 0 \end{aligned} \quad (11)$$

Therefore, to determine $r(\varphi)$, Z , and λ , we have equations (10) and (11) and the isoparametric condition (5), and to determine the unknown variables C_1 and C_2 in the general solution of the Euler equation, we have boundary conditions:

$$r(0) = r(2\pi), \quad r'(0) = r'(2\pi)$$

Let us take a special case of solving the optimization problem for $q_1(\varphi) = \text{const}$. Then

$$r(\varphi) = \text{const}, \quad r'(\varphi) = 0.$$

Equation (10) will be as follows:

$$ZHq_1 + (q_2 + 2\lambda Z)r = 0. \quad (12)$$

Equations (5) and (11) lead to

$$F_0 = \pi Zr^2; \quad Hq_1r + \lambda r^2 = 0. \quad (13)$$

The solution of system (12) and (13) gives

$$r = \sqrt[3]{\frac{HF_0q_1}{\pi q_2}}.$$

Now we pass to the second optimization problem. Note that the second, as well as the third optimization task, can have different objective functions depending on the goal set by the researcher - architect or engineer.

The peculiarity of the second optimization problem of energy flows through the building envelope is due to the fact that heat transfer in winter is determined by the stationary mode, and in the summer there is a significantly unsteady mode. One of our frequent decisions showed [4] that in this case the fencing material should have a minimum coefficient of thermal conductivity and the highest possible value of volumetric heat capacity.

It seems that to some extent this condition is satisfied by wood structures. However, here there is an interesting technical problem of creating a material with low thermal conductivity and high volumetric heat capacity. An optimization problem can also be posed on the optimal arrangement of layers in a multilayer structure.

You can also consider the optimization problem associated with the fact that in summer in a warm climate the temperature of the indoor air due to heat from solar radiation through the windows exceeds the temperature of the outdoor air. In this case, the heat flux is directed from the room and the excess of the role of thermal protection of the fence will increase the temperature of the indoor air. Here, the goal function is to minimize the temperature difference between the outdoor and indoor air and consists in finding such a ratio between the heat and sun protection of the building envelope and the air exchange rate at which the contribution of solar radiation to the room's thermal regime is minimized. It was found that the value of the heat transfer resistance of the external building envelope does not affect the thermal regime of the room, if the following equation is fulfilled:

$$\frac{F_W}{R_{0,W}} \left(\frac{\rho_{wl}}{\alpha_{out,wl}} - \frac{\rho_w}{\alpha_{out,w}} \right) + C_V \lambda_V V_R \frac{\rho_{wl}}{\alpha_{out,wl}} - \beta F_W = 0, \quad (14)$$

where $R_{0,W}$, F_W , ρ_w , $\alpha_{out,w}$ are the resistance to heat transfer of the window, $m^2 \cdot ^\circ C/W$; window area, m^2 ; the absorption coefficient of solar radiation and the heat transfer coefficient of the outer surface of the window, $W/(m^2 \cdot ^\circ C)$; ρ_{wl} , $\alpha_{out,wl}$ are

the absorption coefficient of solar radiation and the heat-transfer coefficient of the outer surface of the wall, $W/(m^2 \cdot ^\circ C)$; C_V , λ_V , V_R are the volumetric heat capacity of the air ($kJ / (m^3 \cdot ^\circ C)$), air exchange rate (h^{-1}), volume of the room (m^3); β is the coefficient of penetration of solar radiation through a permeable fence, taking into account its shadowing by a sun-protection device; J is the average daily value of the intensity of the total solar radiation, W/m^2 .

Equation (14) corresponds to such an energy state at which the temperature inside the room is equal to the conditional temperature of the outdoor air. And consequently, the building envelope separates two media with the same temperature conditions.

We now formulate the third optimization problem as follows: find such a control of energy consumption $Q(t)$ when heating or cooling a room from temperature t_0 to temperature t_1 and such a solution to the system of equations of thermal balance of a given building's building as a single energy system that satisfies the initial conditions for $\tau = 0$ $T = t_0$, for which the functional takes the smallest possible value.

$$W = W = \int_{t_0}^{t_1} Q(t) dt.$$

The solution to this problem was obtained by the method of Academician Pontryagin as a problem of optimal control and presented in [3, 5]. Based on the results of solving the problem of optimal control of the energy expenditure spent on heating or cooling the room, it was concluded: the minimization of energy costs for heating or cooling the premises is achieved if the transition time from the initial room temperature to the desired end the room temperature is minimal (the principle of "maximum performance").

As a result of solving optimization problems, it becomes possible to evaluate the skill of the architect and engineer when designing a building as a single heat and power system using the following equation (for example, when choosing the shape and orientation of a building envelope):

$$\eta = Q_{eff} / Q_{acc},$$

where Q_{eff} is building energy consumption with optimal consideration of the directed action of the outdoor climate; Q_{acc} is energy consumption of the building accepted for design.

If, for example, the value of η is 0.5, then we can assume that the architect did not choose the shape of the building well enough and did not use the positive directional energy impact of the outdoor climate. In the other case, if, for example, $\eta=0.8$, then things are much better.

A similar estimate is possible for the second and third optimization problems.

REFERENCES

1. **Tabunshchikov Yu.A., Brodach M.M.** Matematicheskoe modelirovanie i optimizacija teplovoj jeffektivnosti zdanij [Mathematical modeling and optimization of the thermal efficiency of buildings]. Moscow, AVOK-PRESS, 2002, 194 pages.
2. **Elsgolts L.E.** Differencial'nye uravnenija i variacionnoe ischislenie [Differential equations and calculus of variations]. Moscow, Nauka, 1996.
3. **Moiseev N.N.** Issledovanie operacij. Zadachi, principy, metodologija [Research operations. Tasks, principles, methodology]. Moscow, Nauka, 1988.
4. **Tabunshchikov Yu.A.** O protivorechivosti trebovanij k teplozashhite zdanij v letnih i zimnih uslovijah [On the inconsistency of the requirements for thermal protection of buildings in summer and winter conditions]. // AVOK, 2013, No. 3.
5. **Korobeinik Yu.F., Tabunshchikov Yu.A.** Ob odnoj zadache linejnogo upravlenija i ee prilozhenii k teplotehnike [On a linear control problem and its application to heat engineering]. Moscow, AVOK-PRESS, 2002.

СПИСОК ЛИТЕРАТУРЫ

1. **Табунщиков Ю.А., Бродач М.М.** Математическое моделирование и оптимизация тепловой эффективности зданий. – М.: АВОК-ПРЕСС, 2002. – 194 с.
2. **Эльсгольц Л.Э.** Дифференциальные уравнения и вариационное исчисление. – М.: Наука, 1996.
3. **Моисеев Н.Н.** Исследование операций. Задачи, принципы, методология. – М.: Наука, 1988.
4. **Табунщиков Ю.А.** О противоречивости требований к теплозащите зданий в летних и зимних условиях. // *АВОК*, 2013, №3.
5. **Коробейник Ю.Ф., Табунщиков Ю.А.** Об одной задаче линейного управления и ее приложении к теплотехнике. – М.: АВОК-ПРЕСС, 2002.

107031, Россия, Москва, улица Рождественка, дом 11, 1 корпус, помещение 305; телефон: +7(495)625-16-67; Email: brodatch@abok.ru.

Yuri A. Tabunshchikov, Corresponding Member of the Russian Academy of Architecture and Construction Sciences (RAACN), Professor, D.Sc.; Head of the Department of Engineering Equipment of Buildings and Structures, Moscow Architectural Institute (State Academy); room 305, 11, building 1, Rozhdestvenka Street, Moscow, 107031, Russia; phone: +7 (495) 625-16-67; Email: tabunschikov@abok.ru.

Brodach Marianna Mikhailovna, Professor, Ph.D.; Professor of the Department of Engineering Equipment of Buildings and Structures, Moscow Architectural Institute (State Academy); room 305, 11, building 1, Rozhdestvenka Street, Moscow, 107031, Russia; phone: +7 (495) 625-16-67; Email: brodatch@abok.ru.

Табунщиков Юрий Андреевич, член-корреспондент Российской академии архитектуры и строительных наук (РААСН), профессор, доктор технических наук; заведующий кафедрой «Инженерное оборудование зданий и сооружений», Московский архитектурный институт (государственная академия); 107031, Россия, Москва, улица Рождественка, дом 11, 1 корпус, помещение 305; телефон: +7(495)625-16-67; Email: tabunschikov@abok.ru.

Бродач Марианна Михайловна, профессор, кандидат технических наук; профессор кафедры «Инженерное оборудование зданий и сооружений», Московский архитектурный институт (государственная академия);



АЛЕКСАНДРУ СЕРГЕЕВИЧУ ГОРОДЕЦКОМУ – 85 ЛЕТ

Городецкий А. С. закончил Киевский инженерно-строительный институт в 1955 году по специальности «Промышленное и гражданское строительство».

Работая в проектных и научно-исследовательских институтах УкрНИИпроектстальреконструкция (1955 – 1960, инженер, главный инженер проекта), КиевЗНИИЭП (1960 – 1969, зав. лабораторией), УкрНИИпроект (1969 – 1971, заведующий лабораторией), Гипрохиммаш (1971 – 1976, заведующий отделом), НИИАСС 1976–2009, заместитель директора по научной работе), НИИСП (2009 – 2012, главный научный сотрудник), Киевский национальный университет строительства и архитектуры (2012 – 2016, профессор кафедры), заместитель директора ООО ЛИРА САПР (2011 – по настоящее время) Городецкий А. С. всегда совмещал научно-исследовательскую деятельность с инженерной практикой. Принимал участие в проектировании сложных строительных объектов, большепролетного покрытия Бориспольского аэровокзала (в начале 60-х годов это было самое большое покрытие в виде тонкостенной полой оболочки – пролет 56–48 м), конструкций Республиканского стадиона в г. Киеве (конструкции чаши второго яруса), большепролетных висячих покрытий крытых рынков и киноконцертных залов, сложных конструкций объектов металлургической, химической и угольной промышленности.

При проектировании этих объектов Городецкий А.С. непосредственно принимал участие или руководил как теоретическим обоснованием прочности и надежности конструкций, так и инженерной разработкой.

В 1969 году под руководством и при участии А.С. Городецкого разработаны программные комплексы, в которых впервые в стране для комплексов массового применения был реализован метод конечных элементов, а в 1970 году – и метод суперэлементов.

В 70-х годах научная деятельность Александра Сергеевича Городецкого связана с теоретическим обоснованием метода конечных элементов и его применением в практической инженерной деятельности. Разработаны методы конструирования новых высокоточных конечных элементов, обосновано применение метода конечных элементов при решении нелинейных задач механики. Эти работы обобщены в докторской диссертации Городецкого А. С., которую он успешно защитил в 1978 году. За создание научной школы в области инженерных методов расчета конструкций А.С. Городецкому в 1984 году присвоено звание профессора.

В 80-х научные работы А.С. Городецкого направлены на разработку инженерных методов информатизации проектирования строительных объектов. Под его руководством и при непосредственном участии разработаны программные комплексы, которые позволяют в автоматизированном режиме выполнять весь комплекс проектных работ, включая получение комплекта рабочих чертежей. За эти работы А.С. Городецкий в 1986 году удостоен Государственной премии Украины в области науки и техники.

В 2007 году отмечен Благодарностью Премьер-министра Украины «За значительный личный вклад в обеспечение развития строительной отрасли, за многолетний добросовестный труд и высокий профессионализм».

В настоящее время Городецкий А.С. интенсивно ведет разработку инженерных методов расчета и проектирования конструкций на современных компьютерах.

Большое внимание Городецкий А.С. уделяет методам компьютерного моделирования конструкций, разработке и реализации нелинейных методов строительной механики в программных комплексах, разработке методов расчета конструкций максимально приближенной к их реальной работе, расширению возможностей графических интерфейсов, которые дают возможность широкому кругу инженеров использовать в своей повседневной деятельности современные методы строительной механики.

Городецкий А.С. принимает активное участие в общественной научной деятельности. Он является руководителем отделения «Компьютерные технологии в строительстве» Академии Строительства Украины, является иностранным членом Российской академии архитектуры и строительных наук (РААСН).

А.С. Городецкий является основателем школы компьютерных технологий проектирования конструкций и научным руководителем многих представителей этой школы. Под научным руководством А.С. Городецкого подготовлено два доктора наук и более двадцати кандидатов наук. Разработанные под его руководством и при непосредственном участии программные комплексы ЛИРА, ЛИРА-САПР, МОНОМАХ и другие широко известны и используются практически всеми проектными и научными организациями России, Украины, стран Балтии, некоторых стран Европы и Азии.

Редакция журнала сердечно поздравляет Александра Сергеевича Городецкого с замечательным юбилеем, желает ему здоровья, многолетнего творчества на благо современной науки, благополучия и счастья!

*Редакционный Совет международного научного журнала
“International Journal for Computational Civil and Structural Engineering”*